

OAK RIDGE NATIONAL LABORATORY

operated by

UNION CARBIDE CORPORATION

NUCLEAR DIVISION

for the

U.S. ATOMIC ENERGY COMMISSION



ORNL - TM - 2410

96

~~EMM ESTD~~ JAN 27 1969

IRRADIATED FUEL SHIPPING CASK DESIGN GUIDE

[Handwritten signature]

LEGAL NOTICE

This report was prepared as an account of Government sponsored work. Neither the United States, nor the Commission, nor any person acting on behalf of the Commission:

- A. Makes any warranty or representation, expressed or implied, with respect to the accuracy, completeness, or usefulness of the information contained in this report, or that the use of any information, apparatus, method, or process disclosed in this report may not infringe privately owned rights; or
- B. Assumes any liabilities with respect to the use of, or for damages resulting from the use of any information, apparatus, method, or process disclosed in this report.

As used in the above, "person acting on behalf of the Commission" includes any employee or contractor of the Commission, or employee of such contractor, to the extent that such employee or contractor of the Commission, or employee of such contractor prepares, disseminates, or provides access to, any information pursuant to his employment or contract with the Commission, or his employment with such contractor.

ORNL-TM-2410

Contract No. W-7405-eng-26

CHEMICAL TECHNOLOGY DIVISION

IRRADIATED FUEL SHIPPING CASK DESIGN GUIDE

L. B. Shappert

JANUARY 1969

OAK RIDGE NATIONAL LABORATORY
Oak Ridge, Tennessee
operated by
UNION CARBIDE CORPORATION
for the
U.S. ATOMIC ENERGY COMMISSION

CONTENTS

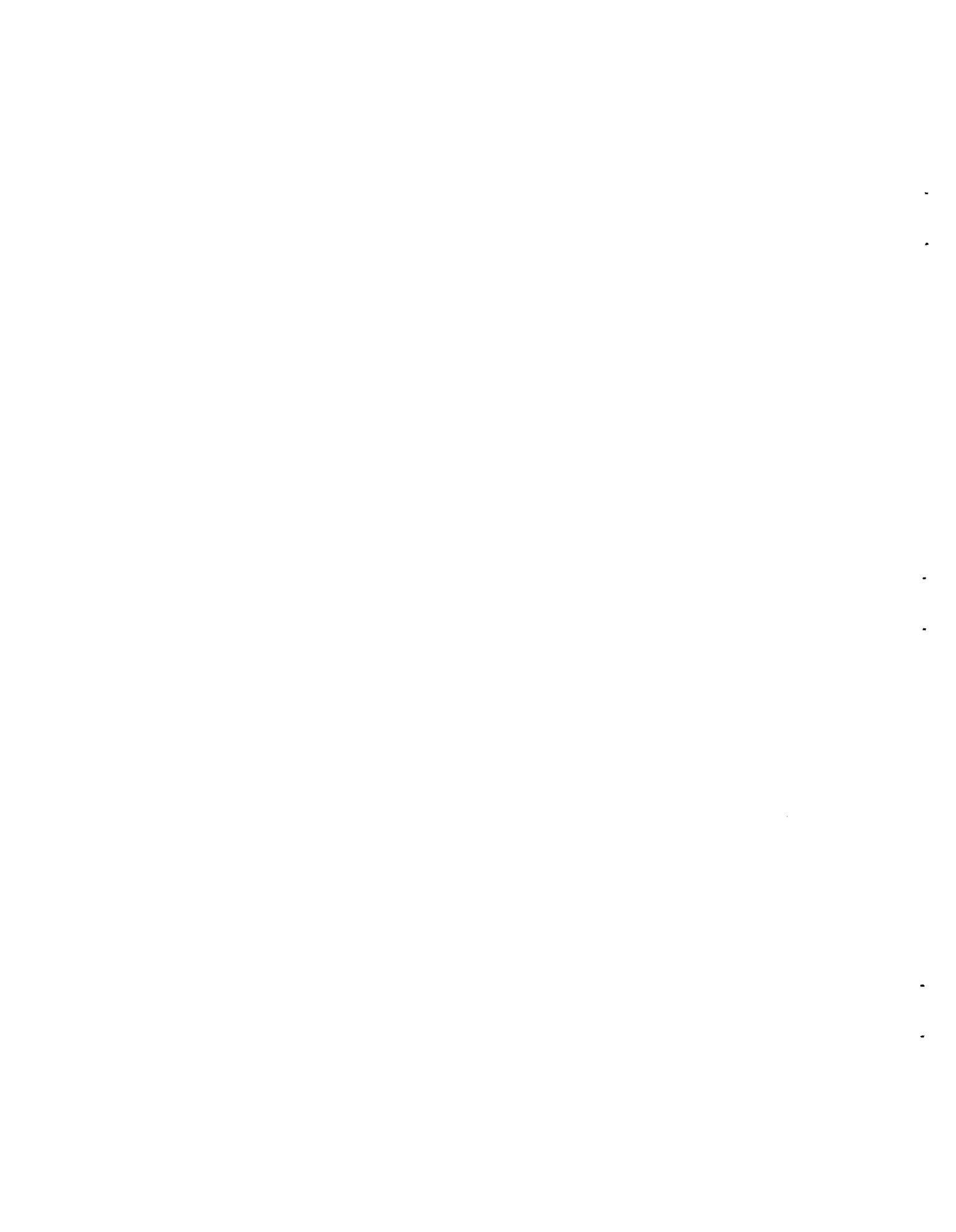
	<u>Page</u>
Abstract	1
1. Introduction	1
1.1 Scope	7
1.2 Cask Nomenclature	7
1.3 Quality Assurance	7
1.4 Acknowledgments	9
1.5 References	10
2. Structural Design	11
2.1 Inner Shell Thickness	11
2.2 Outer Shell Thickness	11
2.2.1 Basis for Equation 2.1	14
2.3 Weld Design	16
2.4 Cask Closure, Gasketing, and Bolting Design	19
2.4.1 Selection and Design of the Gasket	20
2.4.2 Design for Bolts or Studs to Retain Cask Lid	27
2.4.3 Cask Closure Design	31
2.5 Lifting Devices	35
2.6 Tie-Downs	40
2.6.1 General Considerations	40
2.6.2 Tie-Down Methods	42
2.6.3 Methods of Analysis	46
2.7 Effects of a 30-ft Impact on Lead Shielding	46
2.7.1 Material Properties Under Impact Conditions	46
2.7.2 Analysis of a Horizontal Axis Drop of a Cylindrical Cask Without Fins	48
2.7.3 Analyses of an End Drop of a Cylindrical Cask With Nonbuffered Ends	53

	<u>Page</u>
2.8 Shock Absorbing Structures	55
2.8.1 Fins	55
2.8.2 Toroidal Shell-Type Energy Absorbers	57
2.8.3 Protective Buffers	57
2.8.4 Aluminum Honeycomb Characteristics	61
2.8.5 The Army-AEC Vehicle Impact Studies	64
2.9 Testing Requirements	65
2.9.1 Hypothetical Accident Conditions	65
2.9.2 Normal Operating Conditions	67
2.10 Comments on Cask Shielding Material	70
2.10.1 Heat Transfer Under Normal Conditions	72
2.10.2 Heat Transfer Under Accident Conditions	74
2.11 Fuel Magazine Design	76
2.11.1 Protection and Containment of Fuel During Transportation and Handling	76
2.11.2 Dissipation of Heat	77
2.11.3 Control of Criticality	77
2.12 Simple Beam Requirement	80
2.13 References	82
3. Materials	85
3.1 Plate	85
3.2 Pipes and Tubes	87
3.3 Forgings, Fittings, and Bolting	87
3.4 Welding Electrodes, Rods, and Wire	88
3.5 Special Materials	88
3.6 Identification Marking and Purchase Order Requirements ...	88
4. Fabrication	89
4.1 Materials	90

	<u>Page</u>
4.1.1 Mill Test Reports and Marking	90
4.1.2 Cutting Material	90
4.1.3 Repair of Defects in Materials	90
4.1.4 Forming Materials	91
4.2 Identification and Control of Materials	91
4.3 Welding	91
4.3.1 Welding Processes and Filler Metals	91
4.3.2 Qualification of Welding Procedures	92
4.3.3 Qualification of Welders and Welding Operators ...	92
4.3.4 Lowest Permissible Temperatures for Welding	92
4.3.5 Fitting and Alignment	92
4.3.6 Cleaning of Surfaces to be Welded	93
4.3.7 Joints - Alignment Tolerances	93
4.3.8 Finished Joints	93
4.3.9 Miscellaneous Welding Requirements	94
4.3.10 Repair of Weld Defects	94
4.4 Weld-Metal Cladding of Carbon Steel	94
4.4.1 Welding Procedure Qualification Requirements	94
4.4.2 Performance Qualification Test	97
4.5 Joining Integrally Clad or Weld-Metal-Overlay Clad Material	97
4.6 Postweld Heat Treatment	97
4.7 Lead Pouring	98
4.8 Inspection	98
4.8.1 Access for Inspector	98
4.8.2 Inspection of Material	98
4.8.3 Inspection of Surfaces During Fabrication	99
4.8.4 Dimensional Inspection	99
4.8.5 Weld Inspection	100

	<u>Page</u>
4.8.6	Check of Postweld Heat-Treatment Practice 100
4.8.7	Inspection During Fabrication 101
4.9	Testing 101
4.9.1	Shielding Chamber Leak Test 101
4.9.2	Pressure Test 101
4.9.3	Leak Test 102
4.9.4	Heat Transfer Acceptance Test 102
4.9.5	Shielding Integrity Test 103
4.9.6	Lead Bond Integrity Test 103
4.10	Fabrication Record 104
5.	Heat Transfer 106
5.1	Introduction 106
5.2	Heat Sources 108
5.2.1	Decay Heat Load 109
5.2.2	Solar Heat Load 112
5.3	External Heat Transfer 116
5.3.1	Heat Removal from a Cask Surface 116
5.4	Internal Heat Transfer 127
5.4.1	Analytical Method 128
5.4.2	The Parametric Cases 129
5.5	Fire Analysis 134
5.5.1	Graphical Method 138
5.5.2	Analog Method 141
5.5.3	Energy Balance Method 143
5.5.4	Use of Digital Computers in Studying the Thermal Transient Caused by a Fire 156
5.6	References 161

	<u>Page</u>
6. Criticality	164
6.1 Introduction	164
6.2 Methods of Prevention of Criticality	164
6.2.1 Application	165
6.3 Normal Conditions of Transport	168
6.3.1 The Fresh Fuel Assumption	169
6.3.2 Burnup Effects on Reactivity	169
6.4 The Most Reactive Credible Condition of Transport	172
6.5 Criticality Evidence	173
6.5.1 Safe Limits	173
6.5.2 Calculational Evidence	174
6.5.3 Experimental Evidence	178
6.6 Applications for AEC Approval on Criticality	180
6.6.1 Exemptions	180
6.6.2 General Licenses	181
6.7 References	183
6.8 Bibliography of Critical Experiments	186
7. Shielding	197
7.1 General Considerations	197
7.2 DOT Regulations	197
7.3 Shielding Estimates	199
7.3.1 Comparison of Nomograph and Machine Code	199
7.4 Dose Calculations Away from Cask Surface	199
7.5 Example	201
7.6 References	209



IRRADIATED FUEL SHIPPING CASK DESIGN GUIDE

L. B. Shappert

ABSTRACT

The design of irradiated fuel shipping casks is governed not only by the material being shipped but also by the Regulations (AEC Manual Chapter 0529, 10CFR71 and 49CFR171-178) that impose structural performance standards on the cask by a series of postulated accidents. This Guide provides cask design procedures and criteria, developed from extensive analysis and testing programs, that enable the designer to correlate the cask design to its performance as reliably as if the cask were subjected to a physical demonstration.

The Guide covers design areas of cask structural integrity, heat transfer, criticality, shielding materials of construction, and fabrication techniques. The design information presented is discussed within the framework of the AEC regulations along with the rationale and testing program that supported its development.

It has been possible to provide design information in the important areas referred to in the current Regulations. However, the Regulations continue to undergo modification and reinterpretation. In consequence, future editions of the Guide will contain additional data to cover the problems that result from continuing refinement of the Regulations.

1. INTRODUCTION

The domestic transportation of spent fuel elements from power reactors is governed by regulations from the Department of Transportation (DOT) and the U. S. Atomic Energy Commission. The Hazardous Materials Regulations Board of the DOT has recently revised these regulations, making them more general and eliminating much of the detail.¹ The primary aim of the Regulations is, of course, to protect the public by rigorously restricting the amount of radiation and contamination to which people are exposed.

The Regulations referred to throughout this Guide are primarily those of the USAEC² (referred to as AECM 0529 which are almost identical to those published as CFR Title 10 part 71), but occasionally the DOT regulations are mentioned.*

The Regulations are written in terms of performance specification requirements. A cask designer is free to exercise his own judgment as to, first, how to meet these requirements and, second, how to prove that he has done so. Difficulties arise because various cask designers place their own interpretation on the regulations and many develop new methods of structural assessment. No document has been available which correlate tests with an analytical treatment or indicate analysis methods which have withstood a test of time.

Several years ago the Division of Reactor Development and Technology (RDT) suggested that the Oak Ridge National Laboratory develop a Guide which would state in clear, orderly fashion what are considered to be good engineering standards of practice in the design, fabrication, testing, inspection, and maintenance of irradiated fuel shipping casks. It was decided that initially the information in the Guide should apply to lead-shielded spent fuel casks having steel inner and outer shells since this type of cask is most widely used in the United States today; it should be subsequently expanded to include uranium, steel, and other appropriate shielding materials. The Guide should be of such quality that proof of adherence to it would constitute prima facie evidence of satisfying the performance standards of the Federal Regulation. In addition, the Guide should provide detailed engineering backup supporting its provisions with such justifications, derivations and judgments as required to clarify the intent as to the degree of safety and degree of conservatism intended

*The DOT regulations have been made compatible to the International Atomic Energy Agency (IAEA) regulations.³ It is expected that the USAEC will modify their regulations to become more compatible with both the DOT and IAEA regulations.

by the Guide. As a result a framework would exist against which to judge alternative approaches, techniques or materials to assure that a consistent degree of conservatism is applied and to provide a means for encouraging improvement in the art and its incorporation into practice. This report constitutes the initial effort in fulfilling that commitment.

This report will be widely disseminated; readers are asked to review it and submit their comments, suggestions, and recommendations for changes to the author. Especially those methods of analysis that may be used to evaluate experimental results are solicited; any known operating or fabrication limitations will be of interest.

The format was chosen so as to group design subjects of a specific nature under topical headings. In spite of the disadvantage that the topics do not follow the same order as they appear in the regulations it is easier (and strongly suggested) that requests for approvals that are submitted to the AEC follow the format and order of the regulation to avoid confusion.

Methods of analysis suggested in the Guide are intended to provide reasonably accurate information about cask design; however, in some cases where the accuracy of the analysis is not known, a factor of safety is assigned to account for these uncertainties.

The Guide contains seven chapters. Chapter 1 consists of introductory remarks. Chapter 2 is concerned with the structural design of shipping casks. Discussions of the materials of construction and the methods of fabrication, which are intimately associated with design, follow in Chaps. 3 and 4, respectively. Chapter 5 deals with heat transfer. Chapter 6 describes the kinds of evidence that should be considered acceptable for proving that a system conforms to the criticality requirements of existing federal regulations. Information on shielding is presented in Chap. 7.

Early versions of the regulations indicated that for calculational purposes, the impact resulting from the 30-ft free fall could be considered equivalent to applying a 60 g decelerating force to the cask for 0.016 seconds. Although this specification was removed in later versions

of the regulations it is occasionally used to indicate compliance to the 30-ft-drop requirement. Our investigations indicate that the application of such a force will not produce damage similar to that produced by a 30-ft drop. However, damage may be assessed by analytical methods based on the conservation of energy principle as outlined in Chap. 2. In several cases this method has been correlated with experimental results. The methods will be refined and expanded for wider application in other critical areas for future editions of the Guide.

At the present time we do not have sufficient data at our disposal to predict with confidence the best weld joint design. Some limited information based on observations of static tests and personal contacts with first-hand observers of cask impacts leads us to believe that some joint designs will withstand the 30-ft free fall better than others. Thus, until verification tests can be carried out, the joint designs recommended in Chap. 2 are based on what we consider to be good engineering practice.

Although loss of shielding is discussed in Chap. 2, the primary hazard resulting from the 30-ft free fall is a breach of the cask containment; for this reason it is necessary to protect closure regions from impact. Energy absorbers that may be useful for this purpose are discussed in Sect. 2.8.

One of the major requirements of the cask analysis is to show that the integrity of the cask seal can survive the impact. The primary seal is generally maintained by a force on the lid closure which is secured by bolts or studs and for the most part, the problem involves the energy absorption capacity of these bolts or studs. Sufficient data are not available to permit the computation of the capacity of a particular stud or bolt with the desired degree of confidence; until it is, the equations given in Sect. 2.4 will provide conservative bolt pattern designs for closures.

Since the primary aims of cask design are to shield and to contain a source of radioactive material, the materials of construction (discussed in Chap. 3) must be capable of performing satisfactorily when they are

exposed to a wide range of environmental conditions as specified in the regulations. From the standpoint of use as a fabrication material, a steel should have adequate strength, ductility, and toughness at ambient temperatures. We have assumed that materials which require a minimum of 15 ft-lb of energy to break a Charpy keyhole specimen at a temperature of -40°F will function satisfactorily under normal operating conditions, as described in the regulations; such toughness should be sufficient to prevent brittle fracture from occurring at low temperatures.

In contrast to the high degree of reliance placed on steel shells of casks, the requirements for steel used for supports, lifting, tie-down, and similar non-containment structures may be relaxed. The consequence of a failure in these components are minimal since one material failure would not be sufficient by itself to cause any loss of cask contents or shielding.

The designer is free to specify materials other than those recommended in Chap. 3; however, the factors described above must be accounted for in the cask design. To aid the designer, a list of materials that are acceptable for radiation shielding and criticality control in shipping casks is also provided in this chapter.

The fabrication and inspection requirements for shipping casks are not covered by existing codes and standards. Chapter 4, which sets forth minimum quality requirements, has been prepared in such a manner that any section may be incorporated into procurement specifications. To ensure that the requirements are adhered to, an inspector, as a representative of the cask purchaser, would audit the manufacturer's procurement, fabrication, inspection, and testing records to determine compliance with the procurement specifications. Such a system will be worth its cost for the positive assurances of safety and quality of the final product it will afford to both the cask purchaser and the U. S. Atomic Energy Commission.

Two heat sources - solar heat and decay heat - are considered (see Chap. 5) in calculating the maximum temperature of the spent fuel and cask expected under normal shipping conditions. Although both of these loads vary as a function of time, the cask is generally designed for a

specified heat load that accounts for these two sources. Since the heat capacity of massive spent fuel casks is very large and the solar load is applied primarily to the projected surface area of the cask, we feel it is justifiable to base the solar load (in Btu/hr) on the heat input to the cask averaged over a 24-hr day (see the example in Sect. 5.3.1).

The response of a cask to the hypothetical fire stipulated in the regulations is difficult to evaluate accurately. For example, few fire tests of casks have been instrumented properly to permit theoretical and experimental comparisons to be made. Data that have been accumulated thus far indicate that testing should be carried out on a prototype cask rather than a scale model in order to obtain useful results. More recently, it appears that the furnace testing of a cask at 1475°F may not be equivalent to the fire test postulated in the regulations because of the inability to control the emissivity of the source to the stated value of 0.9. In addition, in an actual test there is inevitably a convection as well as a radiation coupling between the cask and heat source that is not alluded to in the regulations. Such a situation makes the correlation of theory and experiment difficult.

Federal regulations require every shipment of fissile material to remain subcritical at all times during normal transport, including loading and unloading, and under hypothetical accident conditions leading to the most reactive credible configuration. Chapter 6 in the Guide is concerned with the proof of adherence to the requirement of subcriticality rather than with the method of maintaining subcriticality. In the interest of economy and practicality, a shipper should be allowed to exercise any practical controls he desires in rendering a system subcritical; however, he must present proof that these controls are adequate. The types of proof considered acceptable are discussed.

Proof of subcriticality can best be substantiated by arranging the desired fuel in the most reactive credible configuration with respect to the shipping cask design. Thus it would be desirable to have the conceptual cask design available at the same time that reactor critical experiments on the fuel are being performed, since only a few additional experiments would be needed to predict the degree of subcriticality that

would be attained during shipment. When this is not possible, the proof of subcriticality must depend entirely upon calculational methods. The accuracy of such methods may be verified by analyzing selected critical experiments in which a similar fuel has been used. The Guide provides an annotated listing of a wide variety of experiments that may be used for this purpose.

Chapter 7 presents information, in the form of a nomograph, that will provide cask reviewers a quick and reasonably accurate method for determining whether the thickness of the lead shielding in a given cask is adequate for a particular purpose. It was found that the nomograph gives values of lead thicknesses generally within 5% of those calculated by a machine code assuming that the source in the cavity is homogeneous.

Since regulations specify dose rates 3 ft from the cask surface as well as surface dose rates, a number of graphs are given that relate surface dose rate to dose rates 3 ft from the surface as a function of cask dimensions.

1.1 Scope

This Guide deals almost exclusively with casks having steel shells and lead shielding since such casks constitute the most commonly used type. Ultimately, other types of shielding materials will be considered.

1.2 Cask Nomenclature

Figure 1.1 shows a cutaway diagram of a spent fuel shipping cask listing the principal components found in such casks. These components are referred to by name throughout this Guide.

1.3 Quality Assurance

The requirements in the Guide are deemed the minimum to provide quality assurance adequate for most shipping casks. The designer must exercise good judgment and adopt stricter requirements where greater performance requirements are warranted.

The cask manufacturer should provide his own inspection and test personnel and facilities to maintain control of the quality of materials, components, and fabrication throughout the cask construction.

The purchaser's inspector must verify that the manufacturing quality control is maintained and all parts and work processes are in accordance with the approved drawings and specifications. The inspector must have the right to stop work on the cask at any time he feels the cask quality assurance is being jeopardized.

ORNL DWG 68-12260

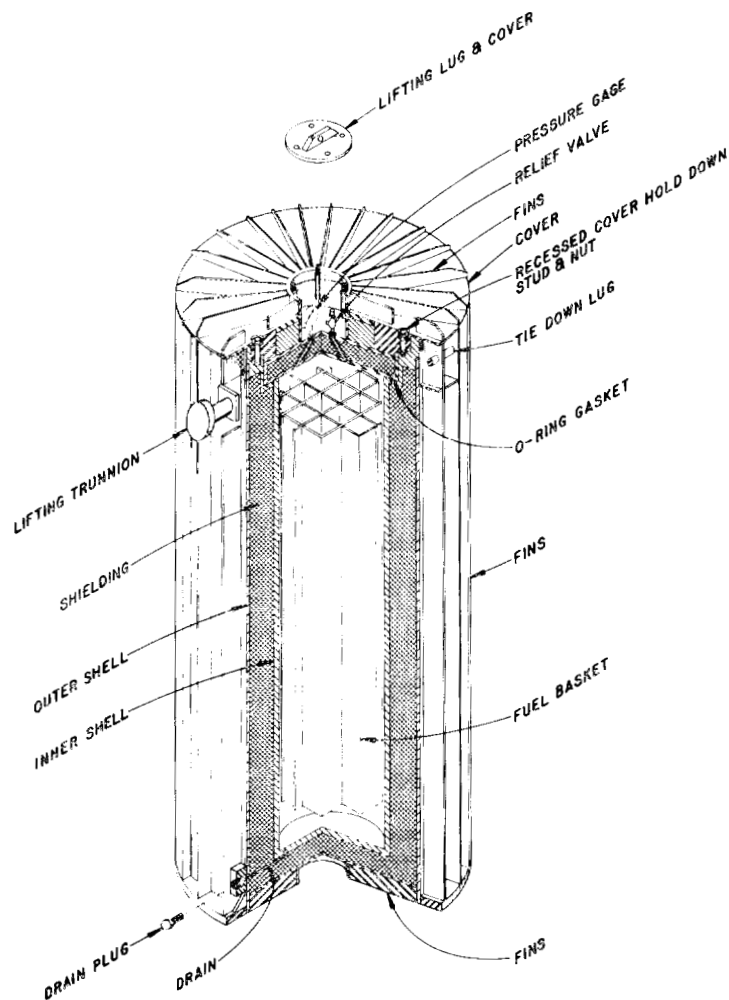


Fig. 1.1. Cutaway Diagram of a Shipping Cask Showing Its Principal Components.

Material test reports, heat treat charts and other documents serving as evidence to document the entire fabrication are required to be maintained in a Fabrication Record (Sect. 4.10) by the Manufacturer and delivered with the cask to the purchaser. The inspector is required to be aware of and to approve all such documents before they are placed in the record. This is to ensure the inspector's complete awareness of all phases of the construction; it does not relieve the cask manufacturer of his responsibility to conform to the design as specified in the drawings.

1.4 Acknowledgments

The Guide represents the efforts of a large number of people; although some of these have worked on more than one chapter, their names are listed after the chapter with which they were primarily concerned.

Chapter 2: W. C. Stoddart, H. A. Nelms, J. H. Evans, A. E. Spaller,*
D. C. Watkin (ORNL) and L. R. Shobe (University of
Tennessee).

Chapter 3: O. A. Kelly (ORNL)

Chapter 4: J. R. McGuffey, R. W. Schneider,** J. N. Robinson (ORNL)

Chapter 5: W. C. Corder, J. D. Rollins, E. C. Lusk, A. W. Serkiz
(Battelle Memorial Institute, Columbus)

Chapter 6: G. E. Edison,*** A. M. Perry (ORNL)

Chapter 7: M. Solomito, H. C. Claiborne (ORNL)

Organization: B. B. Klima, J. N. Baird

*Present address: Tennessee Eastman, Kingsport, Tennessee

**Present address: Bonney Forge, Allentown, Pa.

***Present address: Westinghouse, Pittsburgh, Pa.

1.5 References

1. Code of Federal Regulations, Title 49, Parts 171-178, Federal Register 33 No. 194, Part II (Oct. 4, 1968).
2. Code of Federal Regulations, Title 10, Part 71.
3. Regulations for the Safe Transport of Radioactive Material, Safety Series No. 6, 1967 Edition, International Atomic Energy Agency, Vienna, 1967.

2. STRUCTURAL DESIGN

2.1 Inner Shell Thickness

The inner shell of the cask exclusive of closure devices should be designed as an unfired pressure vessel according to the specifications listed in Sect. VIII of the ASME Boiler and Pressure Vessel Code. These specifications relate size, material of construction, internal and external pressure and weld efficiency to thickness.

It is necessary to establish a shell thickness that will allow the cavity to remain serviceable under all expected internal and external loads. Internal loads will be imposed from the static head of lead during pouring, the shrinkage of lead upon cooling, the expansion of lead resulting from a fire, or the movement of lead as a result of impact. Internal loads occur as a result of coolant pressure in the cavity or possibly from thermal expansion of internal components such as a basket.

Because of the type of environment to which the inner shell is exposed, the material should be capable of being decontaminated without loss of serviceability. Acceptable materials of construction are discussed in Chap. 3.

If it is desirable to perform a more detailed analysis than is afforded by the Pressure Vessel Code, ORNL-TM-1312, Vol. 1, which deals with inner shells of both cylindrical and prismatic casks, should be consulted.

2.2 Outer Shell Thickness

A 40 in. fall of a lead shielded cask onto a 6-in.-diam punch may cause failure* of the cask in one of several ways. The most obvious is a rupture to the outer shell which could result in an excessive loss of lead if the cask were involved in a fire. Less obvious, but nonetheless important, are the possibilities of a gasket failure (if the impact is

*Failure is defined as the inability of the cask to meet the regulations.

in close proximity to the cask closure) or a substantial reduction in shielding (if the indentation is particularly deep).

For an ordinary hot rolled carbon steel outer shell the minimum outer shell thickness required to withstand the punching action of the piston is given by Eq. (2.1).

$$t = (W/s)^{0.71} , \quad (2.1)$$

where

t = shell thickness, in.,

W = cask weight, lb, and

s = ultimate tensile strength of the outer shell, psi.

Figure 2.1 shows a photomicrograph of a section of a steel shell that was damaged to the point of incipient puncture as a result of impact on a punch. Note the partial fracture of the test specimen.

ORNL PHOTO 84426 A

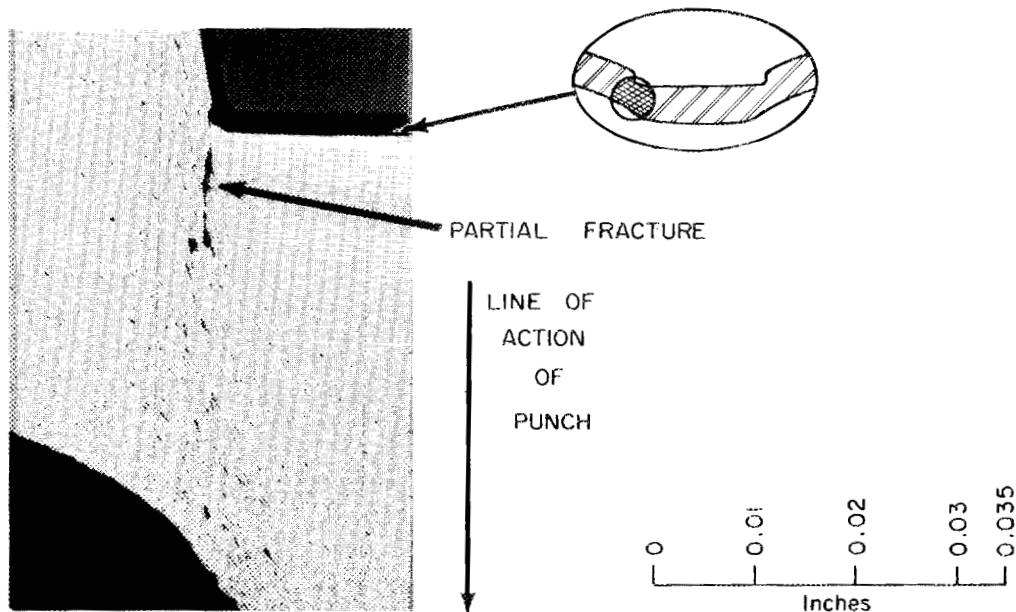


Fig. 2.1. Photomicrograph of Hot-Rolled Steel Plate Tested at Its Incipient Puncture Energy.

A convenient representation of (Eq. 2.1) is given in Fig. 2.2. Equation (2.1) may be used for both prismatic and cylindrical casks within certain limits. Tests have indicated¹ that for cylindrical casks with diameters greater than about 30 in., (Eq. 2.1) gives acceptable results; for diameters less than 30 in., it may give nonconservative results. Until more definitive tests can be performed it is recommended that a factor of 1.3 times the actual cask weight be used in (Eq. 2.1) when it is applied to casks having diameters less than 30 in.

When (Eq. 2.1) is used consideration should be given to the reduction in jacket flexibility caused by various structural features. The energy required to puncture the jacket will be reduced from the value indicated by Eq. (2.2) by "stiffeners" such as fins that are closer than about 9 in. from the center of the impact area. Data to quantitatively evaluate the effect of local stiffeners are not presently available and until this effect is better known, Eq. (2.1) may be considered adequate.

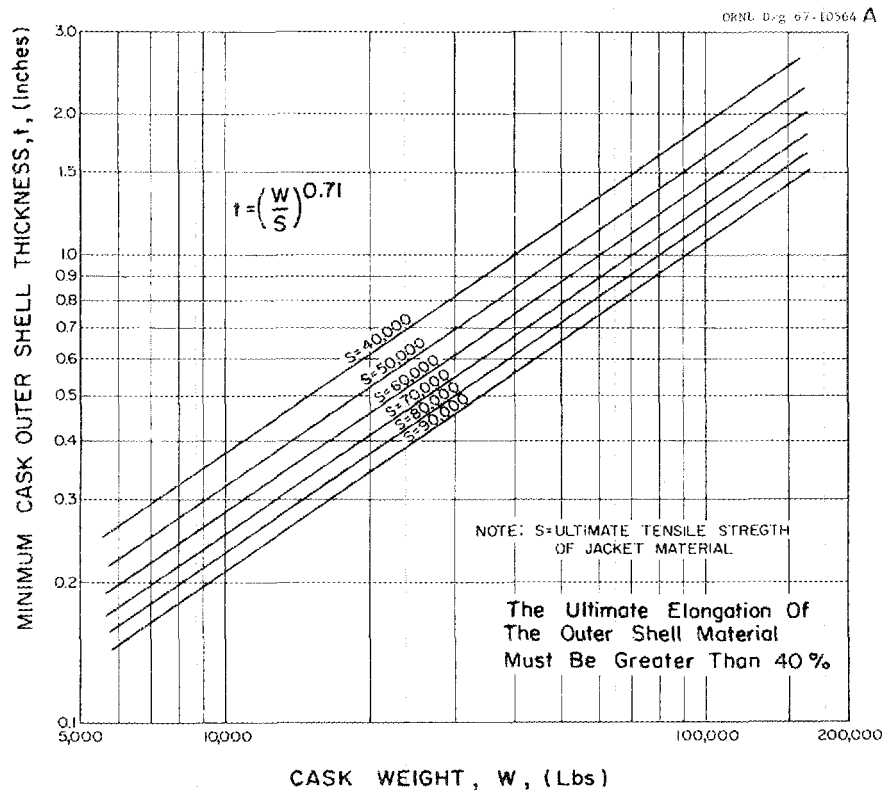


Fig. 2.2. Graph to Estimate Minimum Outer Shell Thickness.

Lead shielded casks based on a three-shell cask wall concept have been designed and built. The design provides inner and outer shells, plus a third shell that is positioned approximately 2 in. inside the outer one; this arrangement provides forming two separate chambers to contain the lead shielding. Under accident conditions the outer shell could be ruptured. However, such an occurrence would be acceptable since the loss of 2 in. of lead shielding in a fire will limit the dose rate increase to approximately a factor of 10. The loss of lead will create an air gap which will reduce the effective heat input to the cask cavity. Impact tests have been performed on the three-shelled wall concept², the results of which appear promising. Considerably more energy is required to rupture the center shell of such a cask than would be expected based on Eq.(2.1).

A similar concept in which puncture of the outer shell may be allowed in an accident is described in a report by the French.³ A layer of wet plaster is poured between the lead shield and the outer shell. If the cask is involved in a fire the outer shell perforates by virtue of fissible plugs and the plaster dries, forming an insulating layer around the lead shield. Results of tests indicate that the layer offers adequate protection from both impact and fire.

2.2.1 Basis for Equation 2.1

An experimental program was initiated to investigate the conditions that would lead to the puncture of steel-jacketed lead-shielded casks.^{1,4} The results are summarized in Fig. 2.3. The three data points are the results of the 86,200 lb prototype model test, and appear to be correlated well by the equation

$$E/S = 39t^{1.4}, \quad (2.2)$$

where

E is the energy (40 W, in in.lb) and the other terms are given above.

Equation 2.2 was developed from a geometrical scale up of data obtained using 1:12 size model test data; i.e., test specimens weighed from 35 to 75 lb and the punch was 0.5 in. diam.

Materials with a broad range of properties backed with lead were tested in the prismatic model phase of the program.¹ It was found that significantly less energy was required to punch through materials which have an ultimate elongation of less than 40% in a 1-in. gage length than those whose elongation was greater than 40%. Above this elongation level the ultimate tensile strength of the shell material was the significant property of the material and, therefore, was used to correlate the data. At impact energies near puncture energy, significant deformations of the jacket were evident over an area whose diameter was about three times that of the punch diameter.

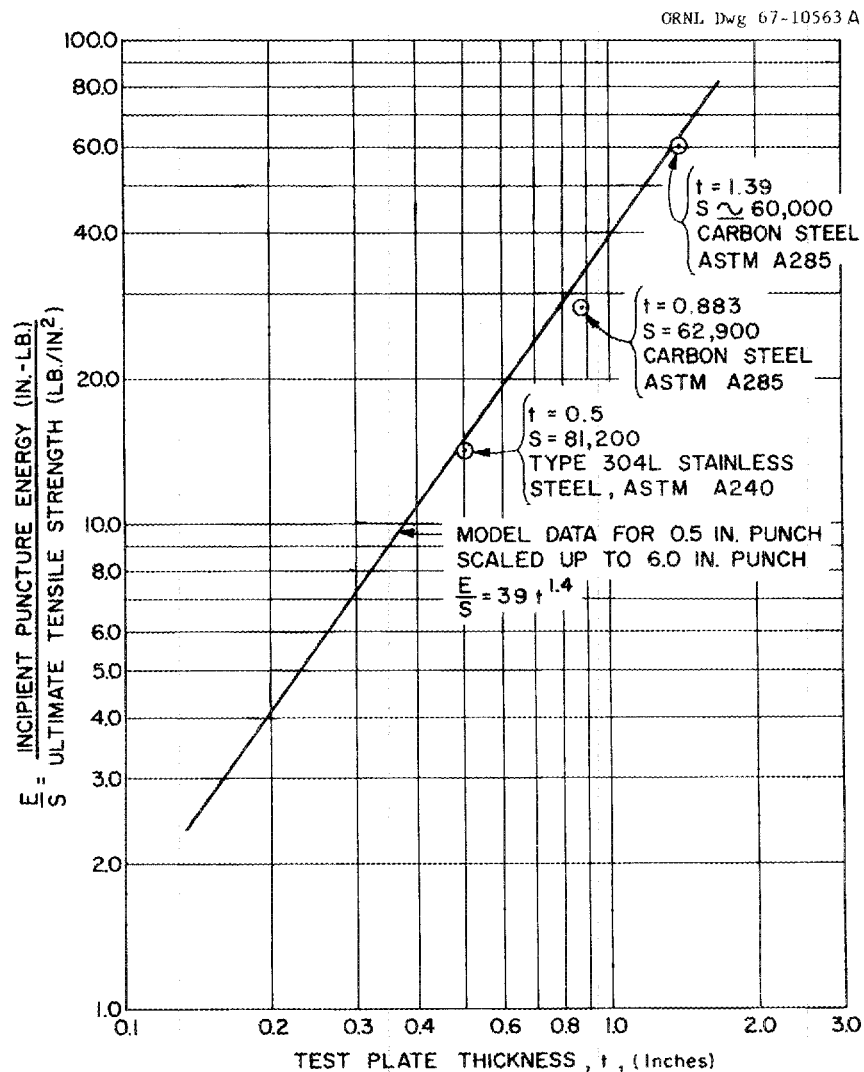


Fig. 2.3. Puncture Test Data.

Cylindrical models from about 4 to 7 in. in diameter with a jacket thickness of 0.075 in. were tested with punches with diameters of 0.4, 0.5, and 0.6 in. In the range of parameters tested, the shells of the cylindrical model were more difficult to puncture than those of prismatic models of similar weight and shell thickness. However, some of the data reported⁵ for impacts of prototype cylindrical casks on 6-in. diam punches suggest that, for casks with diameters less than 30 in., with a punch diameter of 6 in., a cylindrical cask shell will puncture more readily than a prismatic cask shell of the same weight, thickness and material. All tests were made with the line of action of the punch being directed through the center of gravity. This is the basis for the recommending for casks of less than 30 in. diam, the weight should be increased by a factor of 1.3.

2.3 Weld Design

Limited test data has shown that welds are particularly vulnerable regions and subject to fracture in an accident.

Potentially, the greatest loadings to which welds are likely to be subjected would occur as a result of the impact or fire accident conditions. It is, therefore, recommended that a minimum number of joints be made in corner regions and that full penetration welding be used throughout fabrication involving structural components. It is important that no partial penetration welds be used on the cask outer shell since these would provide a built-in crack for rupture initiation under impact or fire conditions.

Data on welds in casks that have been subjected to fire and impact-induced loading are almost non-existent. Until further information becomes available, weld designs given in Table 2.1 are recommended. Other welds may be acceptable, but they should be examined on the basis of ease of fabrication and ability to develop full joint strength. It is permissible to use backup rings or consumable inserts for any of these welds, but backup rings or bars in the lead shielding chamber should be removed prior to lead pouring to prevent porosity in the shield (caused by trapped

Table 2.1. Recommended Weld Joint Configurations.

Joint Appearance	Joint Type	Weld Symbol	Joint Appearance	Joint Type	Weld Symbol
	Square-Groove Joints. Welded Both Sides, Complete Joint Penetration.			Single-Bevel Groove Joints. Complete Joint Penetration, Bead Back Weld.	
	Square-Groove Joints. Welded One Side With Backing, With Complete Joint Penetration.			Single-Bevel Groove Joints. Welded One Side With Backing, Complete Joint Penetration.	
	Double-Vee Groove Joint Welded Both Sides, Complete Joint Penetration. Preferred Joint For Longitudinal Welds On Outer Shell.			Double-Bevel Groove Joints. Welded Both Sides, Complete Joint Penetration.	
	Single-Vee Groove Joints. Complete Joint Penetration, Bead Back Weld			Single-J Groove Joints. Complete Joint Penetration, Bead Back Weld	
	Single-Vee Groove Joints. Welded One Side, With Backing, Complete Joint Penetration.			Double-J Groove Joints. Welded Both Sides, Complete Joint Penetration.	
	Single-Vee Groove Joints. Welded One Side, With Burn Through, Complete Joint Penetration.			Single-U Groove Joints, Complete Joint Penetration, Bead Back Weld	
	a. Gas Tungsten Arc Process Preferred For Root Pass. b. Details Of Joint Developed By Procedure Qualification Are To Be Used In Production.			Double-U Groove Joints, Welded Both Sides, Complete Joint Penetration.	

gases). Welding practices required by Chap. 4 should be adhered to; if economically feasible, the welds should be stress relieved.

If a weld design from Table 2.1 is used in conjunction with the inspections required in Chap. 4, the cask designer may use a joint efficiency of 85% in the design of the inner shell under the recommendations of Sect. 2.1. The joint efficiency can be increased to 100%, provided the designer feels justified based on thorough inspection procedures.

All welds should be made by the processes given in Sect. 4.3.1 and should be of the quality specified by Sects. 4.3.2 and 4.8.5. Welding requirements shown on engineering drawings should conform to AWS A2.0 welding symbols.

The design of a welded joint that is not a part of the cask proper will be left to the discretion of the designer and should be based on good engineering practice.

For most common cask designs at least one weld of the cask shells must be made from one side only. Because of the difficulty in maintaining integrity in an area of high vulnerability and stress concentration, this weld should not be made in a corner but rather at a point in the outer or inner shell as suggested in Fig. 2.4. Caution should be exercised in the design of welds in order to avoid differential expansion difficulties in fabrication or service.

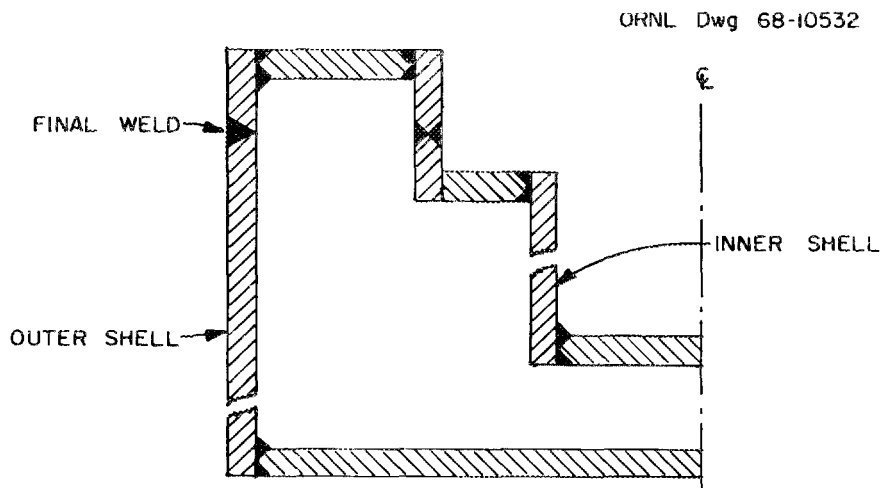


Fig. 2.4. Suggested Positioning of Final Weld.

Consideration should be given to the effects of angular, lateral, and end restraints on the weldment when butt welds are made (as described in Sect. 4.3.5), particularly with respect to material and weld metal having an ultimate strength of 80,000 psi or higher and heavy sections of both low and high-tensile-strength material. The addition of restraints during welding may result in cracks that might not occur otherwise.

Typical recommended corner joint configurations (see Fig. 2.5) are based on composite joints as shown in Table 2.1.

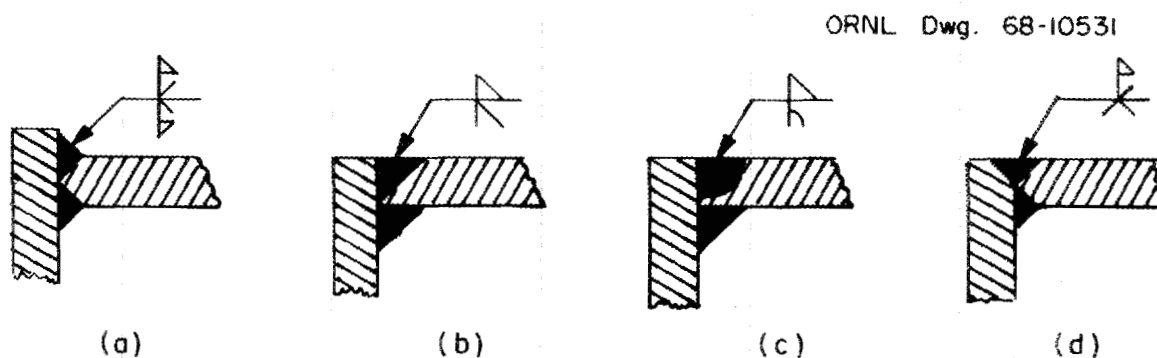


Fig. 2.5. Recommended Corner Joint Configuration Based on Joint Design in Table 2.1.

2.4 Cask Closure, Gasketing, and Bolting Design

The primary functions of the closure are: (1) to provide access to the cavity within the cask and (2) to confine the radioactive material within the cask during normal conditions of transport. Under accident conditions some leakage of radioactivity is allowed; these limits are noted in AECM 0529.

It is realistic that some leakage is permitted; but, unless encapsulated material is being carried, it would be difficult to estimate the

amount of radioactive material that will escape if the seal is breached following an accident. As more knowledge is gained about the mechanism of the escape of radioactive materials under accident conditions, these difficulties may be eased.

The closure design must provide for the load carrying capacity of the gaskets, retaining studs or bolts, flanges, etc. to resist both normal and accident conditions since exposure to the hypothetical 30-ft drop followed by the 0.5-hr fire creates the most difficult closure problems the designer must face. If an analysis indicates that quantities larger than those permitted to escape could exist in the cavity in a mobile form after an accident, containment reliance may have to be placed on some item other than the gasket.

2.4.1 Selection and Design of the Gasket

Large forces and thus distortions that could separate the lid from the body of the cask may occur as a result of the 30-ft impact. Under such conditions the integrity of the seal generally depends upon the design of the flanges and retaining bolts or studs; that is, if the lid and cask flanges are stiff (or if there is no relative movement between the lid and the cask due to impact) and if the gasket is located near the retaining studs, the seal would probably remain intact. These conditions can best be met by providing sacrificial parts such as fins to lessen the shock of impact and to distribute the impact load over a relatively wide area. Such protection is discussed in Sect. 2.8.

Gaskets that are most applicable to use as closure seals fall into several basic groups, as follows:

1. elastomer gaskets,
2. flat asbestos gaskets,
3. jacketed gaskets (e.g., steel over asbestos),
4. corrugated metal gaskets with or without soft filler,
5. spiral-wound gaskets,
6. plain or machined flat metal gaskets,*

7. O-ring-type metallic gaskets, and
8. solid metal gaskets with a round or a special cross section.

The general characteristics of each of these basic groups are discussed in the following paragraphs; design information pertaining to some of the more common types of gaskets is given in Tables 2.2a, 2, 2b, and 2.3.

Normally, elastomer gaskets alone would not be considered satisfactory because their maximum recommended operating temperature is often below that to which the gaskets would be exposed if the cask were involved in a 0.5-hr fire. If other lines of containment have been designed to prevent the escape of radioactivity (e.g., if the fuel is canned prior to shipment), elastomer gaskets are excellent to provide a final, insurance seal. In fact, since elastomer gaskets are desirable under normal conditions of transport, an arrangement of one elastomer and one metallic O-ring gasket may provide the best all-around sealing protection.

To maintain a fluid-tight joint, it is necessary that the parts be tightly bolted together. The initial bolt loading must be great enough to cause local yielding of the gasket when in contact with the inequalities of the metal flange surfaces. The minimum contact pressure necessary to secure a tight joint is called the "yield" value, "y" or "y'," of the gasket; values of y and y' are given in Tables 2.2a and 2.2b.

Any internal fluid pressure above atmospheric in the cask cavity reduces the gasket contact pressure. Experience has shown that the ratio between the contact pressure and the fluid pressure, which is called the gasket factor ("m"), should not be less than a certain value if the joint is to remain tight (see Tables 2.2a and 2.2b).

Design equations using the data from Tables 2.2a and 2.2b are given in Sect. 2.4.2. For design data on special gaskets, such as the Marman or Grayloc types, the manufacturer should be consulted.

Special gasket cross sections shown in Table 2.2b require a fine surface finish in contact with the gasket and close tolerance control, along with careful assembly. The maximum temperature limits that are recommended for solid metal gaskets in continuous service are given in Table 2.3.

Table 2.2a. Design Data for Different Types of Gaskets^a

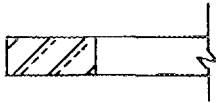
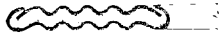
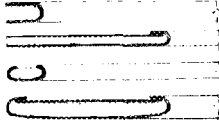
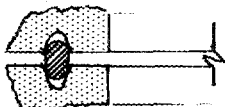
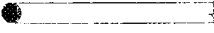
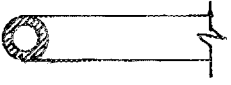
Type	Material	m, Gasket Factor	y, Minimum Design Seating Stress (psi)
 Flat	Rubber (homogeneous)		
	Below 75 Shore durometer	0.50	0
	Above 75 Shore durometer	1.00	200
	Asbestos		
	1/8 in. thick	2.00	1600
1/16 in. thick	2.75	3700	
1.32 in. thick	3.50	6500	
 Spiral Wound Metal Asbestos Filled	Carbon steel	2.50	2900
	Stainless or Monel	3.00	4500
 Corrugated Jacketed, Asbestos Filled	Soft aluminum	2.50	2900
	Soft copper or brass	2.75	3700
	Iron or soft steel	3.00	4500
	Monel	3.25	5500
	Stainless steels	3.50	6500
 Corrugated Metal, Asbestos Cord Cemented in Corru- gations	Soft aluminum	2.75	3700
	Soft copper or brass	3.00	4500
	Iron or soft steel	3.25	5500
	Monel	3.50	6500
	Stainless steels	3.75	7600
 Metal Jacketed, Asbestos Filled	Soft aluminum	3.25	5500
	Soft copper or brass	3.50	6500
	Iron or soft steel	3.75	7600
	Monel	3.50	8000
	Stainless steels	3.75	9000

Table 2.2a (Cont'd.)

Type	Material	m, Gasket Factor	y, Minimum Design Seating Stress (psi)
 Flat Metal, Serrated or Grooved	Soft aluminum	3.25	5500
	Copper	3.50	6500
	Iron or soft steel	3.75	7600
	Monel	3.75	9000
	Stainless steels	4.25	10,100
 Flat Metal	Lead	2.00	1400
	Soft aluminum	4.00	8800
	Soft copper or brass	4.75	13,000
	Iron or soft steel	5.50	18,000
	Monel	6.00	21,800
 Ring Joint	Iron or soft steel	5.50	18,000
	Monel	6.00	21,800
	Stainless steels	6.50	26,000

^aData taken from the "ASME Boiler and Pressure Vessel Code Section VIII, Unfired Pressure Vessels"; from Machine Design, Seals Reference Issue, 36(14), 95 (June 11, 1964); and from M. F. Spotts p. 452 in Design of Machine Elements, 3d ed., Prentice Hall, 1961.

Table 2.2b. Design Data for Different Types of Gaskets^a

Type	Material	y', Minimum Seating Stress (lb/in. of gasket)
 Round Cross Section	Aluminum	1300
	Soft steel (iron)	4500
	Stainless steel	6000
 Wrapped Wire Core	Aluminum jacket - aluminum cores	1500
	Aluminum jacket - stainless steel cores	1500
	Stainless steel jacket - stainless steel cores	6000
 Metal O-Ring	1/16-in.-OD tube x 0.014-in.-thick wall	
	Aluminum	350
	Mild steel	850
	Inconel	1100
	Stainless steel	1300
	1/8-in.-OD tube x 0.012-in.-thick wall	
	Aluminum	100
	Inconel	300
	Stainless steel	320
	1/4-in.-OD tube x 0.012-in.-thick wall	
	Stainless steel	90

^aData taken from the "ASME Boiler and Pressure Vessel Code Section VIII, Unfired Pressure Vessels"; from Machine Design, Seals Reference Issue, 36(14), 95 (June 11, 1964); and from M. F. Spotts p. 452 in Design of Machine Elements, 3d ed., Prentice Hall, 1961.

Table 2.3. Temperature Limits of Metallic Gasket Materials^a

Material	Maximum Temperature (°F)
Lead	212
Common brasses	500
Asbestos	500
Copper	600
Aluminum	800
Stainless steel type 304	800
Stainless steel type 316	800
Soft iron, low-carbon steel	1000
Stainless steel type 502	1150
Stainless steel type 410	1200
Silver	1200
Nickel ^b	1400
Monel ^b	1500
Stainless steel type 309 ^b	1600
Stainless steel type 321 ^b	1600
Stainless steel type 347 ^b	1600
Ceramic fiber ^b	1600
Inconel ^b	2000

^aData taken from Machine Design, Seals Reference Issue, 36(6):19 (June 1964).

^bConsult gasket manufacturer for high-temperature use.

Hollow O-Ring Type Metallic Gaskets. -- Under operating conditions, hollow metallic O-ring gaskets possess certain characteristics that are not found in elastomer O-rings. These metallic O-rings have a natural resiliency somewhat similar to that of elastomer types, but without their temperature limitations, and can be used in both fully confined and semi-confined gasket joints. Such O-rings are dependent upon large compressive forces in the flange faces to create a seal (O-rings require approximately 20 to 30% compression across the small diameter to develop a seal.) The seal is created in a manner similar to that experienced by an ordinary flat gasket.

Stainless steel O-rings are common; 321 stainless steel is the most widely used. However, O-rings fabricated from other metals, such as aluminum and copper, are available.

When designed for low temperature operation, flanges, bolts, and O-rings should be made of the same material. Consideration of the maximum operating temperature in an accident determines the basic O-ring material as follows:

- (1) -40 to 450°F - 321 stainless steel,
- (2) 450 to 800°F - Inconel,
- (3) 800 to 1300°F - Inconel X,
- (4) above 1300°F - consult O-ring manufacturer

Metallic O-rings are often used with a coating of silver or other material to increase sealing effectiveness in seats which have a poor finish and to reduce the probability of seizing or galling when the rings are used in screwed closures. For vacuums and low pressures, an unpressurized hollow stainless steel ring with a silver coating is used. At pressures up to 100 psi, an unpressurized ring with medium wall thickness is used; at pressures above 100 psi, a pressurized ring with a heavy wall is used. Coatings are necessary for rings that seal gases or volatile liquids.

Gases, vacuums, and low-viscosity liquids such as water require a coating or plating, depending upon the maximum design temperature:

- (1) -430 to 1300°F - silver plating,
- (2) above 1300°F - consult O-ring manufacturer,
- (3) in the event that silver is not compatible with fluid - consult O-ring manufacturer.

The thickness of the wall of the tubing used to form these O-rings provides the necessary resistance to the compression that creates the initial seal; the required thickness depends a great deal upon the nature of the material to be confined. Highly viscous liquids are the easiest to seal and can be confined with thin-walled rings. Gases require a coated heavy-wall ring. The heavy wall rings can support heavier flange loads; consequently they provide tighter seals.

Care should be exercised during assembly to assure that the finished surfaces and the O-ring are not marred or scratched.

2.4.2 Design for Bolts or Studs to Retain Cask Lid

Closures should withstand expected decelerating forces resulting from an impact without producing stresses (in the closure fastenings) that exceed the yield strength or 50% of the ultimate strength. Where this recommendation cannot be met, then the bolts or studs should be designed to absorb all the kinetic energy of the cask closure and contents at the impact velocity (generally assumed to be 30 mph resulting from the 30-ft drop). Estimates of the energy absorption capabilities of bolts may be found in ref. 3.

The expected forces experienced by casks protected by crash frames are often amenable to calculation; in other cases the deformation and displacements observed in model testing should provide a basis for estimating deceleration forces.

Four forces must be considered in the development of a design for bolting the cask lid. They are: (1) the force due to internal pressure, F_p , (2) the force due to the apparent weight of the lid and the contents of the cask under impact conditions, F_w , (3) the force required to seat the gasket, F_{sg} , and (4) the force on the gasket required to maintain a tight joint under service conditions, F_{oc} .

The force on a cylindrical cask lid due to the internal pressure in the cask is

$$F_p = \frac{\pi p (d_g)^2}{4}, \quad (2.3)$$

where

p = the differential pressure existing across the gasket, psi,

d_g = the mean diameter of the gasket, in.

If a cask is end-loaded and shipped horizontally, the closure for the lid may be subjected to a force caused by the impact of the cask contents against the lid when the transporting vehicle comes to a sudden stop. The force due to the apparent weight of the cask lid plus the contents of the cask can be calculated from

$$F_w = 2N_g (W_l + W_c), \quad (2.4)$$

where

W_l = the weight of the cask lid, lb,

W_c = the weight of the contents of the cask, lb,

N_g = the mean number of g's to which the lid and contents of the cask are subjected upon impact. A method for accurately obtaining this number is not available at present, but g loadings experimentally measured at points on several cask models are discussed in Sect. 2.8; estimates of N_g may be made by considering the information presented in this section, and the factor 2 is an attempt to account for the effect of dynamic loading.

For a cylindrical lid, the force required to make the gasket material flow into the irregularities of the flange faces and seat is given by

$$F_{sg} = b \pi d_g y, = \pi d_g y', \quad (2.5)$$

where

b = the effective gasket seating width, in. (This value may be obtained from "ASME Boiler and Pressure Vessel Code Section VIII - Unfired Pressure Vessels"),

y = the minimum design seating stress, lb/in.² (see Table 2.2a),

y' = the minimum design specific load, lb/in. (see Table 2.2b).

For cylindrical cask lids, the force required on a flat gasket to maintain a tight joint under service conditions is given by

$$F_{oc} = \pi b d_g m p, \quad (2.6)$$

where

m = the gasket factor (see Table 2.2a).

Proper design requires that F_{oc} be equal to or greater than F_{sg} ; however, care must be exercised to avoid overloading the gasket, particularly in designing large-diameter flanges or even relatively small ones for high-pressure service. Overloading can result in crushing of the gasket or yielding of the flange or both. To avoid this, F_{oc} should not exceed $2 F_{sg}$.

After the gasket has been selected, the minimum bolt area, A_m , is calculated by both Eqs. 2.7 and 2.8; then the largest value is chosen for use in further calculations.

The bolt area is given by

$$A_m = F_{sg} / S_a, \quad (2.7)$$

or

$$A_m = \frac{(F_p + F_w + F_{oc})}{s_a}, \quad (2.8)$$

where

s_a = the bolt yield stress at operating temperatures, psi.

After A_m has been chosen, the actual bolting pattern may be established. A simple procedure for cylindrical lids is as follows:

1. To obtain an approximation of the number of bolts required, allow one bolt for each inch of inside diameter of the lid flange. If the resulting number is not already a multiple

of four, use the next larger number that is a multiple of four.

2. Divide the minimum bolt area, A_m , by the number of bolts determined in step 1; this gives the required area per bolt.
3. Select the bolt size. Because of the danger of overstressing smaller-sized bolts, a 1/2-in. diam bolt is considered the minimum size to be used. The shank diameter should be no greater than the root diameter of the thread.
4. Apply Eq. 2.9 to determine whether the resulting bolt spacing is close enough to maintain adequate unit pressure on the gasket between the bolt holes.⁶

$$\text{Maximum bolt spacing} = [6t/(m + 0.5)] + 2a, \quad (2.9)$$

where

a = the major diameter of the bolts, in.,

t = the thickness of the lid flange, in.,

m = the gasket factor.

5. In an analysis of deformation and fracture of steel bolts, the French considered both plastic deformation and brittle fracture.³ They concluded that, since under high strain rates the outside of bolts undergo considerable plastic deformation while the center fractures, it is better to employ a large number of small bolts rather than a small number of large bolts to maximize their total energy absorption capabilities.

Any changes in the bolting arrangement should be based on practical considerations such as those suggested in step 5, subject only to the requirements for the minimum total bolt area and maximum spacing.

A torque wrench should be used in bolting the cask lid. An approximate relationship between the torque applied to the bolt or nut and the force induced in the bolt or stud for unlubricated conditions is given by:⁷

$$T = 0.2aF, \quad (2.10)$$

where

T = torque, in.-lb,

a = the major diameter of the bolt, in.,

F = the induced force, lb,

The force required to seal the gasket, F_{sg} , was calculated in Eq. 2.5; therefore, the corresponding torque required to seal the gasket is

$$T_{sg} = \frac{0.2aF_{sg}}{N_B}, \quad (2.11)$$

where

N_B = the number of bolts required.

2.4.3 Cask Closure Design

A schematic drawing of a shipping cask, typical of those designed for transporting radioactive materials, is shown in Fig. 2.6. Such designs have been impact tested^{8,9} in the closure region; results indicate relative movement between the cask closure and body occurs frequently, destroying the seal (see Fig. 2.7).

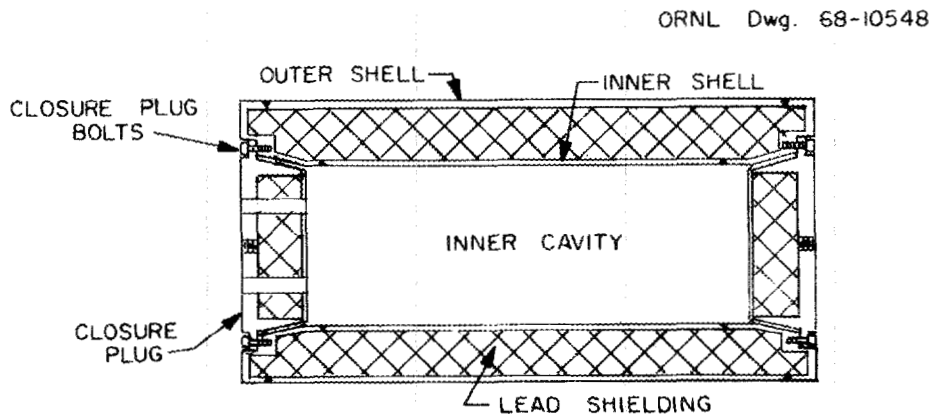


Fig. 2.6. Schematic Drawing of a Typical Radioactive Material Shipping Cask.

ORNL DWG 68-10571

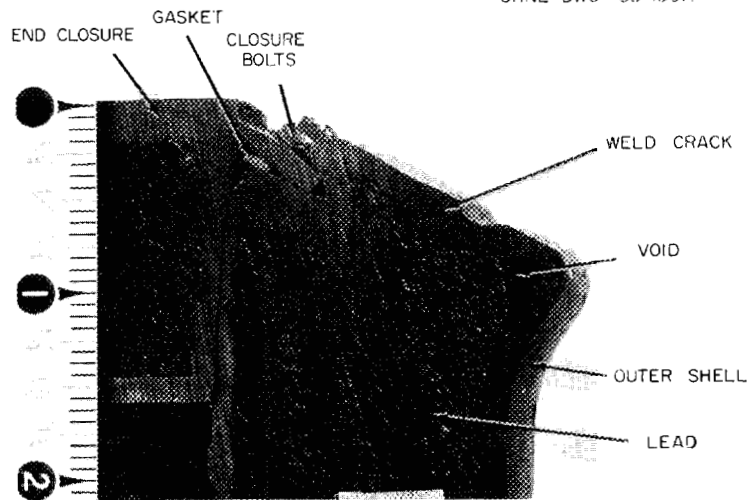


Fig. 2.7. Deformation as a Result of a 30-ft Free Drop Test on a Model Cask Shown in Fig. 2.6. (Courtesy of the University of Tennessee).

A practical solution to the relative movement problem for this and other designs is to buffer the vulnerable impact areas with energy-absorbing parts. For example, a closure, protected by energy-absorbing fins is shown in Fig. 2.8.

ORNL DWG 68-10549-A

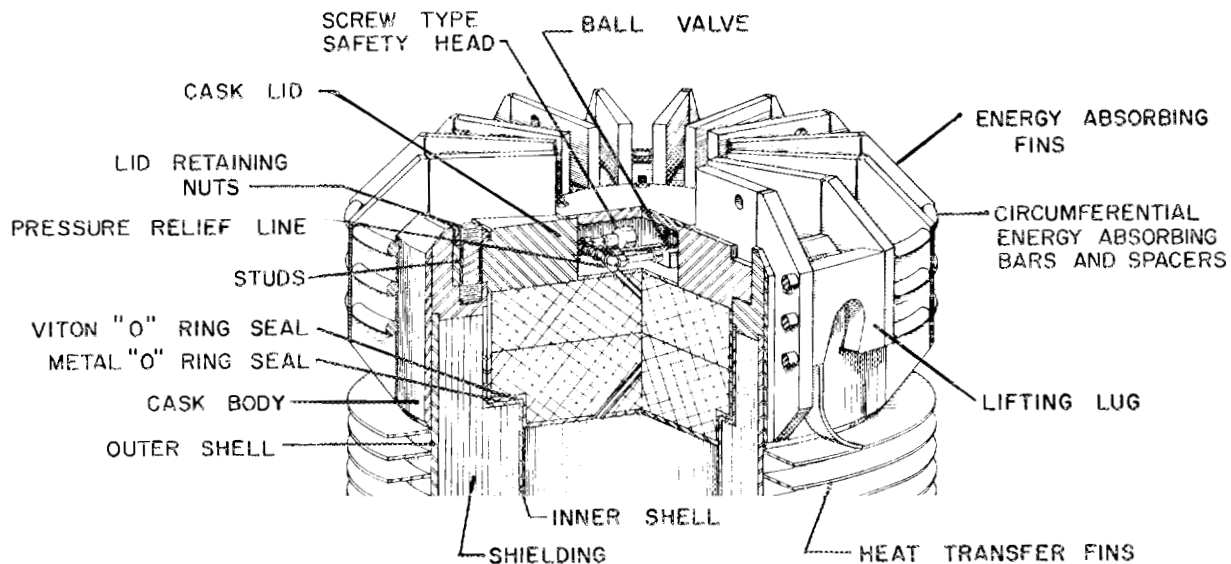


Fig. 2.8. Model Shipping Cask Protected by Energy Absorbing Fins.

A cask,¹⁰ with protective fins similar to those shown in Fig. 2.8 and weighing 372 lb was drop tested on its closure end from a height of 30 ft. The impact damage to the model was restricted to the fins and to one broken bolt in the lid (see Fig. 2.9). The lid was easily removed, and an inspection revealed that less than 0.5 ml of water-soluble oil had leaked across the gasket seal, apparently at the moment of impact since the cavity was still capable of maintaining pressure after impact. Details of the drop and the protection offered by the energy-absorbing fins are discussed in Sect. 2.8.

ORNL PHOTO No. 93140A



Fig. 2.9. Model of Cask with Protective Fins After the 30-ft Closure End Drop Test - Lid Removed.

Figure 2.10 shows a closure design that is less vulnerable to impact.

ORNL DWG. 68-10547RI

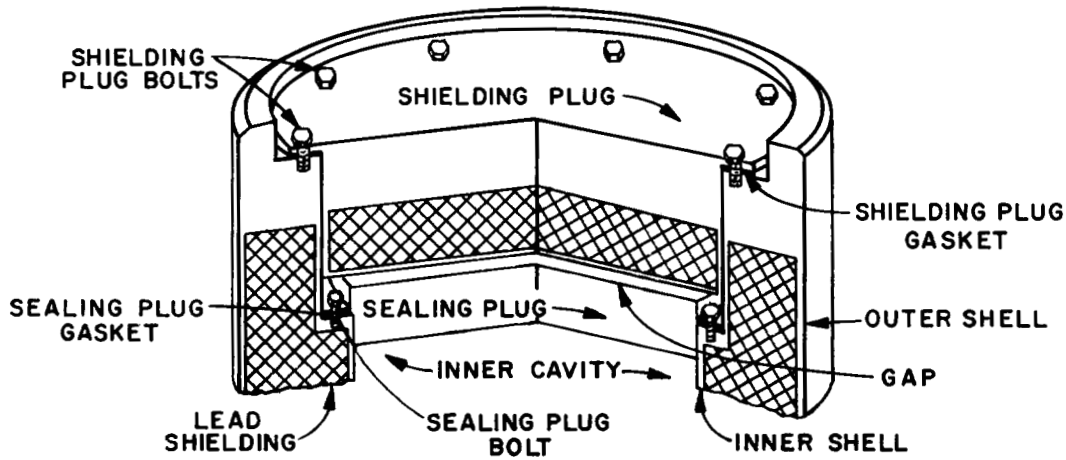


Fig. 2.10. Cask Double Plug Closure.

This design is characterized by the separation of the shielding and sealing functions into two similar plug-type closures. It is expected that this design will survive an impact, provided that the shield plug does not directly contact (and therefore affect) the seal plug in an impact.

A closure design developed by the Knapp Mills Corporation is unique in that the closure bolts are loaded in compression rather than tension (see Fig. 2.11). Of all the closure designs tested, it is likely that this one has the highest probability of retaining the shielding plug in

ORNL DWG 68-10542

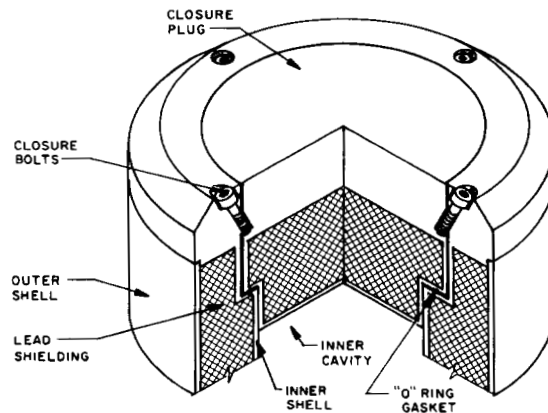


Fig. 2.11. Knapp Mills Type Cask Closure.

position after an impact; however, the problem of maintaining a leakproof seal appears to be no different than for other closures. In addition, removing the plug after the accident may prove difficult.¹⁰

2.5 Lifting Devices

For purposes of this Guide, lifting devices are defined as those items that are attached permanently to a shipping cask whose function it is to transmit the entire load to lifting equipment such as a crane. Such devices are generally designed with the convenience and simplicity that would be required for remote handling (e.g., when a cask is handled underwater or in a shielded cell). Occasionally, lifting devices are used for tiedown. The performance standards required by Paragraph II. A. 3. of the regulations are given below.

1. "A system of lifting devices which is a structural part of the package shall be capable of supporting three times the weight of the loaded package without generating stress in any material of the packaging in excess of its yield strength.
2. "A system of lifting devices which is a structural part only of the lid shall be capable of supporting three times the weight of the lid and any attachments without generating stress in any material of the lid in excess of its yield strength.
3. "For a structural part of the package which could be employed to lift the package and which does not comply with the above requirements, the part shall be securely covered or locked during transport in such a manner as to prevent its use for that purpose.
4. "Each lifting device which is a structural part of the package shall be so designed that failure of the device under excessive lifting load would not impair the containment or shielding properties of the package."

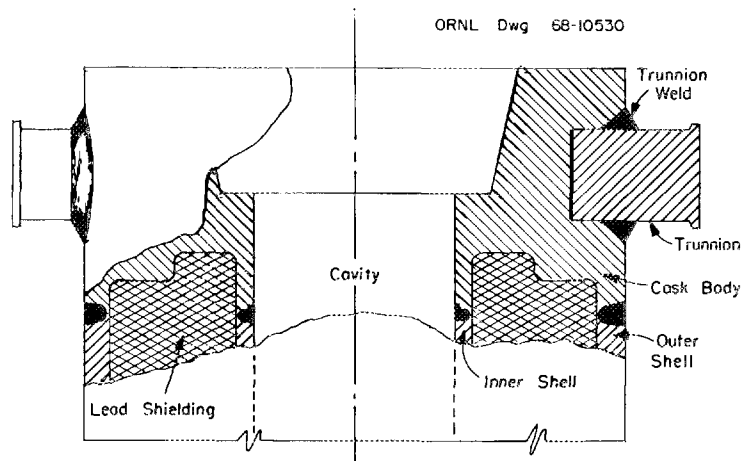
These requirements have been interpreted to mean that the lifting device may not suffer any significant permanent deformation when subjected to a force equal to three times the weight of the cask. This does not eliminate devices that may be subjected to local yielding, over a small area, caused by contact of the lifting device with lifting hooks, etc.

Many types of lifting devices may be designed to meet the regulations by relying on the "strength of materials" approach to solid mechanics. Providing a factor of safety to allow for the approximate nature of this method results in a reasonable balance between engineering effort and conservative design.

This approach may not be justified if the lifting device design is complex or the basic assumptions prove to be invalid. In such cases the designer may rely on a more rigorous method based on elastic behavior. Discussions of such methods may be found in most of the basic "strength of materials" textbooks.

The following paragraphs present a brief description of four general lifting device designs. The detailed analyses of these configurations will be published in ref. 11.

Perhaps the most common design for a lifting device is a pair of short cantilever beams commonly called trunnions (see Fig. 2.12). This



design has the advantage of simplicity of fabrication and, to some extent, simplicity of analysis. Trunnions should be mounted in massive steel blocks as suggested in Fig. 2.12; the base of each trunnion should be inserted to a depth of at least one trunnion diameter into its socket. The weld between trunnion and flange should be designed for minimum concentration of stresses and should be sufficient to develop the full-load capability of the trunnion.

Trunnions welded onto the outer steel shell, as opposed to the massive block shown in Fig. 2.12, may be vulnerable to its punching action in a 30-ft impact. While penetration of the outer shell may not violate regulations, per se, a fire following such an impact might result in the leakage of lead and excessive radiation levels.

Occasionally, a strap that is attached to the shell and the free end of the trunnion is used to minimize any flexing in the trunnion-to-flange-joint weld area. The length of the exposed trunnion should be no more than three trunnion diameters and should be designed only after consideration of the effects of both shear and bending stresses. For lifting systems of this type, a reasonable safety factor is 4.

A second type of common lifting device consists of "ears" with holes through which hooks may be placed for lifting. Often the ears are placed vertically so that the weld is loaded entirely in shear (see Fig. 2.13). This device has been used on lightweight casks and is not recommended for designs weighing over 10,000 lb.

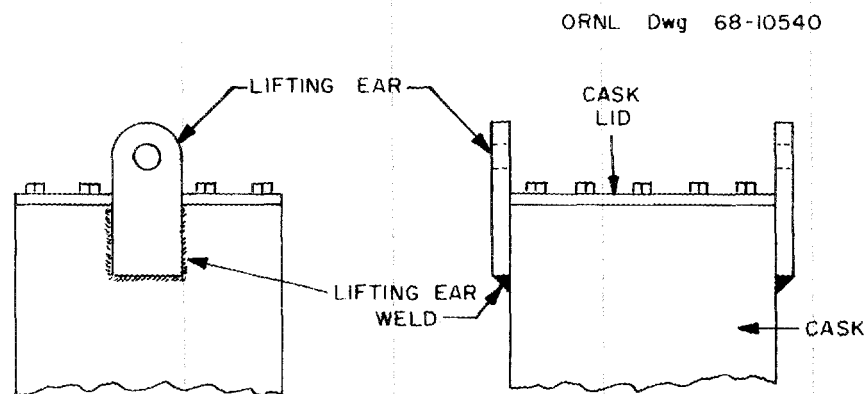


Fig. 2.13. Typical Cask Lifting Ears.

The design features simplicity of fabrication and analysis and a minimum risk of puncture of the shell in the hypothetical accident. However, if the ears are particularly stiff, impact on the closure end could result in high-tensile loadings of the closure bolts.

For the designs shown in Fig. 2.13, the thickness of the ear should be equal to, or greater than, the thickness of the outer shell. The diameter of the hole in the ear should be no more than one-half the width of the ear, and the amount of material above the hole should be equivalent to at least the diameter of the hole.

The length of the ear welded to the cask shell should be at least equal to that portion of the ear (containing the hole) that is not welded to the cask shell. The load carrying capacity of the weld between shell and ear should be at least three times the loaded cask weight and care must be taken not to overstress the metal surrounding the hole under load conditions. For this design, a reasonable factor of safety is 3.

A design that incorporates many of the features of the previous two designs is the mechanical inversion of the trunnion, hereafter called a socket-and-sling lifting device (see Fig. 2.14).

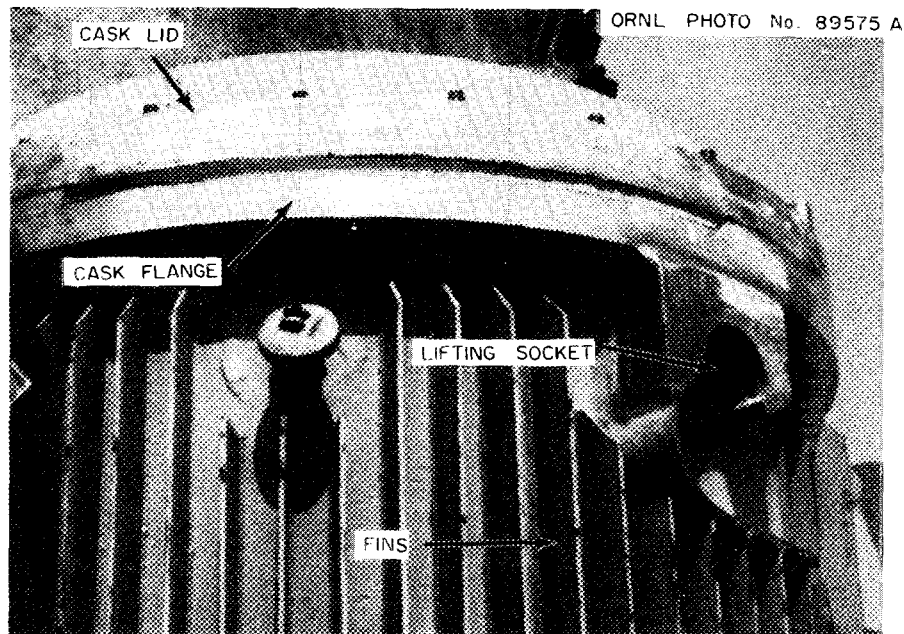


Fig. 2.14. Typical Cask Inverted Trunnion.

The socket-and-sling lifting device minimizes the potential effects of a 30-ft impact with respect to the puncture problem. Although its lifting capabilities are somewhat difficult to analyze and an elaborate sling is required, its advantage of minimizing impact effects makes the design desirable.

Welds are the key to a proper design in that the socket is usually a massive machined piece whose thickness is about one diameter of the pin used in the sling. As a result, the socket is usually stronger than the welds. Although the socket may be located beneath a flange as shown in Fig. 2.14, the socket welds should be capable of carrying the design load. Analysis is somewhat complicated since an eccentric loading caused by the lifting sling produces a torsional load in the weld pattern. A safety factor of 3 is reasonable for this design.

The fourth design is a lifting device which may be thought of as a continuous ring made up of lifting ears welded around the top of the cask (see Fig. 2.15). Although this design is somewhat similar to that of single lifting ears, the analysis is more difficult.¹¹ Because of the more-detailed analysis required, a safety factor of 2 is considered sufficient.

ORNL DWG. 67-12874

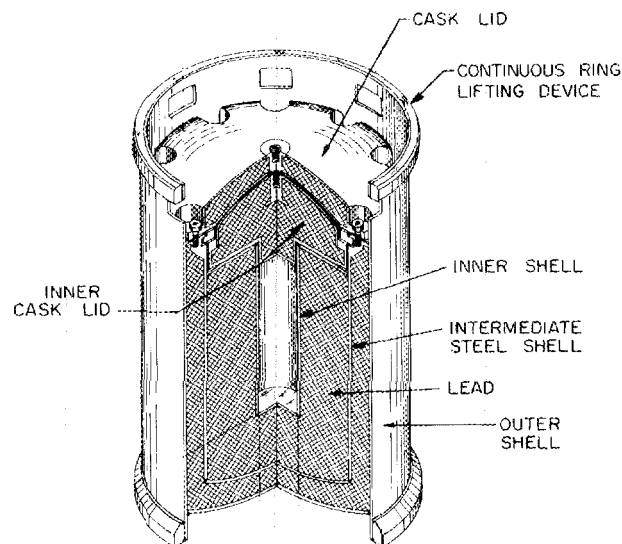


Fig. 2.15. Cask Using Continuous Ring Lifting Device.

2.6 Tie-Downs

2.6.1 General Considerations

The tie-down is a device defined in the regulations as that portion of the system which is rigidly attached to the cask. The tie-down system, including the tie-down device, is used to maintain a controlled geometric relationship between a cask and the transporting vehicle. Such systems are usually designed to facilitate rapid loading and unloading of cargo. This guide considers the analysis of the complete tie-down system.

The performance requirements for tie-down devices are as follows:

1. "If there is a system of tie-down devices which is a structural part of the cask, it shall be capable of withstanding, without generating stress in any material of the cask in excess of its yield strength, a static force applied at the center of gravity of the package having a vertical component of two times the weight of the cask, with its contents, a horizontal component along the direction in which the vehicle travels of ten times the weight of the cask with its contents, and a horizontal component in the transverse direction of five times the weight of the cask with its contents.
2. "Also if there is a structural part of the cask which could be employed to tie the package down and which does not comply with the above paragraph, that part shall be securely covered or locked during transport in such a manner as to prevent its use for that purpose.
3. "Each tie-down device which is a structural part of the package shall be so designed that failure of the device under excessive load would not impair the ability of the device to meet other requirements of the regulations."

Since the prevention of localized yielding in small areas due to contact stresses is virtually impossible under normal usage, these requirements are interpreted to mean that the tie-down must be able to withstand the prescribed loading without suffering any significant permanent deformation.

In this Guide, it is considered good engineering practice to apply these performance requirements, as far as is possible, to the tie-down system rather than just the tie-down device. The designer often has control over the entire tie-down system up to the point where the system is attached to the vehicle. At that point he has to depend upon other personnel to attach the system in positions of adequate strength on the vehicle. This problem can be significant since it is important to maintain control of the load - vehicle system to avoid possible loss of cargo or vehicle instability.

The most commonly used tie-down is one in which the cask is rigidly fastened to the vehicle during normal operating conditions and which is expected to remain with the vehicle under accident conditions. Such tie-downs have proved adequate for most shipments in the past.

Hanford's policy of using tie-downs for their buffered cask on railcars has been somewhat different. Since the buffer that is attached to the cask is designed to reduce the deceleration to which the cask will be subject, the tie-downs are designed to break with a severe shock (about 12 g), allowing cask and buffer to roll free; this would reduce the chance of its being crushed by the colliding railcars. The buffered cask tie-downs are shown in Fig. 2.16; the cask itself is discussed in Sect. 2.8.

In general, casks that have been designed for shipment on a special vehicle can have their tie-down systems designed to provide the necessary strength and energy absorption capability. This is more difficult to provide in the case of smaller casks that are transported by a variety of common carriers.

The United States of America Standards Institute (USASI) subcommittee N 14.2 expects to publish, in the near future, a compendium of tie-down methods that are in use today. In addition, the Oak Ridge National Laboratory is considering various methods for the analysis of common tie-down designs under the prescribed static loading.

A computer program to perform tie-down analysis under static loading conditions has been developed by the Sandia Corporation and may be found in ref. 12. This program considers the sliding mode of displacement only.

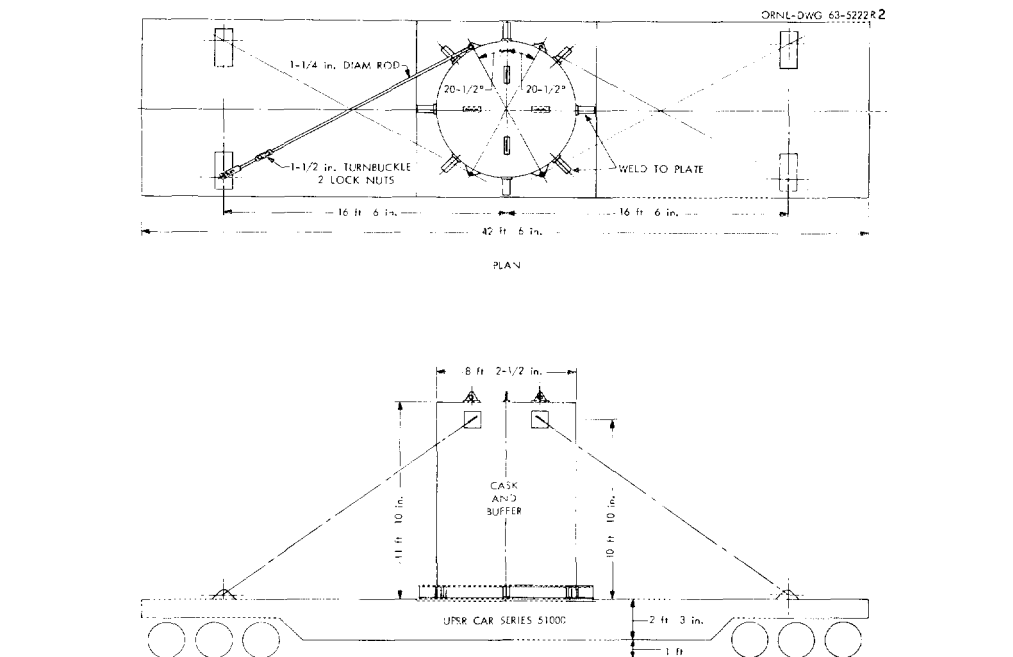


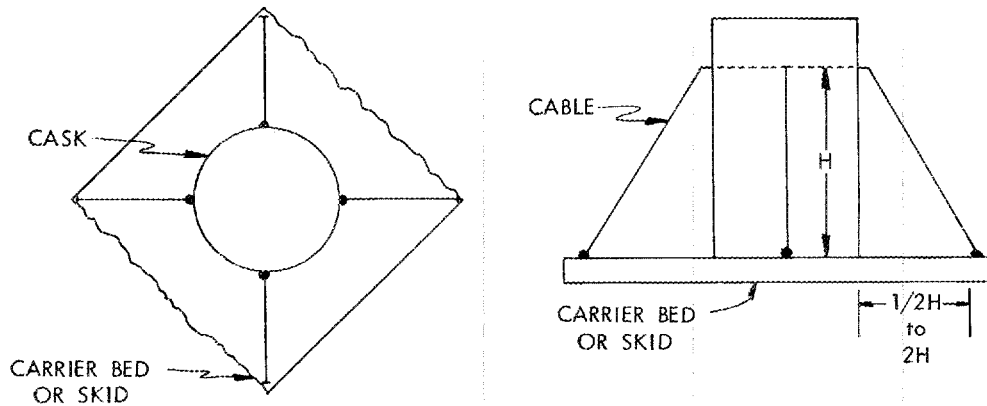
Fig. 2.16. Tiedown of Hanford's Buffered Cask to Railroad Car.

Workers at the Franklin Institute have developed a method of tie-down analysis that is based on idealized dynamic conditions. The method is primarily useful for comparing materials used in tie-down systems.¹³

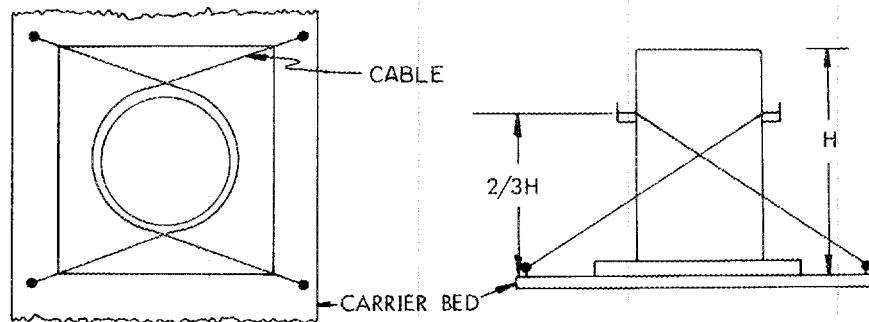
2.6.2 Tie-Down Methods

Spent fuel carriers weighing less than 10,000 lb may be readily transported by truck or rail. If the cask weighs greater than 500 lb, some means must be provided to limit the floor loading to less than 500 lb/ft². A skid or load spreader under the cask will serve this purpose. Acceptable tie-downs for casks in this category are shown in Figs. 2.17 and 2.18. The bottoms of these casks are often held in place by wooden chocks that are nailed to the floor of the vehicle. Routine inspection should ensure that these chocks are adequate and provide reasonable support during transit. Members of the tie-down system are usually cables or chains; however, in certain cases, solid steel struts have been used to obtain a fully rigid system (see Fig. 2.19). Cables are preferred over chains because of their elastic behavior beyond "yield point" loading (a desirable characteristic not available in chains). Recommended cables consist of 5/8-in. (minimum) ploughed steel wire rope fastened to itself with no less than three Crosby clamps at either end (see Fig. 2.18).

ORNL-DWG 64-9131R2



A. Four-Way Tie-Down for Heavy Containers.



B. A Basket Hitch Tie-Down for Light Containers.

Fig. 2.17. Two Typical Tiedown Systems.

Casks weighing more than 10,000 lb but less than 50,000 lb may be shipped by either tractor-trailer or rail. In each case, a skid is usually designed for controlling the floor loading and for tying down the cask. The usual practice is to tie the cask to the skid and then to tie the skid to the vehicle (see Fig. 2.19). Loads of this size occasionally require modification to trailer or rail car beds to provide adequate means of making rigid connections between the skid and the bed. Brackets are often welded to the vehicle to ensure alignment of the holes in the flanges of the skid with those in the vehicle.

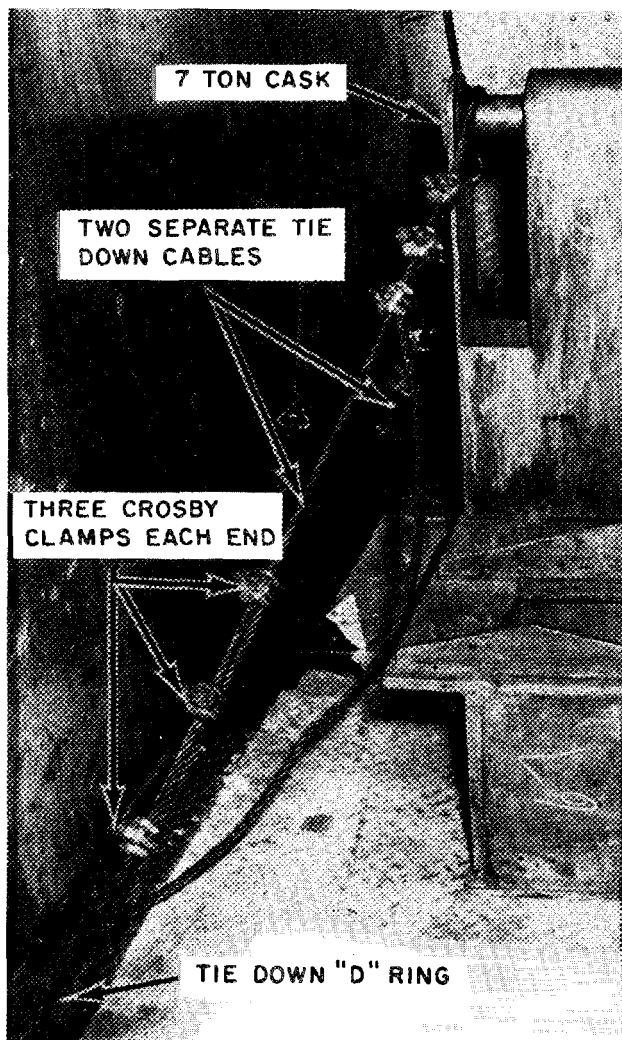


Fig. 2.18. A Four-Way Tiedown on a 7-Ton Cask.

Shipment by rail or barge appears to be the best methods for casks weighing greater than 50,000 lb; however, rail transport is much more prevalent.

Tie-downs for such heavy shipments are often designed specifically for the cask and vehicle. Saddles, with steel holddown straps bolted to the saddles (see Fig. 2.20), may surmount the skid. The number of bolts required to withstand the 2, 5, and 10 g tie-down loadings may be calculated, based on a static loading as discussed in Sect. 2.6.3.

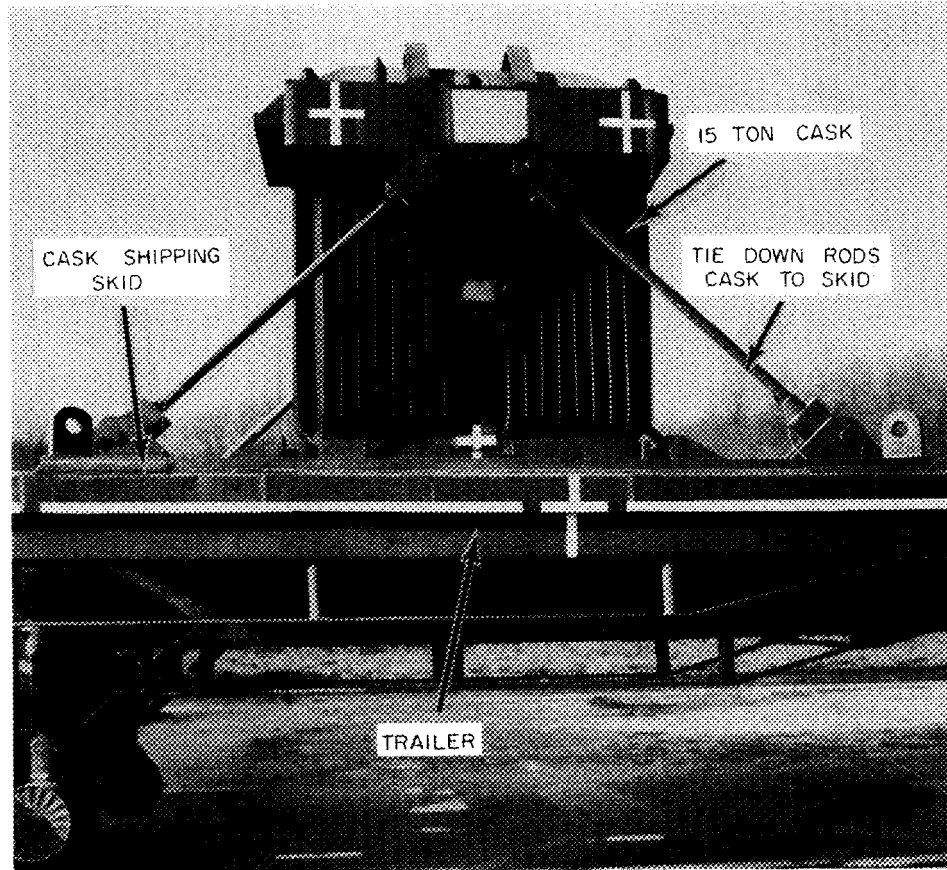


Fig. 2.19. Tiedown of a 15-Ton Cask and Skid to Trailer. (Courtesy of Aberdeen Proving Grounds).

ORNL Dwg. 68-10533

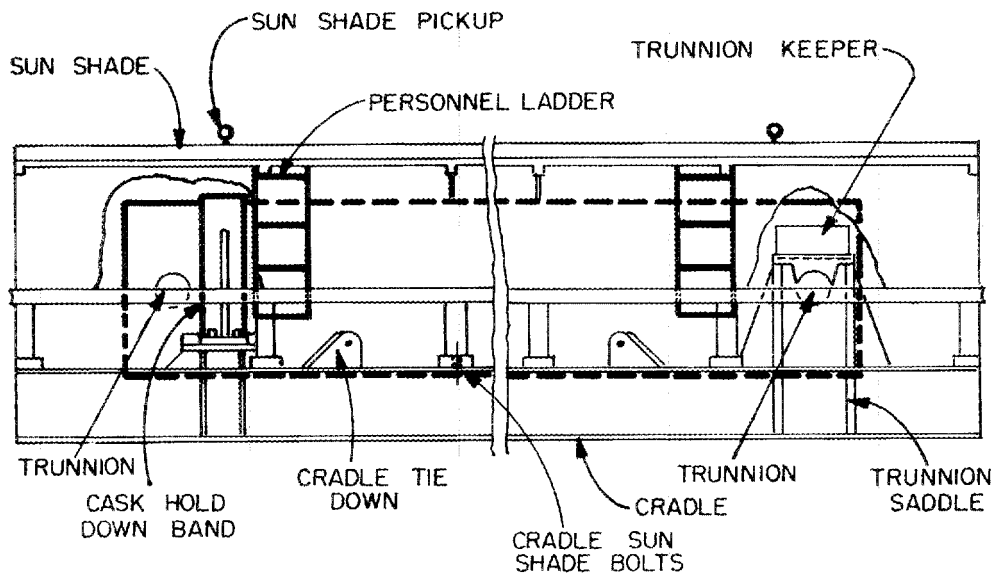


Fig. 2.20. HNPF 6-Element Fuel Shipping Cask Tiedowns.

2.6.3 Methods of Analysis

Tie-down systems may be analyzed by using approximate methods of solid mechanics. These methods will not yield exact results, if compared with strain gauge measurements; nevertheless, tie-down systems designed by using these methods have proved to be adequate.

Dynamic loadings such as might occur in an accident, are not easy to analyze. The behavior of a system of elastic-plastic elements under dynamic loading condition has been under study for a number of years by various workers. Recent work is based on dividing the structure into a number of finite elements and then using the proper descriptive differential equations, converted to finite difference equations, to carry out a solution using numerical integration. Discussion of this technique may be found elsewhere.¹⁴ A direct application of this method is found in reference 15.

2.7 Effects of a 30-ft Impact on Lead Shielding

Lead shielding can be lost in an impact in two ways: (1) An outer surface of the cask can be flattened to the extent that lead is shifted to other areas; thus less shielding would remain in the area of the impact. (2) If an end impact occurs, lead movement may occur at the opposite end of the cask, creating a void space. This section presents analytical procedures and test results that will allow the cask designer to estimate the loss of shielding which occurs in either of these two ways.

2.7.1 Material Properties Under Impact Conditions

The kinetic energy of a cask during an impact must be dissipated either in the cask or its environment. Since regulations stipulate that the impact surface must be unyielding, essentially all the energy must be absorbed by elastic and inelastic deformation of material that may or may not be a part of the cask. The properties of the material under dynamic conditions must, therefore, be known in order to evaluate the effect of impact on the cask.

For steel, tests indicate that at strain rates expected in a 30-ft impact the dynamic yield point is only slightly greater than the static yield point.¹⁶ It is, therefore, recommended that the static yield point stress be used to determine inelastic deformations in steel components of the cask.

The behavior of lead under impact conditions has been studied by a number of workers; however, since the dynamic properties of lead are affected by strain rate, impurities in the lead and other variables, results do not often agree. The mechanical properties determined under static conditions are given in Table 2.4.¹⁷

Table 2.4. Mechanical Properties of Cast Lead

Modulus of Elasticity	2×10^6
Poisson's ratio	0.40 to 0.45
Tensile strength	2300-2800 psi
% ultimate elongation	Approx. 33%
Brinell hardness No.	4.0-6.0

Strain rate affects the relationship between stress and strain. In principle, once the relationship between these properties is known, the damage suffered in any given impact may be predicted by using methods of continuum mechanics. In practice, closed-form solutions to the impact problem are few; and results, using realistic physical models and measured dynamic properties, have been less than satisfactory.

Accepting the limitations of less rigorous methods, dynamic behavior can be related to a pseudo material property called the "dynamic flow pressure." This pressure is defined as the energy that is necessary to displace a unit volume of lead; dimensions are in.-lb/in.³ or psi. The dynamic flow pressure relates the absorbed energy directly to the final displacement without resorting to laborious numerical methods. Results

of the few problems analyzed using the dynamic flow pressure concept have been acceptable when applied to composite structures and excellent when applied to homogeneous bodies. Two examples of this form of analysis applied to composite structures appear as Sects. 2.7.2 and 2.7.3.

The dynamic flow pressure of common plumbers lead, as measured by J. H. Vincent,¹⁸ was found to be between 3700 and 18,850 psi; the magnitude of this range was attributed to variations in the crystal size or orientation and possibly to material impurities. J. P. Andrews^{19,20} found that, in testing lead spheres, the relationship between impact energy and displaced volume of the sphere was a straight line in the range of velocities investigated. In a study of impact of spheres on rigid plates, Clarke²¹ presents a nondimensional strain factor as a function of impact velocity; this factor may be readily converted to a dynamic flow pressure of 8500 psi by using his definition of average radial strain. However, assuming a Brinell hardness No. of 4.0, the dynamic flow pressure (based on very low strain rates) has been calculated to be 5900 psi.

These data indicate that lead tends to resist deformation under dynamic conditions more than under equivalent static conditions and that the energy required to displace 1 in.³ of lead appears to be two to three times the static compressive yield strength as stated in ref. 22. This conclusion is in agreement with information presented in refs. 8 and 23 where penetration tests using cylindrical punches are reported; results indicate a value of 10,300 psi for the dynamic flow pressure.

From the above data it is clear that the dynamic flow pressure of lead depends upon test specimen configuration, strain rate, and method of correlation. However, for engineering purposes, a value of 5000 psi appears to be both reasonable and conservative and is recommended for calculational purposes unless the designers can justify a higher value.

2.7.2 Analysis of a Horizontal Axis Drop of a Cylindrical Cask Without Fins

When dropped in such a manner that their longitudinal axes are horizontal, cylindrical casks with flat end plates and no external energy

absorbers will absorb energy upon impact mainly in three ways: (1) by deformation of the end plates, (2) movement of lead, and (3) stretching of the cylindrical outer shell. A relatively small amount of energy is absorbed in bending the steel shell at the point of impact and is, therefore, neglected in this analysis.

Assuming the cask to be a long cylinder without an internal cavity, the energy absorbed in deformation of the steel ends and of the lead may be calculated from Eqs. (2.11a) and (2.11b), respectively.

$$E_e = R^2 t_e \sigma \left(\theta - \frac{1}{2} \sin 2\theta \right) \quad (2.11a)$$

$$E_{Pb} = R^2 L \sigma_{Pb} \left(\theta - \frac{1}{2} \sin 2\theta \right), \quad (2.11b)$$

where

E = energy absorbed in the lead or steel ends, in.-lb,

R = the outer radius, in.,

L = the cylinder length in.,

t_e = thickness of the steel end plate, in.,

σ_s = the dynamic flow stress in steel, lb/in.²

σ_{Pb} = the dynamic flow stress in lead, lb/in.²

θ = the angle defined in Fig. 2.21, deg.

ORNL Dwg 68-10537

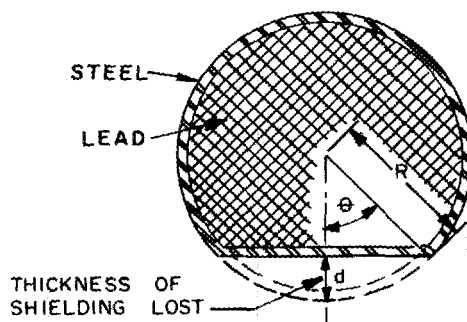


Fig. 2.21. End View of the Deformation in a Steel Encased Solid Lead Cylinder.

Assuming uniform strain, the energy absorbed by the stretching of the outer shell of the cask (due to movement of lead), E_{OS} , may be estimated from

$$E_{OS} = Rt_S L \sigma_S [\sin \theta (2 - \cos \theta) - \theta], \quad (2.12)$$

where

R = the outer shell radius, in.,

t_S = the outer shell thickness, in.,

L = the length of the shell, in.,

σ_S = the dynamic flow stress of the shell, psi

Combining and rearranging Eqs. (2.11a), (2.11b), and (2.12) leads to Eq. (2.13):

$$\frac{WH}{t_S R L \sigma_S} = [F_1(\theta)] \left[\frac{R}{t_S} (\sigma_{Pb}/\sigma_S) + 2(R/L)(t_e/t_S) \right] + F_2(\theta), \quad (2.13)$$

where

W = cask weight, lb,

H = drop height, in.,

$$F_1(\theta) = \theta - \frac{1}{2} \sin 2\theta = \theta - \sin \theta \cos \theta,$$

$$F_2(\theta) = \sin \theta (2 - \cos \theta) - \theta.$$

Equation (2.13) is based on the assumptions that the yield point stress of the steel end piece is the same as that of the shell and that the end pieces are of equal thickness.

In order to use Eqs. (2.11a), (2.11b), and (2.12), the half angle θ and the cask geometry must be known. The angle θ may be determined from Fig. 2.22, which is based on Eq. (2.13). The maximum loss of shielding represented by the outer shell flattening, d , may be calculated by $d = R(1 - \cos \theta)$.

ORNL Dwg 68-10536

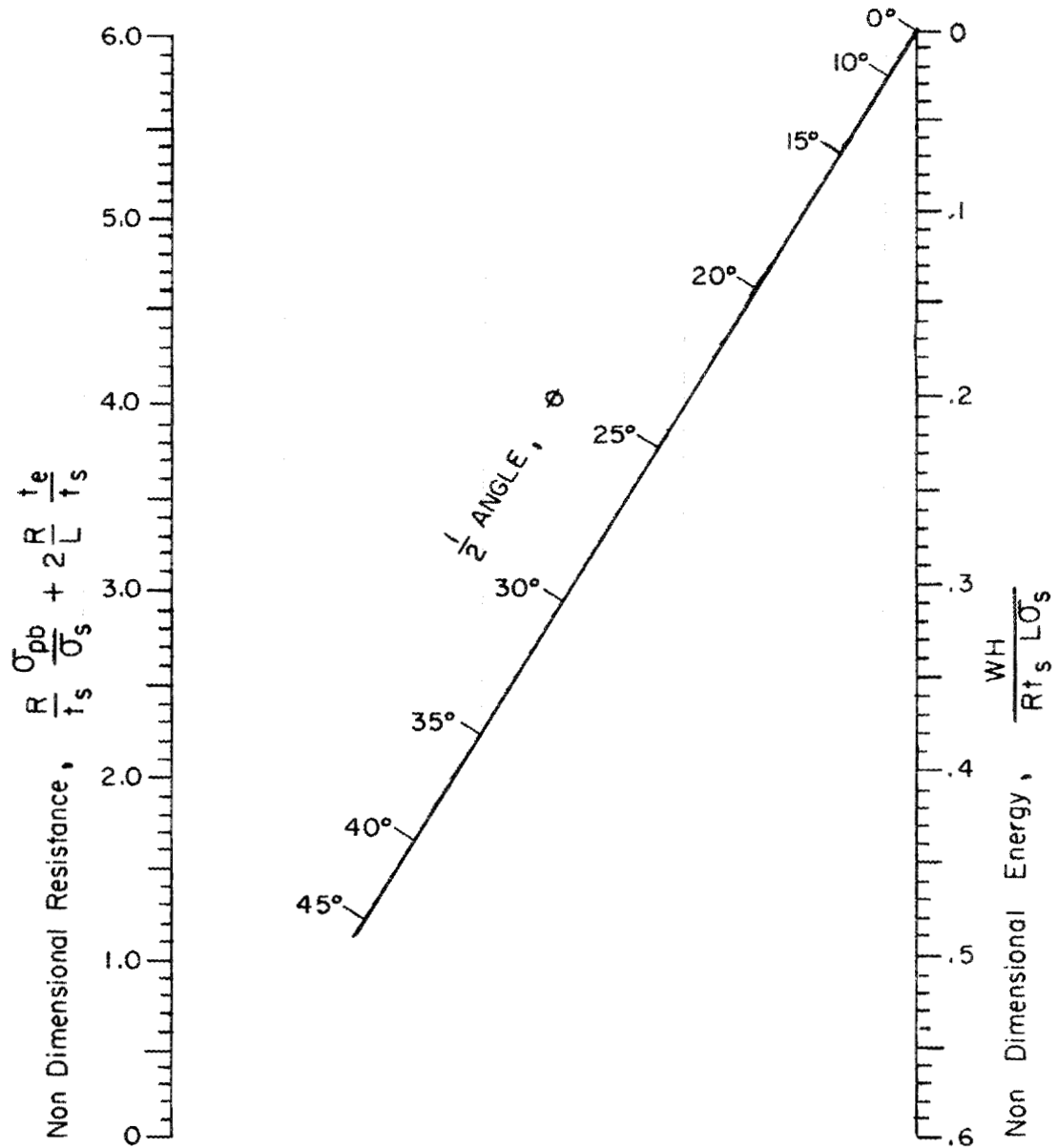


Fig. 2.22. Nomograph for Determining $1/2$ Angle of Flat Developed Due to Impact of a Cylindrical Cask with Axis Horizontal.

Example. - A 1.3-ton cask, shown schematically in Fig. 2.23, was dropped 15 and 29 ft in a horizontal attitude. Results of the deformation produced after the first drop only are reported in ref. 5. Using Eq. (2.13), the expected deformation is predicted and compared with the actual results.

ORNL DWG. 63-3592-A

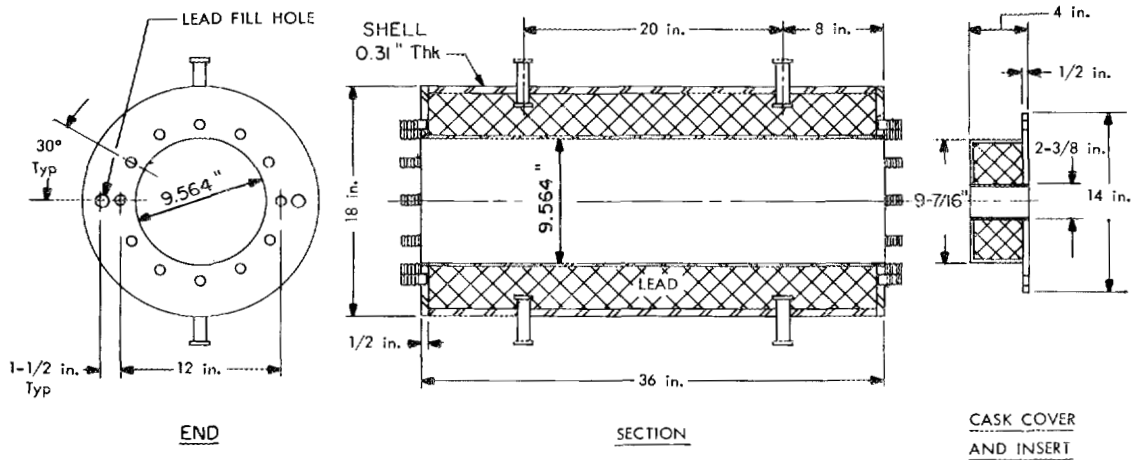


Fig. 2.23. 1.3-Ton Test Cask.

The geometry and properties of the materials of the cask are given below:

$$W = 2600 \text{ lb,}$$

$$H = 180 \text{ in.,}$$

$$t_S = 0.31 \text{ in.,}$$

$$R = 9.0 \text{ in.,}$$

$$L = 36.0 \text{ in.,}$$

$$\sigma_S = 50,000 \text{ psi,}$$

$$t_e = 0.5 \text{ in.,}$$

$$\sigma_{pb} = 5000 \text{ psi.}$$

Computing the parameters given in Fig. 2.13,

$$\frac{R\sigma_{Pb}}{t_S\sigma_S} + \frac{2Rt_e}{Lt_S} = 3.70 \text{ and } \frac{WH}{t_S RL\sigma_S} = 0.09319.$$

From Fig. 2.22 the angle θ is predicted to be 18° , and the maximum reduction in shielding, d , is (9 in.) $[1 - \cos(18^\circ)] = 0.405$ in.

The test data in ref. 5 indicate that the average width of the developed flat is 3.53 in., for which the average half angle is $11^\circ 19'$. The maximum width was determined to be 5.25 in., for which the half angle is $16^\circ 57'$ (e.e., very near the predicted angle of 18°).

The approximate distribution of absorbed energies for this drop, based on Eqs. (2.11a), (2.11b), (2.12), and (2.13), is:

<u>Cask Part</u>	<u>Energy Absorbed (%)</u>
Lead	76
Shell	13
End plates	11

These values are in good agreement with those of the detailed analysis based on brittle coating and strain gage measurements presented in ref. 5.

2.7.3 Analyses of an End Drop of a Cylindrical Cask with Nonbuffered Ends

An end drop of a cask in which the lead is not bonded to the steel shell will cause the lead to settle, thus creating a void in the end opposite the point of impact. An analysis of such an impact, based on the energy absorbed by the lead (as a result of its deformation) and by the outer steel shell (as a result of its circumferential strain from internal lead pressure) has been made.²³

The change in the lead volume in an impact may be estimated from Eq. (2.14):

$$\Delta V = \frac{RWH}{t_S\sigma_S + R\sigma_{Pb}} \quad (2.14)$$

For negligible changes in the outer radius of lead, R , and the inner radius of lead, r , the change in the height of the lead column, ΔH , is

$$\Delta H = \frac{\Delta V}{\pi(R^2 - r^2)}. \quad (2.15)$$

Combining Eqs. (2.14) and (2.15) yields

$$\Delta H = \frac{RWH}{\pi(R^2 - r^2)(t_S \sigma_S + R\sigma_{Pb})}. \quad (2.16)$$

As noted before, Eq. (2.16) is based on an unbonded lead condition since neither the support provided by the steel shells nor the possibility of collapse of the inner shell by buckling is taken into account.

Example. - A model shipping cask (Fig. 2.24) was designed and built to investigate the movement of lead in an end impact. Care was taken to prevent the lead from becoming bonded to the steel shells. The cask (Fig. 2.24) was dropped 30 ft onto its bottom end. Pertinent data of the cask are as follows:

$$W = 163 \text{ lb,}$$

$$H = 30 \text{ ft or } 360 \text{ in.,}$$

$$R = 2,248 \text{ in.,}$$

$$r = 1,3125 \text{ in.,}$$

$$t_S = 0.20 \text{ in.,}$$

$$\sigma_S = 45,000 \text{ psi (seamless cold-drawn tubing),}$$

$$\sigma_{Pb} = 5000 \text{ psi.}$$

The change in the height of the lead column inside the weldment can be estimated from Eq. (2.16) as follows:

$$\begin{aligned} \Delta H &= \frac{(2.25)(163)(360)}{\pi[(2.25)^2 - (1.31)^2] [(0.20)(45,000) + (2.25)(5000)]} \\ &= 0.62 \text{ in.} \end{aligned}$$

Experimental data indicated that the height of lead actually changed 0.7 in., which is in reasonable agreement with the height predicted above.

ORNL Dwg. 67-12865

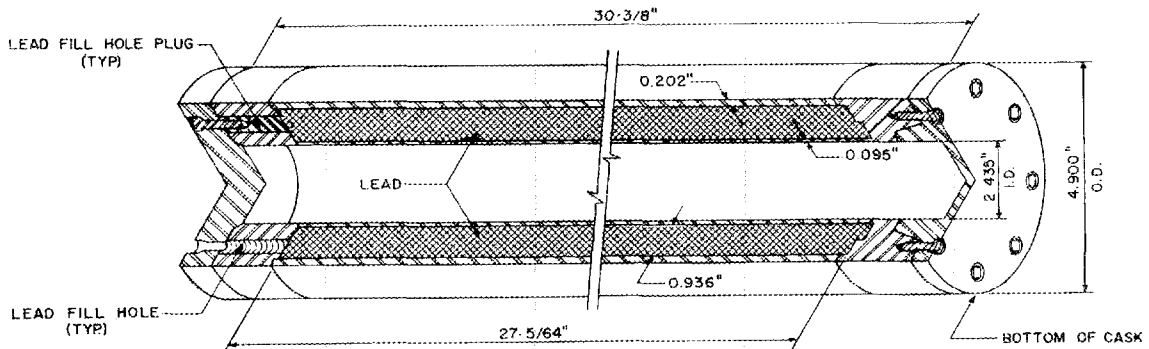


Fig. 2.24. ORNL Constructed 1:75 Model of Hallam 6-Element Shipping Gask (HNPF).

2.8 Shock Absorbing Structures

Often it is desirable to protect a cask from direct impact by surrounding it with a shock-absorbing structure. In an accident the structure will deform and absorb energy that might otherwise cause damage in the cask itself. It is particularly important to protect cask closures from deformation (see Sect. 2.4.3).

2.8.1 Fins

Several types of protective structures have been designed and built. Probably the simplest and least expensive of these are fins that are welded directly onto the cask. Fins are often necessary for heat removal, but their usefulness as shock absorbers should not be overlooked.

Analytical techniques for predicting the amount of energy that can be absorbed during the deformation of fins of various configurations have not been fully developed; however, if the fins are pre-bent in such a manner that their movement in an accident can be predicted with confidence, the energy that they absorb can be estimated by treating each fin as a plastic hinge.

As a part of a larger study program, a model uranium-shielded cask weighing 382 lb was built with $1/4$ -in.-thick fins extending approximately 1 in. above the closure. This cask was dropped 30 ft onto an edge.¹⁰ The protection afforded by fins is illustrated in Fig. 2.25.

ORNL PHOTO No. 93139 A

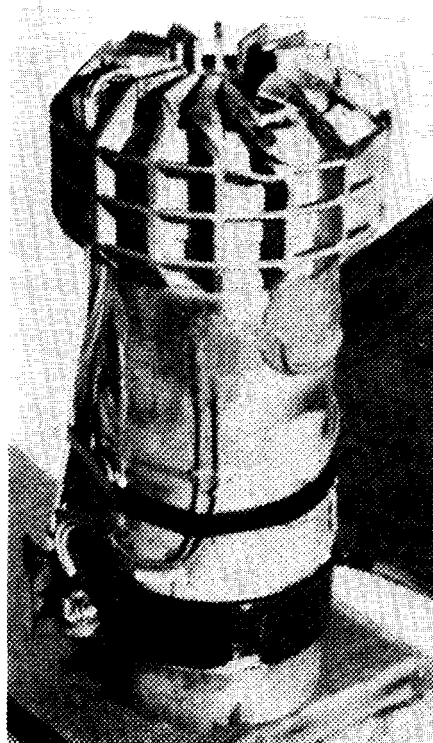


Fig. 2.25. Model Uranium Shielded Cask After 30-ft Drop.

Two accelerometers were placed - one on the top and one on the bottom of the cavity - at an angle normal to the impact surface. Both registered approximately 1100 g's; the peak lasted for approximately 0.001 sec.

The closure (see Fig. 2.9) was apparently well protected since no dimensional changes to the lid and its mating parts were observed after the impact.

The full-size demonstration fuel element shipping cask, designed with protective fins, was also drop tested from 30 ft onto a top edge.²⁴ It was equipped with both elastomer and stainless steel gaskets. The cavity was pressurized to approximately 165 psi before the drop; no evidence of leakage after the drop was noted.

2.8.2 Toroidal Shell-Type Energy Absorbers

The amount of energy that can be absorbed by fins is dependent on the orientation of fins relative to the direction of cask impact. Shell structures, such as the segmented toroidal ring shown in Fig. 2.26, can be designed to circumvent this problem. This ring is designed not only to protect the cask closure in an end drop but will also operate properly regardless of the angle at which the cask impacts on a horizontal surface.

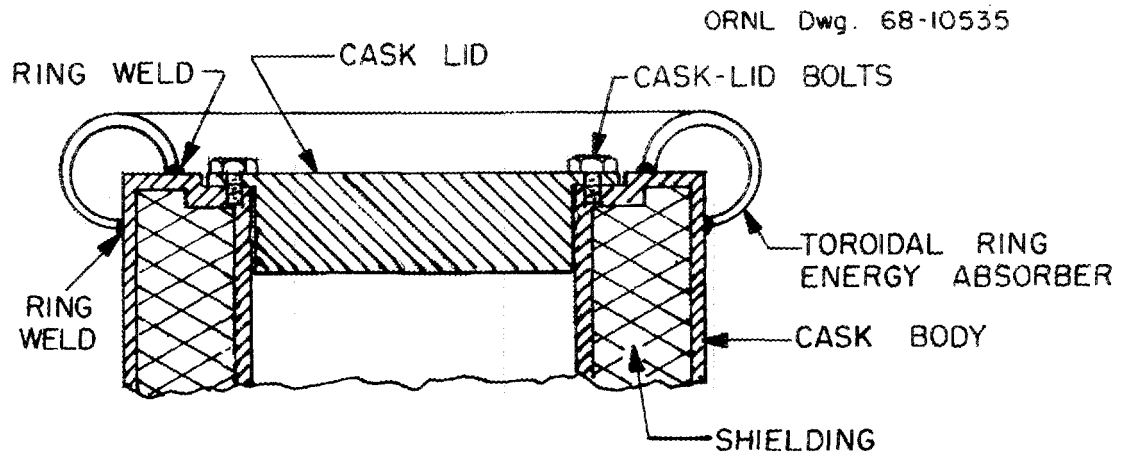


Fig. 2.26. Toroidal Ring Energy Absorber.

Several engineers at the University of Tennessee have investigated protective devices of this design and have found that such rings can supply the energy absorption capabilities necessary to maintain seal integrity and permit closure after a 30-ft impact for cask weights of interest.²⁵ This work is being pursued further in an attempt to accumulate engineering data that will permit the design of a toroidal ring of predictable energy absorption capacity, as would be required in a specific use.

2.8.3 Protective Buffers

An example of a crash frame, designed to protect a cask which, per se, would not meet specifications with regard to the 30-ft-drop, is shown in Fig. 2.27. This crash frame was analyzed by means of a plastic hinge technique.²⁶

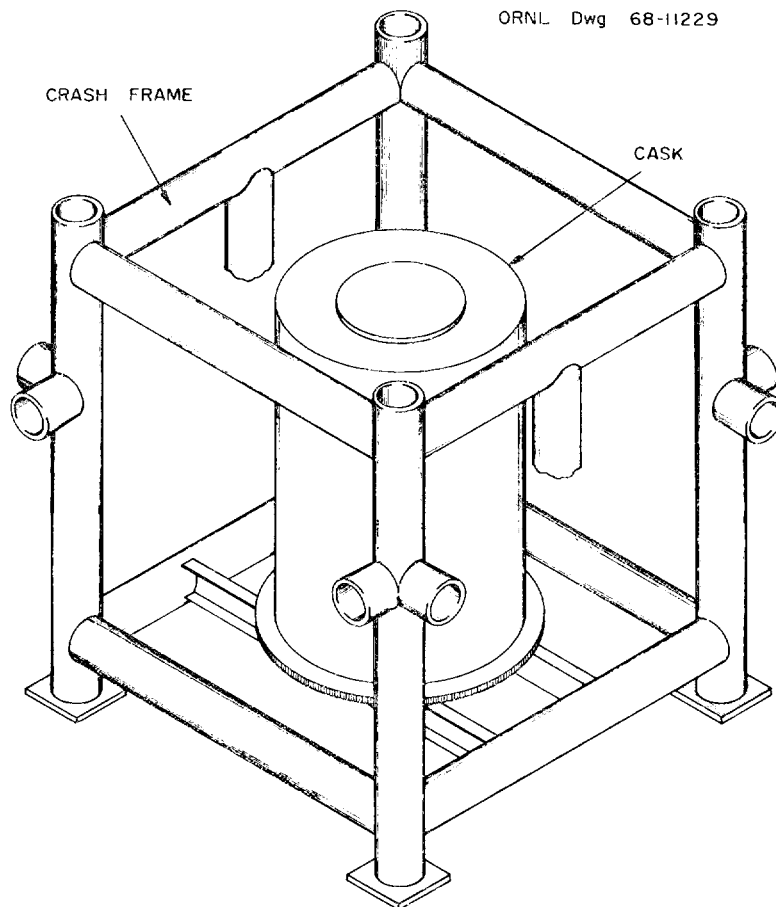


Fig. 2.27. Crash Frame Designed for an Existing Cask.

The validity of the analysis was confirmed by the results from several model test drops; these results indicated that the force loading to the cask and contents can be estimated with a reasonable degree of accuracy.²⁷

A vehicle-cask system can be designed in such a manner that a considerable amount of the impact energy is absorbed in the deformation of material located external to the cask. Such a system was designed by the Westinghouse Electric Corporation to protect their 75-ton Yankee spent fuel shipping cask (see Fig. 2.28). Their analysis of this shock absorbing structure, based on an early version of the regulations, is given in ref. 28.

Another, more elaborate, protective buffer, which can be considered simply as an extension of the cask, was designed by Hanford to protect several of their isotope shipping casks, the heaviest of which weighs

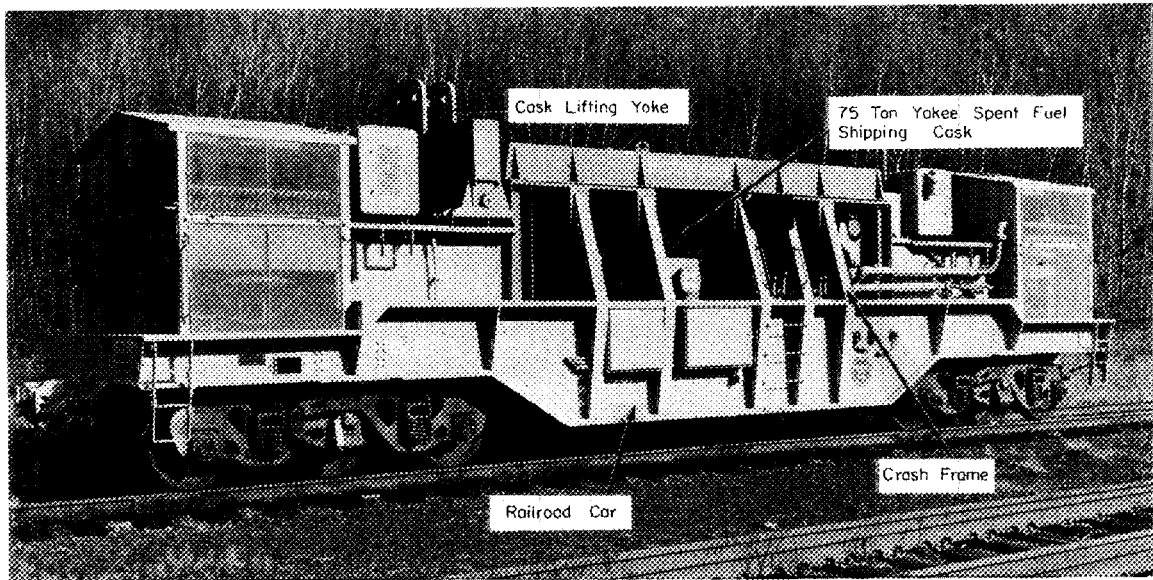


Fig. 2.28. External Crash Frame Mounted on a Railroad Car.
(Courtesy of Westinghouse Electric Corporation).

ORNL DWG. 63-7891R 1

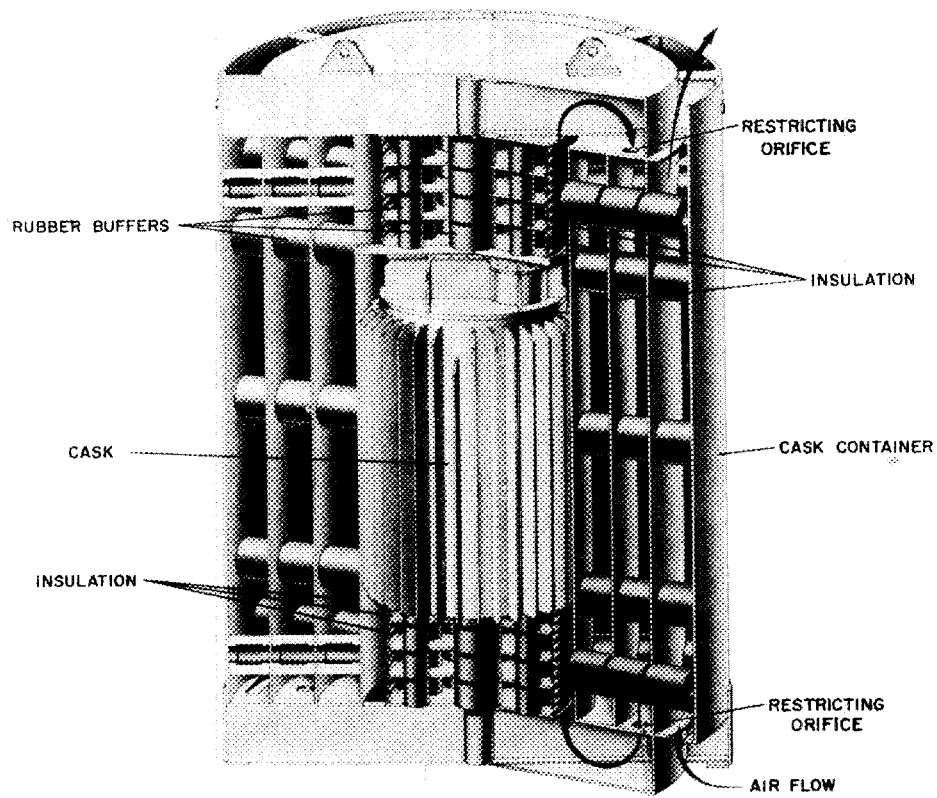


Fig. 2.29. Hanford's 1A Cask and Buffer Shield.

40,000 lb.²⁹ The protective structure (see Fig. 2.29), weighs 35,000 lb and is made of concentric steel shells that surround the lead-shielded cask and are held in place by rubber shock absorbers. This buffer is designed to reduce the impact force on the surface of the cask to 50 g's when the cask-buffer combination is dropped in any orientation on a solid surface from a height of 30 ft. Since most of the kinetic energy of the system is dissipated by the shock-absorbing device, the uniform surface loading on the cask may be specified and controlled.

In order to test the adequacy of the design and to make a complete analysis of the buffering system, an impact testing program of model buffered casks was undertaken at the University of Texas.³⁰ A 0.25-scale model of the HAPO cask-buffer combination was built.

An analysis of the scaling laws indicates that the deceleration received by the cask inside the buffer should be inversely proportional to the scale factor. Since the HAPO system was designed to reduce the deceleration of the cask to 50 g's on impact from a 30-ft fall, a deceleration of 200 g's was expected for the 0.25-scale models when dropped from the same height. Two types of material were used in the buffer to absorb the impact energy: rubber and a specially designed aluminum honeycomb material. The aluminum honeycomb was evaluated because its properties are less susceptible to temperature changes and because this material can be used to design smaller buffers with the same energy absorbing capabilities as those using rubber shock absorbers.

An acceleration, velocity, and displacement record of the rubber buffer model is shown in Fig. 2.30. The maximum deceleration of the cask received in this drop was 224 g's; however, the "smooth peak" value was about 200 g's, which is in excellent agreement with the predicted value.

A similar record for an aluminum honeycomb buffer model is shown in Fig. 2.31. The cask received a peak deceleration of 300 g's; the "smooth peak" value was considerably less than 200 g's. This is certainly within acceptable limits and, if required, the honeycomb could be redesigned in such a manner that the "averaged" impact results will agree more closely with the specifications.

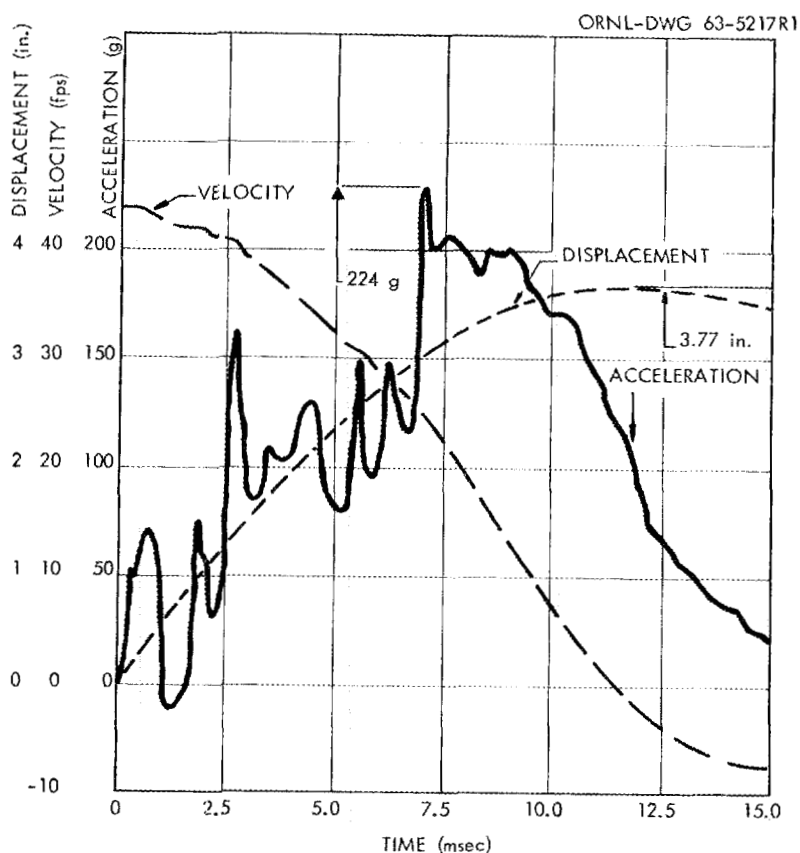


Fig. 2.30. Acceleration, Velocity, and Displacement Record for 30-ft End Drop of a Rubber Buffer Model.

2.8.4 Aluminum Honeycomb Characteristics

Energy absorption characteristics of aluminum honeycomb were studied at the University of Texas.^{31,32} This material has cross-laminated corrugations and is made in various foil thicknesses, corrugation heights, and lamination patterns. Stress-strain curves for a typical honeycomb under static loading and impact velocities of 50 and 100 fps are shown in Figs. 2.32, 2.33, and 2.34. When the honeycomb is compressed to about 20% of its initial thickness (see Fig. 2.32), it becomes almost solid; therefore, further compression is attainable only at high loadings. The energy absorption capability of such a system is essentially irreversible. The characteristics of the honeycomb under static and impact conditions are summarized in Table 2.5. Note that the honeycomb is slightly stronger under static loading than impact loading. The maximum amount of energy that this particular material can absorb under an impact load is about 550 in.-lb/in.³

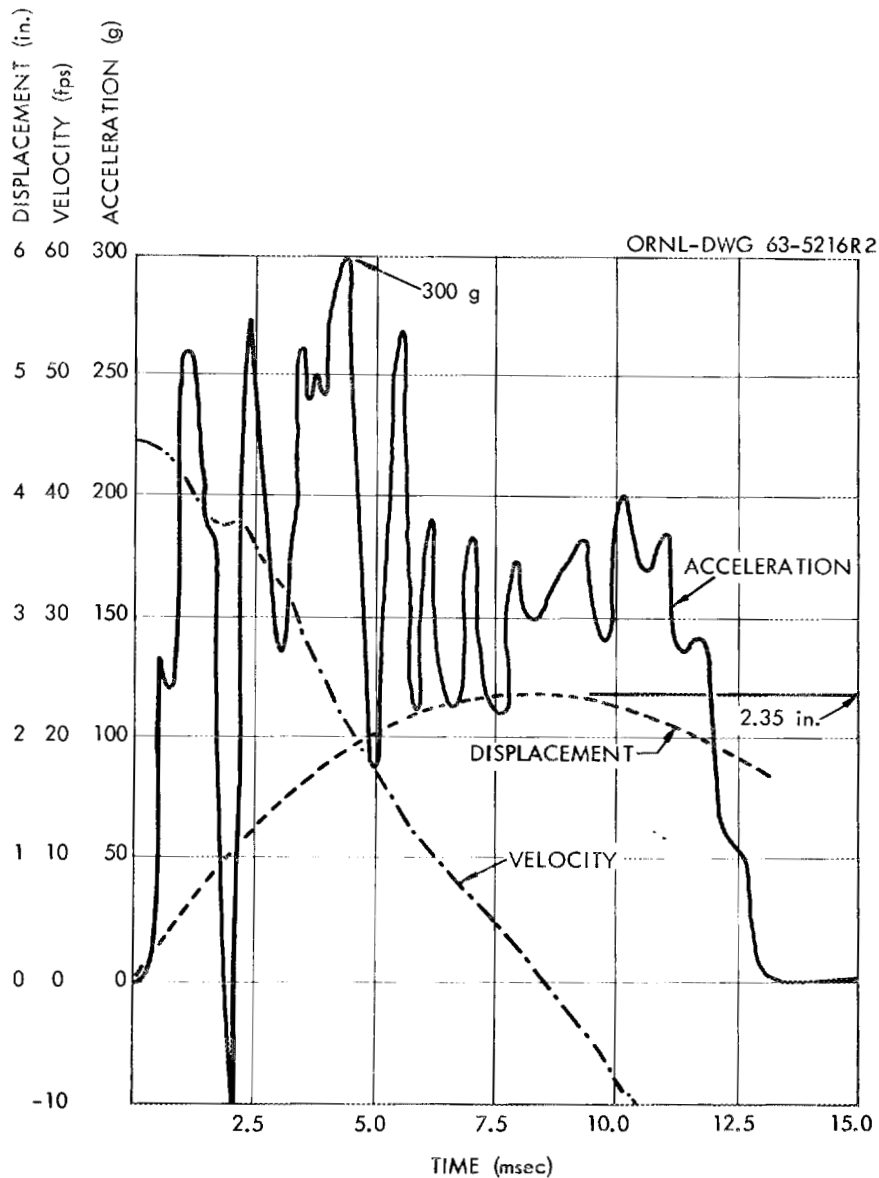


Fig. 2.31. Acceleration, Velocity, and Displacement Record for 30-ft End Drop of an Aluminum Honeycomb Buffer Model.

Table 2.5. Energy Dissipation and Average Stress

Material	Impact Velocity (fps)	Average Stress (psi)	Energy Dissipated (in.-lb/in. ³)	Strain (%)
PR-A-0	0 (static)	798	600	75
PR-A-0	50	713	535	75

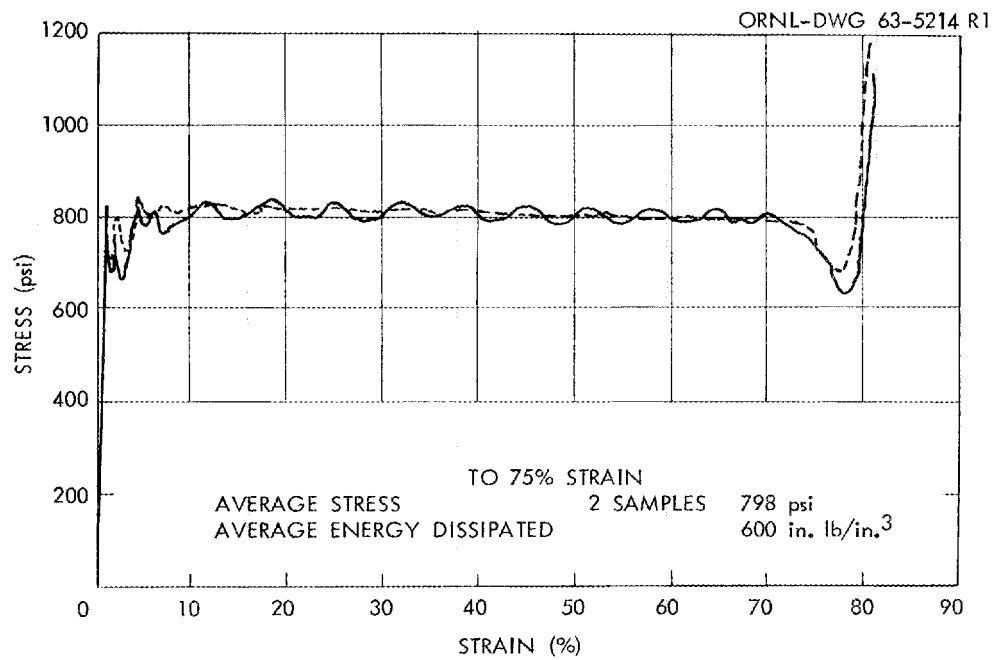


Fig. 2.32. Static Stress-Strain Curves for PR-A-0 Type Aluminum Honeycomb.

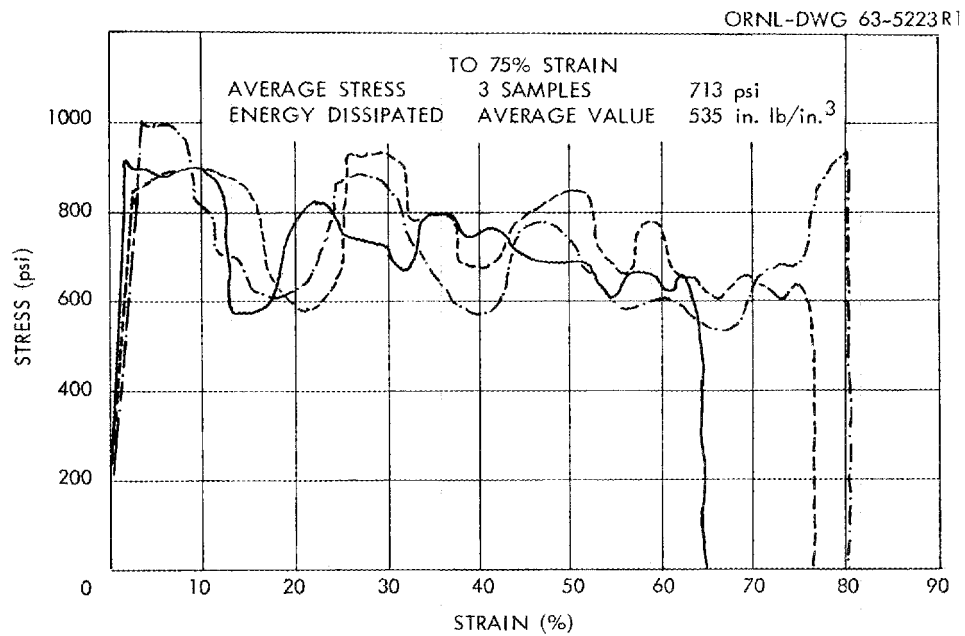


Fig. 2.33. Dynamic Stress-Strain Curves for PR-A-0 Type Aluminum Honeycomb Impacted at 50 FPS.

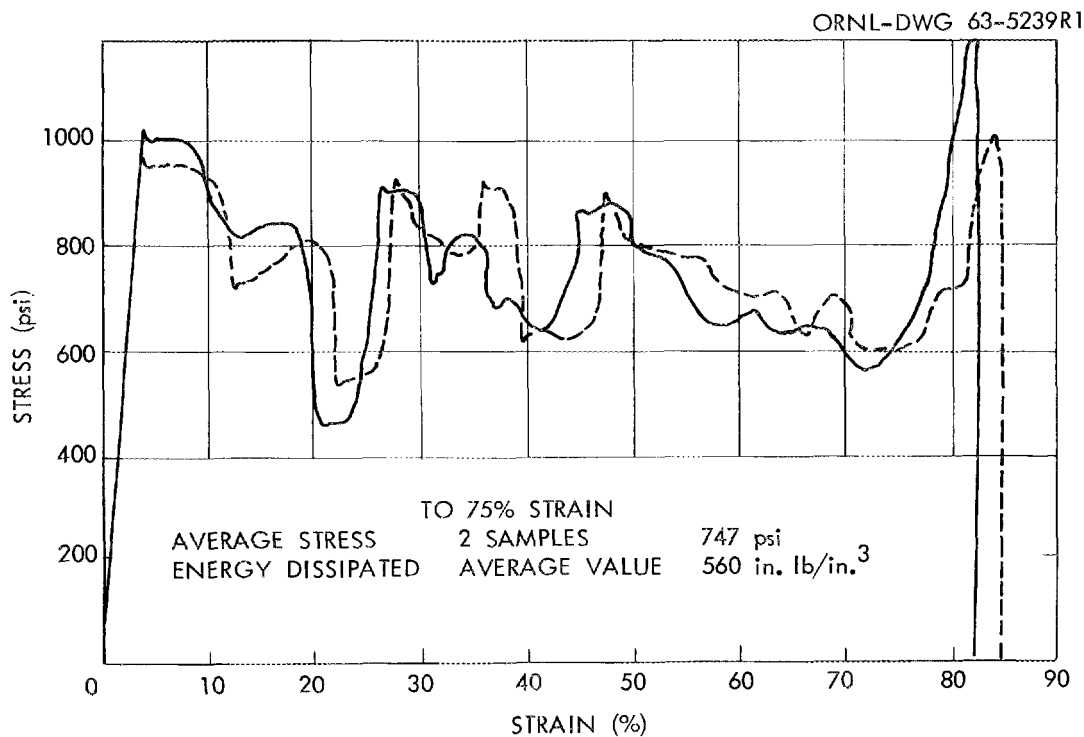


Fig. 2.34. Dynamic Stress-Strain Curves for PR-A-0 Type Aluminum Honeycomb Impacted at 100 FPS.

2.8.5 The Army-AEC Vehicle Impact Studies

Three vehicle impact tests, sponsored by the USAEC and the Department of the Army, have been carried out in order to determine the effects of an accident on the total transport system.³³ The objective of this study was "to provide a realistic understanding of the dynamics of transportation accidents . . . , " particularly with regard to vehicle, cargo, and tie-downs. A massive barrier with a front surface of armor plate was used as the "immovable object" into which the vehicles were driven at velocities varying from 4 to 41 mph. High-speed photography revealed that the barrier did not move during any of the tests.

One of the most significant results of the study was the proof that the fifth wheel is a weak link in a tractor-trailer system; however, if this wheel is reinforced, large fractions of the total energy of the transport system (up to 100%) may be dissipated in the vehicle without seriously involving the cask or tie-downs. For example, DuPont's 15-ton IMF cask was rigidly tied down to a flatbed trailer (see Fig. 2.19); the fifth wheel was reinforced, and the tractor-trailer was driven, by remote means, into the barrier at 28.5 mph. Results showed that even though the cab was

completely demolished and the trailer frame was bent, the cask remained upright and undamaged on the trailer. Although methods of calculating force inputs to a cask in an accident remain somewhat crude, these tests leave little doubt as to the energy absorption capabilities of the vehicle in a front-end impact. Until methods to make reasonable predictions of the energy absorption capabilities of complex structures become available, such tests will have to be considered as the best method for determining the amount of impact protection that is afforded the cask by a vehicle.

2.9 Testing Requirements

Because of the uncertainties and inherent approximations in engineering designs, compliance with regulations must sometimes be demonstrated by subjecting the cask to a series of tests rather than relying entirely on analytical treatment. A decision to test will be affected primarily by the purpose of the cask and the designer's knowledge of the applicability of analytical treatments to his particular design. A compilation of cask test results is in preparation by an ad hoc group of the USASI N14 committee; this compilation can assist designers in deciding if testing is desirable.

Cask tests would appear to constitute complete proof of a design; but, in fact they do not. Only a limited number of tests are made, generally under conditions that the designer feels are most damaging. This fact, however, in no way lessens the importance of cask testing. Tests can often be valuable to more than one designer; and, as additional definitive tests are made, analytical techniques can be improved until test results can be predicted with a known degree of accuracy.

2.9.1 Hypothetical Accident Conditions

Designers usually consider subjecting a cask (prototype or scale model) to tests that involve an impact or a fire. The hypothetical accident conditions given in AECM 0529 Annex 2 are noted below:

1. Free Drop -- "A free drop through a distance of 30 ft onto a flat, essentially unyielding, horizontal surface, striking the surface in a position for which maximum damage is expected.
2. Puncture -- "A free drop through a distance of 40 in. striking in a position maximum damage is expected, the top end of a vertical cylindrical mild steel bar mounted on an essentially unyielding horizontal surface. The bar shall be 6 in. in diameter, with the top horizontal and its edge rounded to a radius of not more than 1/4 in., and of such a length as to cause maximum damage to the package, but not less than 8 in. long.

The long axis of the bar shall be normal to the package surface.

3. Thermal -- "Exposure for 30 min within a source of radiant heat having a temperature of 1475°F and an emissivity coefficient of 0.9, or equivalent. For calculational purposes, it shall be assumed that the package has an absorption coefficient of 0.8. The package shall not be cooled artificially until after the 30-min test period has expired and the temperature at the center of the package has begun to fall.
4. Water Immersion -- "Immersion in water for 24 hr to a depth of at least 3 ft."

These conditions are to be applied to a cask, either by calculational methods or by test, in the sequence listed. As a result, the reduction in shielding should not be sufficient to increase the external radiation dose rate to more than 1000 mr/hr (or equivalent) at 1 m from the external surface of the cask. The cask will not release any radioactive material except gases or contaminated coolant (release limits are given in AECM 0529, Para. II.F.1.b.) and the material in the cask will remain subcritical.

Both prototype and scale model casks have been used in testing programs. However, the fire test should be performed on a prototype cask because the response of the full-scale cask would be difficult to predict based on test results of a model.

One cask that has recently been subjected to a rather complete testing program was built by Union Carbide Corporation, Paducah Plant, using laminated uranium for shielding. Tests were made to study the structural capabilities of a uranium shielded cask. A detailed description of these tests, their objectives, and the resulting data and conclusions, reported in ref. 25, is recommended as a guide to testing procedures.

The question of instrumentation of the test specimens frequently arises. To date, strain gages, accelerometers, and brittle lacquer have been used on casks subjected to impact, while thermocouples, heat-sensitive paint or thermo sticks are most frequently used in connection with fire testing. While the impact data are interesting, frequently no satisfactory method is available to translate such information into expected cask damage. The most useful accelerometer readings have been obtained from buffered cask tests in which the cask itself (i.e., the shielding and cavity) decelerates uniformly; such data are discussed in Sects. 2.8.1 and 2.8.3.

2.9.2 Normal Operating Conditions

Normal operating conditions, presented in Annex 1 of AECM 0529, are given below. Each of the conditions is to be applied separately to determine its effect on the cask.

1. Heat -- Direct sunlight at an ambient temperature of 130°F in still air.
2. Cold -- An ambient temperature of -40°F in still air and shade.
3. Pressure -- Atmospheric pressure of 0.5 times standard atmospheric pressure.
4. Vibration -- Vibration normally incident to transport.

5. Water Spray -- A water spray sufficiently heavy to keep the entire exposed surface of the package, except the bottom, continuously wet during a period of 30 min.
6. Free Drop -- Within 2.5 hr after conclusion of the water spray, a free drop through the distance specified below onto a flat essentially unyielding horizontal surface. Impact with the surface occurs in a position for which maximum damage is expected.

Free Fall Distance

<u>Package weight (lb)</u>	<u>Distance (ft)</u>
< 10,000	4
10,000 to 20,000	3
20,000 to 30,000	2
> 30,000	1

7. Corner Drop -- A free drop onto each corner of the package in succession, or, in the case of a cylindrical package, onto each quarter of each rim, from a height of 1 ft. This test does not apply to packages that are not constructed primarily of wood or fiberboard, to packages exceeding 10,000 lb in weight.
8. Penetration -- Impact of the flat circular end of a vertical steel cylinder, 1.25 in. in diameter and weighing 13 lb, dropped from a height of 4 ft impacting normally onto the exposed surface (of the package) that is expected to be the most vulnerable to puncture.
9. Compression -- For packages not exceeding 10,000 lb in weight, a compressive load equal to either five times the weight of the package or 2 lb/in.² multiplied by the maximum horizontal cross section of the package, whichever is greater. The load shall be applied, for a period of 24 hr, uniformly against the top and the bottom of the package. The package should be positioned as in normal transport.

It is not always necessary to subject a spent fuel shipping cask to these normal conditions of transport in order to determine whether the cask is adequate; calculational methods often suffice. There are, however, exceptions.

The effect of vibration on the cask contents may be impossible to calculate analytically; this may also be true of the penetration requirement (No. 8), particularly if the penetrator strikes an exposed valve. Tests could be used to resolve the problem.

In addition, Paragraph III.C.2. of AECM 0529 requires the cask, before its initial shipment, to be tested at 50% higher than the normal operating pressure (if the latter exceeds 5 psig). The test should be carried out with the cask at the maximum normal operating temperature; if this is not possible, the test may be made at a lower temperature but at a higher pressure (see ASME Code Sect. VIII, Paragraph UG 99b; Standard Hydrostatic Test).

It is also wise to demonstrate the capability of the cask to dissipate the amount of heat generated by the fuel to an ambient temperature of 130°F in direct sunlight. A test of this type is discussed in Sect. 4.9.4.

Often, spent fuel shipping casks are loaded and unloaded under water. If the normal operating cask temperatures are high, the cask will be subjected to a thermal shock during this type of unloading procedure. Although not required by the regulations, the consequences of such a thermal shock should be evaluated either by testing or some other method. It is possible that welds could crack under this treatment; visual inspection of such vulnerable areas should be made if the test is performed.

Although a radiation attenuation test is not required by the regulations, it is recommended. Dose rate measurements made when the source is first loaded into the cask will suffice; however, it is frequently desirable to check the effectiveness of the shielding during fabrication. Tests of this nature are discussed in Sect. 4.9.5.

2.10 Comments on Cask Shielding Material

Its low cost (presently about \$0.15/lb), high density, and ability to be easily fabricated, even in odd shapes, make lead the most common material of construction used in the United States for a gamma shield. However, disadvantages of using lead as the primary shielding material are several fold. For example, lead must usually be encased in steel for fabrication, protection, and handling purposes. Also, since lead contracts appreciably upon solidification from the molten state (more than 3% by volume), care must be taken during the pouring of large steel-encased shields to prevent the introduction of unwanted voids. In addition, the unsatisfactory wetting or bonding of lead to stainless steel can also contribute to the formation of unwanted voids.

Fire presents a hazard to lead-filled casks. The coefficient of thermal expansion for lead is higher than that of steel, which is normally used to encase the lead (Fig. 2.35).^{34,35} High pressures, which may develop in the cask during exposure to a fire, could result in broken welds and subsequent loss of shielding.

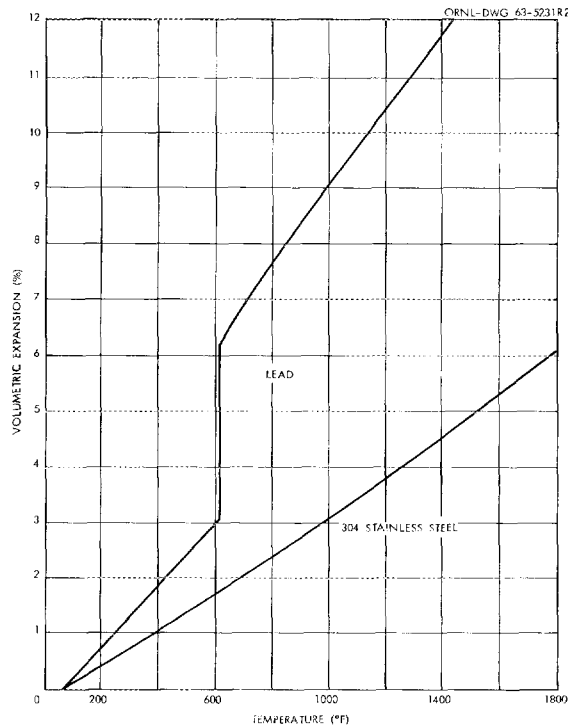


Fig. 2.35. Volumetric Expansion of Lead and Steel as a Function of Temperature.

The British have performed some heat tests on small lead-filled, steel-shelled casks³⁶ and found that even the use of controlled voids in the cask shield to provide thermal expansion space for the lead was not entirely satisfactory. Melting of the lead would not always take place around the void area; thus these areas did not prevent pressure buildup and the loss of lead in other areas. In addition, the position of the void after cooling (even when no lead was lost) was not predictable and could result in areas of inadequate shielding. Such arguments against voids are compelling; nevertheless, it is premature to argue that properly designed voids do not give the protection for which they are designed and that the resulting redistribution of lead may offer less protection than if the voids had not been there.

Other shielding materials that may be used to advantage include uranium and steel. Uranium is structurally about as strong as steel; both shielding materials can resist the consequences of an accidental fire better than lead. Neither material is easily deformed and consequently will impart a higher shock loading to the cask contents when involved in a 30-ft impact unless buffering is supplied.

The British have made a number of large casks from cast iron or steel containing no lead or other high-density material. This eliminates the problem of differential thermal expansion found in the lead cask with their steel shells. The shielding does not melt when involved in a normal petroleum fire, and the cask impact qualities are apparently improved.

The unit cost of a steel cask is about \$0.40 to \$0.50/lb, but its total cost is comparable to that of a lead cask with the same cavity size. It has been reported that, in the United Kingdom, the expected costs of steel casks, ordered in large quantities, might have unit costs as low as \$0.18/lb.^{37,38}

The main disadvantage of steel casks is that, for an identical cavity size, a steel cask is larger and weighs considerably more than a lead-shielded cask. This, in turn, means that transportation charges for the steel cask will normally be higher.

Depleted uranium has been used for shielding in casks. Uranium is a more dense metal than lead and, for the same cavity size, will result in a smaller cask weighing less than a lead cask. Because of the pyrophoric nature of uranium (even though it is difficult to get large solid pieces to burn), uranium shields should be encased in steel.

Uranium may be cast and machined, or rolled in sheets, formed and welded. A uranium casting is generally limited by the size of the fabrication equipment; at present, the maximum size is about 10,000 lb. However, sheets that have been rolled and formed may be nested and welded into a modular type of construction of almost any size.

Unassayed depleted uranium may be obtained from the United States Government as UF_6 at a base cost of about \$1.13 per pound of contained uranium. The uranium hexafluoride must be reduced to metal and then cast or rolled. The total cost of a uranium cask from a vendor would be more expensive when compared to the cost of a lead-filled cask; however, the price may be justified to obtain a maximum cavity volume for minimum shield weight. The physical properties of lead, steel, and uranium are given in Table 2.6.

2.10.1 Heat Transfer Under Normal Conditions

When lead-shielded casks are to be used for transporting fuel that generates a large amount of heat, the thermal resistance between the lead and steel shells should be as low as possible; air gaps between the lead and the steel shells of the cask could cause excessive temperatures in the cask cavity. To minimize the normal operating temperature of the cask and contents, many cask designers desire a metallurgical bond between the outer shell and the lead shield.

It is possible to design the cask in such a way that a good bond between the lead and the outer shell is not required for efficient heat removal. Figure 2.36 schematically shows a sectioned cask in which the fins are welded or brazed to the inside of the outer shell.³⁹ These fins are designed to move as the lead expands and contracts under varying

Table 2.6. Physical and Chemical Properties of Some Shielding Materials

	Uranium ^a	Lead ^b	Iron	Stainless Steel ^c
Density, g/cc	18.9	11.34	7.87	7.9
lb/in. ³	0.683	0.410	0.284	0.29
Melting point, °C	1133	326	1537	1400-1454
°F	2070	618	2798	2550-2650
Boiling point, °C	3900	1525	3000	-
°F	7052	2777	5430	-
Ultimate tensile strength, psi	60,000-100,000 ^d	2300-3000	95,000-130,000 ^d	80,000
Yield strength, psi	25,000-45,000 ^d	1180-1380	60,000-125,000 ^d	30,000
Modulus of elasticity, psi x 10 ⁶	24 ^d	2	28.5	28
Poisson's ratio	0.21	0.45	0.29	9.30
Hardness, Brinell No.	185-385 ^d	4.3	149-170 ^d	150
Thermal expansion, (in./in.-°C) x 10 ⁻⁶	6.8 to 15 ^d	29	11.7	10.4
Specific heat, cal/g-°C	0.028	0.031	0.11	0.12
Thermal conductivity (at 100°C) cal/cm-sec-°C	0.063	0.082	0.18	0.039
Btu/hr-ft-°R	14.0	19.9	4.3	9.4

^aUnalloyed depleted uranium.^bChemical lead ASTM B29-55.^cType 304L, annealed.^dVaries with treatment.

heat loads while still maintaining mechanical contact with the lead; this provides a good path for heat to be conducted from the lead to the outer steel shell.

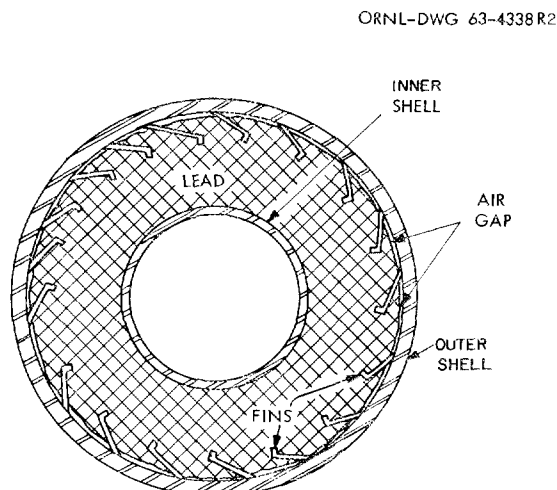


Fig. 2.36. Cask Containing Internal Heat Transfer Fins.

2.10.2 Heat Transfer Under Accident Conditions

Although the probability of a cask being involved in a fire may be low, an examination of the consequences is far from academic since the potential monetary loss is significant. As its temperature increases, lead expands at a faster rate than steels that normally contain it. Consequently, molten lead could rupture the steel shell and flow out. Cavity pressure would increase, particularly if a liquid coolant were present, which could cause the containment to be violated with the attendant loss of coolant; fission products could thus be dispersed.

The current regulations require that a cask be able to withstand the environment of a 0.5-hr fire at 1475°F without exceeding the prescribed loss of contents or increased dose limits shown in Table 5.1. Because of the small amount of test data presently available, as well as the impracticality of testing many casks, the task of designing in terms of the consequences of the 0.5-hr fire is primarily a matter of good engineering judgment.

Normally, the cask is designed to provide a path for heat to flow from the source to the cask surface. This, however, results in a path for heat to be transferred from the surface of the cask to the cavity. Since, in a fire, much of the energy is transferred by radiation, it is desirable to build a cask that would reject heat by convection and not accept thermal energy by radiation. The HAPO cask is designed to do this by providing several concentric steel shells surrounding the cask to act as buffers (see Fig. 2.29). Under normal conditions, air cools the cask by flowing around the cask, then past the cask, and finally out the top of the buffer. In a fire, the hot gases are not expected to pass the few entrance barriers, and the radiant energy of the flame will be intercepted by the outer surface of the buffer.

Since the addition of a fire shield would add to the total cost and since proper operation of the fire shield following the 30-ft drop is difficult to guarantee, this technique has seen limited use.

A second method of protection is to design the shield in two portions: an inner shield to contain lead and an outer shield to contain lead or wet plaster.³ In a fire, material in the outer compartment is sacrificed either by melting and running out holes designed in the outer shell (in the case of lead) or by driving water vapor out pressure relief valves (in the case of wet plaster). The void thus created would provide a thermal buffer against continuing radiant energy emanating from the fire.

Casks of both types have been built, but testing has been limited. A schematic of the three-shelled cask containing lead in the outer compartment is shown in Fig. 2.15.

Calculations made for a large lead-shielded cask indicate that, in the 30-min 1475°C fire, an unrestrained (no circumferential fins) outer shell of a cask will deform by plastic strain.²⁶ Such strains can be shown to be low in magnitude (below the ultimate elongation at the elevated temperatures), thus indicating that lead will not be lost. Calculations of this type can indicate compliance of the regulations since the specified fire is assumed to provide a uniform heat source around the cask. It does not account for practical problems such as local hot spots or restraints caused by, for example, fins or a cask cradle.

2.11 Fuel Magazine Design

The function of the spent fuel shipping cask magazines (or baskets) is to:

1. Protect and contain the fuel assemblies during transportation and handling.
2. Assist in the dissipation of decay heat.
3. Control criticality.

Since the decay heat dissipation problem is one of the chief factors in limiting cask capacity under normal conditions, the selection of thermally efficient materials can be an important economic factor.

2.11.1 Protection and Containment of Fuel During Transportation and Handling

The magazine serves to segregate each fuel assembly, and to keep the assemblies from abrading each other while in transit.

Testing reactor fuel assemblies are normally shipped in a vertical orientation which is identical to their orientation during operation. With this in mind, the magazines designed for these assemblies are usually readily removable from the casks. They serve also to safely move the fuel in both the loading or unloading pool.

Because of their length, power reactor fuel assemblies are normally shipped in the horizontal orientation. These assemblies are designed to operate in the vertical position, however, and excessive strain may be applied to the fuel pins if insufficient support is provided for the assemblies in the horizontal position. The fuel magazines must be designed to provide this support as uniformly as possible over the entire fuel assembly length. During an impact accident, the magazines are designed to limit the movement of each assembly and to minimize loading applied to an assembly other than that due to its own weight.

The designer must consider the following items in the selection of materials of construction of the cask magazine:

1. Compatibility of fuel, coolant, and cask cavity materials. This compatibility includes possible corrosion tendencies under cask operating conditions and thermal expansion during the operation and life of the equipment.
2. The most efficient use of cask cavity space while meeting the requirements of criticality, thermal conduction, protection of fuel elements, radiation shield capability, and structural integrity.
3. The optimum selection of fabrication techniques and construction costs.

2.11.2 Dissipation of Heat

Fuel magazines provide a significant path for the transfer of decay heat to the cask wall. In the normal operating condition, the magazine fuel assembly should be designed to provide efficient flow channels for circulating coolant. In the loss-of-liquid-coolant condition, the magazine structure provides heat conduction paths from the hot fuel elements to the shielding. When fixed (welded in place) baskets are used the heat paths will extend directly from the fuel assemblies to the shielding, making a very efficient heat removal system.

2.11.3 Control of Criticality

One of the best methods to control criticality is to alloy neutron absorbing material with the structural members of the magazine. For heat dissipating purposes, the magazine structural members often range from 0.25 in. to 0.75 in. in thickness; such thicknesses permit the use of small alloy percentages of high thermal neutron cross-section materials for effective control of criticality.

Fuel magazines consisting of cavities lined with boral (35% B_4C + Al) are used in shipping aluminum-clad testing reactor fuel assemblies (see Fig. 2.37). Fire test and loss-of-coolant conditions as defined in AECM 0529 and Title 10 CFR part 71, may restrict the usefulness of boral as a structural material. Such weakness may be overcome by cladding the boral

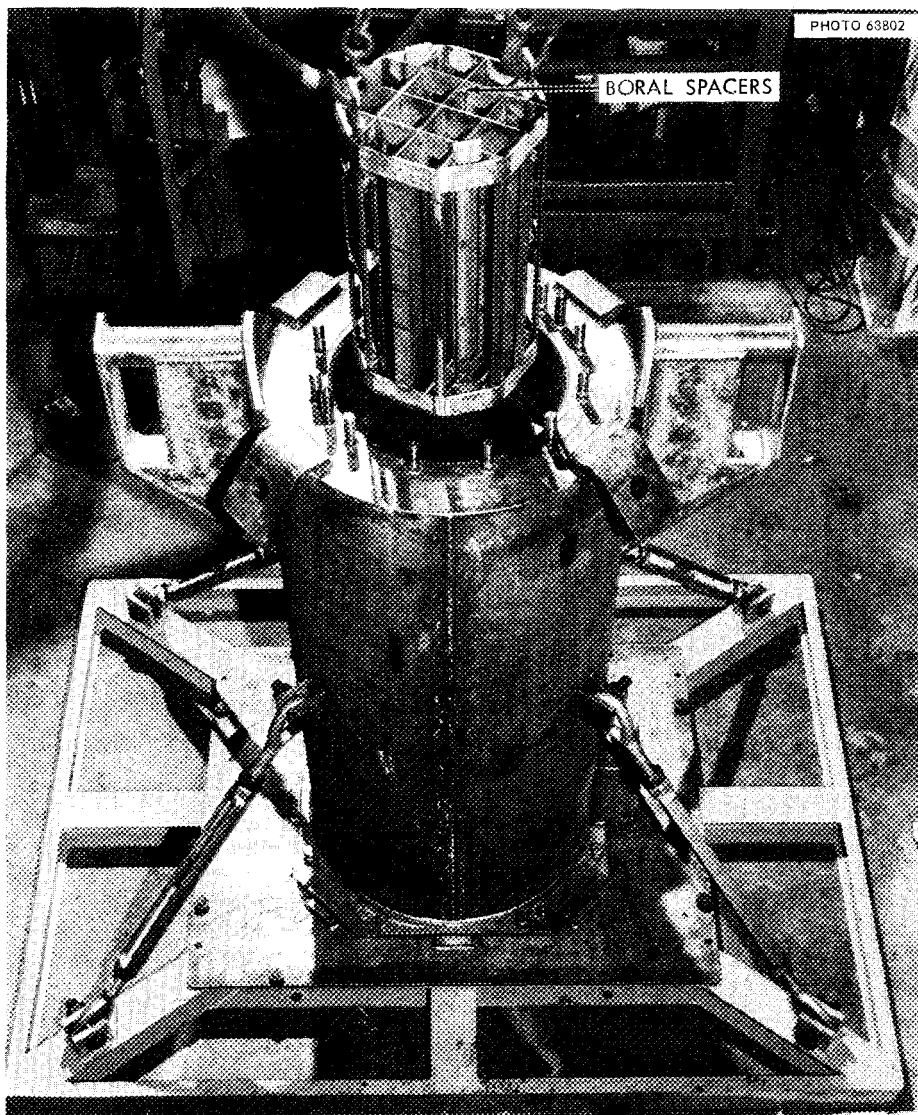


Fig. 2.37. BMI-1 Shipping Cask with One Fuel Basket Removed.
(Courtesy of Battelle Memorial Institute).

with stainless steel; tests performed at Battelle Memorial Institute indicate this clad material functions with adequate structural integrity above 1400°F.

Borated stainless steel has been employed as a poison by some designers. Although it is an effective poison, borated stainless steel has the disadvantages of high initial cost, difficulty of procurement, relatively low thermal conductivity, and a history of embrittlement after welding.

Copper, alloyed with either cadmium or boron, is also a very effective neutron absorbing material and in addition is a very good thermal conductor. Such alloys are difficult to fabricate, however, and add considerably to the magazine cost; they may also require cladding to (1) protect the coolant water from copper particle contamination and (2) permit magazine and cask decontamination by acid solutions.

Geometric or spatial control of criticality can be achieved with proper magazine designs. However, this method of control may lead to inefficient use of cask space when compared to the use of neutron absorbing materials.

Table 2.7 is a list of pertinent data describing typical materials used in the construction of magazines for spent fuel assembly shipment.

Table 2.7. Properties of High Cross-Section Magazine Alloys

Name	Minor Alloy Constituent, %	Thermal Conductivity, Btu ft/hr sq ft °F	Σ_a Macroscopic Thermal Neutron Cross Section cm^{-1}	lb/cu in.	Methods of Construction
Boral	35 B ₂ O	25 (200°F) 19 (500°F)	15.6 ^a (1/8 in. thick) 11.8 (1/4 in. thick)	0.091	Bolt, rivet weld clad with SS
Borated SS	0 - 1	12	3.4	.28	Weld, bolt, clad with 300 series SS
Boron copper	0 - 2	140 (est.)	8.1	.318	Cast, roll, machine, weld
Cadmium copper	0 - 3	2% = 150 (est.) ^b	4.8	.319	Cast, roll, machine, weld

^a Experimentally determined.

^b Thermal conductivity tests made from various alloys are reported to range from 180-140 Btu ft/hr sq ft °F.

2.12 Simple Beam Requirement

When regarded as a simple beam supported at its ends along any major axis the cask must be capable of withstanding a static load, normal to and uniformly distributed along its length, equal to five times the fully loaded cask weight without generating stresses in any material of the cask in excess of the yield strength of that material. This portion of the regulations is usually interpreted as being applied to the outer shell alone. The strength of the lead shielding and the local stresses that would occur around the support points are neglected.

Stresses in the outer shell resulting from the uniform load can be determined analytically using the following equation:

$$S = \frac{MC}{I} \quad (2.17)$$

where

S = the stress, lb/in.²

M = the bending moment, in./lb

C = one-half (1/2) the height of the cask in the direction of bending, in.

I = the cross section moment of inertia, (in.)⁴

The bending moment is given by:

$$M = \frac{5WL}{8} \quad (2.18)$$

where

5W = five times the total cask weight as required in the regulations and L is the length between supports.

The cross section moment of inertia for a cylindrical cask is calculated from:

$$I = \frac{\pi}{4} (r_2^4 - r_1^4) \quad (2.19)$$

where

r_2 = the outside radius

r_1 = the inside radius, both of the outer shell in inches
(see Fig. 2.38a).

The cross section moment of inertia for a prismatic cask (see Fig. 2.38b) is:

$$I = \frac{1}{12} (b_2 d_2^3 - b_1 d_1^3) . \quad (2.20)$$

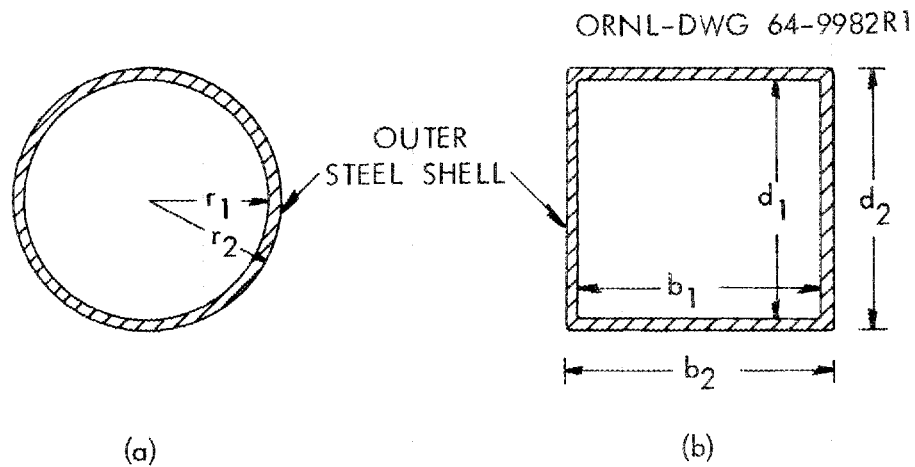


Fig. 2.38. Cross Section of a Cylindrical and a Prismatic Cask.

The strength provided by the lead shielding prevents local buckling of the outer shell; this helps ensure the validity of the assumptions which lead to the use of Eq. (2.17).

2.13 References

1. H. Nelms, Structural Analysis of Shipping Casks Vol. 3 Effects of Jacket Physical Properties and Curvature on Puncture Resistance, ORNL-TM-1312 Vol. 3 (June 1968).
2. H. G. Clarke, Proceedings International Symposium for Packaging and Transportation of Radioactive Materials, p. 261, SC-RR-65-98 (Jan. 1965).
3. Examination of the International Atomic Energy Agency's Regulations for the Safe Transport of Radioactive Materials, EUR-3485e, f, Vol. IV (1968).
4. A. E. Spaller, "Structural Analysis of Shipping Casks, Vol. 2. Resistance to Puncture" USAEC Report ORNL TM-1312, Vol. 1. (Sept. 1966).
5. D. W. Goodpasture and L. B. Shappert, Energy Absorption Capability of Steel Determined from Cask Impact Tests, ORNL TM-680 (Jan. 6, 1964).
6. Products for Piping and Pressure Vessel Construction, 2d ed., Taylor Forge and Pipe Works Catalog 571, 1961.
7. M. F. Spotts, p. 204 in Design of Machine Elements, 3d ed., Prentice Hall, 1962.
8. L. B. Shappert, A Guide to the Design of Shipping Casks for the Transportation of Radioactive Material, ORNL TM-681 (April 1965).
9. F. E. Shadid, Analytical Investigation of Procedures Proposed for the Design of a Shipping Cask for Radioactive Materials, M.S. thesis, University of Tennessee, Knoxville (December 1967).
10. C. B. Clifford, The Design, Fabrication, and Testing of a 1/4 Scale Model of the Demonstration Fuel Element Shipping Cask, KY-546 (June 10, 1968).
11. J. H. Evans and W. C. Stoddart, Structural Analysis of Shipping Casks, Vol. 5, Lifting Devices, ORNL-TM-1312 Vol. 5 (in preparation).
12. R. O. Letourneau, Loads in Shipping Container Tie-down Lines, SC-TM-65-320 (July 1965).

13. H. G. Clarke and K. D. Doshi, Structural Integrity of Shipping Containers for Radioactive Materials. Part III: Analysis of Container Tie-down During Collision of Highway Vehicles, NYO-2539-2 (February 1966).
14. J. M. Biggs, Introduction to Structural Dynamics, McGraw-Hill, New York, 1964.
15. K. D. Doshi, Structural Integrity of Shipping Containers for Radioactive Materials. Part IV: An Analytical Study of Longitudinal Vehicle Collisions, NYO-2539-4 (Nov. 1965).
16. J. Marin, Engineering Materials, p. 231, Prentice-Hall, Inc., New York, 1952.
17. Lead in Modern Industry, Lead Industries Associated, New York, 1952.
18. J. H. Vincent, Proc. Cambridge Phil. Soc. X, 332 (1898-1900).
19. J. P. Andrews, Phil. Mag., Series 7, 8, 53, Suppl. (Dec. 1929).
20. J. P. Andrews, Phil. Mag., Series 7, 9, 58 (1930).
21. H. G. Clarke and W. E. Onderko, Model Impact Tests Pertaining to Shipping Containers for Radioactive Materials, TID-7651, p. 238.
22. D. Tabor, The Hardness of Metals, Oxford Clarendon Press, London 1951.
23. B. B. Klima, L. B. Shappert, and W. C. Stoddart, Structural Analysis of Shipping Casks. Impact Testing of a Long Cylindrical Lead-Shielded Cask Model, ORNL-TM-1312, Vol. 6 (March 1968).
24. C. B. Clifford, Demonstration Fuel Element Shipping Cask from Laminated Uranium Metal, Part III. Tests and Demonstrations, KY-552 (to be published).
25. C. T. Welch, An Experimental Investigation of the Effects of Impact on a Cylindrical Container of Lead and Steel Construction, M. S. thesis, University of Tennessee, Knoxville (December 1967).
26. J. H. Evans, Structural Analysis of the Brookhaven National Laboratory Mobile Gamma Irradiator, ORNL-TM-2178 (September 1968).

27. J. H. Evans, Structural Analysis of the Brookhaven Shipboard Irradiator, ORNL-TM-2064 (January 1968).
28. Shipment of Irradiated Yankee Fuel Elements, WCAP-1859, Westinghouse Electric Corp., Pittsburgh, Pa. (October 1961) (Revised January 1962).
29. C. W. Smith et al., "Application of External Impact Energy Sorption to Large Radioisotope Shipping Casks," p. 265 in Summary Report of the AEC Symposium on Packaging and Regulatory Standards for Shipping Radioactive Material, Germantown, Md., Dec. 3-5, 1962, TID-7651.
30. E. A. Ripperger, Model Studies of Buffered Shipping Containers for Fission Products, HW-77963, Structural Mechanics Research Laboratory, University of Texas (May 1963).
31. J. M. Lewallen and E. A. Ripperger, Energy Dissipating Characteristics of Trussgrid Aluminum Honeycomb, SMRL-RM5, The University of Texas.
32. E. A. Ripperger and M. D. Reifel, Size Effects of Trussgrid Aluminum Honeycomb, SMRL-RM-6, The University of Texas.
33. Y. Kamita and R. Morgan, Final Report on Engineering Test of Transportation of Nuclear or Fissile Materials, DPS-2582 (November 1967).
34. Lead in Modern Industry, Lead Industries Association, New York, 1952.
35. T. Lyman (ed.), Metals Handbook, 8th ed., Vol. 1, p. 422, American Society of Metals, 1961.
36. F. E. Dixon, "The Design of Shielded Containers to IAEA Standards," p. 331 in Summary Report of AEC Symposium on Packaging and Regulatory Standards for Shipping Radioactive Material, Germantown, Md., Dec. 3-5, 1962, TID-7651.
37. H. E. Goeller and W. H. Lewis, personal communication, Jan. 25, 1960.
38. R. Morris, Atomics, p. 29 (February 1963).
39. E. C. Lusk, Patent No. 3,005,105, issued Oct. 17, 1961.

3. MATERIALS

The primary objectives of cask design are to shield and contain a source of radioactive material. The properties of the materials of construction must be such that these objectives can be carried out under a number of environmental conditions as specified in the regulations.

This chapter provides guidelines for selecting materials. Some materials which have the desirable properties recommended below are given in tabular form along with their ASTM material specification.

To be acceptable, a material should have adequate strength, ductility and toughness at sub zero (-40°F), ambient and elevated temperatures. In addition, factors such as its corrosion resistance, cost, availability, and ease of fabrication, as well as its ability to withstand decontamination solutions, must be considered.

The necessity that materials of construction have adequate strength at -40°F is probably the most restrictive requirement and the one that removes many otherwise acceptable materials from the tables given below. We have arbitrarily considered materials which require a minimum of 15 ft-lb of energy to break a Charpy keyhole specimen at temperatures of -40°F as adequate to meet the regulations; such toughness should be sufficient to prevent brittle fracture from occurring at low temperatures.

The designer may specify materials other than those recommended in this chapter provided he considers the factors described above; and the design analysis reflects these considerations.

A listing of special materials used in shipping casks for radiation shielding and criticality control is also provided to assist the designer.

3.1 Plate

Recommended carbon, low alloy and stainless steel plate specifications are listed in Table 3.1. These materials have good strength and ductility and are adequate for service at -40°F . The ASTM A300 steels are given mandatory impact tests and are specially manufactured for low temperature service by control of composition, melting practice and heat

treatment; this material is difficult to procure in small quantity with reasonable delivery schedules. However, the ASTM A516 grades 55 and 60, not procured to A300 requirements, have proven to be sufficiently tough at low temperatures that individual impact tests of different heats is not required; this material is available in small quantities. A533, a nuclear reactor grade steel, is also considered to be an acceptable material.

Several grades of austenitic stainless steel plate conforming to ASTM Specification A240 are listed. Stainless steel, although more expensive, has inherent characteristics which are often ideally suited for certain portions of a shipping cask. The material has good strength and ductility over a wide range of temperatures; has no ductile-to-brittle transition at low temperatures; has excellent corrosion resistance particularly for chemicals used in decontamination, and good forming and welding properties. The particular grades recommended were selected to provide a balance of all the factors involved. ASTM A240 type 304 is suggested unless the application requires the added corrosion resistance for decontamination in the heat-affected weld zone that is provided by 304L, 321, and 347.

Stainless steel clad plate is listed for the situation in which the designer desires to take advantage of both carbon and stainless steel in his cask design.

Table 3.1 Recommended Plate Materials

Material Type	ASTM Specification and Grade	
Carbon and low alloy steel	A300	A516 all grades A203 A and B
	A516 ¹	Grades 55 and 60
Low alloy steel	A533	Grades A, B, and C
Stainless steel	A240	Types 304, 304L, 321, and 347
Stainless clad steel	A264 with A300 or A516 base metal and A240 cladding	

¹Manganese content shall be 0.85 to 1.20% All plate shall be normalized by the mill and so marked.

3.2 Pipes and Tubes

Suggested carbon and stainless steel pipe and tube specifications are shown in Table 3.2. These steels have adequate resistance to brittle fracture at -40°F and like the plate materials, they are weldable grades of moderately strong, ductile materials.

Table 3.2 Recommended Pipe and Tube

Material Type	ASTM Specification and Grade
Carbon steel pipe	A333 Grades 1 and 6
Stainless steel pipe	A312 Types 304, 304L, 321, and 347
Carbon steel tube	A334 Grades 1 and 6
Stainless steel tube	A213 Types 304, 304L, 321, and 347

3.3 Forgings, Fittings, and Bolting

Forging, weld fitting and bolting materials having mechanical and chemical properties comparable or better than those listed for plate are given in Table 3.3. The low alloy steels selected are specifically produced for sub zero temperature applications. The stainless steels listed have good strength at both -40°F and elevated temperatures.

Table 3.3 Suggested Material Specifications
for Forgings, Fittings, and Bolting

Material Type	ASTM Specification and Grade
Low alloy steel forgings	A350 Grades LF1 and LF2 A508 Classes 4, 4A, 5, and 5A
Stainless steel forgings	A182 Types 304, 304L, 321, and 347 A473 Types 304, 304L, 321, and 347
Low alloy steel fittings	A420 Grade WPL1
Stainless steel fittings	A403 Grades WP304, 304L, 321, and 347
Low alloy steel bolting	A320 Grade L7, L10, and L43
Stainless steel bolting	A193 Types B8, B8C, and B8T

3.4 Welding Electrodes, Rods, and Wire

The following filler metal specifications are applicable to shipping cask fabrication: ASTM A316, A371, B295, and B304. The filler metal used in a particular weld will depend upon the base metal or metals being joined together.

3.5 Special Materials

Lead used for shielding is normally specified as ASTM B29, pig lead, chemical grade. A 4% antimony-lead alloy has been used for greater rigidity and because of its ability to wet steel. However, these gains are partially offset by the lower melting point of 570°F versus 618°F for chemical lead.

Three materials used for criticality control are as follows:

Pure cadmium metal purchased to ASTM B440.

Stainless steel containing small quantities of natural boron or boron enriched in ^{10}B .

Boral plate, a uniform dispersion of boron carbide crystals in aluminum with a cladding of commercially pure aluminum such as produced by Brooks and Perkins, Inc. of Detroit, Michigan.

3.6 Identification Marking and Purchase Order Requirements

Information regarding identification marking and purchase order requirements of materials are given in Sect. 4.1 of this guide.

4. FABRICATION

The fabrication and inspection requirements for shipping casks are not covered by existing codes and standards. This chapter sets forth minimum quality assurance requirements as part of the Guide; it has been prepared so that any or all sections may be incorporated into procurement specifications.

The designer is expected to prepare engineering drawings and specifications as appropriate for the particular requirements of the shipping container. The specifications shall include as a minimum the applicable requirements of this chapter as a quality assurance program to be followed during fabrication and testing. Additional requirements may be added as necessary.

The purchaser shall bear the primary responsibility for assuring that the shipping container is fabricated in accordance with the appropriate regulations.

The Inspector is the representative of the purchaser. He is responsible for auditing the manufacturer's procurement, fabrication, inspection, and testing to the extent that he is satisfied that the shipping container complies with the contract. The Inspector is expected to visit or be in residency at the fabricator's plant as required to discharge his responsibilities.

The manufacturer is responsible to conform to the contract. As part of this responsibility, he shall provide competent quality control personnel who will perform the prescribed inspections and tests to the satisfaction of the purchaser's inspector. In addition, he shall maintain a Fabrication Record including such information as mill test reports, in-plant procedures, standards and specification, heat treat charts, all approved deviations, test and inspection results, and "as-built" drawings. This Record shall be delivered to the purchaser at the completion of the contract.

4.1 Materials

Only materials of construction which conform to the drawings and specifications shall be used in fabrication.

4.1.1 Mill Test Reports and Marking

Purchase orders for material except for ASTM A403 and A420 shall include the requirement that a certified mill test report be furnished. The mill test report shall include the ASTM Specification number, the manufacturer's name, the heat number, and the results of all chemical analysis and mechanical properties test results. Orders for A403 welding fittings shall state that the manufacturer shall furnish a certification of conformance. Orders for A420 welding fittings shall state that the manufacturer shall provide the results of the chemical analysis, the results of the impact tests and the heat treatment applied to the material and the test pieces.

The purchase order should also state that all material shall be marked in accordance with the applicable ASTM Specification.

4.1.2 Cutting Material

When oxyacetylene or an arc process is used for cutting material, all slag and previously molten material shall be removed by mechanical means prior to further fabrication or use.

Edges that will be exposed in the finished cask shall be rounded (grinding is permitted) to a radius of at least 1/8 in. or chamfered at 45° to at least 5/32 in. flat.

4.1.3 Repair of Defects in Materials

Minor defects in material may be repaired, provided that the Inspector approves the method and the extent of repairs. Defective material that cannot be satisfactorily repaired shall be rejected.

4.1.4 Forming Materials

Materials may be formed to the required shape by any process that will not unduly impair the physical properties of the material.

4.2 Identification and Control of Materials

The marking on each piece of material shall be retained until fabrication is complete. If the material is cut into two or more parts, or if the marked surface is to be removed, the marks shall be carefully transferred prior to cutting.

Unless it can be positively identified, any piece of material whose marking is lost or removed must be classified as "not fully identified" material and subjected to the tests of Sect. 4.8.2 before it is re-marked and used in fabrication.

The manufacturer shall maintain a detailed record that lists the description and marking of each piece of material used in the fabrication, and shall correlate this information with material test reports. This record shall be incorporated into the Fabrication Record (see Sect. 4.10.)

4.3 Welding

Production welding shall not be undertaken until both the welding procedure and the welders or welding operators have been qualified. All such qualifications must be approved by the Inspector. Brazing and pressure welding processes are not permitted.

4.3.1 Welding Processes and Filler Metals

Stainless Steel to Stainless Steel. - Any arc-welding process may be used without including impact tests as a part of the procedure qualification.

Stainless Steel to Carbon Steel. - Any arc-welding process may be used. The filler metal shall be stainless steel ASTM A298 or A371 Class E309, or Inconel ASTM B295 Class E Ni CR Fe-2 or ASTM B304 Class ER Ni CR Fe-6.

No impact tests are required.

Carbon Steel to Carbon Steel. -- The shielded metal-arc process may be used with ASTM A316 Class E3016 or 8018-C1, C2, C3 electrodes without requiring impact tests as a part of the procedure qualification. The use of other electrodes with the metal-arc process, or the use of other processes such as the gas-metal arc or submerged-arc processes, requires three impact tests of the deposited weld metal; the weld must have an average of 15 ft-lb of impact energy (Charpy keyhole) at -40°F in order to qualify as an acceptable process.

4.3.2 Qualification of Welding Procedures

Each welding procedure to be used in construction shall be qualified by the manufacturer in accordance with Sect. IX of the ASME Boiler and Pressure Vessel Code. A copy of the Procedure Qualification Test Report and the Welding Procedure shall be, after approval by the Inspector, incorporated into the Fabrication Record.

4.3.3 Qualification of Welders and Welding Operators

Performance qualification of welders and welding operators shall conform to Sect. IX of the ASME Boiler and Pressure Vessel Code. A copy of the Performance Qualification Test Report shall be, after approval by the Inspector, incorporated into the Fabrication Record.

A test conducted by one Manufacturer shall not qualify a welder to do work for any other Manufacturer.

4.3.4 Lowest Permissible Temperatures for Welding

When the temperature of the base metal is lower than 60°F, the area to be welded shall be preheated until it is warm to the hand. All surfaces shall be dry and protected from rain, snow, and high winds.

4.3.5 Fitting and Alignment

Edges to be welded shall be uniform and free of all foreign material (see Sect. 4.1.2).

Parts to be welded shall be fitted, aligned, and retained in position during the welding operation.

Bars, jacks, clamps, tackwelds, or other appropriate means may be used to hold the edges to be welded in line. Tackwelds may be incorporated in the final weld, provided they are free of visible defects.

The edges of butt joints shall be held during welding in such a manner that the tolerances stated in Sect. 4.3.7 are not exceeded in the completed joint.

4.3.6 Cleaning of Surfaces to be Welded

Surfaces to be welded shall be clean and free of foreign material such as grease, oil, lubricants, and marking paints, for a distance of at least 1 in. from the welding edge. Detrimental oxides shall be removed from the weld preparation area. When weld metal is to be deposited over a previously welded surface, any slag shall be removed.

4.3.7 Joints - Alignment Tolerances

Abutting edges of parts at joints shall not, after being welded, have an offset from each other at any point in excess of one-eighth of the nominal thickness of the part at the joint.

4.3.8 Finished Joints

Joints shall have complete penetration and shall be free from cracks, undercuts, overlaps, abrupt ridges, or valleys. Fillet welds shall have complete fusion at the root of the fillet. To ensure that the weld grooves are completely filled so that the surface of the weld metal at any point does not fall below the surface of the adjoining part, weld metal may be built up as a reinforcement on each side of the joint. The thickness of this reinforcement shall not exceed the following dimensions:

<u>Thickness of Part (in.)</u>	<u>Maximum Thickness of Reinforcement (in.)</u>
Up to 1/2, inclusive	3/32
Over 1/2 to 1, inclusive	1/8
Over 1	3/16

4.3.9 Miscellaneous Welding Requirements

The reverse side of double-welded butt joints shall be prepared by chipping, grinding, or melting out, so as to secure sound metal at the root of the weld before applying filler metal from the reverse side. This requirement is not intended to apply to any process of welding by which proper fusion and penetration are otherwise obtained and by which the base of the weld remains free from impurities.

If the welding is stopped for any reason, extra care shall be taken in restarting the process to achieve the required penetration and fusion. For submerged arc welding, chipping out a groove in the crater is recommended.

Where single-welded joints are used, particular care should be taken in alignment to ensure complete penetration and fusion at the root of the weld over its full length.

In the case of plug welds, a fillet around the bottom of the hole should be deposited first.

4.3.10 Repair of Weld Defects

Visible defects such as cracks, pinholes, and incomplete fusion, as well as defects that can only be detected by prescribed examinations or tests, shall be removed and the joint rewelded (see Sect. 4.1.2).

4.4 Weld-Metal Cladding of Carbon Steel

4.4.1 Welding Procedure Qualification Requirements

A separate welding procedure shall be qualified for the corrosion-resistant weld-metal overlay cladding of carbon-steel-base metal, in accordance with Sect. IX of the ASME Boiler and Pressure Vessel Code. In addition, when any of the changes listed below are made, the procedure shall be requalified; other changes do not require requalification, but the procedure specification must be corrected to show the changes.

For All Welding Processes:

- (1) A change from one welding process to any other welding process or combination of welding processes.
- (2) A change in the composition of the deposited weld metal from one A-Number in Table Q-11.3 of Sect. IX of the Code to any other A-Number or to an analysis not listed in the table; however, each AISI type of A-7 or A-8 analysis (Table Q-11.3) requires separate qualification.
- (3) The addition of welding positions other than those already qualified.
- (4) A change in the specified preheating temperature range.
- (5) A change in the specified heat-treating temperature or an increase of 25% or more in the total time at temperature.
- (6) A change from a multiple weld layer to a single weld layer, or vice versa.

For Shielded Metal-Arc Welding:

- (1) A change in the electrode diameter used for the first layer.
- (2) A change from one F-Number in Table Q-11.2 to any other F-Number (notes 2 and 3 in Table Q-11.2 shall apply).
- (3) An increase of more than 10% in the amperage used in the application of the first weld layer.

For Submerged-Arc Welding:

- (1) A change in the composition or type of flux used. Requalification is not required for a change in flux particle size.
- (2) A change from single-wire to multiple-wire techniques.
- (3) A change from ac to dc or from dc to ac current, or a change in the polarity of the current.
- (4) The addition or elimination of oscillation of the electrode.

- (5) A variation of more than 10% in travel speed.
- (6) A change in wire diameter.

For Gas Tungsten-Arc Welding or Gas Metal-Arc Welding:

- (1) A change from one gas to another, or to a mixture of gases.
- (2) A reduction of 25% in the rate of gas flow.
- (3) A change from an inert gas or a mixture of inert gases to a shielding gas containing more than 2% of an active gas (e.g., oxygen or hydrogen).
- (4) A change from single-wire to multiple-wire techniques.
- (5) A change from ac to dc or from dc to ac current, or a change in the polarity of the current.
- (6) The addition or elimination of oscillation of the electrode.
- (7) A variation of more than 10% in travel speed.
- (8) A change in wire diameter.

The procedure qualification shall be made on a test plate that simulates the conditions to be used in production with respect to essential variables, except that the test plate may be thinner than the material used in production but shall not be less than either 3/4 in. or the thickness of the fabrication material, whichever is less. The postweld heat treatment of the test plate shall be equivalent to that to be applied to the parts, except that the total time at temperature may be achieved during one heating cycle.

The weld overlay surface shall be examined using a liquid penetrant in accordance with Sect. 4.8.5. Following this examination, the test plate shall be sectioned to make four side-bend test specimens, two parallel and two perpendicular to the direction of welding. These shall have dimensions identical to those of the guided side-bend specimens noted in Sect. IX of the ASME Boiler and Pressure Vessel Code. The specimens shall be bent in a test jig and shall meet the acceptance requirements of Sect. IX, except that the maximum allowable defect in the cladding

shall be 1/16 in. In addition, a chemical analysis shall be obtained from the overlay at a depth from the surface of at least 0.020 in. The chemical analysis obtained shall be within the range of analysis given in the procedure specification.

4.4.2 Performance Qualification Test

Welders and welding operators shall be qualified on metal plate that is either not less than 3/4 in. thick or the thickness of the material to be used in fabrication, whichever is thinner, in accordance with the requirements of a qualified weld-metal overlay cladding procedure specification.

The essential variables of Paragraph Q-22 of Sect. IX of the Code shall apply. The test plate shall be subjected to the penetrant and bend tests as noted in Sect. 4.4.1, except that the chemical analysis need not be made. Any welder or welding operator who qualifies the procedure is automatically qualified.

4.5 Joining Integrally Clad or Weld-Metal-Overlay Clad Material

Each welding procedure used in joining clad material shall be qualified by the Manufacturer in accordance with Sects. VIII and IX of the ASME Boiler and Pressure Vessel Code using clad material. A separate welding procedure and qualification is required for welds that join clad material to austenitic stainless steel. Test welds shall be heat treated if the fabricated material is to be heat treated.

The performance qualification of welders to join clad material shall conform to Sects. VIII and IX of the ASME Boiler and Pressure Vessel Code. Performance tests should be made, using clad material before a welder is permitted to weld base metal, cladding, or the composite joint.

4.6 Postweld Heat Treatment

Postweld heat treatment is neither required nor prohibited.

Any postweld heat treatment shall be documented and made a part of the Fabrication Record.

4.7 Lead Pouring

Lead pouring shall be done in a single, continuous operation unless a method is developed and proven by a test which will assure no high, local radiation at lead interfaces resulting from multiple pours.

The manufacturer should prepare a detailed lead-pouring procedure which will provide such information as to the grade and purity of the lead, the grade of any tinning compounds, a description of the heating, pouring and cooling facilities (including sketches), the sequence of operations, a precleaning or pretinning procedure (if used), the method and speed of pouring, preheating and controlled cooling methods, temperature control requirements and measurements, and details of pouring and vent connections.

After approval by the Inspector, the lead pouring shall be performed in accordance with the procedure and a copy of the Lead Pouring Procedure shall be incorporated into the Fabrication Record.

4.8 Inspection

4.8.1 Access for Inspector

The Inspector shall be permitted free access, at all times while work on the fabrication is being performed, to all parts of the manufacturer's shop concerned with the fabrication. The manufacturer shall keep the Inspector informed of the progress of the work, and shall notify him reasonably in advance of any required tests or inspections.

4.8.2 Inspection of Material

The Inspector shall assure himself that all materials used comply in all respects with the material requirements given in Chap. 4.1.

The manufacturer shall make available to the Inspector certified mill test reports or certification of compliance records in the case of ASTM A403 and A420 material prior to the use of the material. The Inspector shall satisfy himself that the material complies with the specifications and is properly marked and correlated with the mill test reports.

A copy of all approved test reports and certifications shall be incorporated into the Fabrication Record.

If there is a question regarding the identity or adequacy of the material, the fabricator shall perform chemical analysis and mechanical tests to verify that the material complies with the applicable specification. Reports of such tests shall be reviewed by the Inspector and if approved, such records shall be placed in the Fabrication Record.

All materials to be used in fabricating a cask shall be inspected for the purpose of detecting, as far as possible, defects that would affect the adequacy of the fabrication.

Particular attention should be given to cut edges and other parts of rolled plate that would disclose the existence of serious laminations, shearing cracks, and other objectionable defects.

The Inspector shall assure himself that the thickness and other dimensions of the material comply with those specified on the design drawings.

4.8.3 Inspection of Surfaces During Fabrication

As fabrication progresses, the edges of plates, openings, and fittings shall be examined to detect defects as well as to determine that the work has been properly done.

4.8.4 Dimensional Inspection

The Inspector shall satisfy himself that components conform to the prescribed shape and meet thickness requirements after forming.

The Inspector shall assure himself of the proper fit, to the curvature of the surface, of appurtenances to be attached to curved surfaces.

During and after fabrication, such dimensional inspections as are necessary shall be performed to ensure that the completed fabrication conforms to the design drawings and that mechanical parts can be physically assembled.

Any critical feature requiring special inspection, such as the flatness or the surface finish of gasket seats, shall be specifically indicated on the design drawings. A report of the dimensional inspection of all such features shall be incorporated into the Fabrication Record.

4.8.5 Weld Inspection

The Inspector shall assure himself that the welding procedures employed in the fabrication have been qualified under the provisions of this Criteria.

The Inspector shall assure himself that only welders and welding operators that are qualified under the provisions of this Criteria are being used to fabricate the weldment.

The Inspector shall have the right, at any time, to call for and to witness tests of the welding procedure or tests to determine the ability of any welder or welding operator.

All welds, including the heat-affected zone, shall be inspected at least twice with liquid penetrants, using Procedure A-2 or B-3 of ASTM E165, or with magnetic particles, using ASTM E109, first on completion of the root pass, after preparing the second side of welds made from two sides, (if appropriate) and second, after completing the weld. Finished welds shall be inspected on both surfaces after heat treatment and/or any machining. Cracks, in-line porosity, or other linear defects should be removed down to sound metal and then repaired. Adequate penetrant inspection will, in most cases, require some grinding of the welds.

4.8.6 Check of Postweld Heat-Treatment Practice

The Inspector shall satisfy himself that any postweld heat treatment is correctly performed and that the temperature readings conform to the requirements. A copy of the heat-treatment procedure and furnace charts shall be incorporated into the Fabrication Record.

4.8.7 Inspection During Fabrication

The Inspector shall inspect each component, at such stages of construction as he deems necessary, to assure himself that fabrication is in accordance with the design drawings.

Interior surfaces of enclosed chambers shall be examined as completely as possible before final closure is made.

4.9 Testing

4.9.1 Shielding Chamber Leak Test

Before any shielding chamber is filled with shielding material, the integrity of the chamber shall be demonstrated by a leak test. A shielding chamber that is partly completed at the time of introduction of shielding material shall be leak tested twice: before shielding material is added, and when the chamber is completed. In any instance, testing shall be performed while joints are accessible for repair and before any leak paths can be plugged with shielding material.

Leak tests may be performed by any procedure that can be demonstrated to have a sensitivity of 1 cm^3 (STP) of air per hour. Acceptable test methods are: mass spectrometry, helium leak detection, halogen leak detection, vacuum rate-of-pressure-rise, and pressurized soap bubble.

If leakage is indicated, the leaks shall be located, repaired, and the test repeated.

4.9.2 Pressure Test

After fabrication is complete, the cavity and any other chamber that is pressurized in service shall be subjected to a pressure test to demonstrate structural integrity.

Each chamber to be tested shall be separately filled with water and pressurized to twice the maximum normal operating pressure or 40 psig, whichever is the greater. Pressure shall be held for 10 min.

For the purposes of this test, gaskets other than service gaskets may be used.

4.9.3 Leak Test

After the pressure test is complete, the cask shall be assembled with a service gasket, and the cavity shall be subjected to a leak test.

The cavity shall be pressurized to 1-1/2 times the maximum normal operating pressure or 7-1/2 psig, whichever is greater, with a gaseous mixture containing at least 10% of a test gas to which the leak detector is sensitive. Testing may be done by using a helium mass spectrometer or a halogen leak detector if the testing procedure has been demonstrated to have a sensitivity equivalent to 1 cm³ (STP) of air per hour at the test differential pressure. All accessible welded and mechanical joints shall be surveyed.

Any indication of leakage shall require repair and retesting of the cask.

4.9.4 Heat Transfer Acceptance Test

If heat-transfer calculations indicate a cask surface temperature of 180°F or greater under normal conditions of transport, a heat-transfer test shall be performed before the cask is accepted by the purchaser.

The heat source provided in the cask cavity for use in the test shall be equal to or greater than 25% of the design heat load of the cask. The cask will be sealed, so far as is possible, in a manner ready for transport when the test is performed.

Temperatures shall be measured and recorded (using either thermocouples or temperature-sensitive paint) at a minimum of three points each on the inner and the outer cask shell. In addition, the temperature should be measured at points inside the cavity that could come in contact with the fuel (e.g., nuclear-poison divider plates).

Measured temperatures must be less than those calculated for the test heat load input, or the discrepancy reconciled. A report of these

tests, along with the original temperature records, shall become a part of the Fabrication Record.

The Inspector shall witness all heat-transfer tests and shall sign the original temperature record.

4.9.5 Shielding Integrity Test

Prior to initial use in shipping irradiated materials, the integrity of the shielding of each cask shall be demonstrated by loading the cask with the material for which it is designed or equivalent, insofar as is practical, and surveying the entire outer surface for radiation in excess of the allowable limits.

Gamma Scanning and Probing. -- Gamma scanning and probing inspection to determine the soundness of the lead as part of the manufacturing procedure is an optional test which may be required. In such cases the requirements are as follows:

The manufacturer shall prepare a gamma probe procedure which includes information concerning: the electronic equipment, radiation source and strength, calibration standards for both scanning and probing, grid pattern, scintillation crystal size, positioning equipment, the method of reading and recording the radiation detected, the measuring technique and acceptance requirements. The procedure shall be acceptable to the Inspector prior to its application. The procedure and all results shall be made a part of the Fabrication Record. If the above gamma scan and probe inspection is not carried out then prior to initial use and insofar as is possible, each cask shall be loaded with the material that it is intended to carry and the entire outer surface shall be surveyed for radiation in excess of the allowable limits.

4.9.6 Lead Bond Integrity Test

In those cases where the design requires a metallurgical bond between the lead and the shell and/or the lid, the manufacturer shall determine the percentage of bond by an ultrasonic inspection procedure. A detailed

procedure based on a standard shall be prepared and approved by the Inspector prior to its application. The information required by paragraph 7.7.1.2 of MIL-STD-2710 (SHIPS) shall be provided in the procedure.

The cask surfaces which will be contacted by the couplant and transducer shall be free of scale and foreign material. The Inspector shall be notified prior to the ultrasonic inspection so that he may have the option of witnessing any or all of the work. The procedure and all results shall be made a part of the Fabrication Record.

4.10 Fabrication Record

The manufacturer shall maintain currently in a Fabrication Record documents indicating compliance with this Criteria which includes, but is not limited to, the following:

- (1) A Material Record shall be kept and shall specify the following:
 - (a) Product form and heat number
 - (b) Correlation of part and test report
 - (c) Cask component name or part numberMarked drawings or annotated bills of material may be necessary to satisfy this requirement.
- (2) In compliance with the stipulations listed in Chap. 3, Material Test Reports for each item of material, or other evidence of acceptability, shall be incorporated into the Fabrication Record after the material has been accepted.
- (3) Welding procedure, procedure qualification, welder performance records, and lead pouring procedure.
- (4) Reports of all inspections and tests, including liquid penetrant examinations, dimensional inspections, and pressure and leak tests, shall be prepared in such detail that compliance with this Criteria is clearly demonstrated. If any radiographic inspection is performed, the radiographs shall be made a part of the Fabrication Record.

- (5) Reports of any required check analysis, clearly identified with the material they represent.
- (6) Where heat treatment is performed, the procedure followed, together with furnace temperature charts, shall be included in the Fabrication Record.
- (7) Any deviation, for any reason, from this Criteria shall be reported in detail in the Fabrication Record.
- (8) If, for any reason, the fabrication process deviates significantly from the design drawings, and those drawings do not present a clear and correct description of the construction of the cask or show proper sizes of materials and location and geometries of welds, the manufacturer shall prepare as-built drawings to accomplish this purpose. As-built drawings shall be verified and certified by the Inspector.

The Fabrication Record shall be assembled by the manufacturer and shall be kept current at all times. The Inspector shall have access to the Fabrication Record and, at regular intervals, shall assure himself that it is complete and correct. Any deficiencies found shall be promptly rectified by the manufacturer. On completion of the fabrication, the Fabrication Record shall be reviewed by the manufacturer and by the Inspector, each of whom shall certify, in writing, that the record is correct and complete and that the fabrication is (with noted exceptions) in complete conformity with this Guide. The Fabrication Record shall then be transmitted to the Purchaser.

The Inspector shall maintain a log in which he shall record the dates of his visits to the manufacturing plant, status of work at those times, notations of materials accepted, notations of inspections witnessed, difficulties encountered in fabrication, deviations from design details and specification, and a chronological record of the progress of the work. On completion of the job, the Inspector's log shall be incorporated into the Fabrication Record.

5. HEAT TRANSFER

5.1 Introduction

All shipping casks should be evaluated to determine their temperature response in thermal environments under normal and accident conditions. Specifically, the temperatures which should be determined are the maximum cask surface temperature and maximum fuel element temperature under normal conditions, the temperature distribution through the shield, and the maximum fuel element temperature under accident conditions.

The normal ambient temperature range is defined in the regulations to be -40°F to $+130^{\circ}\text{F}$. As a result of exposure to these temperatures there must be no release of radioactive material from the containment vessel. Under accident conditions the cask will experience a fire, whose temperature is 1475°F , for 0.5 hr. As a result, radioactivity released from the cask must not exceed the limits given in Table 5.1.

Table 5.1 Limits for Release¹

No radioactive material, except gases and contaminated coolant, may be released from the cask; the total radioactivity content of the coolant must not exceed either 0.1% of the total radioactivity of the cask contents or the following designated limits:

<u>Transport Group</u> *	<u>Curies</u>
I	0.01
II	0.5
III & IV	10.
Inert gases	1000.

*Specific isotopes are arranged in transport groups. The complete list is given in ref. 1.

Regulations do not specify temperature limitations on the cask or fuel; however, since fuel temperatures affect fuel integrity which in turn affects potential contamination if a cask leaks, temperature limitations should be considered by a designer for his specific cask and type of fuel. That is, it is prudent to restrict the temperature of the accessible surface of the cask system to 180°F under normal operating conditions. Such a temperature restriction, while presently not required for domestic shipments, is imposed by IAEA regulations for a cask being shipped "exclusive use." Secondly, the temperature of a lead shield should be restricted to below the melting point of lead (621°F). Finally, the temperature of the fuel should be kept as low as possible to help prevent release of activity from the fuel to the primary coolant.

For example, the fuel temperature under normal operating conditions can be restricted to that which was experienced by the fuel during reactor operation assuming such a temperature did not produce failed fuel elements. There may be an economic justification for operating at higher temperatures and the safety of such operating temperature should be specifically stated.

Under the 0.5 hr fire accident condition, fuel element temperatures will increase. The maximum temperature which the fuel should be permitted to reach under accident conditions will be affected by cladding material of construction, cladding thickness, fuel material, burnup, cooling time, specific power, fuel damage caused by impact, etc. It is impossible to indicate precisely how or to what extent each item will affect the maximum permissible fuel temperatures but some general statements may be made.

The maximum temperature reached by the cladding under accident conditions should be less than the temperature at which the fuel ruptures, releasing gross quantities of fission products to the cask cavity. This perforation temperature will vary with the fuel cladding material, its thickness, history in the reactor, fuel element geometry, etc. It should be calculated for each type of fuel element under the accident conditions if the cask designer wishes to push his temperature to the maximum. Other

things being equal, stainless steel clad fuel can generally withstand higher temperatures than Zircaloy-clad fuel.

If embrittlement of the cladding has occurred to a significant extent as a result of high burnup or high specific power and/or if the buildup of pressure in the gas space in the fuel element produces excessive stresses in the cladding at the cask operating pressure, the perforation temperature could be affected.

If the fuel elements are individually contained in sealed canisters, temperature limitations should be considered on the basis of good engineering practice by the cask designer.

The subjects covered in this chapter include heat sources, external heat transfer under normal conditions, internal heat transfer under loss-of-coolant conditions and fire analysis of the shield. This will allow estimation of the first three temperatures which were suggested as necessary in the first paragraph of Sect. 5.1. Maximum fuel element temperatures can be calculated utilizing numerical methods capable of determining individual fuel element response under transient conditions. Digital computer codes utilizing such methods are available^{2,3,4,5} and have been used for this purpose. Each code requires considerable experience to obtain best results for a given problem and thus no comparison of the codes is made here.

5.2 Heat Sources

The cask surface temperature under normal operating conditions is dependent upon the heat which the cask must dissipate to the environment. The heat stems from two sources; namely, the decay heat load caused by radioactive decay of isotopes within the material being shipped, and the solar heat load which results from the impingement of solar radiation on the surface of the cask. Both sources change with time, but variations in the decay heat load is generally insignificant during shipment. Decay heat is usually the major portion of the total heat load that must be dissipated.

The contribution of solar radiation to the total cask load rarely exceeds 15% of the entire amount of heat that the cask must reject. The solar heat load depends on the projected surface area of the cask, the condition of the cask surface, the season of the year, the hour of the day, and other factors enumerated in Sect. 5.2.2.

5.2.1 Decay Heat Load

The amount of decay heat generated by a spent fuel element is dependent on the time the fuel element spends in the reactor (irradiation time), the number of fissions occurring per unit time in the element and the time an element has to decay before it is shipped (cooling time). A "typical" thermal power reactor fuel element with a cooling time of 120 days would be expected to generate heat at a rate of from 2 to 7 kw.

One of the most recent calculational tools recommended for determining decay heat is a code developed at Oak Ridge National Laboratory⁶ in which experimental data^{7,8,9} has been used to cover a wide range of cooling periods. The code utilizes the fission rate (operating power), irradiation time, and cooling time as input variables. A parametric representation of the decay heat source that was constructed by use of the code is presented in Fig. 5.1. Figure 5.2 presents the same data replotted such that the effect of burnup and specific power on the decay heat can be seen. The data used in the construction of Figs. 5.1 and 5.2 were based on the decay of fission products resulting from the thermal fission of ^{235}U . Fission product yields vary with neutron energies and the fissionable isotopes;^{10,11,12,13} however, the data for ^{235}U can be used for the thermal fission of ^{239}Pu and the fast fission of ^{235}U and ^{239}Pu with little error in the calculation of decay heat.

Figures 5.1 and 5.2 may be used to determine Q_d , the decay heat generation rate, of an average fuel element by determining the information given in List 1. Items 4a and 4b may be used to calculate Item 3.

List 1

1. Reactor operating power in megawatts
2. Cooling time in days

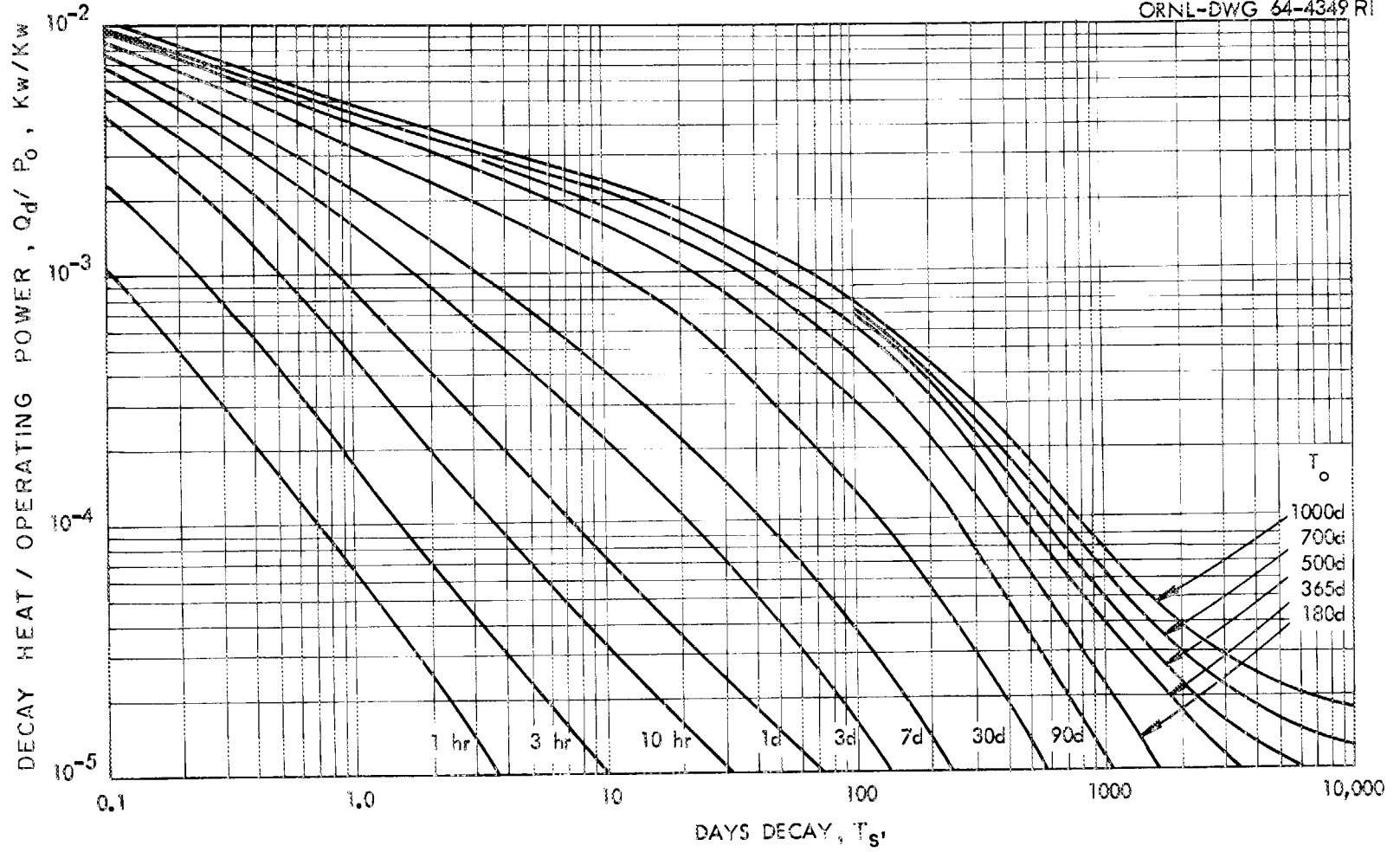


Fig. 5.1. Decay Heat, Q_d , from ^{235}U Fuel as a Function of Operating Power, P_o , Operating Time, T_o , and Decay Time, T_s .

ORNL DWG 67-6893 R1

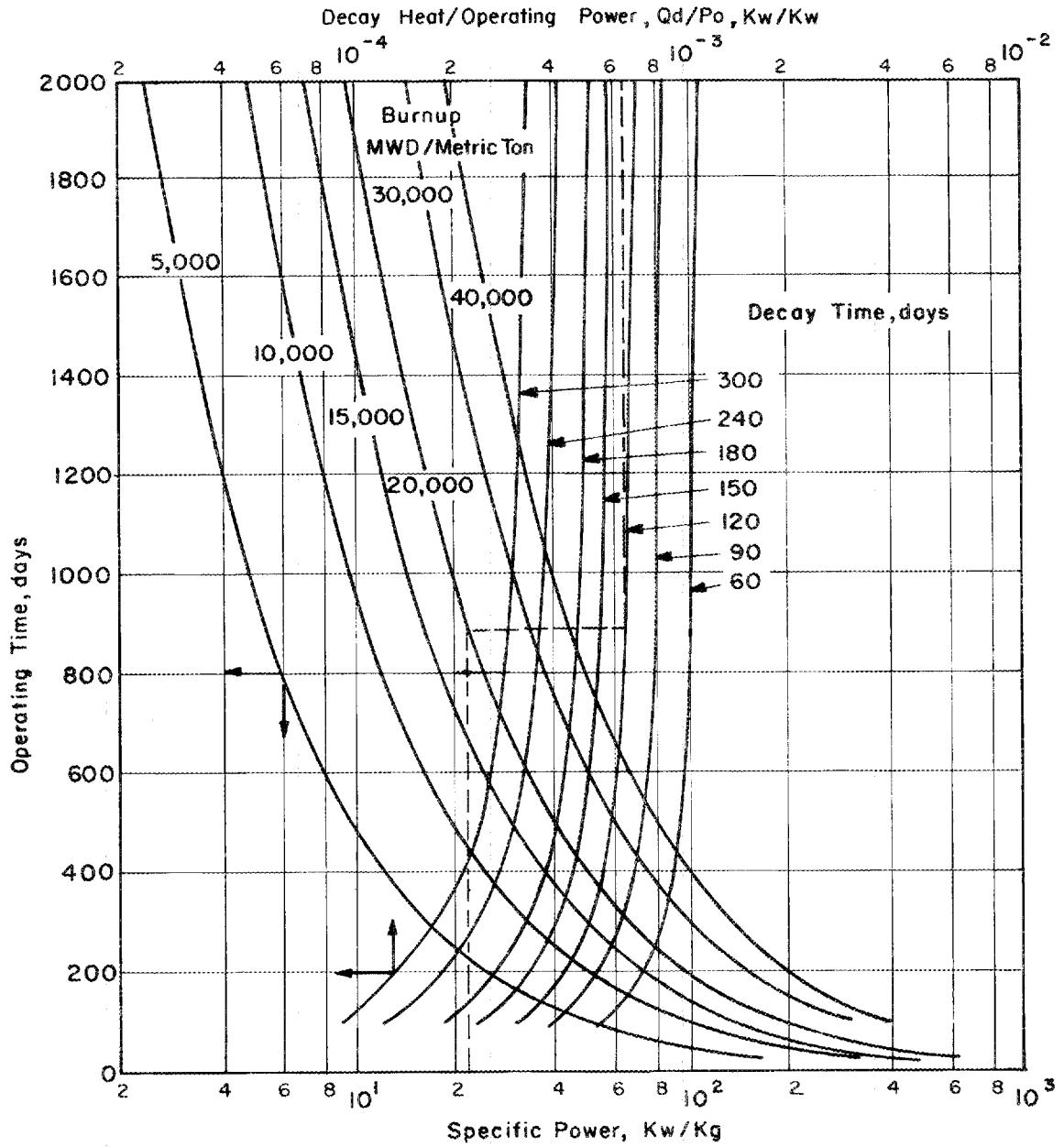


Fig. 5.2. Ratio of Decay Heat to Power for Spent Fuel Elements.

3. Reactor operating time, days
4. a) Fuel burnup, MWD/metric ton
 - b) Reactor fuel loading, kg

Example: If a reactor had the following design characteristics, determine the decay heat of one average fuel assembly that has been allowed to cool for 120 days.

Reactor burnup	20,000 MWD/metric ton fuel
Reactor fuel loading	4350 Kg
Operating power of one reactor	100,000 Kw
Number of fuel assemblies	20
Specific power =	$\frac{100,000 \text{ Kw}}{4350 \text{ kg}} = 23 \text{ Kw/Kg}$

Applying this data to Fig. 5.2, we obtain a value of 6.5×10^{-4} for the ratio of decay heat/operating power. (Note Fig. 5.2 could be entered from either the ordinate or abscissa.)

Assuming that the operating power of one average fuel assembly is $\frac{100,000 \text{ kw}}{20 \text{ assemblies}} = 5000 \text{ kw/assembly}$, the decay heat may then be computed by

$$Q_d = (5000 \text{ kw/assembly})(6.5 \times 10^{-4}) = 3.25 \text{ kw/assembly}$$

5.2.2 Solar Heat Load

The rate at which the earth intercepts solar energy on a surface normal to the sun's rays at a point above the earth's atmosphere is 142 Btu/hr-ft², or 10,600 Btu/ft²-day; this value, known as the solar constant, increases (decreases) 3.5% in December (June). The amount of solar radiation received at a point on the surface of the earth on a clear day when the sun is at the zenith varies, but 70% of the solar constant value generally is considered sufficiently accurate for engineering purposes.

Total solar radiation is made up of both direct radiation from the sun and diffuse or scattered solar radiation; this latter contribution is small and can be neglected when considering maximum daytime heating rates.

Values of the solar heat load can be calculated for each surface of the cask and the sum of these values yields the total solar heat load which is then normally added to the decay heat load to estimate the heat which must be rejected by the cask.

Exact values as a function of latitude, time of day, time of year, tilt of the surface, etc. can be calculated by referring to standard heat transfer texts,^{14,15} but a quick estimation of hourly solar heating rates on clear summer days on variously oriented surfaces¹⁶ may be made by referring to Fig. 5.3.

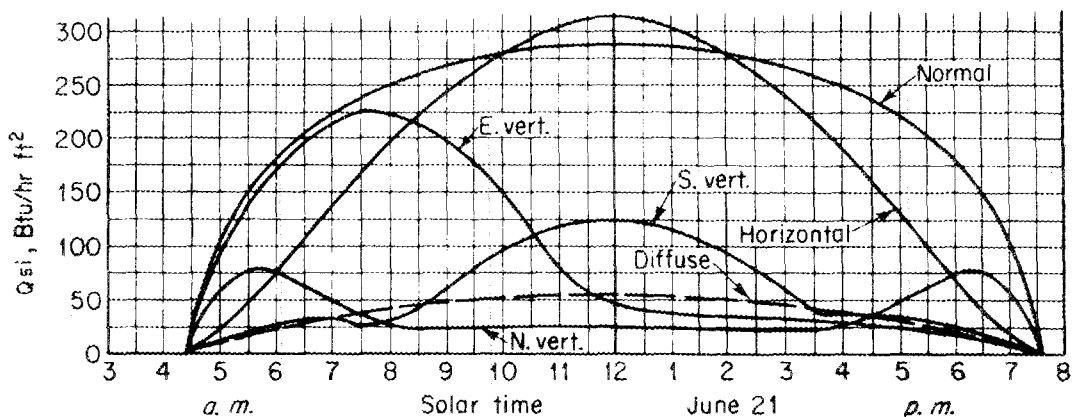


Fig. 5.3. Incident Solar Energy on Clear Days, Latitude 42°N.

The curves marked N. Vert., S. Vert., and E. Vert. indicate the total amount of solar plus scattered radiation received by vertical surfaces facing north, south, and east, respectively. The solar energy received by a vertical west wall may be considered as the mirror image of that given for E. Vert. rotated around the 12:00 noon line. The curves marked horizontal and normal indicate the solar energy received by a horizontal surface and a surface that is always normal to the sun's rays.

All curves, except that one referring to the normal surface, include the contribution of diffuse radiation to the total heat load; the diffuse radiation for a horizontal surface is separately noted in Fig. 5.3.

Figure 5.4 gives the relative total daily radiation incident on a horizontal or south-facing vertical surface as a function of latitude.¹⁷ Multiplication of the appropriate values from Fig. 5.4 by the 24-hour solar constant (10,600 Btu/ft² day) and the local mass transmittance of the earth's atmosphere (~ 0.7) gives the daily incidence on a vertical or horizontal surface. Scattered radiation is not included.

To determine the heat load affecting a given surface, the incident heating value, Q_{si} , given in Fig. 5.3 must be multiplied by the absorptivity (emissivity), α_{solar} , of that surface; i.e., $Q_s = Q_{si} (\alpha_{solar})$. Values of α are given in Table 5.2.

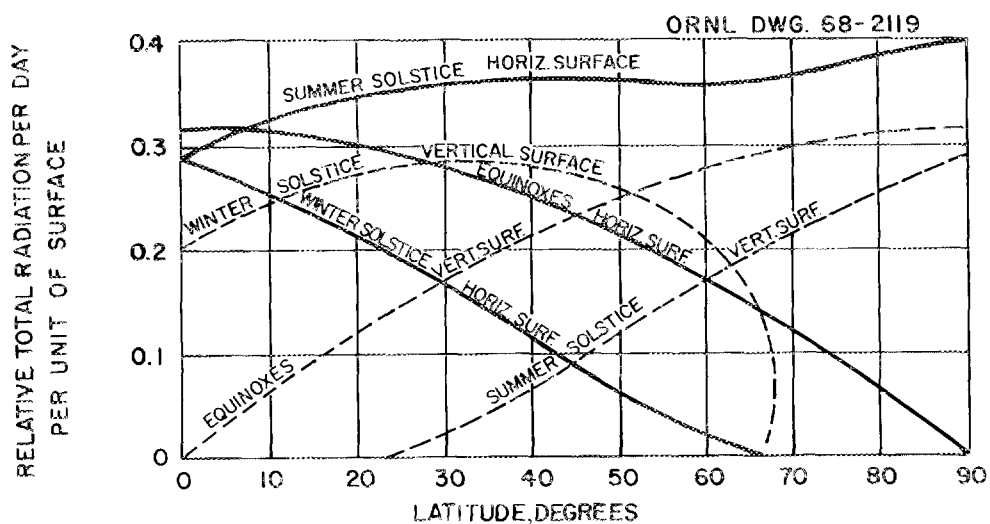


Fig. 5.4. Relative Total Daily Solar Radiation Incident on a Horizontal or South Facing Vertical Surface as a Function of Latitude.

Note that, for most polished metals, the emissivity (absorptivity) of the surface is higher when exposed to solar radiation than when exposed to lower temperatures or longer wavelength radiation. There are paints that may be applied to such surfaces to reverse the situation. White zinc oxide paint has a low value of emissivity at solar wavelengths (0.18), but at 100°F the emissivity is high (0.95). This is the ideal situation since a surface freshly painted with zinc oxide paint

Table 5.2. Emissivities of Various Materials

Material	Temperature	
	100°F ^a	Solar ^a
<u>Metals</u>		
Aluminum		
Polished	0.04	.26
Oxidized	0.11	
24-ST weathered	0.4	
Anodized (at 100°F)	0.94	
Chromium		
Polished	0.08	0.49
Iron		
Polished	0.06	0.45
Cast, oxidized	0.63	
Galvanized, new	0.23	0.46
Galvanized, dirty	0.28	0.89
Steel plate, rough	0.94	
Stainless steel		
18-8, polished	0.15	
18-8, weathered	0.85	
<u>Paints</u>		
Aluminized lacquer	0.65	
Cream paints	0.95	
Lacquer, black	0.96	
Lampblack paint	0.96	0.97
Red paint	0.96	0.74
Yellow paint	0.95	0.30
Oil paints (all colors)	0.94	
White (ZnO)	0.95	0.18

^aSee refs. 14 and 15.

would absorb little solar radiation, yet would have a high emissivity at lower operating temperatures.

5.3 External Heat Transfer

The analytical procedures described below were developed to analyze heat transferred from the external surface of a cylindrical cask and to account for variations in the cask geometry (i.e., the cask may be either finned or unfinned, and be positioned vertically or horizontally). It is assumed that the container is resting on its shipping skid and is surrounded by essentially stagnant air. Heat is transferred from the cask surfaces by radiation and by natural convection to the environment. At cask surface and ambient air temperatures normally encountered, both the amount of heat transferred by convection and radiation are significant and neither can be neglected.

The surface area (of a typical cylindrical cask) that is available for rejecting its heat load is not easily defined. The major portion of the total surface area consists of the cylindrical sides of the cask which will not be uniformly effective in transferring heat because a portion of the surface may be either in contact with, or facing, a solid surface (the vehicle deck) of indeterminate temperature and surface emissivity. This is particularly true when the cask is designed to be shipped with its major axis oriented horizontally. Occasionally the ends of the cask are neglected when considering external heat transfer although under some circumstances they could reject a significant fraction of the heat load.

A finned surface on a cask is quite common, particularly for casks designed for large heat loads. The fins are designed either circumferential or longitudinal depending on the expected orientation of the cask during shipping.

5.3.1 Heat Removal from a Cask Surface

The basic equation that describes convection and radiation from the cask surface is

$$Q_T = h_c A_c (T_s - T_a) + 0.173 \bar{F}_{12} A_r \left[\left(\frac{T_s + 460}{100} \right)^4 - \left(\frac{T_a + 460}{100} \right)^4 \right] \quad (5.1)$$

where

Q_T = total heat transferred, Btu/hr

h_c = the convective heat transfer coefficient, Btu/hr-ft²-°F

A_c = the effective convective surface area, ft²

A_r = the effective radiative surface area, ft²

T_s = the cask surface temperature, °F

T_a = the ambient temperature, °F

\bar{F}_{12} = the gray-body shape factor

This equation, which assumes a uniform cask surface temperature, cannot easily be expressed parametrically in graphical form owing to the difference in A_c and A_r . If the cask is unfinned, however, $A_c = A_r = A$ and Eq. (5.1) can be simplified to

$$Q_T = h_t A (T_s - T_a) \quad (5.2)$$

where h_t accounts for both convection and radiation.

The following stepwise procedures, which treat the unfinned and finned types of shipping container, are recommended for calculating the heat rejected from the cask surface to the environment under normal conditions.

Analysis of an Unfinned Cask. - If the total heat load of an unfinned cylindrical cask is known, determination of the external surface temperature, T_s , involves a trial-and-error solution of Eq. (5.1) with $Q_T = Q_d + Q_s$ (Q_d is the decay heat and Q_s the solar heat load). The procedure is as follows:

1. Compute the Heat Transfer Area. - If we neglect the ends of an unfinned cask, the areas available for the rejection of heat by convection and radiation are equal and are given by:

$$A_c = A_r = A = \pi D_o L . \quad (5.3)$$

2. Assume a Cask Surface Temperature, T_s .

3. Determine the Heat Transfer Coefficient. - McAdams^{1,8} recommends the simplified dimensional equation (for cylinders or plane surfaces in air under turbulent conditions),

$$h_c = C (T_s - T_a)^{1/3} \quad (5.4)$$

where C is assigned the value of 0.19 for vertical planes and cylinders, 0.18 for horizontal cylinders, 0.22 for heated plates facing up. The value of h_c calculated by Eq. (5.4) can be used under laminar flow conditions with only a slight loss of accuracy.

It is convenient to determine an equivalent radiant heat-transfer coefficient so that a total heat-transfer coefficient may be computed as follows:

$$h_t = h_c + h_r . \quad (5.5)$$

The heat transferred by radiation can be expressed by the equation:

$$Q = h_r A (T_s - T_a); \quad (5.6)$$

then by setting Eq. (5.6) equal to the second term on the right side of Eq. (5.1), the effective radiant heat-transfer coefficient may be calculated by:

$$h_r = 0.173 \bar{F}_{12} \left[\frac{(T_s + 460)^4 - (T_a + 460)^4}{T_s - T_a} \right] \quad (5.7)$$

If the surroundings are large compared to the cask then \bar{F}_{12} may be approximated by ϵ , the emissivity of the cask surface. After substituting

ϵ for \bar{F}_{12} , the solutions to Eq. (5.7) and Eq. (5.4) are plotted in Fig. (5.5) as a function of $(T_s - T_a) = \Delta T$.

4. Find the Surface Emissivity. The proper value of ϵ may be selected from Table 5.2.

5. Solve Equation (5.2). Select a T_s to determine ΔT and with the ϵ determined above find h_c and h_r from Fig. 5.5. Add these coefficients as in Eq. (5.5) and evaluate Eq. (5.2) using the assumed ΔT . If Q_t thus determined does not equal $Q_d + Q_s$, Steps 3 through 5 must be repeated assuming a different value for T_s .

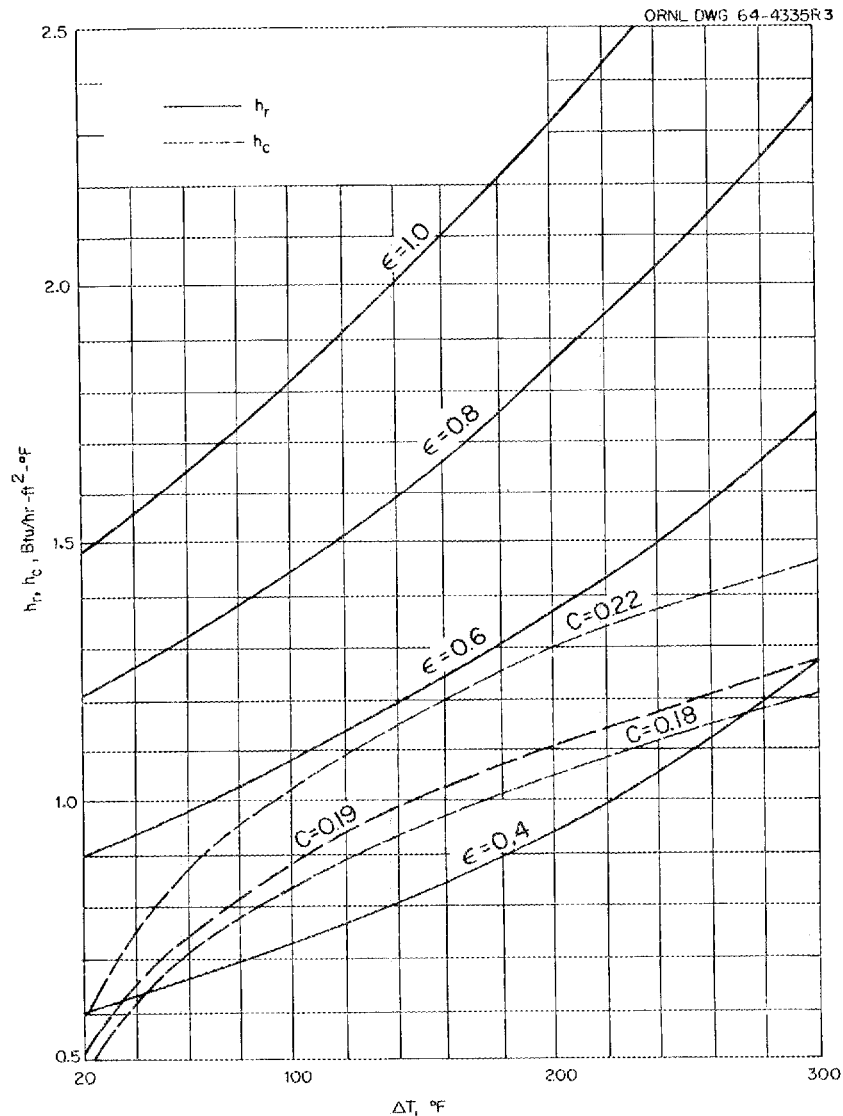


Fig. 5.5. Convective and Radiative Heat Transfer Coefficients as a Function of ΔT when $T_a = 130^\circ\text{F}$.

Analysis of a Finned Cask. - For finned casks, the procedure to be used for the prediction of the cask surface temperature is more involved. The recommended trial-and-error procedure is as follows:

1. Compute the Heat Transfer Area. The area for convection does not equal the area for radiation in the case of finned casks. For the cask shown in Fig. 5.6

ORNL Dwg 67-11688 R1

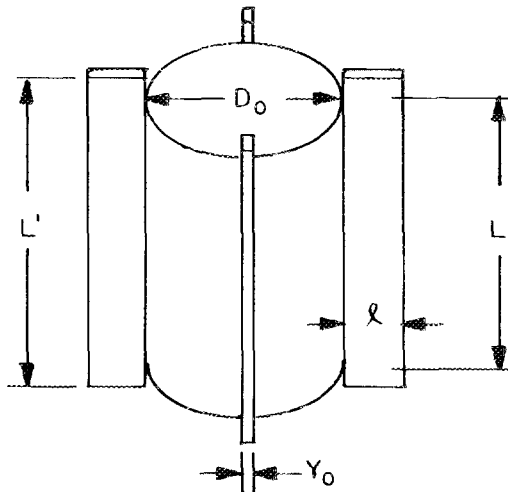


Fig. 5.6. Longitudinally Finned Cask Oriented Vertically.

$$A_c = (\pi D_o - n_f y_o) L + \eta n_f (2lL') , \quad (5.8)$$

where

D_o = cask outer diameter, ft

n_f = number of fins

y_o = fin thickness, ft

L = cask length, ft

η = fin efficiency (see Step 5)

l = fin height, ft

L' = fin length, ft

For a cask with circumferential fins of rectangular profile oriented horizontally (see Fig. 5.7)

$$A_c = \pi D_o (L - n_f y_o) + 2\pi (r_L^2 - r_o^2) n_f \eta_c \quad (5.9)$$

where

η_c = fin efficiency for circumferential fins.

The radiation heat transfer area of the finned cask is taken as the "string" area of the cask; this is the area of the total cask envelope, and irrespective of the type of fin can be calculated by:

$$A_r = \pi (D_o + 2\ell) L \quad (5.10)$$

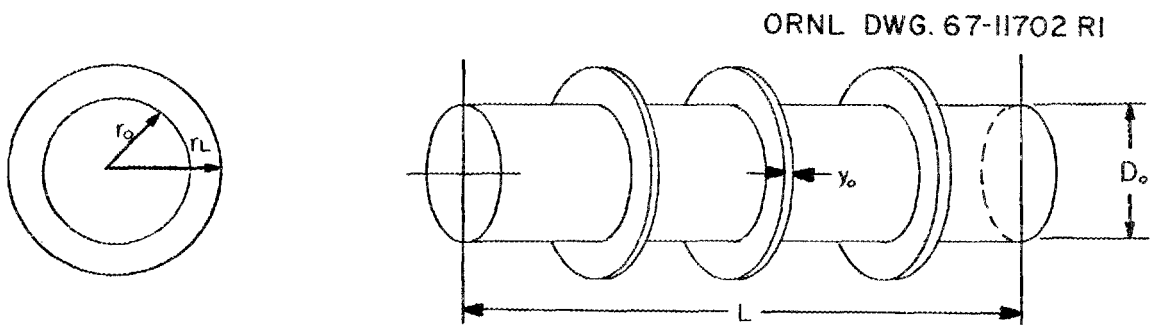


Fig. 5.7. Circumferentially Finned Cask Oriented Horizontally.

2. Determine the Effective Emissivity. Since, for finned casks, the sides are considered cavity-type radiators,¹⁹

$$\epsilon = \frac{1}{1 + \frac{s}{S} \left(\frac{1}{\epsilon_r} - 1 \right)} \quad (5.11)$$

where

ϵ_r is the surface emissivity of the cask shell and fins,

s is the average face-to-face distance between fins and S is defined as:

$$S = s + 2\ell$$

Typical values for ϵ_r are given in Table 5.2.

3. Assume a Cask Surface Temperature, T_s .
4. Determine the Convection Heat Transfer Coefficient. Use Fig. 5.5.
5. Calculate the Fin Efficiency as Indicated in Step 5 for Unfinned Casks. The useful heat transfer area is dependent on the fin efficiency η , which in turn depends on the convection heat transfer coefficient. Figure 5.8 is based on the following two equations from Jacob²⁰ for longitudinal fins and can be used for any materials of construction:

$$\eta = \frac{\tanh(b)}{b} \quad (5.13)$$

Where:

$$b = \text{fin parameter} = \ell \sqrt{\frac{2h_c}{ky_0}} ;$$

and k is the thermal conductivity of the fins.

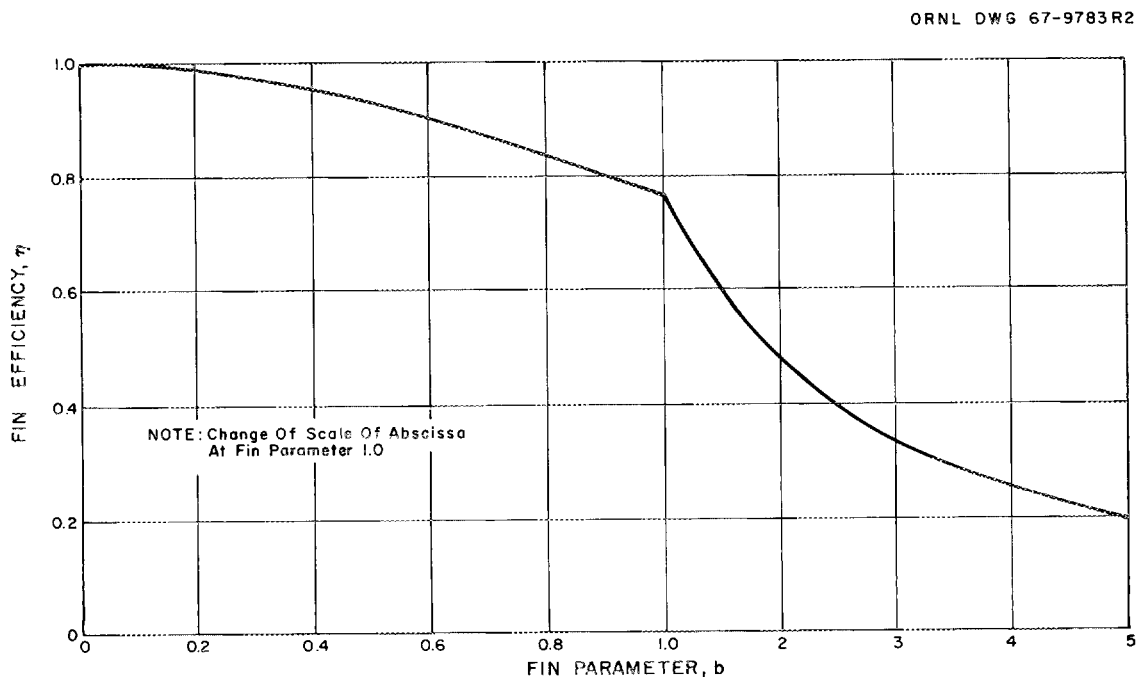


Fig. 5.8. Fin Efficiency for Straight Fins of Rectangular Cross Section vs Fin Parameter.

Figure 5.9 can be used to determine η for stainless steel fins by first calculating b/l and by knowing l , computing b . Substituting b in Eq. (5.12) (or utilizing Fig. 5.8) will yield a value for η .

If circumferential fins of rectangular profile are used, a correction factor, $\Delta\eta$, must be added to Eq. (5.14) (see Fig. 5.10); that is,

$$\eta_c = \eta + \Delta\eta . \quad (5.14)$$

After η and/or η_c has been determined the calculations can be completed since the convection and radiation heat transfer areas are completely determined.

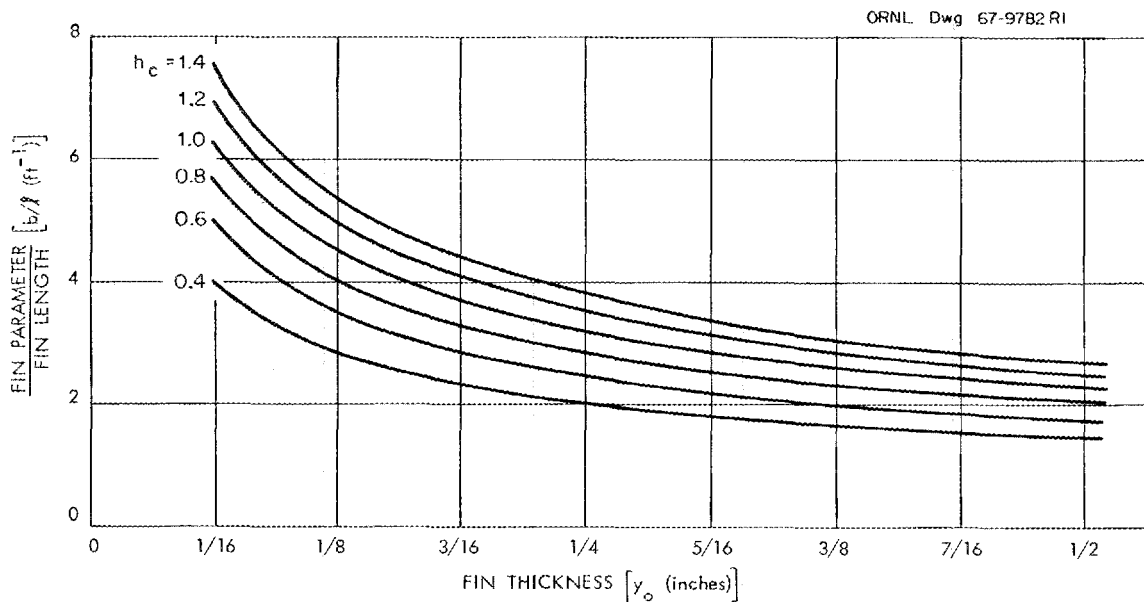


Fig. 5.9. Graph of (Fin Parameter/Fin Length) for Longitudinal Fins of Rectangular Profile, 304 Stainless Steel.

6. Solve Eq. (5.6). If the value obtained by solution of Eq. (5.1) does not equal $Q_d + Q_s$, a new surface temperature must be chosen and Steps 3 through 6 repeated until $Q_T = Q_d + Q_s$.

Example using Heat Transfer Equations. Assume it is required to determine a value for the surface temperature of a circumferentially

finned cask which is transported horizontally. The cask is designed to transport two fuel elements from a reactor whose characteristics are described in the example of Sect. 5.2.1. Suppose the cask has the following characteristics:

- Material of construction (outer shell and fins) ... 304 SS
- Outside diameter of cask, D_o 3 ft
- Radius from cask center to tip of fin, r_L 1.75 ft
- Radius from cask center to base of fin, r_o 1.50 ft
- Cask length, L 9 ft
- Number of fins, n_f 54
- Fin length, ℓ 0.25 ft (3 in.)
- Fin thickness, y_o 0.0208 ft
(.25 in.)
- Approximate fin spacing (center to center) 0.167 ft
(2 in.)
- Fin width, L' 9 ft

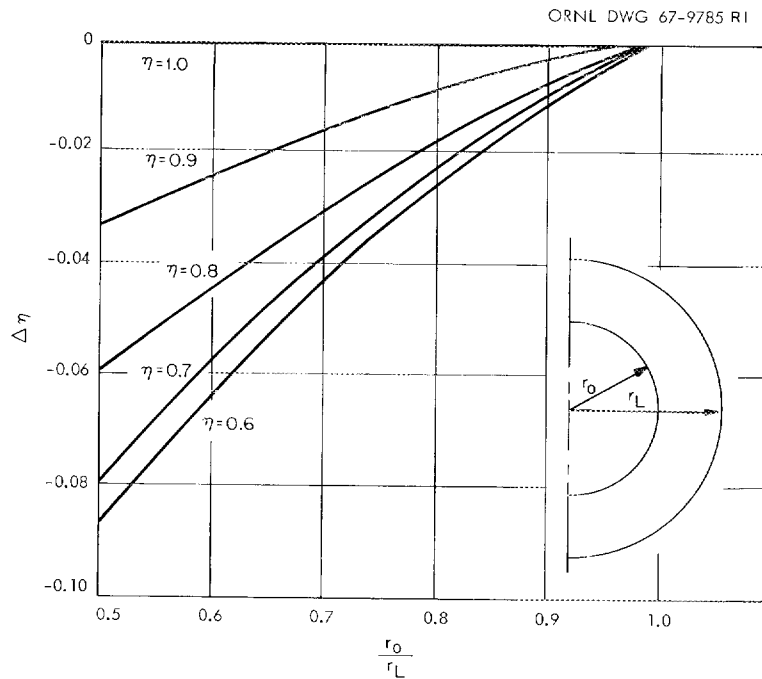


Fig. 5.10. Reduction Term $\Delta\eta$ for Circumferential Fins of Rectangular Profile. $\eta_c = \eta + \Delta\eta$

First the heat load, $Q_d + Q_s$, should be calculated. From the example in Sect. 5.2.1 for fuel cooled 120 days, $Q_d = (2 \text{ assemblies}) (3.25 \text{ kw/assembly}) = 6.50 \text{ kw}$.

The solar heat load, Q_s , varies with the season, the latitude, the weather, etc. Assuming the cask will be transported at a latitude of 42° during the summer solstice, an average heat load can be calculated.

Because of the cyclic nature of the solar heat load and the large thermal capacity of spent fuel shipping casks, it seems reasonable to average the total load over 24 hr.

Integrating the curve denoted as "normal" in Fig. 5.2 gives $3445 \text{ Btu/ft}^2\text{-day}$; this equals $144 \text{ Btu/ft}^2\text{-hr}$ or 42 watts/ft^2 of projected cask surface. The total solar heat load is therefore $(3 \text{ ft}) (9 \text{ ft}) (0.042 \text{ kw/ft}^2) = 1.1 \text{ kw}$.

Proceeding step-by-step as previously indicated for a finned cask,

1. From Eq. (5.9),

$$\begin{aligned} A_c &= \pi(3)[9 - 54(0.0208)] + 2\pi(1.75^2 - 1.50^2) 54 \eta_c \\ &= 74.3 + 276 \eta_c \text{ ft}^2 \end{aligned}$$

$$\begin{aligned} A_r &= \pi(3 + 2 \times .25)9 \\ &= 99 \text{ ft}^2 \end{aligned}$$

2. Determine the effective emissivity using Eq. (5.11).

$$s = 2 - .25 = 1.75 \text{ sq in./in.}$$

$$S = 1.75 + 2(3) = 7.75 \text{ sq in./in.}$$

$$\frac{s}{S} = \frac{1.75}{7.75} = 0.226$$

A value for ϵ_r may be obtained from Table 5.2 or other suitable reference. For partially weathered stainless steel:

$$\epsilon_r \approx 0.5$$

Thus,

$$\frac{1}{\epsilon_r} - 1 = 1$$

And from Eq. (5.11)

$$\epsilon = \frac{1}{1 + 0.226} = 0.814$$

3. Assume $T_s = 200^\circ\text{F}$.

4. Since $T_a = 130^\circ\text{F}$, $\Delta T = 70^\circ\text{F}$ and from Fig. 5.5.

$$h_c = 0.781$$

5. From Fig. 5.9, for $y_o = 1/4$ in. and $h_c = 0.781$,

$$\frac{b}{z} = 2.8 \text{ ft}^{-1}$$

hence,

$$b = 2.8 (0.25) = 0.700 .$$

Using Fig. 5.8 for $b = 0.700$

$$\eta = 0.87$$

From the cask geometry

$$\frac{r_o}{r_L} = \frac{1.50}{1.75} = 0.857$$

From Fig. 5.10 for $\eta = 0.87$ and $r_o/r_L = 0.857$,

$$\Delta\eta = -0.007$$

Making the correction for circumferential fins,

$$\eta_c = 0.870 - 0.007 = 0.863$$

$$A_c = 74.3 + 276 (0.863) = 312.5 \text{ ft}^2$$

6. From Eq. (5.1), the solution for Q_T yields:

$$Q_T = (.781)(312.5)(200-130) + 0.173 (.814)(99.0)[6.6^4 - 5.9^4]$$

$$Q_T = 26,647 \text{ Btu/hr} = 7.81 \text{ kw}$$

Since $Q_T = Q_d + Q_s$, $= 6.50 + 1.1 = 7.6 \text{ kw}$, the cask surface temperature is slightly lower than the 200°F value assumed.

By repeating Steps 3 through 6 a temperature of 199°F is found to dissipate the requisite amount of heat.

5.4 Internal Heat Transfer

Present regulations do not place a limit on the maximum temperature of a spent fuel element. What they do require is that under normal conditions of transport no radioactive material will be released from the containment vessel; and under the hypothetical accident conditions some activity release, up to specified limits, may be tolerated. It is, therefore, prudent to keep fuel element temperatures as low as possible and, if coolant is lost, below temperatures which are capable of causing cladding failure.

The internal heat transfer analysis involves consideration of the transfer of the decay heat generated in the fuel elements, through the fuel cladding, the primary coolant region, the cask inner shell, the biological shield region, and the cask outer shell. No treatment has been given to the heat transfer analysis in the usual case involving water as a primary coolant since accident conditions normally imply that liquid coolants have been replaced with air.

In some cases it will be desirable to contain each fuel element in its own canister although canned fuel elements often impose economic penalties. Such a canister becomes the primary line of containment and the cask's main purpose is then to shield and transfer heat, and provide a secondary line of containment. This system often has the disadvantage

of increasing the temperature difference for the heat that must be transferred, but the increased ability to contain the fuel generally offsets this. Presently few cask designs employ this containment philosophy.

This section presents temperature maps of one specific cask cavity containing two fuel element designs under several different conditions. Its purpose is to indicate how the temperature distribution changes as these conditions are varied.

The following information should provide a "feel" for maximum temperatures and indicate the magnitude of temperature variations caused by changing various parameters.

5.4.1 Analytical Method

This data was developed using the heat transfer computer code THTC (17), which considers conductive, convective, and radiative heat transfer simultaneously and determines steady state temperature distributions by a relaxation technique.

For the square 3 x 3 fuel assembly array studied the system parameters which were used as input to the code are summarized as follows:

1. Number of fuel pins per assembly
2. Fuel pin diameter (D_p)
3. Fuel pin spacing (S_p)
4. Fuel element assembly linear heat generation rate
5. Basket configuration
6. Basket web thickness
7. Mode of basket attachment to cask inner shell

The overall geometry upon which the nodal network is based is shown in Fig. 5.11, and is defined as a 45° wedge with two adiabatic boundaries. This system permits simultaneous radiative, conductive, and convective coupling throughout the cavity and biological shield. The external ambient conditions were assumed to be 130°F . An emissivity and solar

absorptivity equal to 0.5 respectively, were chosen for the exterior cask surface.

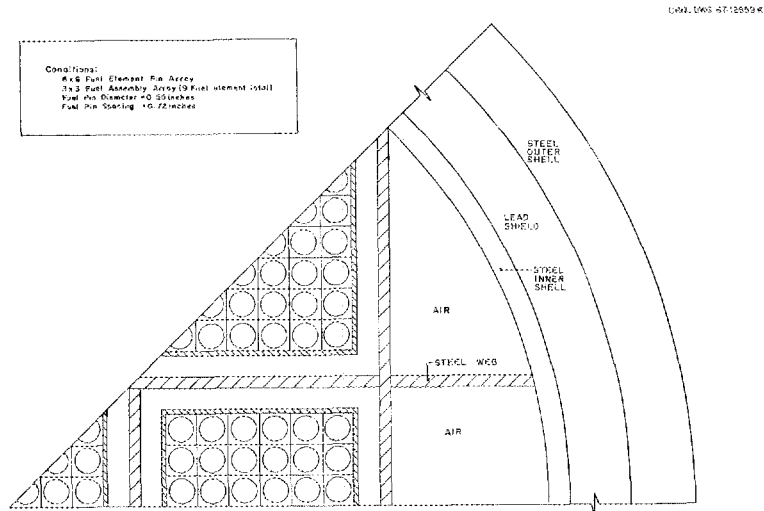


Fig. 5.11. Thermal Nodal Model Used as Basis for Loss of Coolant Investigations.

5.4.2 The Parametric Cases

The basic geometric model for the fuel assemblies in the cask cavity consists of a square array of rods or "pins." A range of pin diameters and pin spacings was derived from a review of the fuel assembly designs of existing and proposed power reactors; these data are presented in Table 5.3.

Table 5.3. Fuel Parameters in Typical Water Reactor Systems

Reactor System	Pin Array	Active Length, ft	Pin Diameter, in.	Pin Spacing, in.	Fuel Assembly Cross Section in. x in.	Q_1 , Btu/hr	Q_2 , Btu/hr-ft
Oyster Creek	7 x 7	12	0.57	0.738	5.27 x 5.27	12,620	1,050
Senn	9 x 9	9.07	0.534	0.705	7.36 x 7.36	9,046	1,000
SOE	15 x 15	12	0.22	0.562	9 x 9	49,859	4,160
Yankee	18 x 18	7.68	0.34	0.422	8.6 x 8.6	33,405	4,350

The first "base" case was made considering the following specific values of the parameters required by the THTC code to determine each individual pin temperature in air:

Case 1

1. 6 x 6 fuel pin array
2. $D_p = 0.55$ in.
3. $S_p = 0.72$ in.
4. $Q_2 = 1000$ Btu/hr-ft of fuel assembly
5. 3 x 3 basket array
6. Basket web thickness = 0.25 in.
7. Web welded to cask inner shell

The temperature distribution resulting from the calculation is given in Fig. 5.12. Variations were then made in parameters (4), (6), and (7). The temperature maps are presented in Figs. 5.13 through 5.16.

Figure 5.17 graphically presents the temperature distribution as a function of cask radius taken along the abscissa of Figs. 5.12, 5.13, 5.14 and 5.16. As might be expected, the inside web is cooler than either row of adjacent fuel pins.

A second base case was investigated in which the number of fuel pins was increased from 36 to 144. Pertinent data of the fuel element is given below:

Case 2

1. 12 x 12 fuel pin array
2. $D_p = 0.20$ in.
3. $S_p = 0.40$ in.
4. $Q_2 = 1000$ Btu/hr-ft
5. 3 x 3 basket array
6. Basket web thickness = 0.25 in.
7. Web not welded to inner shell

The linear heat source, Q_2 , was changed to 500 and 1500 Btu/hr-ft. Temperature maps of the results are shown in Figs. 5.18, 5.19, and 5.20. The maximum temperature picked from these three figures is plotted as a function of linear heat generation in Fig. 5.21 and is compared to the maximum temperatures of the 6 x 6 fuel pin array given in Figs. 5.12 through 5.14.

Results of the Parametric Analysis

Pertinent conclusions which may be drawn from the data are:

1. As the heat generation rate per unit length increases, the maximum fuel element temperature increases to approximately the 0.5 power (see Figs. 5.12 through 5.14 and 5.18 through 5.20).
2. Welding of the basket web to the cask shield inner liner/inner shell apparently does not significantly affect the maximum pin temperatures with respect to heat transfer, (compare Figs. 5.12 and 5.15).
3. Increasing the basket web thickness from 1/4 in. to 3/4 in. results in a significant decrease in maximum pin temperature (about 200°F for the case analyzed; compare Figs. 5.12 and 5.16).
4. If Q_2 , the linear heat generation rate is constant, increasing the number of fuel pins in the fuel assembly (keeping the fuel assembly approximately the same size) does not significantly increase the maximum pin temperature. One of the reasons for this is that as the number of pins per fuel assembly increases, the heat source per pin decreases proportionally.

5.5 Fire Analysis

In the analysis of transient heat transfer many methods exist for obtaining approximate temperature distributions through the use of mathematical models. These range from one dimensional models that cannot

ORNL DWG 68-10594

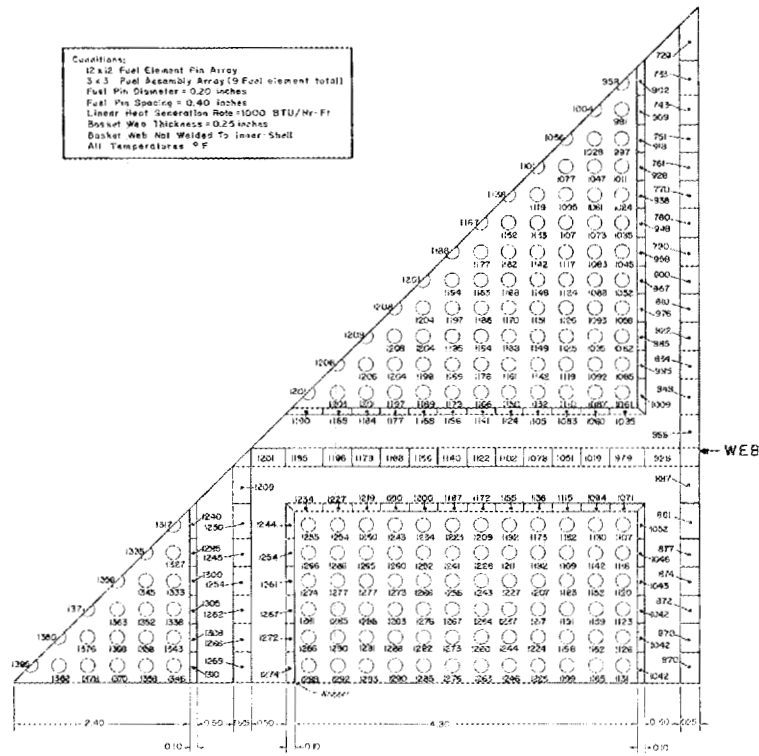


Fig. 5.18. Temperature Distribution Under Conditions of Case 6.

ORNL DWG 68-10597

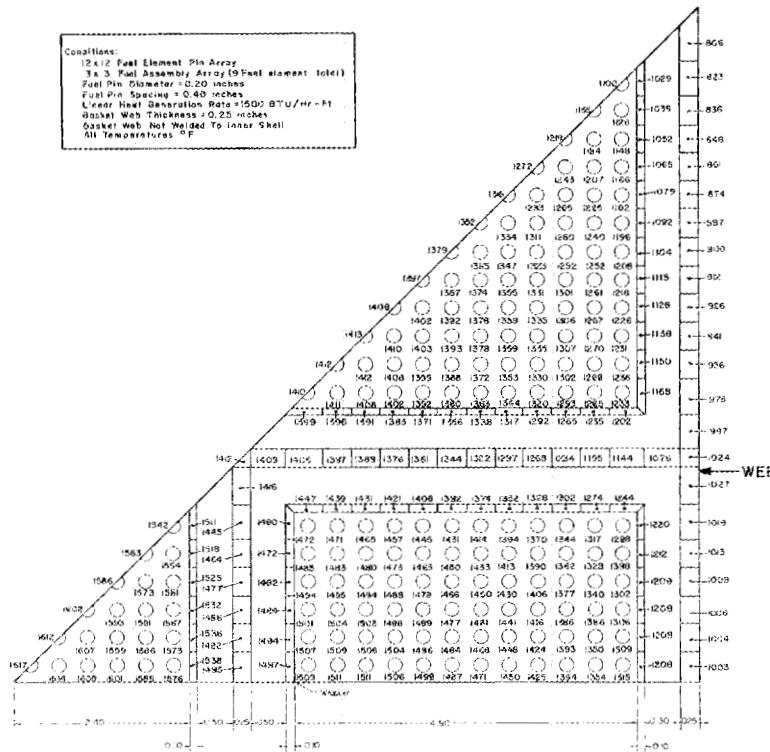
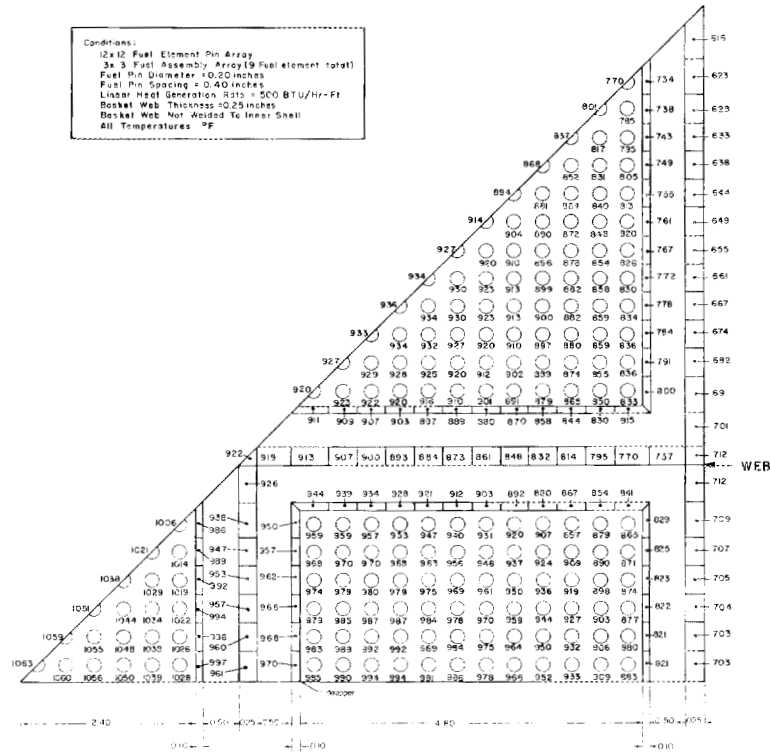


Fig. 5.19. Temperature Distribution Under Conditions of Case 7.

ORNL DWG. 68-10596



account for a change of phase (which may be readily handled using finite difference solutions) to three dimensional models that can account for melting for which sophisticated computer codes have been written. The following paragraphs present a brief overview of methods which have yielded acceptable results in analyzing cask response to a 0.5 hr fire. The fire will affect, 1) the strength of materials of construction, 2) the ability of the cask to shield the contents during and after the fire, 3) the cask seal, and 4) the mobility of the activity in the cask. Any analysis of the cask involved in the specified fire must aim at determining whether the cask can maintain its shielding and sealing characteristics. Certainly criticality must also be considered, since the fuel or poison plates could change position or form, but in general high temperatures will not create a criticality problem.

In attempting to assess the damage that a fire is capable of inflicting on a cask many techniques have all been employed. The objective of most of these methods is to determine the temperature profile through the cask shield as a function of time and to determine the maximum fuel element temperature and what portion of the shield, if any, melts. This information may then be used, in principle, to estimate, 1) both thermal and mechanical stresses induced in the outer and inner shell, 2) the ability of the cask seal to be maintained, and 3) the amount of fission products which may escape from the fuel to the primary coolant.

The techniques of analysis will be somewhat affected by the peculiarities of the cask to be analyzed. In several cases when unirradiated material was to be transported in an insulated container, and the process may be considered one dimensional, graphical methods were employed to calculate the temperature profile through the cask as a function of time. These methods often are relatively quick and easy, and the accuracy is generally good. For a complete description of the theory and method, the reader is referred to refs. 14 and 18.

5.5.1 Graphical Method

The graphical technique discussed here, known as the Schmidt method is relatively simple even when the boundary conditions become complicated, but is limited to temperatures below the melting point of the cask materials.

The unsteady state equation, which applies to heat conduction in a thick-walled cylinder, is

$$\frac{\partial T}{\partial \theta} = \left(\frac{\partial^2 T}{\partial r^2} + \frac{1}{r} \frac{\partial T}{\partial r} \right) a \quad (5.15)$$

where T is temperature, θ is time, a is the thermal diffusivity, and r is the radius. This equation may be transformed into the finite difference Eq. (5.16).

$$T_n^{t+1} - T_n^t = \frac{2a\Delta\theta}{(r\Delta\eta)^2} \left(\frac{T_{n+1}^t + T_{n-1}^t}{2} - T_n^t \right) \quad (5.16)$$

To use Eq. 5.16, the walls of the cylinder must be subdivided into concentric cylinders of constant thickness (Δr), and it is the temperature at the planes between these intervals that is determined as a function of time.

In Eq. (5.16) the superscripts indicate the number of time increments ($\Delta\theta$'s) that have elapsed, the subscripts to the position through the cylinder wall, and $\Delta\eta = \frac{\Delta r}{r}$.

Assuming the thermal diffusivity of the system remains constant over the temperature range of interest and if $\Delta\theta$ or $r\Delta\eta$ is chosen such that

$$\frac{2a\Delta\theta}{(r\Delta\eta)^2} = 1 \quad (5.17)$$

then Eq. (5.16) would become

$$T_n^{t+1} = \frac{T_{n+1}^t + T_{n-1}^t}{2} \quad (5.18)$$

which indicates that the temperature at position n at time increment $t + 1$ is equal to the arithmetic mean of the temperature at position $n + 1$ and $n - 1$ measured at time increment t , and implies temperature at any point changes at alternate time intervals. This, therefore, permits a stepwise calculation of temperature as a function of time and temperature history.

Example

A container, designed to transport unirradiated fissile material, was built by inserting Foamglas^{*} insulation into a 30-gal drum. It was fire tested by inserting it into an oven preheated to 1725°F and both inside and outside surface temperatures were measured as a function of time.²² The container was removed from the furnace at the end of one hour.

The temperature of the inner surface was calculated by the Schmidt method using the measured outer surface temperature as input data and assuming there were no end effects (a non conservative but reasonable assumption). A drawing of the container is shown in Fig. 5.22.

^{*}TM of Pittsburgh Corning Company

ORNL DWG. 68-872 RI

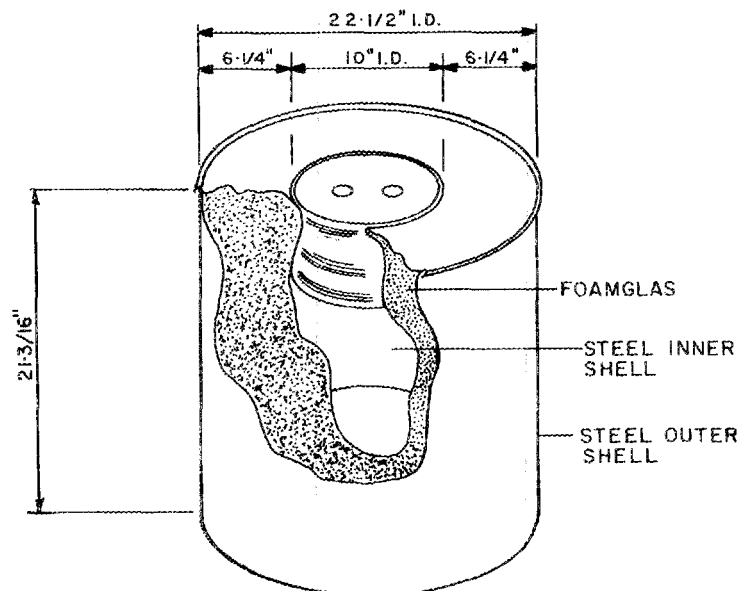


Fig. 5.22. Y-12 Foamglas Insulated Shipping Container.

The insulation was divided up into six 1-in.-thick cylinders; $\Delta\eta$, calculated for each cylinder (see Table 5.4), was used to graphically determine the temperature as a function of time (see Fig. 23).

Table 5.4 Determination of $\Delta\eta$

Seg. No.	Radius, r (in.)			$\Delta\eta = \frac{\Delta r}{r}$
	Inner	Outer	Mean	
1	5	6	5.5	0.182
2	6	7	6.5	0.154
3	7	8	7.5	0.134
4	8	9	8.5	0.118
5	9	10	9.5	0.105
6	10	11	10.5	0.095

The thermal diffusivity (a) of Foamglas at room temperature is given as $0.0175 \text{ ft}^2/\text{hr}$. The average temperature of the insulation during the fire is in the range of 400°F and the thermal conductivity is known to increase appreciably with temperature. For these reasons " a " was assumed to be $0.0278 \text{ ft}^2/\text{hr}$. This number seems reasonable and when used in Eq. (5.20) gives a convenient value for $\Delta\theta$.

That is:

$$\begin{aligned}\Delta\theta &= (r\Delta\eta)^2/2a = [1/12]^2/[2(0.0278)] \\ &= 0.125 \text{ hr} = 7.5 \text{ min} .\end{aligned}$$

Equation (5.18) is solved graphically in Fig. 5.23.

The calculated value of the inner surface temperature as a function of time is compared with the measured inner and outer surface temperatures in Fig. 5.24. Results compare reasonable although the maximum calculated temperature is about 60°F below the measured maximum. Greater accuracy could have been obtained by decreasing the thickness of the slabs (Δr) thereby shortening $\Delta\theta$.

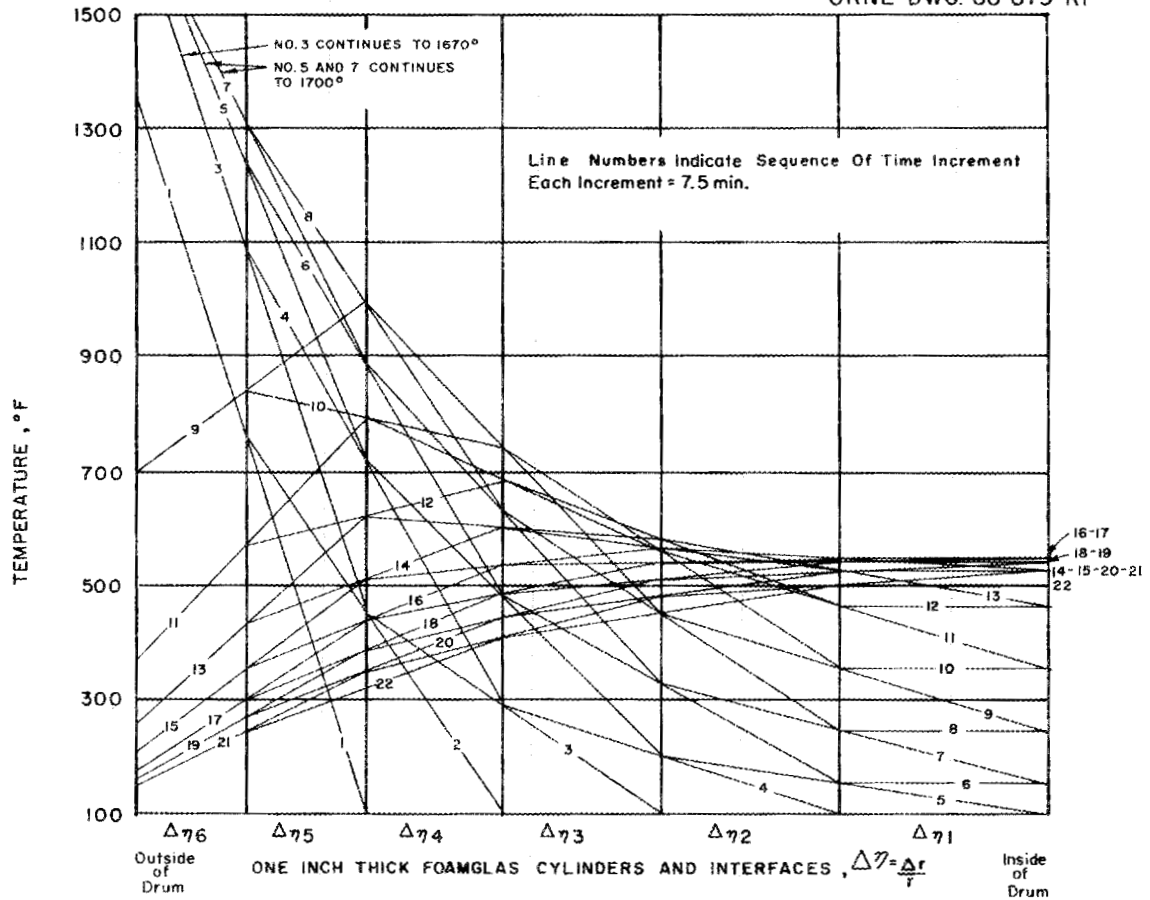


Fig. 5.23. Temperature Distribution Through the Annular Foamglas Insulation.

5.5.2 Analog Method

An electrical analog network for a thermal analysis of a lead shielded cask under fire conditions has been reported by Bonilla and Strupczewski.²³ Their analysis can account for fins, an external fire shield, a fire shield situated inside the lead, and both convection and radiation heat transfer at the outer surface. Their network does not allow for internal (decay) heat generation although it would not be difficult to add to the program.

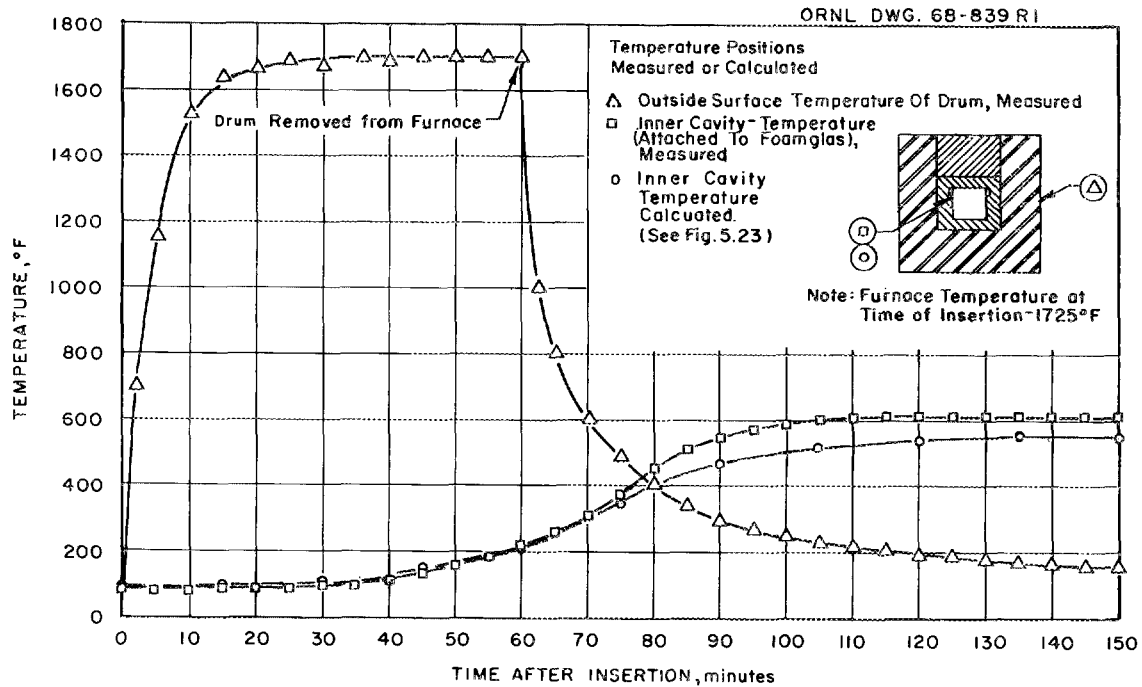


Fig. 5.24. Time-Temperature Curves of the Foamglas Container.

Their analysis of a lead-shielded MTR shipping cask produced some interesting, albeit not surprising, results. An external asbestos fire shield greatly reduced the cask temperatures resulting from the fire environment to the point that without a high wind velocity present, very little lead melted after an hour's exposure; this compares to complete melting of the lead after 1½ min without the shield.

The use of steel thermal shields placed in the shielding cavity was also considered. In a fire, the lead between these steel shells would melt and flow away through drainage holes provided in the lower part of the cask. The resulting voids would provide a thermal shield

for the remaining portion of the lead. Results indicated that with four such gaps complete melting of the remaining lead took about 45 min.

5.5.3 Energy Balance Method

An empirical method of calculating the inner and outer shell temperatures and the amount of lead that melts in the specified 30-min fire has been proposed by Wachtell and Langhaar.²⁴ The method, based on a heat balance deduced from both theory and experiment, is essentially a one-dimensional analysis but does account for melting in cask corners.

Advantages in using this method are several. First, the method is relatively quick and easy and does not require a computer. Second, it takes into account the convection of molten lead; that is, vertical temperature gradients, found in actual fire tests of lead shielded casks, are calculated. Third, superheat of molten lead before all lead has melted is recognized and considered. Experimental results have shown during lead melting, the molten portion is considerably hotter than 621°F, the melting temperature of lead.

Disadvantages are that the temperature gradients across the shield cannot be calculated as a function of time and fins are ignored so far as heat transfer from the fire to the cask is concerned. This latter point is probably not a severe limitation if the cask being analyzed is at least of moderate size; tests tend to confirm this supposition. If the cask is small, however, and the fin height is an appreciable fraction of the cask radius (e.g., > 25%), neglect of the fins could be significant.

In addition, the method does not account for air gaps, fire shields, or other features which would significantly affect the flow of heat. Nevertheless, for a number of cases the method may prove useful. The physical constants that may be assumed for these calculations are tabulated below.

	<u>Stainless Steel</u>	<u>Carbon Steel</u>	<u>Solid Lead</u>	<u>Liquid Lead</u>
k = thermal conductivity, Btu/hr ft °F	11	25	18.6	9.3

	<u>Stainless Steel</u>	<u>Carbon Steel</u>	<u>Solid Lead</u>	<u>Liquid Lead</u>
C_P = specific heat capacity, Btu/lb °F	0.125	0.125	0.0325	0.038
ρ = density, lb/ft ³	485	487	687	657
H_F = latent heat of fusion, Btu/lb			10.55	
T_{MP} = melting temperature, °F			621	

In these calculations, time is divided into three intervals: t_0 to t_1 , t_1 to t_2 , and t_2 to t_3 ; where t_0 is the initial time at the start of the fire test, t_1 is the time required to start melting of the lead in the center of a face away from the corners of the cask, t_2 is the time required to complete melting of the lead, and t_3 is the time to arrive at a temperature higher than the melting point of lead. The following steps are required to estimate the temperature of the outer and inner cask shells.

1. Calculate the weight and area of the parts of the cask,
2. estimate the average surface temperature of the cask between time t_0 and t_1 ,
3. estimate the average net absorbed heat flux between time t_0 and t_1 ,
4. estimate the average temperature of solid lead at time t_1 ,
5. estimate the temperature of the inner shell at time t_1 ,
6. estimate the value of t_1 ,
7. estimate the total heat absorbed by the cask at time t_1 ,
8. estimate the amount of molten lead at time t_1 ,
9. estimate the superheat of molten lead,
10. estimate the surface temperature of the cask at time t_2 ,
11. estimate the net absorbed heat flux between time t_1 and t_2 ,

12. estimate the total heat absorbed by the cask at time t_2 ,
13. estimate the value of t_2 ,
14. estimate the amount of molten lead at 0.5 hr,
15. estimate the maximum inner wall temperature at 0.5 hr,
16. repeat appropriate steps for cask lid if necessary.

Step 1

The weights and areas tabulated below must be computed.*

<u>Symbol</u>	<u>Description</u>	<u>Units</u>
A	effective external heat transfer surface**	total ft ²
W_F	weight of fins	total lb
W'_F	weight of fins	lb/ft ² of outer shell
W_{OS}	weight of outer shell	total lb
W'_{OS}	weight of outer shell	lb/ft ² of outer shell
W_{IS}	weight of inner shell	total lb
W'_{IS}	weight of inner shell	lb/ft ² of outer shell
W_L	weight of lead	total lb
W'_L	weight of lead	lb/ft ² of outer shell

Step 2

The average temperature of the cask under normal operating conditions, T_0 , must be estimated (see Sect. 5.3). From T_0 and the curve shown in Fig. 5.25, the average surface temperature of the cask, T_{s-1} between time t_0 and t_1 may be obtained. The curve in Fig. 5.25 was determined from Eq. (5.19).

*For a cylindrical cask the weights are based on a wedge-shaped segment.

**This surface area is calculated as if there were no fins welded to the cask.

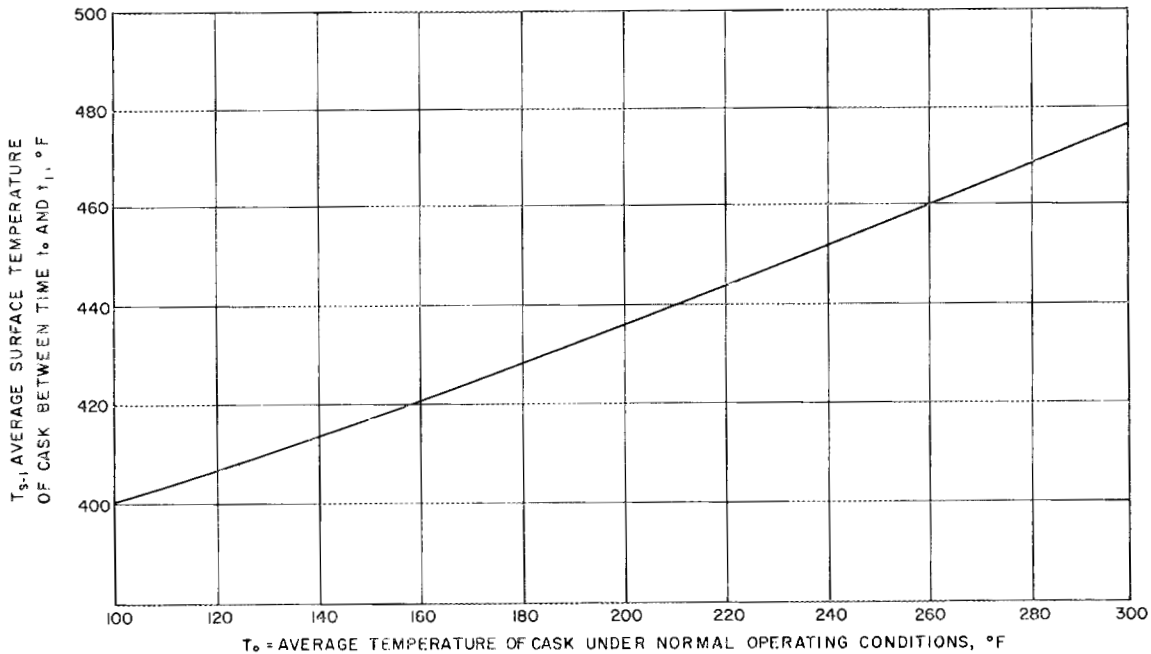


Fig. 5.25. The Average Surface Temperature of the Cask Between Time t_0 and t_1 , as a Function of the Average Temperature of the Cask Under Normal Operating Conditions.

$$T_{s-1}^4 = T_0^4 + 2T_0^3 (T_{MP} - T_0) - 2T_0^2 (T_{MP} - T_0)^2 + T_0 (T_{MP} - T_0)^3 + \frac{1}{5} (T_{MP} - T_0)^4, \quad (5.19)$$

where T_{MP} is the melting-point temperature of the lead. All temperatures are in degrees Rankine.

Step 3

with a fire temperature of 1475°F (1935°R), a flame emissivity of 0.9, and a cask absorption coefficient of 0.8, as required by the regulations, the average heat flux between the time t_0 and t_1 is given by

$$\bar{Q}_1 = (1935^4 \times 0.9 - T_{s-1}^4)(0.173 \times 10^{-8})(0.8) \text{ Btu/hr ft}^2. \quad (5.20)$$

The value for \bar{Q}_1 may be found from the curve shown in Fig. 5.26 by knowing T_{s-1} .

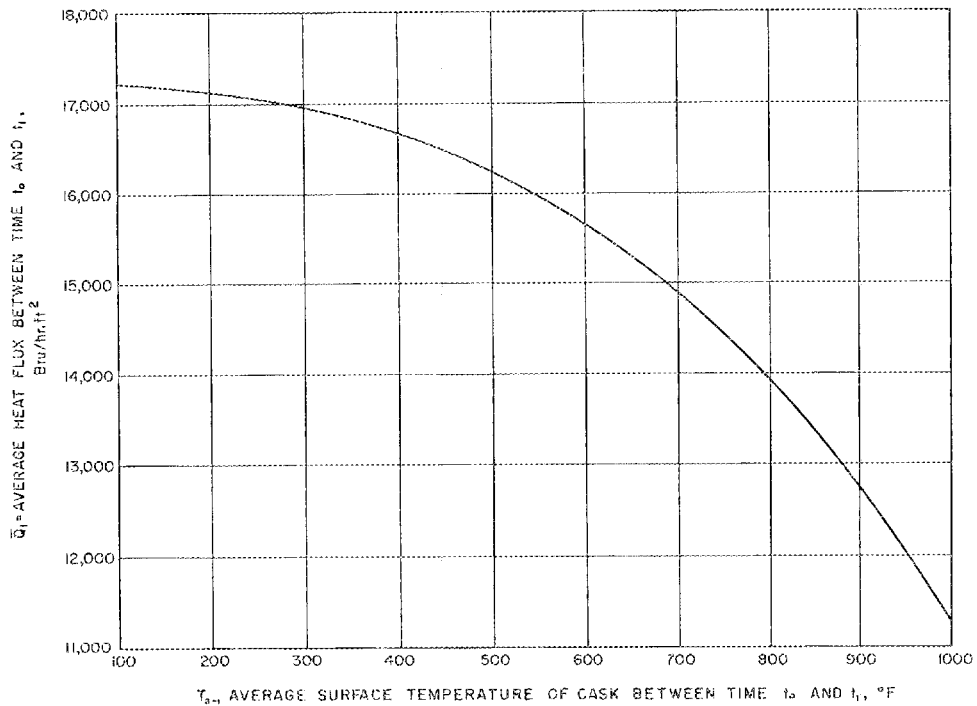


Fig. 5.26. Average Heat Flux Between Time t_0 and t_1 as a Function of the Temperature of the Surface of the Cask.

The average temperature of solid lead in the cask at time t_1 is given by

$$T_{L-1} = 621 - \frac{\bar{Q}_1 D}{36k} \quad (5.21)$$

where D = the thickness of the lead shield in in. The value of T_{L-1} can be determined from the nomograph shown in Fig. 5.27.

Step 5

The average temperature of the inner shell of the cask at time t_1 may be calculated from

$$T_{is-1} = 621 - \frac{\bar{Q}_1 D}{24k} \quad (5.22)$$

The value of T_{is-1} can be determined from the nomograph shown in Fig. 5.28.

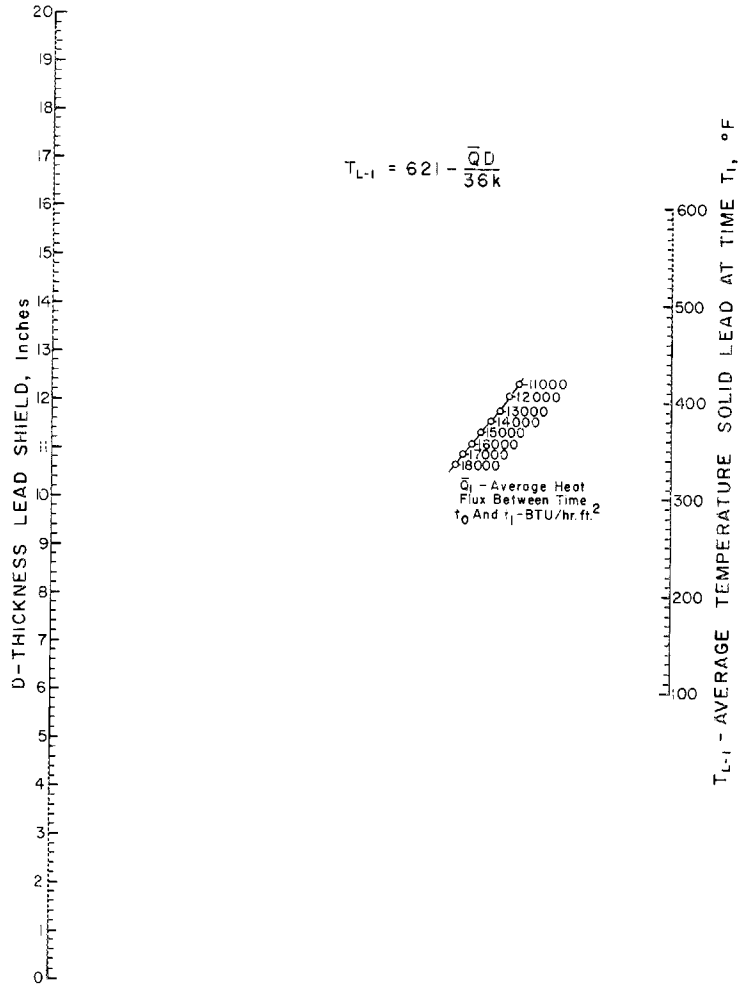


Fig. 5.27. Nomograph to Determine the Average Temperature of the Solid Lead as a Function of the Lead Thickness and the Heat Flux.

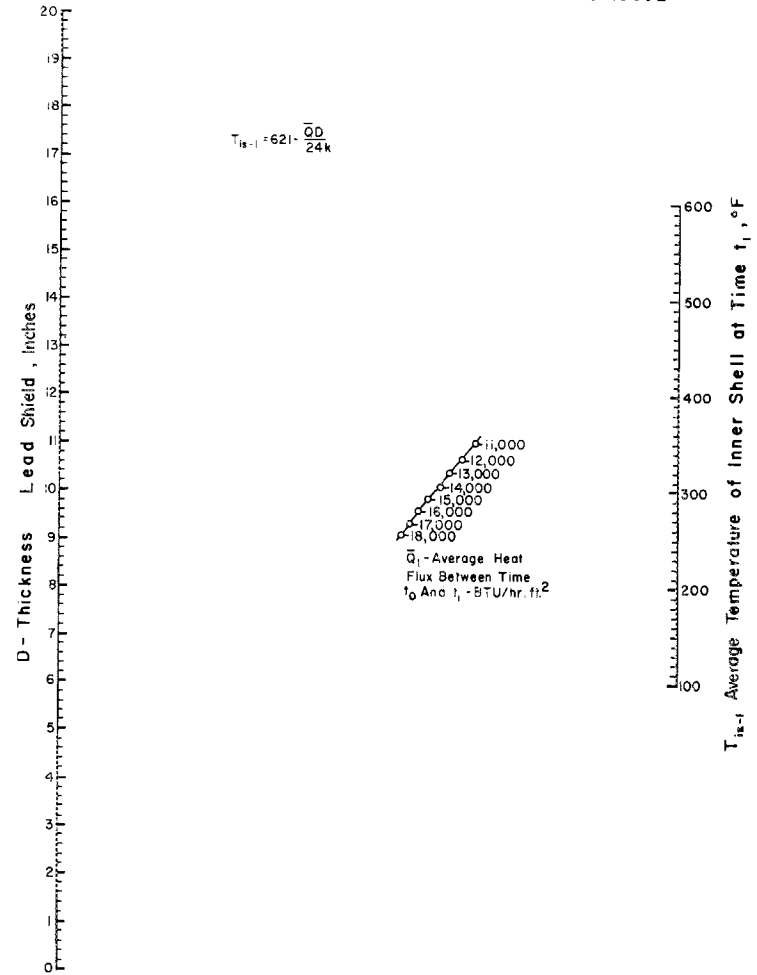


Fig. 5.28. Nomograph to Determine the Average Temperature of the Inner Shell of the Cask as a Function of the Thickness of the Lead and the Heat Flux.

Step 6

To determine a value for t_1 , the quantity of heat absorbed per square foot of cask surface at time t_1 must be calculated. The temperature of the outer shell and the fins must first be calculated by using Eqs. (5.23a) and (5.23b). For the outer shell:

$$T_{OS-1} = 621 + \frac{\bar{Q}_1 \chi}{24k}; \quad (5.23a)$$

where χ = the thickness of the outer shell in in.

For the fins:

$$T_{F-1} = 621 + \frac{\bar{Q}_1 \chi}{12k} \quad (5.23b)$$

These temperatures may easily be found for carbon and stainless steel materials of construction by referring to Figs. 5.29 through 5.32. For the nomographs, it was assumed that k for carbon steel = 25 Btu/hr ft °F, and that k for stainless steel = 11 Btu/hr ft °F.

Assuming that W'_F , W'_{OS} , W'_{is} , and W'_L are the weights of the fins, outer shell, inner shell, and lead per square foot of outer shell area respectively, the total heat absorbed per square foot at time t_1 , H'_{T-1} , is the sum of that absorbed by the parts of the cask. That is:

$$H'_{F-1} = W'_F (T_{F-1} - T_0) 0.125$$

$$H'_{OS-1} = W'_{OS} (T_{OS-1} - T_0) 0.125$$

$$H'_{is-1} = W'_{is} (T_{is-1} - T_0) 0.125$$

$$H'_{L-1} = W'_L (T_{L-1} - T_0) 0.0325$$

$$H'_{T-1} = MC_p \Delta T \text{ Btu/ft}^2$$

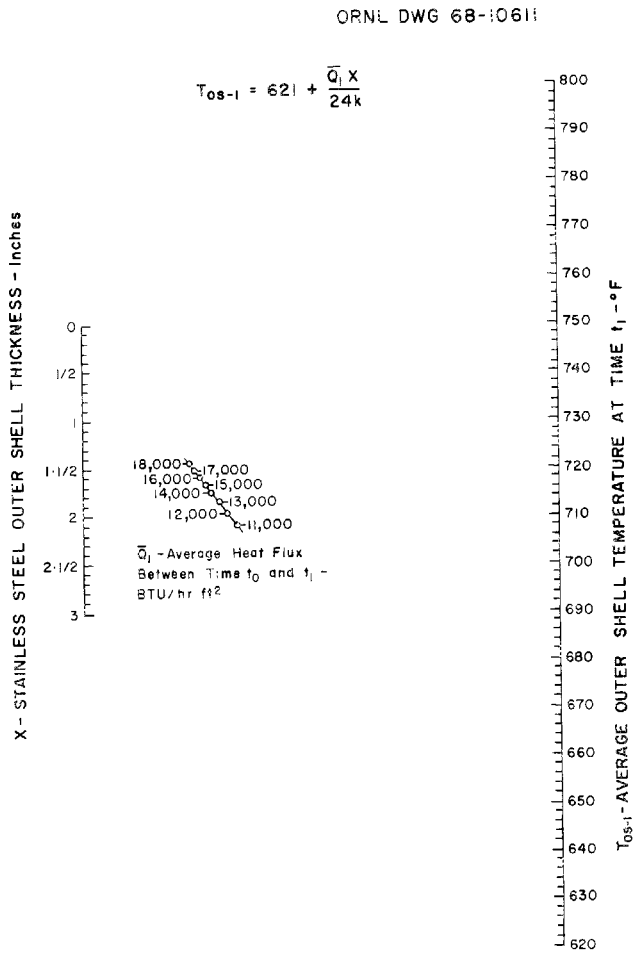


Fig. 5.29. Nomograph to Determine the Average Outer Stainless Steel Shell Temperature at Time t₁ as a Function of the Outer Shell Thickness and the Heat Flux.

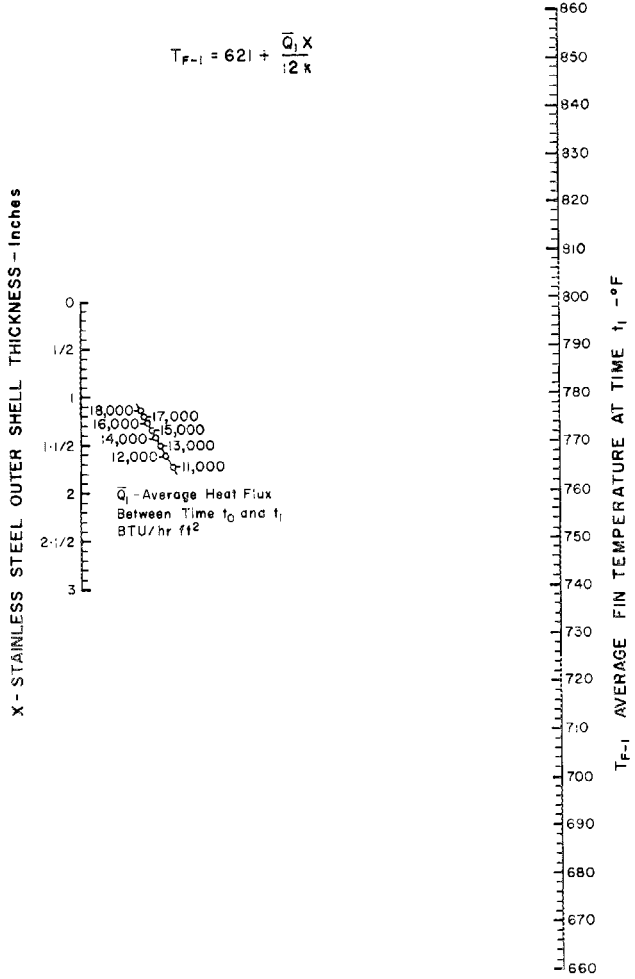


Fig. 5.30. Nomograph to Determine the Average Stainless Steel Fin Temperature at Time t₁ as a Function of the Outer Shell Thickness and the Heat Flux.

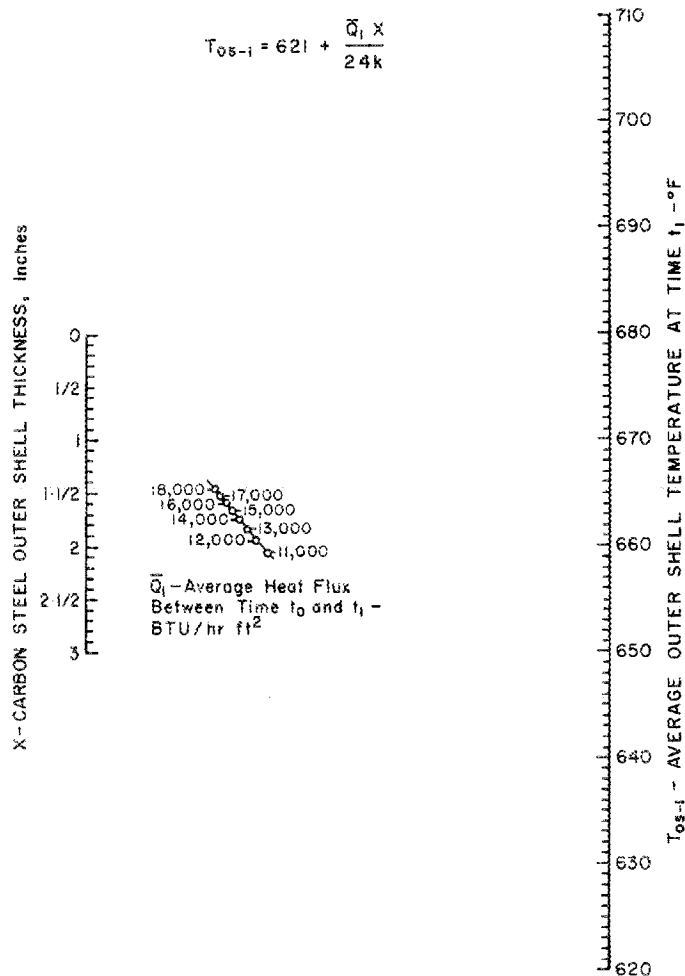


Fig. 5.31. Nomograph to Determine the Average Outer Carbon Steel Shell Temperature at time t_1 as a Function of the Outer Shell Thickness and the Heat Flux.

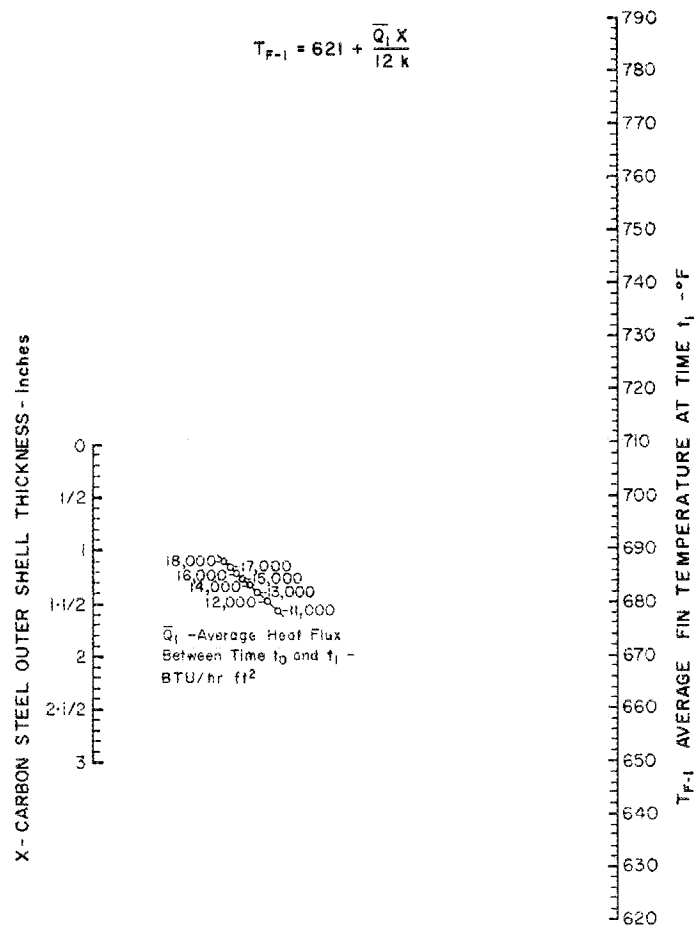


Fig. 5.32. Nomograph to Determine the Average Carbon Steel Fin Temperature at Time t_1 as a Function of the Outer Shell Thickness and the Heat Flux.

Then t_1 is given by:

$$t_1 = \frac{H'_{T-1}}{\bar{Q}_1} \quad (5.24)$$

Step 7

Knowing t_1 , the total heat absorbed by the cask at time t_1 may be calculated from the equation:

$$H^*_{T-1} = \bar{Q}_1 = H'_{T-1} A . \quad (5.25)$$

Step 8

The amount of lead that is molten at time t_1 may be estimated by calculating the heat absorbed by the cask if all the lead were solid and each component of the cask was at the same average temperature as it was in Step 6.

If W_F , W_{OS} , W_{IS} , and W_L are the total weights of the fins, outer shell, inner shell, and lead, respectively, the total heat absorbed by the cask at time t_1 if all the lead were solid, H_{T-1} , is the sum of that absorbed by the parts. That is:

$$H_{F-1} = W_F (T_{F-1} - T_0) 0.125$$

$$H_{OS-1} = W_{OS} (T_{OS-1} - T_0) 0.125$$

$$H_{IS-1} = W_{IS} (T_{IS-1} - T_0) 0.125$$

$$H_{L-1} = W_L (T_{L-1} - T_0) 0.0325$$

$$H_{T-1} \text{ Btu.}$$

Thus:

$$\Delta H_{T-1} = H^*_{T-1} - H_{T-1}$$

Values for \bar{Q}_2 may be obtained from the curve shown in Fig. 5.33.

Step 12

The total amount of heat absorbed by the cask at time t_2 , H_{T-2}^* , (when the lead is completely melted) may be calculated from the following equations:

$$H_{F-2} = W_F(T_{F-2} - T_0)0.125$$

$$H_{OS-2} = W_{OS}(T_{S-2} - T_0)0.125$$

$$H_{is-2} = W_{is}(621 + T_{sup} - T_0)0.125$$

$$H_{LM} = W_L(621 - T_0)0.0325$$

$$H_{LS} = W_L(T_{sup})0.038$$

H_{T-2}^* Btu.

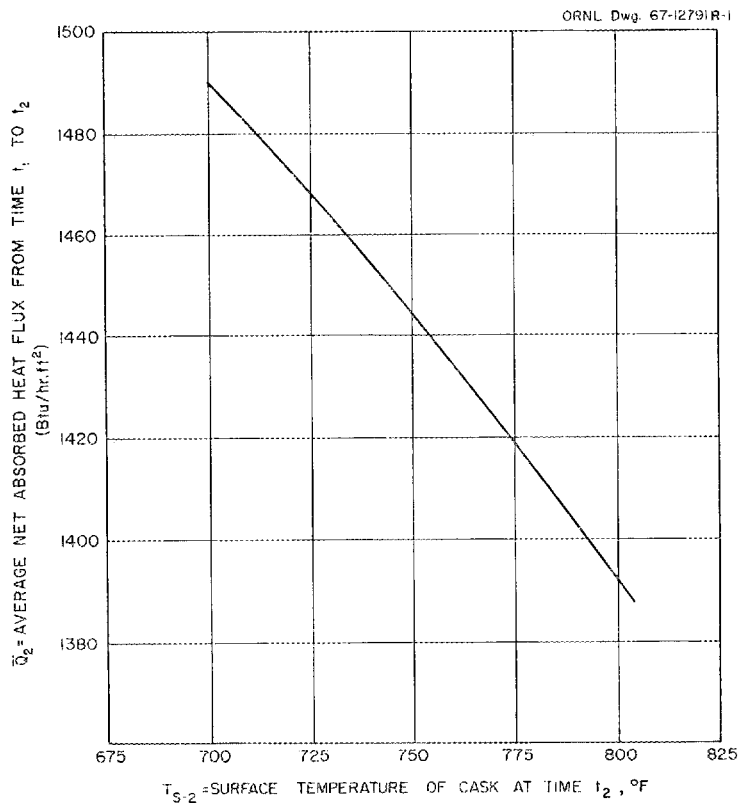


Fig. 5.33. Net Heat Flux Absorbed from Time t_1 to t_2 as a Function of the Surface Temperature of the Cask.

The weight of the molten lead can now be calculated from Eq. (5.27)

$$W_{ML-1} = \frac{\Delta H_{T_{L-1}}}{(621 - T_{L-1})(0.0325) + 10.55} \quad (5.27)$$

Note that if the cask were an infinitely long cylinder or a semi-infinite slab, there would be no molten lead at time t_1 because the onset of melting would be uniform over the surface. Finite cask geometries that have edges and corners create spots for lead to start melting quickly.

Step 9

The superheat of the molten lead has been estimated to be 4.3°F per vertical inch for a 1475°F fire. The average temperature of the superheated lead, T_{sup} is, therefore, given by

$$T_{\text{sup}} = (4.3^\circ\text{F})\frac{h}{2}, \quad (5.28)$$

where h = the vertical dimension of the cask in the fire.

Step 10

The surface temperature of the cask at time t_2 is given by:

$$T_{S-2} = T_{F-1} + T_{\text{sup}} \quad (5.29)$$

The average temperature of the outer shell of the cask at time t_2 is:

$$T_{OS-2} = T_{OS-1} + T_{\text{sup}} \quad (5.30)$$

Values of T_{F-1} and T_{OS-1} were computed in Step 6.

Step 11

The net heat flux absorbed from time t_1 to t_2 may be calculated from:

$$\bar{Q}_2 = \left[1935^4(0.9) - T_{S-2}^4 \right] (0.173 \times 10^{-8})(0.8) . \quad (5.31)$$

Step 13

A value for t_2 may now be computed.

$$(t_2 - t_1) = \frac{H_{T-2}^* - H_{T-1}^*}{\bar{Q}_2 A} \quad (5.32)$$

$$t_2 = t_1 + (t_2 - t_1) . \quad (5.33)$$

Step 14

If time t_2 is greater than 0.5 hr, then all of the lead will not be melted at the end of the 30-min fire test. In this event, the quantity of the lead that is melted may be computed by using Eq. (5.34).

$$W_{ML-2} = W_{ML-1} + (W_L - W_{ML-1}) \frac{(0.500 - t_1)^{1.5}}{(t_2 - t_1)^{1.5}} \quad (5.34)$$

Step 15

The temperature of the inner shell may be calculated by assuming that the body of the cask is at a uniform temperature. The total heat absorbed per degree F by the steel and lead in the cask up to the melting point of lead is given by:

$$H_S^* = 0.125 (W_{os} + W_{is} + W_F) . \quad (5.35)$$

$$H_L^* = 0.0325 W_L . \quad (5.36)$$

$$H_T^* = H_S^* + H_L^* \text{ Btu/}^\circ\text{F}, \quad (5.37)$$

$$\text{The heat absorbed at the end of 0.5 hr} = Q_{0.5} = H_{T-1} (0.5 - t_1) \bar{Q}_2 A \quad (5.38)$$

The average temperature of the inner shell may then be calculated from:

$$T_{is-2} = T_0 + \frac{Q_{0.5}}{H_T^*} \quad (5.39)$$

5.5.4 Use of Digital Computers in Studying the Thermal Transient Caused by a Fire

In recent years digital computer programs have been written to provide solutions to general and specific transient heat transfer problems. The development of such programs has been prompted by a variety of reasons such as to analyze heat transfer in three dimensions, to include temperature dependent material properties and to incorporate time dependent boundary conditions. Such codes are valuable in studying the thermal response of a cask to the hypothetical fire condition.

The programs used have ranged from those which provide numerical evaluation of closed form analytical solutions of heat transfer equations to those which involve direct mathematical models of the heat transfer phenomena. A discussion of some of the characteristics of computer codes useful in analyzing the response of a cask to the hypothetical fire is discussed below.

Several codes have been developed to obtain a solution to the differential heat transfer equations written in finite difference form for specific geometries. An excellent reference on the principles used in finite difference solutions to problems in heat transfer is the text by G. M. Dusenberre.²⁵ Examples of this are the FACF²⁶ code and the code described in a paper given by K. H. Veith.²⁷ These programs are aimed at specific cask geometries and each have limitations in their ability to provide detailed information regarding thermal behavior. However, they provide a reasonably detailed analysis of cask behavior coupled with economical use of computer memory and running time.

A second major class of computer codes are those based on finite element representation. The SIFT-TOSS²⁸ and TRUMP²⁹ codes are examples of such general application codes not intended for use on any specific geometry. Both codes provide for computer input in terms of physical coordinates which describe material boundaries; the codes allow the various material volumes to be divided into a large number of smaller regions thus providing the flexibility to model a specific problem.

The heat transfer equations in these codes are used to describe heat flow in a medium including the ability of the medium to retain heat and

resist heat transfer in each individual small volume. For each small time increment a heat balance is made on each elemental volume; this results in a temperature change for that volume from its previous temperature. Solutions to the problem of transient heat transfer are carried out in a manner closely resembling that in codes using finite difference representation of the equations.^{26,27}

Severe problems of storage and machine running time may result from using a very finely divided network since such networks reduce the heat capacitance of the individual volume elements. The method of solution used in the SIFT-TOSS and TRUMP codes requires that the time increment used in each heat balance be dictated by the smallest heat capacitance used in the network. Even with present day high speed digital computers it is not uncommon for the execution time of some analyses to exceed the real time being modeled.

Codes like SIFT-TOSS and TRUMP have limitations on the geometry which may be easily accepted by the machine. One example is that SIFT-TOSS does not have a mesh generator for spherical coordinates. The incorporation of mesh generators into codes like SIFT-TOSS and TRUMP require relatively large amounts of memory thus reducing the number of elements that may be utilized in a given problem. In order that a larger number of elemental volumes may be considered, the input generator (SIFT) of the SIFT-TOSS code may be bypassed and the TOSS portion only of the code used.

In certain cases of analysis advantages will be found in "building" a specialized program from a family of subroutines incorporated in problem-oriented codes such as CINDA-3G.³⁰ This code is a series of numerical routines for solution by direct or iterative methods. This allows an almost unlimited ability to model thermal transient problems in terms of number of elements considered but also requires vast amounts of input to describe a given problem. A family of codes is currently being developed at ORNL which will combine the best features of codes like SIFT-TOSS with the flexibility of CINDA-3G to minimize the tedious input generation problem.

NOMENCLATURE FOR ENERGY BALANCE METHOD, SECT. 5.5.3

- A = effective external surface area of cask, ft^2
 C_p = specific heat capacity, $\text{Btu/lf } ^\circ\text{F}$
 D = thickness of lead shield, in.
 H_f = latent heat of fusion, Btu/lb
 H_{F-1} = heat absorbed by cask fins at time t_1 , Btu
 H'_{F-1} = heat absorbed per sq ft of fin at time t_1 , Btu/ft^2
 H_{F-2} = heat absorbed by cask fins at time t_2 , Btu
 H_{is-1} = heat absorbed by inner shell of cask at time t_1 , Btu
 H'_{is-1} = heat absorbed by inner shell of cask per sq ft at time t_1 ,
 Btu/ft^2
 H_{is-2} = heat absorbed by inner shell of cask at time t_2 , Btu
 H_L^* = heat absorbed by lead to its melting point, $\text{Btu/}^\circ\text{F}$
 H_{L-1} = heat absorbed by lead at time t_1 , Btu
 H'_{L-1} = heat absorbed by lead per sq ft at time t_1 , Btu/ft^2
 H_{LL} = heat absorbed by melting lead, Btu
 H_{LM} = heat absorbed by solid lead to melting, Btu
 H_{LS} = heat absorbed by superheating lead, Btu
 H_{OS-1} = heat absorbed by outer shell of cask at time t_1 , Btu
 H'_{OS-1} = heat absorbed by outer shell of cask per sq ft at time t_1 ,
 Btu/ft^2
 H_{OS-2} = heat absorbed by outer shell of cask at time t_2 , Btu

H_S^* = heat absorbed by steel on cask to the melting point of lead,
Btu/°F

H_T^* = total heat absorbed by the cask to the melting point of lead,
Btu/°F

H_{T-1}^1 = total heat absorbed by the cask per sq ft at time t_1 , Btu/ft²

H_{T-1}^* = total heat absorbed by the cask at time t_1 , Btu

H_{T-1} = total heat absorbed by the cask if all the lead were solid,
Btu

ΔH_{T-1} = heat available for melting lead at time t_1 , Btu

H_{T-2}^* = total heat absorbed by the cask at time t_2 , Btu

h = vertical dimension of cask in fire test calculations, in.

k = thermal conductivity, Btu/hr ft °F

M = weight of cask per unit area of outer shell area, lb/ft²

\bar{Q}_1 = average heat flux between time t_0 and t_1 , Btu/hr ft²

\bar{Q}_2 = average heat flux between time t_1 and t_2 , Btu/hr ft²

$Q_{0.5}$ = heat absorbed at the end of 0.5 hr, Btu

T_0 = average temperature of cask under normal operating conditions,
°F

T_{F-1} = average fin temperature at time t_1 , °F

T_{F-2} = average surface temperature of fins at t_2 , °F

T_{is-1} = average temperature of inner shell of cask at time t_1 , °F

T_{is-2} = average temperature of inner shell of cask at time t_2 , °F

T_{L-1} = average temperature of solid lead at time t_1 , °F

T_{MP} = melting temperature of lead = 621°F = 1081°R

- T_{OS-1} = average temperature of outer shell of cask at time t_1 , °F
 T_{OS-2} = average temperature of outer shell of cask at time t_2 , °F
 T_{S-1} = average surface temperature of cask between time t_0 and t_1 , °F
 T_{S-2} = surface temperature of cask at time t_2 , °F
 T_{sup} = average temperature of superheated lead or the increase above 621°F at time t_2 , °F
 t_0 = initial time at start of fire test
 t_1 = time required to start melting lead in center of cask face, hr
 t_2 = time required to complete melting of lead, hr
 t_3 = time required to arrive at a temperature higher than the melting point of lead, hr
 W_F = weight of fins, lb
 W_F' = weight of fins per unit of outer shell area, lb/ft²
 ΔT = differential in temperature, °F
 W_{iS} = weight of inner shell, lb
 W_{iS}' = weight of inner shell per unit of outer shell area, lb/ft²
 W_{ML-1} = weight of molten lead at time t_1 , lb
 W_{ML-2} = weight of melted lead at time t_2 , lb
 W_{OS} = weight of outer shell, lb
 W_{OS}' = weight of outer shell per unit of outer shell area, lb/ft²
 χ = thickness of the outer shell, in.
 ρ = density, lb/ft³

5.6 References

1. "Safety Standards for the Packaging of Radioactive and Fissile Materials," AEC Manual Chapter 0529 (August 1966, revision).
2. THT-D (Transient Heat Transfer Program). Originator: The General Electric Company.
3. NETHAN-II and III (Network Thermal Analyzer). Originator: Applied Physics Laboratory. Developer: Communications Satellite Corp.; modified by Battelle Memorial Laboratory.
4. CINDA (Chrysler Improved Numerical Differencing Analyzer). Originator: Space Division of the Chrysler Corporation.
5. J. S. Watson, Heat Transfer from Spent Reactor Fuels During Shipping: A Proposed Method for Predicting Temperature Distribution in Fuel Bundles and Comparison with Experimental Data, ORNL-3439, May 27, 1963.
6. E. D. Arnold, PHOEBE - A Code for Calculating Beta and Gamma Activity and Spectra for ^{235}U Fission Products, ORNL-3921 (July 1966).
7. R. W. Peelle, W. Zobel, and T. A. Love, "Measurement of the Spectrum of Short-Lived Product Decay Gamma Rays Emitted from a Rotating Fuel Belt," Applied Nuclear Physics Division Annual Report, ORNL-2081 (September 1956); W. A. Zobel and T. A. Love, "Time and Energy Spectra of Fission Product Gamma Rays Measured at Short Times After Uranium Sample Irradiations," ibid.
8. J. F. Perkins and R. W. King, "Energy Release from the Decay of Fission Products," Nucl. Sci. Eng. 3(6), (June 1958).
9. J. O. Blomeke and M. F. Todd, Uranium-235 Fission Products Production as a Function of Thermal Flux, Irradiation Time, and Decay Time, ORNL-2127 (Aug. 19, 1957).
10. C. A. Anderson, Jr., Fission Product Yields from Fast (\sim MeV) Neutron Fission of Pu-239, LA-3384 (Dec. 30, 1965).

11. Yu A. Zysin, A. A. Lbov, and L. I. Sel'chenkov, Fission-Product Yields and Their Mass Distribution (Consultants Bureau, New York, 1964); Russian publication in 1963.
12. S. Katcoff, "Fission-Product Yields from Neutron-Induced Fission," Nucleonics 18 (11), 201 (1960).
13. L. Burris, Jr. and I. G. Dillon, Estimation of Fission Product Spectra in Discharged Fuel from Fast Reactors, ANL-5742 (July 1957).
14. Frank Kreith, Principles of Heat Transfer, pp. 217-227, International Textbook Co., Scranton, Pa., 1958.
15. A. I. Brown and S. M. Marco, Introduction to Heat Transfer, 2nd ed., p. 68, McGraw-Hill, New York, 1951.
16. F. I. Hand, "Insulation on Clear Days at the Time of Solstices and Equinoxes for Latitude 42°N, Heating and Ventilation" 47 92 (Jan. 1950); 51 97 (Feb. 1954).
17. H. C. Hottel, Mark's Engineering Handbook, 6th Ed. 1958. pp. 12-114.
18. W. H. McAdams, Heat Transmission, 3d ed., pp. 172-178, McGraw-Hill, New York, 1954.
19. C. S. Williams, J. Opt. Soc. Am. 51, 564 (May 1961).
20. M. Jacob, Heat Transfer, Vol. 1, p. 236, Wiley, New York, 1956.
21. S. C. Skirvin, User's Manual for the THTC Computer Program, General Electric Company, Cincinnati, Ohio.
22. J. D. McLendon, Summary Report of AEC Symposium on Packaging and Regulatory Standards for Shipping Radioactive Material, TID-7651,
23. C. F. Bonilla and A. L. Strupczewski, Nuclear Structural Engineering (2), No. 1, pp. 40-47 (1965).
24. G. P. Wachtell and J. W. Langhaar, Fire Test and Thermal Behavior of a 15-ton Lead-Shielded Cask, DP-1070, Oct. 1966.

25. Heat Transfer Calculations by Finite Differences, G. M. Dusenberre, International Textbook Company, 1961.
26. W. C. Corder, Battelle Memorial Institute, FACP Code, Personal communication.
27. K. H. Veith, Assessment of the Thermal Behavior of Irradiated Fuel Casks, 2nd International Symposium on Packaging and Transportation of Radioactive Materials, October 14-18, 1968, pp. 306-319.
28. SIFT: An IBM 7090 Code for Computing Heat Distributions, David Bagwell, K-1528, Oak Ridge Gaseous Diffusion Plant; TOSS, David Bagwell, K-1494, December 1, 1961.
29. TRUMP: A Computer Program for Transient and Steady State Temperature Distributions in Multi-Dimensional Systems, A. L. Edwards, UCRL 14754 Rev. 1, May 1, 1968.
30. CINDA-3G, D. R. Lewis, J. D. Gaski, L. R. Thompson, TN-AP-67-287, October 20, 1967, Chrysler Corp. Space Division.

6. CRITICALITY

6.1 Introduction

The criticality evaluation problem considered here is not so much concerned with the method of maintaining subcriticality as it is with the proof of adherence to the requirement of subcriticality. In the interest of economy and practicality, a shipper should be allowed to exercise any practical controls he so desires in rendering a system subcritical; however, the shipper must present proof that his controls are adequate. Therefore, this chapter deals with the determination of the kinds of evidence that should be considered as acceptable in proving that a system conforms to the criticality requirements of existing federal regulations.

These regulations require every shipment of fissile material to remain subcritical at all times during normal transport, including loading and unloading, and under hypothetical accident conditions leading to the most reactive credible (hereafter denoted by MRC) configuration. In complying with these regulations, shippers of irradiated reactor fuels normally carry out a criticality evaluation of their casks.

Proof of system subcriticality can hardly be better substantiated than with an experiment using the fuel in question arranged in the MRC configuration with respect to the shipping cask design. Many times such information is not available and proof of subcriticality is based on calculational methods.

It is therefore highly desirable to at least have the cask concept in mind at the time critical experiments are being performed to obtain information in the physics of a new reactor core. Under such conditions additional experiments may be performed to predict the degree of subcriticality during shipment.

6.2 Methods of Prevention of Criticality

The criticality of a system is often discussed in terms of an effective multiplication factor, k_{eff} , which is defined as the ratio of the neutron production rate to the neutron loss rate in the system. The

cask-fuel system must remain subcritical so that k_{eff} is less than unity. This may be accomplished by the adjustment and control of several physical and nuclear variables which either limit the neutron production rate (i.e., fission rate) or provide an adequate neutron loss rate (capture plus leakage). These variables are:

1. Mass of fissionable material
2. Degree of moderation
3. Internal geometry details
4. Parasitic poison effectiveness
5. Geometrical shape of assembly
6. Reflector effectiveness

Control of the first three variables can serve to limit the fission rate either by limiting the amount of fissionable material or by controlling the energy and spatial distribution of the neutrons which cause fission. The second, third, and fourth factors may be adjusted to provide an adequate loss rate through neutron capture, while the second, fifth, and sixth variables may be controlled to achieve the desired neutron leakage.

6.2.1 Application

An example of a shipment in which the mass of fissionable material was the primary criticality control was the shipment of MTR-type fuel from the Swedish AER2 reactor. Previous experiments at Oak Ridge had shown that, under optimum conditions, 2.5 kg of ^{235}U in MTR-type fuel elements was required for criticality. The cask for the Swedish shipment was designed to hold nine fuel elements. The particular fuel to be shipped contained 200 g of ^{235}U per element, or a total of 1.8 kg. It was clear that this shipment was and would remain subcritical by virtue of a limited mass.

Another example of criticality control achieved by limiting the mass of fissile material is the Consolidated Edison Company cask, used for shipping fuel from the Indian Point reactor. Critical experiments

indicated that six fuel elements were required for criticality. The cask was designed to hold two fuel elements, giving an estimated k_{eff} of about 0.86.

Fuel assembly geometry is usually fixed by the reactor design and is not changed for shipment. However, spacing between assemblies is often changed to a less reactive separation. In this case one should note that the critical experiments performed during the reactor design may no longer be applicable to the cask - fuel assembly system unless performed in geometry in question. Also, if the fuel assemblies are placed in an awkward or irregular geometry, the difficulty of a criticality evaluation is increased.

Moderation as a primary criticality control has not often been used in the transportation of reactor fuel elements because of the difficulty of guaranteeing the presence or absence of moderator water in the cask in the event of an accident.

Uranium enriched to less than approximately 5% in ^{235}U requires a moderator to make the system critical. This fact forms the basis of criticality safety for the shipment of large quantities of UF_6 enriched to less than 5 wt % ^{235}U . A single container may hold hundreds of pounds of UF_6 and moderation is the primary method of criticality control in these shipments. This often constitutes many critical masses if optimum water moderation ever occurs. However, the cylinders have shown their ability to protect the UF_6 and, consequently have demonstrated the safety of this shipping procedure.¹

Reflector effects are not normally used to control criticality because the reactivity associated with reflector changes is not great in large systems and it is difficult to assure the absence or presence of reflector water around the fuel containment basket.

Although water is recognized to be one of the most effective reflectors that exists, one should note that the replacement of a water reflector by a lead or depleted uranium reflector can increase the reactivity of an assembly. Critical experiment data for different reflectors were being obtained at ORNL at the time of this writing;

preliminary experiments indicate that lead, depleted U, and under some circumstances, stainless steel are superior to water in their reflector properties. An increase in k_{eff} of at least 0.01 is possible in some assemblies by replacing an effectively infinite water reflector with a 6-in. lead reflector and a 3/4-in. water gap (the most reactive combination) between the lead and the core.

The criticality control technique which has practical application in fuel transport is the use of fixed heterogeneous poisons. Large reductions in reactivity can be safely assured with properly fabricated poisoned casks.

To be effective as the primary criticality control method, both the presence of the poison and the effectiveness of the poison must be assured. Physical and chemical processes which could alter the above two conditions include:

1. Selective leaching of the poison by coolants
2. Melting and redistribution of the poison
3. Mechanical fracture and redistribution of the poison
4. Loss of moderation near a thermal neutron absorbing poison
5. Failure to install the poison

The decay heat from irradiated fuel or large heat loads imposed by a fire could melt or soften a poison and change its geometry, thereby reducing its effectiveness. Such undesirable effects must be considered when using Boral (B_4C particles in aluminum) which softens below 800°C or boron-impregnated polyethylene which melts at about 100°C .

In addition to Boral and boron polyethylene, use has been made of boron-clad stainless steel, boron-stainless steel alloy, cadmium clad stainless steel, cadmium-copper, and cadmium-aluminum alloy. The latter two materials have excellent heat transfer properties.

An example of a cask in which a heterogeneous fixed poison constituted a primary method of criticality control is shown in Fig. 2.37.

This cask is capable of transporting 24 MTR type fuel elements in two vertically stacked baskets. The central divider plates are constructed of Boral.

Liquid poisons are generally considered to be an unsatisfactory method of controlling the criticality of a fuel shipment because of the potential leakage problem that accompanies all shipments. If, however, the fissile material is in the liquid form and mixed with the poison, this could be an acceptable method since the poison could not be lost without losing the fuel.

6.3 Normal Conditions of Transport

The purpose of a criticality analysis for the normal condition is to identify the nuclear characteristics of the system that are expected to prevail during shipment and, in addition, provide a point of departure for establishing the most reactive credible condition that might reasonably result from an accident during transport (see Sect. 6.4). Normal conditions of transport are presented in annex 1 of AEC manual Chapter 0529 and consider such environmental conditions as heat, cold, pressure, vibration water spray, impact, and compression.

As part of the normal conditions of transport the following items should be considered:

1. Any differences in normal transportation and normal loading or unloading environments; i.e., occasionally fuel is shipped dry but loaded or unloaded under water.
2. The expected configuration of the fuel-poison system. Is breakage, crumbling or movement of the fuel, poisons, or supporting structural materials expected as a result of vibration during transportation and/or normal handling procedures?
3. The fissile classification for the shipment should be established in accordance with regulatory requirements.^{2,3,4}

4. Structural irregularities and heterogeneities which will exist in the inner cavity and which cannot or will not be rigorously represented in nuclear calculations and other forms of criticality evidence.
5. The actual reflector system during transportation; e.g., an inch of water surrounded by 1/2 in. of steel surrounded by 9 in. of lead.
6. The expected fuel and moderator temperatures.
7. Expected corrosion in the inner cavity which could result in redistribution of the fuel or poisons.

6.3.1 The Fresh Fuel Assumption

A criticality analysis should be made for the case where the fuel is in the most reactive condition in which it will be transported. If the reactivity of the unirradiated fuel system continuously decreases with exposure, which is often the case, the nuclear analysis should be based on a cask containing fresh fuel. Usually, criticality analyses for the commercial thermal power reactors are made on this basis because, in addition, the physical form and composition of fresh fuel are known more accurately than those of irradiated fuel and/or evidence in the behavior of a fresh fuel system may already be in hand from core design experiments and calculations. Moreover, the fresh fuel assumption could be quite realistic if it becomes necessary to remove and ship unexpectedly low burnup fuel because of mechanical or other problems. If the reactivity of the fuel system increases at any time during irradiation, however, then the effect of burnup on reactivity should be considered, and the fresh fuel assumption may not be appropriate.

6.3.2 Burnup Effects on Reactivity

If the fresh fuel assumption is not applicable, it will be necessary to determine the exposure at which the fuel system is most reactive since the criticality analysis will have to be based on this condition. Even if the fresh fuel assumption is applicable, the shipper may want to

consider fuel burnup so that he can ship more fuel in a given cask. However, because several key parameters are a function of exposure, and because the fuel exposure will probably not be uniform, the reactivity of irradiated fuel is more difficult to predict than the reactivity of fresh fuel. The following items must be considered when developing a criticality safety analysis for irradiated fuel:

1. Credit to be taken for burnup of the fissionable material.
2. Buildup of plutonium or ^{235}U .
3. Depletion of burnable poisons.
4. Credit to be taken for poisoning due to fission products.

The main problem in accounting for burnup of ^{235}U is that the gradual control rod withdrawal and, in some cases, changes in moderator density during exposure make the axial variation of neutron flux (and therefore burnup) difficult to predict. In a region of low thermal but high resonance flux, it is possible to generate more fuel than is consumed. If credit is taken for burnup of fissile ^{235}U atoms, then buildup of ^{239}Pu or ^{233}U must be considered.

It is recommended that, unless acceptable evidence is provided of the isotopic abundance of plutonium in the fuel, all plutonium be considered as ^{239}Pu . In a typical PWR reactor, about 70% of the total plutonium is fissile Pu.⁵ A most important point is that statements of fissile concentration in irradiated fuel should be supported by acceptable evidence which includes the associated uncertainty of fissile content and the basis for determining that uncertainty.

Prior to 1967, credit for burnup of ^{235}U was claimed in only one shipment of irradiated fuel. This shipment was an in-plant transfer of Yankee reactor fuel. Assuming no burnup, the calculated k_{eff} was about 0.97 for ten oxide fuel elements enriched to 4.1% in ^{235}U . The calculated k_{eff} for the fuel assuming a burnup of 12,000 Mwd/metric ton U was 0.88.

Many thermal power reactors use burnable poison for power flattening and reactivity lifetime control. Often, the poison burns out faster than

the fuel, resulting in increasing reactivity with burnup. The reactivity increase may continue until most of the burnable poison is depleted, at which time the reactivity will begin to decrease due to fuel burnup. Again, the fuel system may reach its maximum reactivity some time after reactor startup, depending on the type, amount, and location of any burnable poisons in the system. The initial reactivity worth of burnable poison in power reactors is usually several percent and may be as large as $\Delta k_{\text{eff}} = 0.1$. Calculation of the poison reactivity worth as a function of exposure may be difficult because of nonuniform axial burnup as well as changing flux depression in the poison. The problem of predicting burnable poison depletion can usually be sidestepped since it is normally conservative for a criticality calculation to neglect any poisoning effects due to burnable poisons. The rapid burnout of most poisons often leaves only a small poisoning effect after any appreciable burnup, so that only a minor penalty in permissible payload may be incurred by neglecting it.

In order to support a claim of fission product poison worth, some valid treatment of fission product poisoning is needed. Very few experiments have been performed for comparison with calculation. However, one such comparison⁶ indicated that an uncertainty of at least 10% can be expected in the calculated poisoning effects of fission products.

The effect of fission product poisoning has been treated in detail at Oak Ridge National Laboratory.⁶ The uncertainty in the calculated fission product worth in irradiated fuels is estimated⁷ to be less than 15% using the Long Fission-Product Treatment (LFPT). This treatment is sufficiently detailed and well enough established to permit its use as a validating calculational method. If a given fission product treatment compares favorably with LFPT, it should be considered safe engineering practice to allow credit for about two thirds of the calculated fission product reactivity worth in the shipment of irradiated fuel.

Except for ^{135}Xe , about 95% of the fission product poisoning in thermal reactors results from fission products with half lives greater than about two years. Excluding those fission products with half-lives of less than two years, a typical fission product worth in a PWR power

reactor is about 4 to 5% Δk for a burnup of 10 to 12,000 Mwd/metric ton U; for a burnup of 40 to 60,000 Mwd/metric ton U, the worth is about 6 to 7% Δk . The fractional neutron absorption by fission products tends to saturate at very high burnups and the poison worth of long-lived fission products is not expected to exceed about 8% in any practical power reactor.

6.4 The Most Reactive Credible Condition of Transport

The most restrictive criticality requirement for nuclear safety in shipping is that the shipping container must remain subcritical in its most reactive credible configuration (MRC condition); such a configuration could be the result of the container becoming involved in a transportation accident. A series of hypothetical accidents which must be withstood is described in the regulations and consists essentially of the container falling 30 ft onto a solid, unyielding surface followed by a 40-in. drop onto a 6-in. diam piston, followed by a 1/2-hr fire, followed by immersion in water.

Some typical problems that must be considered when determining the MRC condition of a cask after the accident series are given below.

1. The fuel, fixed poisons, and moderators may become broken and redistributed into a more reactive configuration. This is particularly important for irradiated ceramic fuels with long exposures and brittle cladding.
2. Optimum moderation and/or reflection by water may occur inside and outside the cask as a result of impact damage followed by immersion or loss of coolant.
3. Loss of coolant may cause melting of fuel and/or nuclear poisons, resulting in redistribution into a more reactive configuration. Irradiated fuels with intense γ -heating and fixed neutron absorbers with low melting temperatures are cases in point.
4. Unless specifically designed to prevent such an occurrence, inleakage of water after impact may result in a violent reaction with Na- or NaK-bonded fuels, causing redistribution of the fuel into a more reactive configuration.

5. Under certain conditions radioactive decay may increase reactivity while the fuel is in the cask. For example, in the case of thorium-bearing fuels, the decay of ^{233}Pa to ^{233}U can increase the inventory of fissionable material.
6. Nuclear interaction with fissile material in neighboring casks should be considered.

6.5 Criticality Evidence

When the normal and MRC conditions have been identified for a particular fuel shipment, various types of criticality evidence may be compiled. If relatively small quantities of fissile material are involved, it may only be necessary to provide assurance that certain exemption limits on the fuel system parameters will not be exceeded. For larger shipments with highly heterogeneous fuel-poison geometries and compositions, experimental evidence and well-validated calculational evidence may be necessary. The purpose of this section is to establish the kinds of evidence that should be considered acceptable in determining whether and to what degree a system will be subcritical in the normal and MRC conditions, with emphasis on the application to low-enriched water-moderated power reactor fuels.

6.5.1 Safe Limits

Many shipments of fissile material will be made which exceed the exempt quantities and yet are small enough not to pose a serious criticality problem. Parametric limits below which criticality cannot occur in single units are considered in various nuclear safety guides.^{7 - 13} Some of these parametric limits, modified by a small safety factor are given in Table 6.1.

If any one of the limits in Table 6.1 and the conditions for which it applies are maintained, the system cannot become critical under the considered accident conditions. The limits are for uniform aqueous solutions and do not apply to mixtures of fissile isotopes. In addition, the limits are only applicable when the multiplication factor of

Table 6.1 Parametric Limits for Criticality of Single Units*

Parameter	Limit	
	U ²³⁵	Pu ²³⁹
Mass (grams)	700	500
Cylinder diameter (cm)	13.5	12.5
Slab thickness (cm)	4.38	3.6
Volume (liters)	5.8	5.5
Concentration (g/liter)	11.0	7.0
Enrichment of ²³⁵ U in Uranium (wt %)	1.0	-

*This assumes the unit is isolated and therefore has no interaction with other fissile materials.

the system in the presence of neighboring reflectors, fissionable materials and sources is less than or equal to the multiplication factor of the system with an infinite reflector of water.

A safety standard is now being developed¹³ which will specify single parameter limits for use in maintaining nuclear safety of fissionable materials. This proposal is intended as a revision of the American Standard, ASA N6.1-1964 and is being prepared by Subcommittee ANS-8 of the Standards Committee of the American Nuclear Society. While the parameter limits of that document are still being revised, they are expected to be close to the values given in Table 6.1 and, in addition, are expected to be more comprehensive.

6.5.2 Calculational Evidence

The purpose of this Guide is not to require that certain pieces of evidence be developed utilizing specific codes and cross sections; it is

assumed that competent personnel utilizing their own machines, codes, and cross sections can produce reliable evidence as to the k_{eff} of the system in question.

However, it is necessary to provide a framework by which the AEC can assess the confidence level expected in the calculation of k_{eff} . For example, an acceptable calculation of k_{eff} of a fissile assembly should have, as a supporting basis, at least one favorable comparison of the calculational method with a critical experiment which has a fuel-moderator-poison-reflector system similar to the given assembly in the MRC condition. If heterogeneous neutron absorbers are present in the system to be shipped, the calculation should be compared with an experiment having the same poison material and approximately the same poison concentration, geometry, and associated neutron energy spectrum as the system in the MRC condition. If the presence of neighboring fissile assemblies is included in the MRC condition, the calculation-experiment comparison should be made on a critical experiment having the same interspersed moderator and approximately the same size and edge-to-edge spacing of individual assemblies.

If a similar critical experiment does not exist, two or more critical experiments should be calculated to bracket the parameters of interest over not too wide a range. A certain amount of judgement will be required to establish a reasonable parameter range. As a rough estimate for water-moderated power reactors, the fuel rod diameter, water-to-uranium volume ratio, and ^{235}U enrichment of the assembly of interest should not differ by more than about 20% from the corresponding parameters in the validating critical experiment.

The supporting calculational comparisons should use the same assumptions, computer codes, homogenization schemes, input data preparation, neutron energy group structure, and basic cross sections as the calculation which is to provide acceptable evidence of subcriticality during transportation. The sophistication of the calculational technique is not overly important in establishing the reliability and accuracy of the method over a narrow range of parameters. Criticality calculations are somewhat of an art, and it is possible for a two-group diffusion

calculation of k_{eff} to give better results than a ten-group S_{16} transport calculation particularly if the parameters of the diffusion calculation happen to be tailored to the specific problem at hand. It is important, however, that any calculational technique be validated by comparison with experiment for the parameter range of interest. As an aid in finding related critical experiment data for use in the calibration of calculational techniques, a bibliography of selected references has been prepared and is presented in the appendix. Each reference is accompanied by a brief description of the nuclear system(s) investigated.

Whatever the form and quality of calculational evidence, an error analysis should be performed which indicates the uncertainty in the calculated k_{eff} . Generally a calculation will have greater accuracy if the system being described is just critical; therefore, the detail of the error analysis should be commensurate with the proximity of the nuclear system to the critical condition.

Methods of calculation have been fairly well established for isolated fissile assemblies similar to water-moderated thermal power reactors.^{14,15} Experience has shown^{16,17,18} that, with the exercise of reasonable care, it is possible to predict k_{eff} within about 1 to 2% in thermal reactors. In contrast, accurate calculational methods and nuclear cross section data have not yet been generally established for unmoderated systems. A recent comparison of calculations for a dilute plutonium-fueled fast critical assembly of particularly simple design indicated¹⁹ that calculated values of k_{eff} deviated from experiment over a range from -3.6% to +2.4%. The calculations were submitted by domestic and foreign laboratories and by private industry. On the basis of the above comparison, and in view of the general lack of experience in calculations for unmoderated assemblies, we recommend special attention be given to the calculational techniques for unmoderated assemblies to ensure that the results are reasonably conservative.

When several fissionable assemblies are to be transported together, the calculation of interaction effects between neighboring assemblies is often necessary. The multiple-assembly analysis is usually the source of a greater uncertainty in the calculated k_{eff} than for a single

isolated assembly. Several calculational methods have been developed which may be used to treat the interaction effect. The three methods used most extensively in the U.S. are the density analog method,²⁰ the solid angle (interaction potential) method,^{21,22} and the Monte Carlo method.²³ The Monte Carlo method is superior to the others both in accuracy and in the capability of representing geometrically complicated configurations; several computer codes employing the technique are available for criticality calculations.^{24,25,26} While limited experience has been gained with the method in the U.S.^{26,27} which indicates that k_{eff} may be predicted with an uncertainty of about 2%, it is being utilized to a much greater extent than ever before.

Considerable experience has been accumulated with the solid angle and density analog methods, both of which give conservative estimates of k_{eff} when properly used. Comparisons with experiment²⁸ indicate that the criticality factor of a regular air-spaced array may be calculated with an accuracy of about 5 to 10% using the solid angle method. The density analog method has also been checked against experiment and, because of its simplicity, versatility, and accuracy, has been recommended by Brown²⁹ as the method of calculating critical arrays that is most applicable to transportation problems. It may also be used to extend the information already obtained from Monte Carlo calculations.

The above three methods of treating interaction effects have been checked with experiments on regular air-spaced arrays of similar units containing highly enriched fuel. Until more experience is obtained, none of the methods should be considered as proven for application to low-enriched arrays having an interspersed moderator (particularly a hydrogenous material); for this application two different methods should be used, one as a check on the other.

In summary, the following guideline is recommended for evaluating the acceptability of calculational evidence. If a calculational technique has been properly validated by comparison with critical experiments having a geometry and composition range which includes the assembly under consideration, a calculation for the system in the MRC condition should generally be considered as sufficient evidence of subcriticality for the

safe transport of low-enriched well-moderated power reactor fuels having k_{eff} below about 0.90. Above this approximate level of reactivity, calculational evidence should be supplemented with some type of experimental evidence. For high-enriched or unmoderated systems, supplemental experimental evidence may be desirable if the calculation indicates a system k_{eff} even below 0.90 because of the greater change in k_{eff} with small changes in size, mass, or moderation of the system.

6.5.3 Experimental Evidence

Two general types of experimental evidence are considered below: (1) related evidence, which includes relevant data from safety guides and also critical experiments on the given fuel under conditions different from those expected in transport, and (2) direct evidence, which includes reactivity determinations for loaded casks in the normal and/or MRC conditions. While critical experiments with irradiated fuel elements could be considered excellent direct evidence, such experiments are rarely performed in a shipping cask environment and are not included in this discussion.

Related Evidence. - Critical Experiments Before Irradiation. -

Perhaps the most convincing criticality evidence is derived from critical experiments with the given fuel before irradiation. This type of experiment is often carried out during the design of a reactor. The evidence is particularly useful if the fuel elements can be shown to have their maximum reactivity (at any time during life) when they are fresh and unirradiated. The minimum number of fresh fuel elements required for criticality can then be established. If this number is determined for a system having the same moderator and the same fuel element geometry and spacing that is used in the shipping cask, it should be considered excellent criticality evidence. Advance planning can improve the quality of the evidence through experiments with the same reflector, fixed poison, and structural arrangement that will exist in the cask. In the past, core design critical experiments have not been used to full advantage in providing criticality evidence for future shipping and storage safety requirements.

Critical experiment data obtained for a specific fuel-moderator-poison-reflector system are considered excellent evidence in establishing a case for subcriticality of a given system. As a general guideline, this type of evidence, when accompanied by a validated calculation of k_{eff} , should permit safe transport of low-enriched well-moderated power reactor fuels having k_{eff} (with the system in the MRC condition) below about 0.95.

Related Evidence. - Safety Guides and Criticality Data. - The most readily available sources of criticality evidence are the nuclear safety guides.^{9,10,12} These systematic presentations of experimental criticality data are extremely useful in estimating nuclearly safe dimensions, masses, moderator-to-fuel ratios, etc. for a variety of systems. Data from safety guides constitute excellent criticality evidence for many homogeneous and simple heterogeneous fuel systems. The safety guides also have established some safe nuclear parameter correlations which represent excellent evidence when they are applicable. In the case of more complicated systems, cautious extrapolation and interpolation of criticality data may be necessary. Many commercial reactor fuel shipments contain poison rods, fuel rods of several enrichments and diameters, etc.; for these complex systems, the quality of criticality evidence obtained from safety guides should be judged on the basis of the amount of extrapolation or interpolation involved.

Direct Evidence. - Direct experimental methods of reactivity determination represent a potential source of excellent criticality evidence. An advantage of this type of evidence is that the measurements can be made on the very system which is of interest, e.g., a loaded shipping cask submerged in water, or a storage array. Because of the effort and equipment usually required, this type of experiment is normally not performed on shipping casks except in monitoring the loading procedure. However, if the confidence derived from such an experiment were to permit a significantly greater amount of fuel to be shipped than is ordinarily the case, the performance of such an experiment on a shipping cask might be justified.

Several experimental techniques for reactivity measurements have been discussed by Keepin.³⁰ Methods most applicable to loaded shipping casks include: the multiplication measurement, the pulsed neutron method, the Rossi- α technique, and the source-jerk experiment. In general, the present technology of the multiplication experiment is inadequate for the accurate prediction of k_{eff} . However, a multiplication experiment can serve as a useful monitoring procedure during the loading of fuel into a shipping cask.

The best technique for evaluating the reactivity of subcritical moderated assemblies appears to be the pulsed neutron method. The prompt fundamental decay constant, α , can be measured quite accurately and, when normalized by a measurement at a known k_{eff} , or supplemented with a calculation of prompt neutron lifetime, can be used to establish a value of k_{eff} with an accuracy of 1 to 2% for $0.9 < k_{\text{eff}} < 1.00$. Approximately this same accuracy can be obtained from the Rossi- α method when it is applied to unmoderated, strongly-coupled, fast neutron systems. Considerably less accuracy is to be expected from Rossi- α measurements on well-moderated systems. Experience with the source-jerk technique has been limited in the U.S., and accurate predictions of k_{eff} cannot generally be made with this method at the present time.

Problems of measurement and interpretation of data accompany each of the direct experimental methods. For example, in the presence of strong γ -ray activity such as is associated with irradiated fuel elements, one must assure himself that his detector response is primarily determined by the neutron flux and not the γ -rays. As another example, the measured data (and consequently the inferred value of k_{eff}) will probably vary with detector location, and several detectors may be necessary to get an accurate space-averaged result. Reasonable care and attention must be given to such problems to obtain the accuracy mentioned above.

6.6 Applications for AEC Approval on Criticality

6.6.1 Exemptions

Before making application to cover a proposed shipment, examine the shipment to see whether or not a specific license is required.

Exemptions are provided in the regulations for a small quantity of any fissile material; for thorium, depleted uranium, natural uranium, or a very slightly enriched uranium containing insignificant amounts of plutonium or ^{233}U ; and for highly moderated fissile material. The packages which are exempted are those which contain less than a large quantity of material, as defined in the regulations, and may include:

1. Not more than 15 grams fissile material,
2. Thorium, depleted uranium, or natural uranium with insignificant ^{233}U or Pu content,
3. Homogeneous substances with 1% ^{235}U enrichment or less, and no significant ^{233}U or Pu content.
4. Homogeneous substances with 500 grams or less of fissile material, when the H/X ratio is greater than 7600; or 800 grams or less of ^{235}U when the H/ ^{235}U ratio is greater than 5200, and no significant ^{233}U or Pu is present; or 500 grams or less of ^{233}U and ^{235}U when the H/ ^{233}U plus 235 ratio is greater than 5200, and no significant Pu is present.

The "secondary" fissile isotopes mentioned are considered to be insignificant when they are less than 1% of the primary fissile isotope.

6.6.2 General Licenses*

For licensees covered by the Code of Federal Regulations, Title 10 Part 71, a general license is issued by the AEC to transport certain quantities of fissile material without meeting the packaging standards (Subpart C of 10 CFR 71). All shipments made under the general license are to be made either as Class II or Class III shipments. In addition, no package may contain a large quantity of material. If the shipment is to be made as a Class III shipment, the following is generally licensed:

- 500 grams or less ^{235}U ,
- 300 grams or less ^{233}U , ^{238}Pu , ^{239}Pu , and ^{241}Pu ,

*Based on information obtained from the Criticality Branch of the Division of Materials Licensing, U.S. Atomic Energy Commission, Bethesda, Maryland.

Any combination of ^{233}U , ^{235}U , and Pu, following the Unity Rule.**

2500 grams ^{238}Pu , ^{239}Pu , and ^{241}Pu as Pu-Be neutron sources, with no more than 400 grams ^{238}Pu , ^{239}Pu , and ^{241}Pu per package.

If the shipment is to be made as a Class II shipment, the following is generally licensed for each individual package:

Up to 40 grams ^{235}U

Up to 30 grams ^{233}U

Up to 25 grams Pu

Up to 400 grams Pu as Pu-Be neutron sources

Any combination of ^{233}U , ^{235}U , and Pu, following the Unity Rule** for a selected radiation unit.

The above general licenses are issued automatically to persons holding a specific license issued pursuant to any special nuclear material or by-product material license issued by the Commission.

A general license is issued to persons holding a specific AEC license for a shipment which is to be made in a specification container in compliance with the regulations of the ICG, 49 CFR 73. A specification container is one which is listed by the ICG as being approved for certain specified quantities and forms of material. In accordance with the AEC-ICG Memorandum of Understanding, specification packages will have been previously evaluated by the AEC before approval by ICG.

**The Unity Rule states that when fissile isotopes are shipped in combination, the sum of the ratios of the quantity of each isotope to its specified limit shall not exceed unity.

6.7 References

1. Oak Ridge Gaseous Diffusion Plant, "Standard Shipping Containers for 8- and 12-in. diam UF_6 Cylinders," KD-1930, Sept. 27, 1966.
2. U.S. Atomic Energy Commission, "Packaging of Radioactive Material for Transport," Part 71 of Title 10, Code of Federal Regulations, Federal Register, V. 31, No. 141, July 22, 1966.
3. U.S. Atomic Energy Commission, "Safety Standards for the Packaging of Radioactive and Fissile Materials," AEC Manual Chapter 0529, August 22, 1966.
4. Regulations for the Safe Transport of Radioactive Materials International Atomic Energy Agency. Safety Series No. 6, Vienna, 1965.
5. M. W. Rosenthal et al., "A Comparative Evaluation of Advanced Converters," USAEC Report ORNL-3686, pp. 146-179, January 1965.
6. T. R. England, "Time-Dependent Fission-Product Thermal and Resonance Absorption Cross Sections," USAEC Report WAPD-TM-333, p. 48 (Nov. 1962).
7. Private Communication with L. L. Bennett and D. R. Vondy, ORNL, January, 1967.
8. American Standards Association Sectional Committee N6, Project 8 of the American Nuclear Society Standards Committee, "Nuclear Safety Guide," TID-7016 (Rev. 1), 1961.
9. H. K. Clark, "Handbook of Nuclear Safety," USAEC Report DP-532, Jan. 1961.
10. H. G. Paxton, J. T. Thomas, A. D. Callihan, E. B. Johnson, "Critical Dimensions of Systems Containing ^{235}U , ^{239}Pu , and ^{253}U , TID-7028, June, 1964.
11. American Standards Association Sectional Committee N6, "Safety Standard for Operation with Fissionable Materials Outside Reactor," American Standard ASA NG.1-1964, published by The American Society of Mechanical Engineers.

12. American Standards Association Sectional Committee N5, "Guide for Design and Operation of Shipping Containers for Irradiated Solid Fuel from Nuclear Reactors," American Standard ASA N5.3-1964, published by The American Institute of Chemical Engineers.
13. Private Communication with Dixon Callihan, ORNL, January 1967.
14. A. Radkowsky, Naval Reactors Physics Handbook, Vol. I, 1964.
15. Argonne National Laboratory, "Reactor Physics Constants," USAEC Report ANL-5800, July, 1963.
16. Panel on Light Water Lattices, Light Water Lattices, Report of a Panel Held in Vienna, June 1, 1962, Technical Report Series No. 12, IAEA.
17. L. E. Strawbridge, "Calculation of Lattice Parameters and Criticality for Uniform Water Moderated Lattices," USAEC Report WCAP-3269-25, p. 25, Sept. 1963.
18. G. E. Edison, M. L. Winton, "Power Distribution and Reactivity Calculations for the MH-1A Reactor," USAEC Report ORNL-TM-1654, p. 10, January 1967.
19. W. G. Davey, "Intercomparison of Calculations for a Dilute Plutonium-Fueled Fast Critical Assembly (ZPR-3 Assembly 48)," International Conference on Fast Critical Experiments and Their Analysis, ANL, October 10-13, 1966.
20. H. C. Paxton, "Criticality Control in Operations with Fissile Material," LA-3366, p. 32, December, 1964.
21. H. F. Henry, J. R. Knight, C. E. Newlon, "Self-consistent Criteria for Evaluation of Neutron Interaction," K-1317, December, 1956.
22. H. F. Henry, C. E. Newlon, J. R. Knight, "Extensions of Neutron Interaction Criteria," K-1478, July, 1961.
23. M. A. Meyer (editor), Symposium on Monte Carlo Methods, Wiley, New York, 1956.

24. T. C. Longworth, "The GEM Monte Carlo Code and its Use in Solving Criticality Problems," Proceedings of the Symposium on Criticality Control of Fissile Materials, Stockholm, November, 1965.
25. D. C. Irving, R. M. Freestone, Jr., F. B. K. Kam, "O5R A General-Purpose Monte Carlo Neutron Transport Code," USAEC Report ORNL-3622, February, 1965.
26. G. E. Whitesides, G. W. Morrison, E. C. Crume, "Few-Group Monte Carlo Criticality Calculations," ANS Transactions, V. 9, No. 1, p. 133, June, 1966.
27. E. C. Crume, Jr., "The Reliability of Criticality Safety Calculations Using the New Codes GSC and KENO," USAEC Report Y-KC-96, April 21, 1967.
28. C. E. Newlon, "The Elements of Neutron Interacting Arrays-Part I," K-1619, October, 1964.
29. G. L. Brown, "Criticality Safety in Transportation and Storage," Proceedings, Nuclear Criticality Safety, p. 177, December 13, 1966.
30. G. R. Keepin, Physics of Nuclear Kinetics, Ch. 8, Addison-Wesley Publishing Company, Inc., 1965.

6.8 Bibliography of Critical Experiments

A bibliography of selected critical experiments is presented for use in validating calculational methods of reactor analysis. Only systems with a well-defined geometry and composition are included. The experiments are classified according to the system parameter of major interest. Particular attention was given to water cooled and moderated uranium systems of low enrichment since these make up the bulk of power reactor fuel shipments. The bibliography is accompanied by a concise description of the nuclear systems investigated in each reference.

A. Low Enriched UO_2 ; Water Moderated

- A1. P. W. Davison et al., "Yankee Critical Experiments - Measurements on Lattices of Stainless Steel Clad Slightly Enriched Uranium Dioxide Fuel Rods in Light Water," USAEC Report YAEC-94, April, 1959.
- A2. P. W. Davison et al., "Two Region Critical Experiments with Water Moderated Slightly Enriched UO_2 Lattices," USAEC Report YAEC-142, November, 1959.
- A3. R. D. Leamer et al., "Critical Experiments Performed with Clustered and Uniform Arrays of Rodded Absorbers," USAEC Report WCAP-3269-39, November, 1965.
- A4. R. M. Ball, A. L. MacKinney, and J. H. Mortenson, "MARTY Critical Experiments Summary of 4% - Enriched UO_2 Cores Studied for NMSR," USAEC Report BAW-1216, May, 1961.
- A5. Quarterly Technical Report, SPERT Project, IDO-17030, p. 40, April, 1964.

References A1, A2, and A3

Critical experiments were performed with stainless steel-clad UO_2 rods of 2.7, 3.7, and 4.4% enrichment. An unclad fuel pellet diameter of 0.300 in. was used. The square lattice pitch was in the range 0.4 - 0.7 in., permitting W/U ratios between 2 and 11. The oxide density was about 10.2 g/cm³. Cylindrical configurations with an active height of

4 ft were water reflected. In some of the experiments at 3.7% enrichment, 0.4-in. diam pellets clad with Zircaloy 4 were used. A few experiments were also done with 5.7% enriched pellets of 0.357-in. diam.

Reference A4

Lattices of UO_2 rods enriched to 3% and 4% were investigated using a square pitch of about 0.6 in. An unclad fuel pin diameter of 0.444 in. resulted in W/U ratios of 2.6 and 3.6. The fuel had a density of about 7.2 g/cm³ and was clad in either stainless steel or aluminum. The lattices were cylindrical with a water reflector and an active fuel height of about 5-1/2 ft.

Reference A5

Uranium dioxide rods of 4.8% enrichment were studied in the course of the SPERT project. The fuel pellets, 0.420 in. in diameter, were clad with stainless steel and aluminum and had an oxide density of 10.5 g/cm³. The square lattice pitch was about 0.6 in. The W/U ratio appears to be less than 1.0 - nonmoderator to moderator ratios of 1.9 and 2.2 were reported. Both cylindrical and rectangular configurations were made, with an active fuel length of 38.3 in.

B. Low Enriched U Metal; Water Moderated

- B1. W. G. Davey, K. R. Smith, "Exponential Experiments with Enriched Uranium-Natural Water Systems," British Report AERE-RP/R-1788 October, 1955.
- B2. H. Kouts and R. Sher, "Experimental Studies of Slightly Enriched Uranium, Water Moderated Lattices," USAEC Report BNL-486 (T-111), September, 1957.
- B3. C. R. Richey, R. G. Lloyd, and E. D. Clayton, "Criticality of Slightly Enriched Uranium in Water Moderated Lattices," Nucl. Sci. and Eng., 21: p. 217, February, 1965.
- B4. J. K. Fox, J. T. Mihalczko, and L. W. Gilley, "Critical Experiments with 2.09% ²³⁵U Enriched Uranium Metal Plates in Water," USAEC Report ORNL-CF-58-8-3, 1958.

B5. Private Communication with E. B. Johnson, Oak Ridge National Laboratory, (December, 1966).

Reference B1

Most of the square pitch lattice experiments with uranium metal were performed at Harwell Laboratory in England. One series of exponential and approach-to-critical experiments used metal rods of 0.93% enrichment with first aluminum and then stainless steel cladding. The unclad fuel rod diameters were 0.75 and 1.20 in. The lattice pitch varied from 0.94 to 1.85 in. corresponding to a W/U range of 0.59 - 1.94. Water-reflected cylindrical configurations with an active fuel length of about 30 in. were employed.

Reference B2

A series of exponential experiments was performed at BNL using 1.0, 1.15, and 3.3% enriched U metal rods clad with aluminum. The unclad fuel rod diameter was 0.600 in., and the active length was 4 ft. The triangular pitch was varied between 0.85 and 1.31 in. to give a W/U ratio ranging from 1 to 4. Cylindrical core configurations were arranged with a water reflector.

Reference B3

Approach-to-critical and exponential experiments with unclad U metal rods of enrichment 2.0% and 3.06% were carried out at Hanford. The triangular pitch was varied from about 0.28 in. to 1.81 in. for fuel rods whose diameter ranged from 0.175 to 0.925 in. The W/U ratio varied from about 2 to 12. Water-reflected cylindrical configurations were used with the active height varying from about 16 in. to 32 in.

Reference B4

Uranium metal plates enriched to 2.09% were studied at ORNL. The plate spacing varied from 0.0 to 5/8 in. Groups of plates were also studied with group spacings of 5/8 - 1-1/8 in. The plate size was 1/4 in.

thick, 3-1/8 in. wide, and 30 in. long. The W/U ratio varied from 2.5 to 4.5. Rectangular geometry with a water reflector was used in many cases.

Reference B5

Currently, critical experiments with 4.9% enriched uranium metal rods are underway at ORNL. Unclad rods of different diameters up to 1 in. are being studied in both triangular and square pitch lattices. The results for 0.5- and 0.8-in. diam rods are already in hand but unreported as of January 1, 1967. Lattice pitch is expected to be varied from about 0 to 2.4 in. with resulting W/U ratio of about 2 - 12. Water-reflected configurations with active fuel lengths of about 12 and 24 in. have been constructed in rectangular and cylindrical geometries.

C. Highly Enriched Uranium

- C1. J. C. Hoogtemp, "Critical Masses of Oralloid Lattices Immersed in Water," USAEC Report LA-2026, November, 1955.
- C2. J. K. Fox, L. W. Gilley, A. D. Callihan, "Critical Mass Studies, Part IX, Aqueous ^{235}U Solutions," USAEC Report ORNL-2367, (March, 1958).
- C3. E. B. Johnson and R. K. Reedy, "Critical Experiments with SPERT-D Fuel Elements," USAEC Report ORNL-TM-1207, July, 1965.
- C4. G. E. Hansen et al., "Critical Plutonium and Enriched-Uranium Metal Cylinders of Extreme Shape," Nucl. Sci. Eng., 8: p. 570, 1960.

Reference C1

Multiplication measurements at Los Alamos were used to determine critical mass data for fully enriched uranium metal. Lattices of unclad metal cubes having an edge length up to 1 in. were arranged into cubic arrays with water as moderator and reflector. The square lattice pitch was varied from 0.75 to 2.25 in. Some experiments were done with rods in cylindrical arrays. The rods were 1/8 in. in diameter, and the pitch ranged from 0.5 to 1 in. Water-to-uranium volume ratios varied up to about 80.

Reference C2

Critical experiments were performed with homogeneous solutions of fully enriched uranium. The solutions had H:²³⁵U atomic ratios between 27.1 and 74.6. Experiments were made with and also without a water reflector and with and without a cadmium lining in the container. In some cases interacting arrays of as many as seven vessels were tested. Cylindrical vessels of diameters up to 30 in. were used.

Reference C3

A series of water moderated and reflected experiments with SPERT-D fuel elements were performed at ORNL. The spacing between fuel in adjacent elements was varied up to about 2 in. Rectangular geometry was used in all cases except one in which a rounded lattice was made. The elements were 2 ft long in most experiments; a few experiments were done with 6-ft elements. The fuel element consists of a 3-in. square aluminum alloy tube containing 22 parallel fuel plates 60 mils thick and spaced 47 mils apart. Each fuel plate is a 20-mil thick alloy of uranium and aluminum containing 23.8 wt % of fully-enriched uranium sandwiched between two 20-mil thicknesses of aluminum alloy cladding. In some of the experiments, the outer rows of elements were only partially loaded to achieve criticality, the individual plates being removable.

Reference C4

Multiplication measurements were used to establish critical configurations with: a) fully-enriched uranium metal, and b) plutonium metal of composition 95% ²³⁹Pu and 5% ²⁴⁰Pu. Elongated and squat cylinders of extreme shape were built up, having height-to-diameter ratios ranging from about 0.05 to 0.3 and 4 to 15.

The uranium cylinders were of two diameters -- 15.00 and 3.24 in. The plutonium cylinder diameters were 2.2 and 6.0 in. Experiments were made with different reflectors which included water, uranium, graphite, polyethylene, and beryllium.

D. Critical Experiments with Poisons

- D1. E. B. Johnson and R. K. Reedy, Jr., "Critical Experiments with SPERT-D Fuel Elements," USAEC Report ORNL-TM-1207, July, 1965.
- D2. G. D. Hickman, J. A. Bistline, L. A. MacNaughton, "Water Moderated Cores with Boron Steel Septa at Elevated Temperatures," Nuclear Sci. and Eng. 8: p. 381, 1960.
- D3 R. A. Haffley, R. A. Watson and W. Skolnik, "Measurement and Calculation of Relative Poison to Fuel Capture Ratios in Slab Cores," USAEC Report KAPL-M-6528, November, 1965.
- D4. R. H. Clark, M. L. Batch and T. G. Pitts, "Lumped Burnable Poison Program - Final Report," USAEC Report BAW-3492-1, January, 1966.
- D5. P. W. Davison et al., "Yankee Critical Experiments - Measurements on Lattices of Stainless Steel Clad Slightly Enriched Uranium Dioxide Fuel Rods in Light Water," USAEC Report YAEC-94, April, 1959.
- D6. E. B. Johnson et al., "Applied Nuclear Physics Division Annual Progress Report," USAEC Report ORNL-2389, p. 3, September, 1957.

Reference D1

In some of the experiments with SPERT-D fuel elements, already described under reference C3, cadmium plates 25 mils thick were inserted in the water gaps between rows of elements. Also, in a few experiments soluble boron was added to a dilute solution of uranyl nitrate which served as moderator and reflector.

References D2 and D3

Experiments at KAPL were conducted using boron-stainless steel plates and Ni-B¹⁰ plates. The boron-stainless steel plates were 30 mils thick and contained various loadings of B¹⁰ up to 1.24 wt %. The Ni-B¹⁰ plates were 50 mils thick with a B¹⁰ content of 0.55 wt %. In some of the experiments, water gaps were introduced near the poison; in others, the plates were placed near the water reflector. The fuel lattice consisted of Zircaloy-clad fully enriched uranium metal plates 1.61 in.

wide and 0.0015 in. thick with 13-mil and 38-mil water gaps and 29-mil Zircaloy spacer plates interspersed.

Reference D4

Lumped poison experiments were performed by Babcock and Wilcox. Borosilicate glass rods (12.6% B_2O_3) of 0.460- and 0.326-in. diameters were used as well as silica glass rods (3.00% B_2O_3) of 0.326-in. diam and aluminum-clad B_4C rods. The poison rods were substituted for fuel rods at various locations. The fuel consisted of UO_2 rods of 2.5 and 4% enrichment with OD = 0.475 in. The square lattice pitch was 0.644 in., corresponding to a non-moderator to moderator volume ratio of 0.750. The oxide density was 9.5 - 10.2 g/cm³. The active fuel length was about 5 ft for the 2.5% enriched rods and about 5-1/2 ft for the 4% enriched rods.

Reference D5

A number of critical experiments were conducted with the Yankee 2.7% enriched UO_2 using soluble boron (boric acid) in the moderator. A summary of the lattice parameters is given under the reference A1.

Reference D6

Experiments with stainless steel and boron-loaded aluminum plates were performed using BSR fuel elements (see description of ref. C6). The steel plates ranged in thickness from 32 to 125 mils. The B_4C aluminum plates had boron loadings from 1 to 50 g of natural boron and were clad with aluminum. The plates with 16 g or less of boron were 52 mils thick and the plates with higher loadings were 114 mils thick. The poison plates were substituted for fuel plates at several different positions.

E. Critical Experiments with Different Reflectors

- E1. E. C. Mallary, "Oralloy Cylindrical Shape Factor and Critical Mass Measurements in Graphite, Paraffin, and Water Tampers," USAEC Report LA-1305, October, 1951.

- E2. R. E. Donaldson and W. K. Brown, "Critical Mass Determinations of Lead-Reflected Systems," USAEC Report UCRL-5255, June, 1958.
- E3. G. E. Hansen and D. P. Wood, "Precision Critical Mass Determinations for Oralloloy and Plutonium in Spherical Tuballoy Tampers," USAEC Report LA-1356, February, 1952.
- E4. G. E. Hansen, H. C. Paxton and D. P. Wood, "Critical Masses of Oralloloy in Thin Reflectors," USAEC Report LA-2203, January, 1958.
- E5. R. C. Lane and O. J. E. Perkins, "Measurements of the Critical Mass of 37-1/2% Enriched Uranium in Reflectors of Wood, Concrete, Polyethylene and Water," AWRE Report No. NR 1/66, February, 1966.
- E6. Private communication with E. B. Johnson, Oak Ridge National Laboratory, December, 1966.

Reference E1

Multiplication experiments were done using infinite reflectors of graphite, paraffin, and water. Reciprocal multiplication plots were extrapolated to yield critical masses. The cores were unmoderated cylinders or spheres of 93.9% enriched uranium. The core diameters ranged from 3.25 in. to 12.4 in.; most of the units had diameters between 4 and 7.5 in.

Reference E2

Spheres and cylinders of fully-enriched uranium reflected by lead were the subjects of multiplication measurements at Livermore. The uranium cylinder diameters were about 3.9 and 4.4 in., and the sphere diameters were 5.6 and 5.9 in. Critical sizes were determined for lead thicknesses of about 3.5, 5.0, 5.2, and 6.8 in. The lead density was 11.3 g/cm³.

Reference E3

Multiplication measurements were made using a natural uranium reflector of different thicknesses up to 9 in. The spherical core was made

of fully enriched uranium. Some experiments used a spherical plutonium core with a natural uranium reflector.

Reference E4

Critical masses were determined for 5-1/4-in. diameter cylinders of fully-enriched uranium surrounded by 1/2- and 1-in. thick reflectors of Be, graphite, Mg, Al, Ti, steel, Cu, W alloy, natural U, Ni, Co, Mo, Al₂O₃, Mo₂C, and polyethylene. Also, critical masses were measured for fully-enriched uranium spheres with ~2- and ~1/4-in. thick reflectors of W alloy, Fe, Ni, Ni-Ag, Cu, Zn, Th, Be, BeO, C, and natural U. Extrapolated inverse multiplication data were used to establish critical masses. Values of reflector savings were also determined.

Reference E5

Safety-oriented experiments were done at Aldermaston, England using reflectors of wood, concrete, polyethylene, and water. The reflector thickness was varied up to about 8 in. Unmoderated stacks of uranium metal plates of 37.7% enrichment were used for the cores which were in slab and rectangular geometries. The reflector densities were: (a) wood - 0.693 g/cm³, (b) concrete - 2.37 g/cm³, (c) polyethylene - 0.919 g/cm³, and (d) water 1.0 g/cm³. The water content of the concrete was 7.85 wt % of which 2.64 wt % could be driven off by heating. Reflector savings were determined, as well as critical masses and dimensions.

Reference E6

In some of the experiments currently in progress at ORNL (described under ref. B5) with 4.9% enriched water moderated uranium metal rods, reflectors of lead, steel, and water have been used in thicknesses up to 8 in. Also, the water gap between fuel and reflector was varied from 0 to 1/4 in. The fuel was arrayed in rectangular geometry and the reflectors were placed on one or two sides, leaving water on the others. Critical sizes and reactivity worths were determined by the calibrated water-height method.

F. Arrays of Interacting Units

- F1. J. T. Thomas, "Critical Three-Dimensional Arrays of Neutron-Interacting Units," USAEC Report ORNL-TM-719, October, 1963.
- F2. L. W. Gillet et al., "Critical Arrays of Neutron Interacting Units," USAEC Report ORNL-3193, p. 159, September, 1961.
- F3. J. K. Fox, L. W. Gilley, A. D. Callihan, "Critical Mass Studies, Part IX, Aqueous ^{235}U Solutions," USAEC Report ORNL-2367, March, 1958.

Reference F1

Five-liter cylinders of concentrated uranyl nitrate solution were arranged in critical arrays. The uranium concentrations were 63.3, 279, and 415 g/liter with a ^{235}U content of 92.6 wt %, resulting in H/ ^{235}U atomic ratios of 440, 92, and 59, respectively. The plexiglas cylinders which contained the fuel were about 8 in. in diameter and 7-1/2 in. high and had a 1/4 in. wall thickness. The surface-to-surface separation of the cylindrical units ranged from zero to 6-1/2 in. Arrays of 8, 27, 64, and 125 units were assembled in cubic and parallelepipedal geometry. Some of the arrays were reflected by paraffin and plexiglas in thicknesses up to 6 in.

Reference F2

Cylindrical bottles of enriched uranyl nitrate were arranged into arrays of as many as 100 units. In some experiments neither reflector about the arrays nor interspersed moderator was present. In others, the moderator and reflector thickness was varied. The fuel concentration was 410 g of uranium per liter containing 92.6 wt % ^{235}U . Three kinds of cylindrical bottles were used. Two of the types were polyethylene with inner diameters of about 4.7 and 5.1 in., length about 4 ft, and capacities about 13 and 15 liters, respectively. The third type of container was an aluminum cylinder 6 ft long with a 6-in. ID. The units were arranged vertically with their bases in a linear, square, or triangular pattern. Surface-to-surface spacings up to 8-1/2 in. were employed. The array periphery was either square or hexagonal.

Reference F3

In some of the experiments described under ref. C2, interacting arrays of as many as seven cylinders of fully-enriched uranyl nitrate were constructed. The cylinders were arranged in hexagonal, triangular, and linear patterns with edge-to-edge spacings up to 24.5 in. One set of experiments was performed with three units in a triangular pattern. One of the cylinders was then moved to various positions, forming isosceles triangles with different vertex angles.

7. SHIELDING

7.1 General Considerations

The shielding of any shipping cask must reduce the external dose rate from the largest expected source to below specified tolerance levels. This is done for the most part with lead. This chapter will be devoted primarily to the use of that material although steel, depleted uranium, concrete, and other materials can be used to advantage under various circumstances.

There are a number of textbooks and reference documents available covering the subject of shielding; consequently, the theory and calculational methods will not be discussed here. In addition, to help people involved in shielding design, a listing of shielding computer codes and topical reports are available through the Radiation Shielding Information Center. Inquiries should be addressed to:

Radiation Shielding Information Center
Oak Ridge National Laboratory
P. O. Box X
Oak Ridge, Tennessee 37830, U.S.A.

The purpose of this chapter is intended to provide AEC personnel with a quick and reasonably accurate method of determining whether the shielding in a given cask will be adequate for the specified source by using the nomograph given in Fig. 7.1. It is not intended that Fig. 7.1 be used in lieu of analytical shielding methods.

7.2 DOT Regulations

Recent changes have been made in permissible dose rates allowed at the surface or at specified distances from a spent fuel shipping cask. The latest information concerning the shielding requirements of casks has been published by the Department of Transportation¹ and are reproduced below.*

*It is expected that these regulations will be superseded shortly by new regulations developed by the Department of Transportation (DOT). It is unlikely that the dose rate requirements will vary greatly from those given here.

"All radioactive materials, liquid, solid and gaseous must be packaged in suitable containers (shielded, if necessary) so that any time during transportation the radiation dose rate does not exceed any of the limits specified in the following subparagraphs.

.

1. 200 millirem per hour at any point on the external surface of the package
2. 10 millirem per hour at three feet from any accessible external surface of the package.

"Packages for which the radiation dose rate exceeds the limits specified above but does not exceed at any time during transportation any of the limits specified in subparagraphs (1) through (4) below, may be transported in a vehicle (except aircraft) assigned for the sole use of that consignor, and unloaded by the consignee from the transport vehicle in which originally loaded.

1. 1000 millirem per hour at three feet from the external surface of the package (closed transport vehicle only);
2. 200 millirem per hour at any point on the external surface of the car or vehicle (closed transport vehicle only);
3. 10 millirem per hour at six feet from the external surface of the car or vehicle; and
4. 2 millirem per hour or equivalent in any normally occupied position in the car or vehicle except this does not apply to private motor carriers."

7.3 Shielding Estimates

It is often quite useful to be able to determine quickly whether a cask's shielding is adequate for a given service. For this purpose, a nomograph is given² which permits the estimation of the shielding required to reduce the dose rate from spent fuel elements to 100 mr/hr on a cask surface (see Fig. 7.1). Surface dose rates different from 100 mr/hr can be estimated by noting that the dose rate changes by a factor of 2 for about 0.6 in. change in lead thickness.

Figure 7.1 is based on the assumption that a large source has the same activity and mass per unit volume as the average for a cask cavity and that the fuel is either fairly well distributed or approximately centered in the cavity. This model is suitable when the product, wD , exceeds about 200, where w is the average density of the cask contents, in pounds per cubic foot, and D is the minimum cross-sectional dimension of the cavity, in feet. For values of wD as small as 100, however, the conservatism of the method results in less than 1/2 in. of added thicknesses.

7.3.1 Comparison of Nomograph and Machine Code

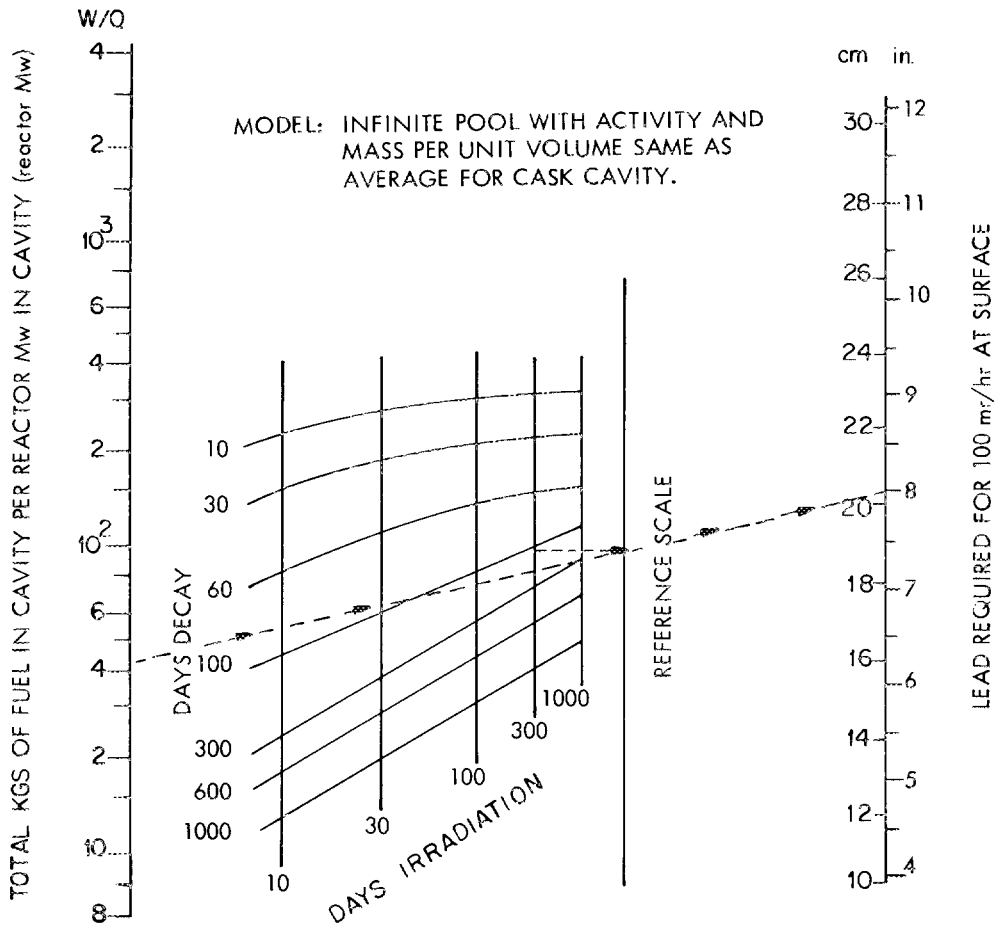
Calculations made to determine the shielding thickness required to produce a dose rate of 100 mr/hr on the cask surface were determined using the QAD-P5A code³ (which uses a kernel technique with the buildup factor calculated by the moments method) and compared with those values obtained in Fig. 7.1.

It was found that the nomograph gave values of lead thicknesses generally within 5% of those calculated using the QAD-P5A code, the extreme being -7.6% and +5.4%.

7.4 Dose Calculations Away From Cask Surface

In many cases, the dose rate at some distance from the cask surface may be controlling (see Sect. 7.2).

The direct application of the point kernel technique using infinite medium buildup factors in calculating the dose rate away from the surface



DIRECTIONS: From proper point in irradiation-decay grid, project perpendicularly to reference scale. Then project from W/Q scale through point on reference scale.

Fig. 7.1. Nomograph for Estimating Amount of Shielding for Casks. (Reference 2)

of a cask may be too far removed from the infinite medium assumption since the detector actually "sees" the entire surface as a source. For calculating surface doses, however, this method should give good results because no surface sources can be "seen" and the infinite medium condition applies, particularly in the case of lead where the backscattering is small. However, point kernel techniques normally predict higher dose rates at the surface than are experimentally measured.

Certainly the dose rate away from the surface may be accurately calculated if the angular flux on the surface is known. Unfortunately, no general correlations exist between a cask design with its source and the flux distribution on the cask surface; each case must be examined individually. Some limited amount of evidence⁴ indicates that the angular flux ϕ on the surface of large casks may be represented by a \cos^3 distribution where ϕ is measured normal to the cask surface.

A series of graphs for cylindrical containers was developed in which are plotted the ratio of the dose at some point in space to the surface dose rate against a distance parameter for flux distributions ranging from isotropic to the highly forward-peaked $\cos^6 \phi$ distribution.

Figures 7.2 through 7.8 refer to the dose ratio at the side of a cylindrical cask and Fig. 7.9 refers to its circular end. Dose ratios for rectangular surfaces are presented in Figs. 7.10 through 7.13.

For dense shielding materials such as lead and uranium, we presently recommend use of the $\cos^3 \phi$ distribution to determine the dose rate away from the surface relative to the dose rate on the surface. As more evidence becomes available, this recommendation may be modified.

7.5 Example

A cylindrical shipping cask is 6.35 ft high and 1.64 ft in diameter. It contains fuel that has been irradiated 300 days and cooled 100 days. The cavity contains 100 lb of fuel and other material per megawatt of original reactor power. Determine a) the amount of shielding required to reduce the surface dose rate to 100 mr/hr, b) the dose rate at both the side and end of the cask 3 ft from the surface.

Answer: From Fig. 7.1 it is determined that 8 in. of lead are required to reduce the surface dose rate to around 100 mr/hr.

To determine the dose rate at 3 ft, the following calculations are made (see figures for nomenclature):

$$\frac{\text{Cask height}}{\text{Cask diameter}} = \frac{6.35}{1.64} = 4.0$$

$$R = 0.82 \text{ ft}$$

$$r = 3 \text{ ft}$$

$$\frac{r}{R} = \frac{3.00}{0.82} = 3.66$$

Assuming the flux on the cask surface has a $\cos^3 \phi$ angular distribution, from Fig. 7.5 for $r/R = 3.66$ and $H/D = 4.00$, the dose rate at 3 ft is:

$$\frac{\text{Dose rate at 3 ft}}{\text{Dose rate at surface}} = 0.18$$

$$\begin{aligned} \text{Dose rate at 3 ft} &= (0.18) (100 \text{ mr/hr}) \\ &= 18 \text{ mr/hr} \end{aligned}$$

Assuming the same $\cos^3 \phi$ flux distribution on the surface of the end of the cask and since

$$\frac{r}{R} = \frac{3 \text{ ft}}{1.64 \text{ ft}} = 1.83$$

from Fig. 7.9 for $n = 3$

$$\frac{\text{Dose rate at 3 ft}}{\text{Dose rate at surface}} = 0.135$$

Assuming the same surface dose rate of 100 mr/hr, the dose rate at 3 ft from the end of the cask is

$$(.135) (100) = 13.5 \text{ mr/hr}$$

These results indicate the surface dose rate is within requirements, but the dose rate at 3 ft from the side of the cask is almost a factor of two too high.

An additional 0.6 in. of lead shielding should allow the cask to meet the DOT regulations.

ORNL DWG 67-11635R1

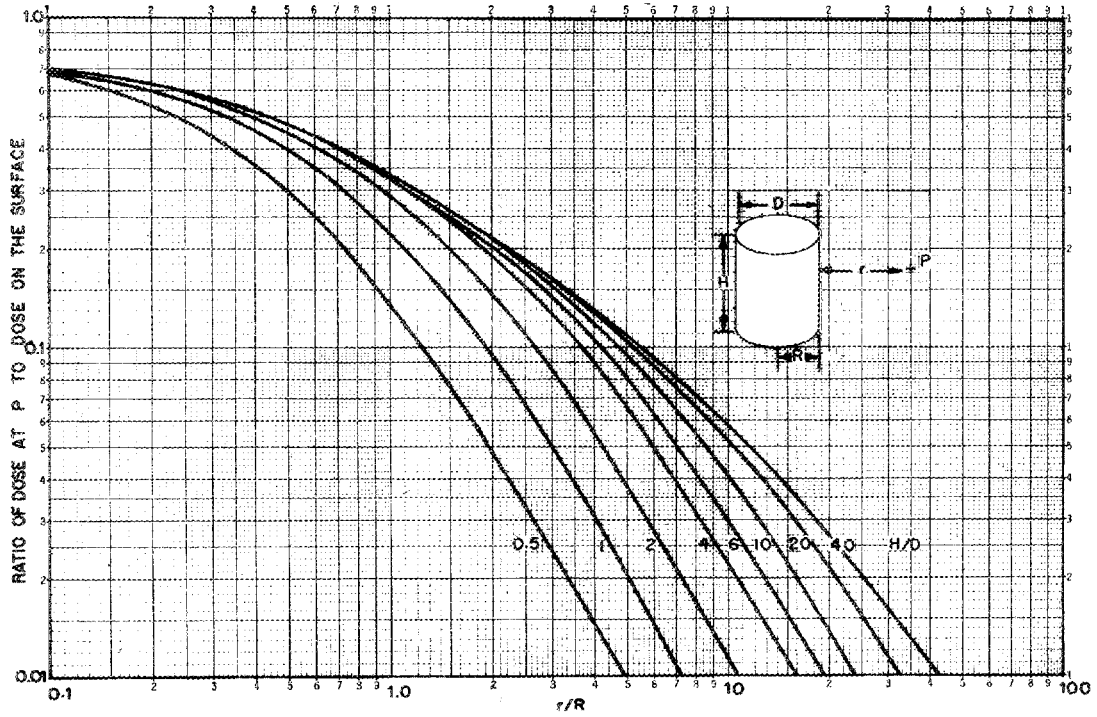


Fig. 7.2. Ratio of Dose at P to Dose on the Surface Based on Isotropic Flux Distribution on Surface.

ORNL DWG 67-11646R1

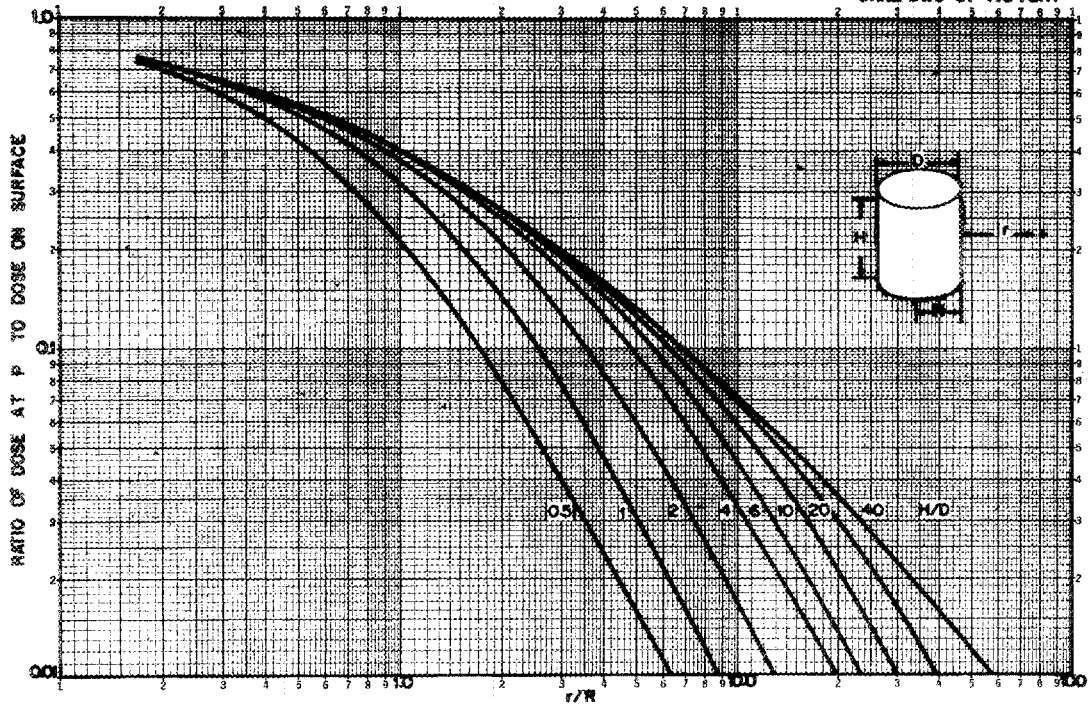


Fig. 7.3. Ratio of Dose at P to Dose on the Surface Based on Cosine¹ Flux Distribution on Surface.

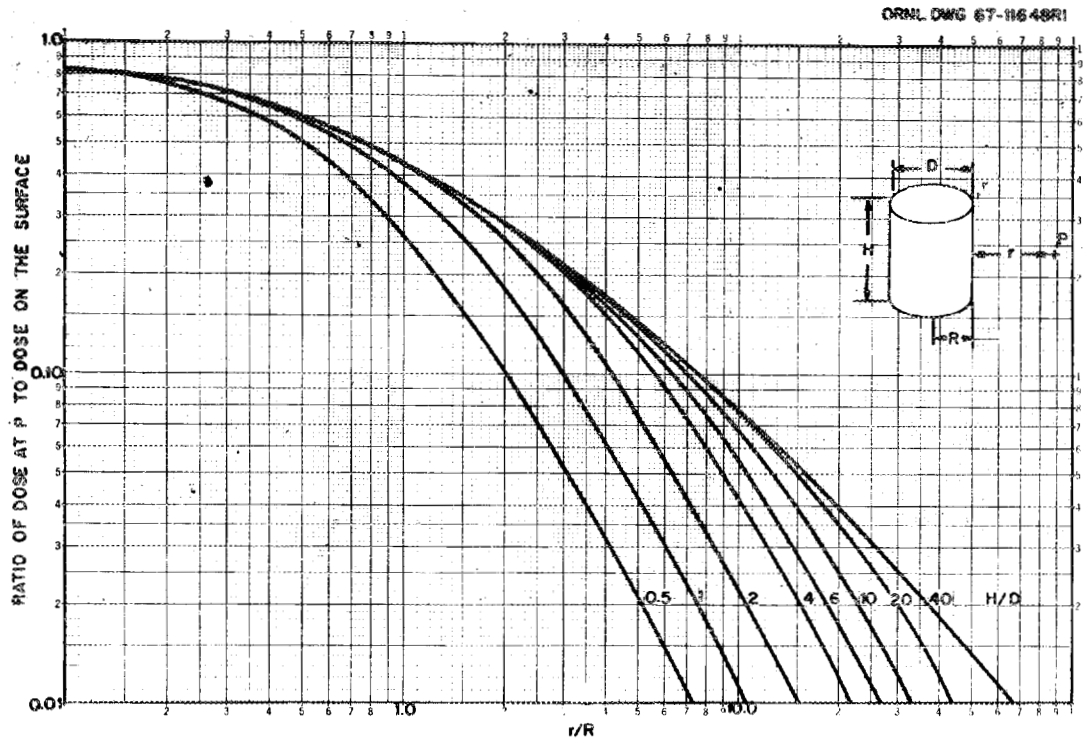


Fig. 7.4. Ratio of Dose at P to Dose on the Surface Based on Cosine^2 Flux Distribution on Surface.

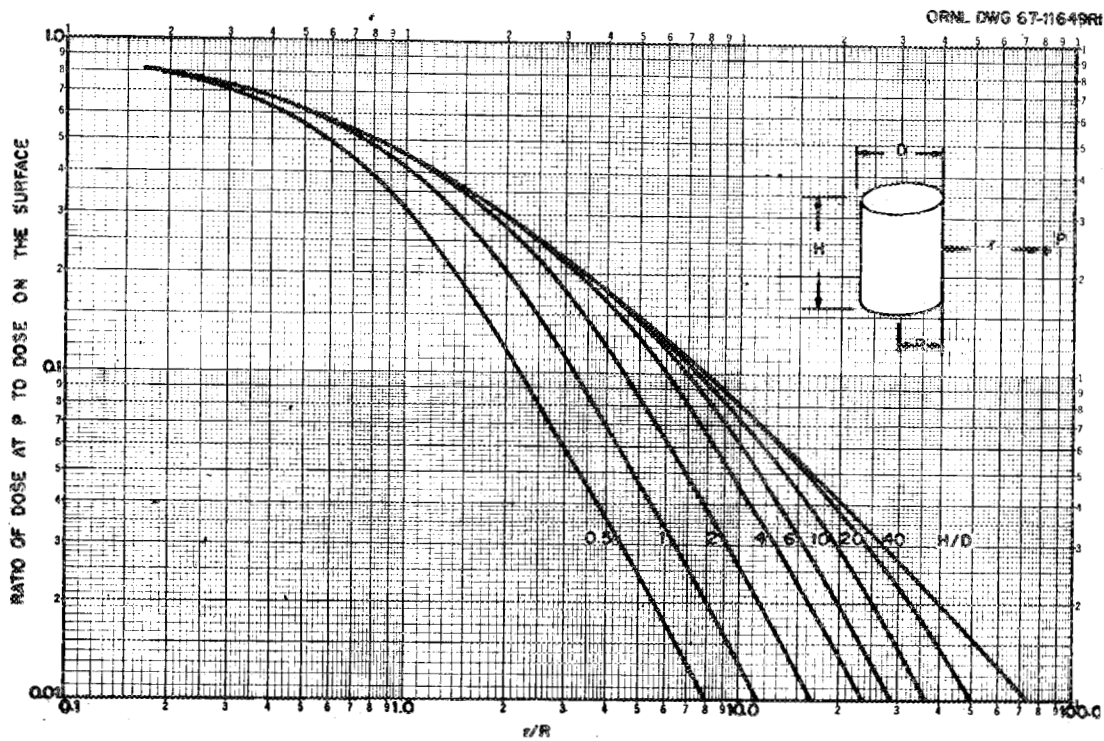


Fig. 7.5. Ratio of Dose at P to Dose on the Surface Based on Cosine^3 Flux Distribution on Surface.

ORNL DWG 67-11650R1

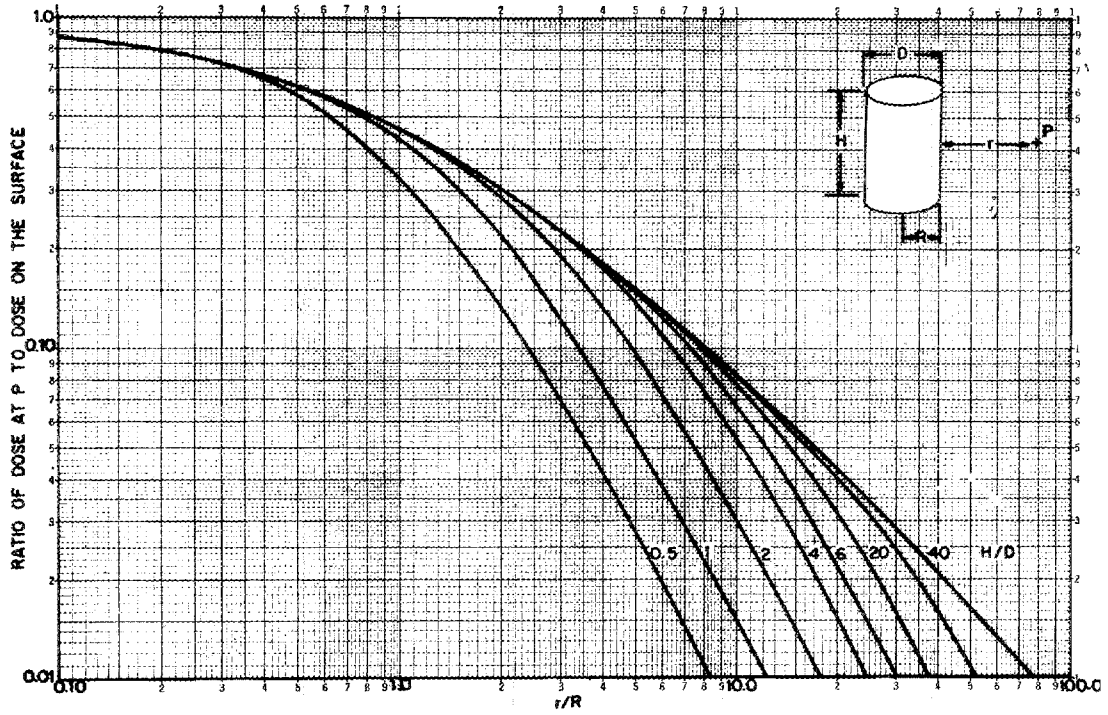


Fig. 7.6. Ratio of Dose at P to Dose on the Surface Based on Cosine^4 Flux Distribution on Surface.

ORNL DWG 67-11651R1

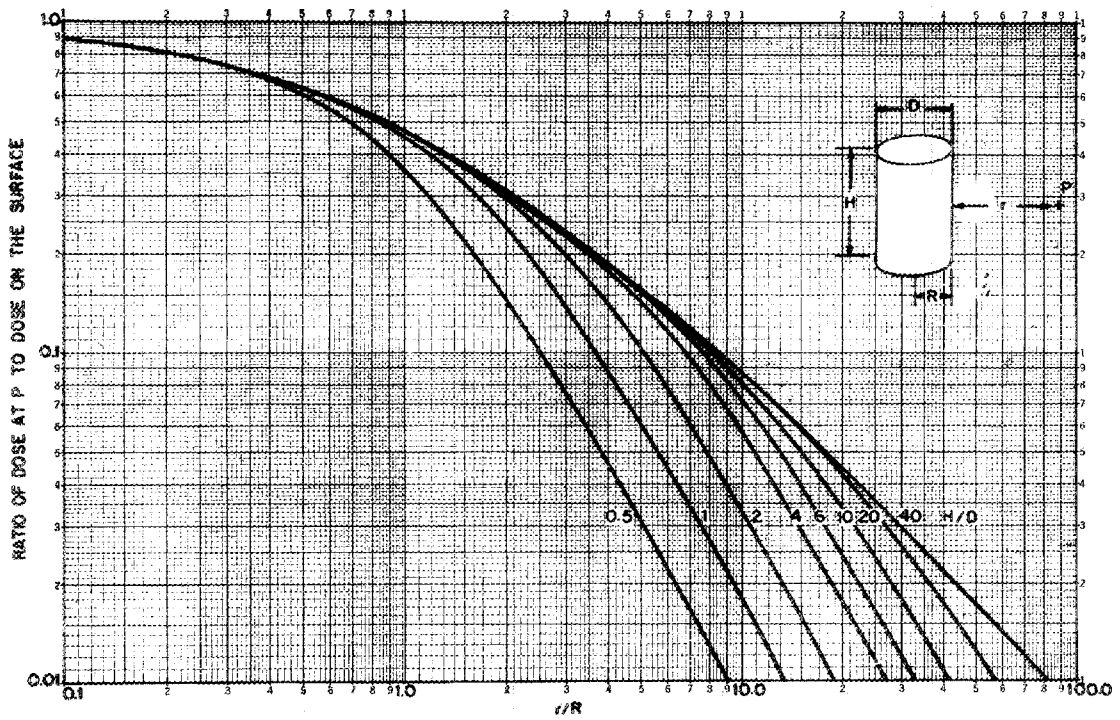


Fig. 7.7. Ratio of Dose at P to Dose on the Surface Based on Cosine^5 Flux Distribution on Surface.

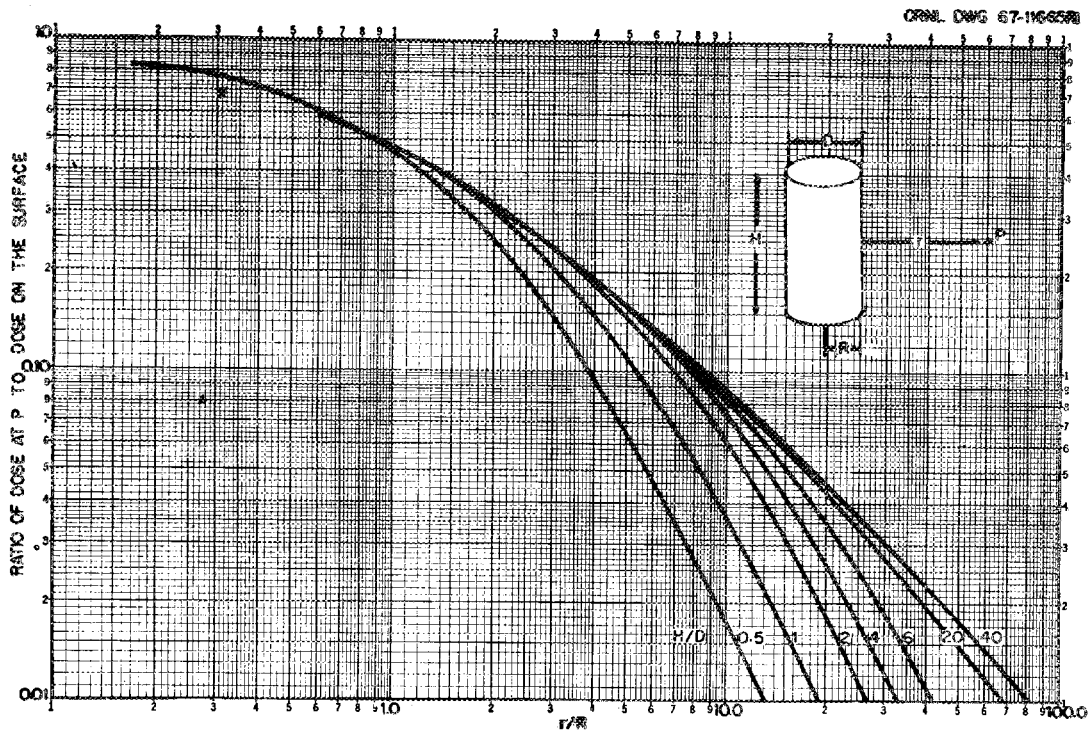


Fig. 7.8. Ratio of Dose at P to Dose on the Surface Based on Cosine⁵ Flux Distribution on Surface.

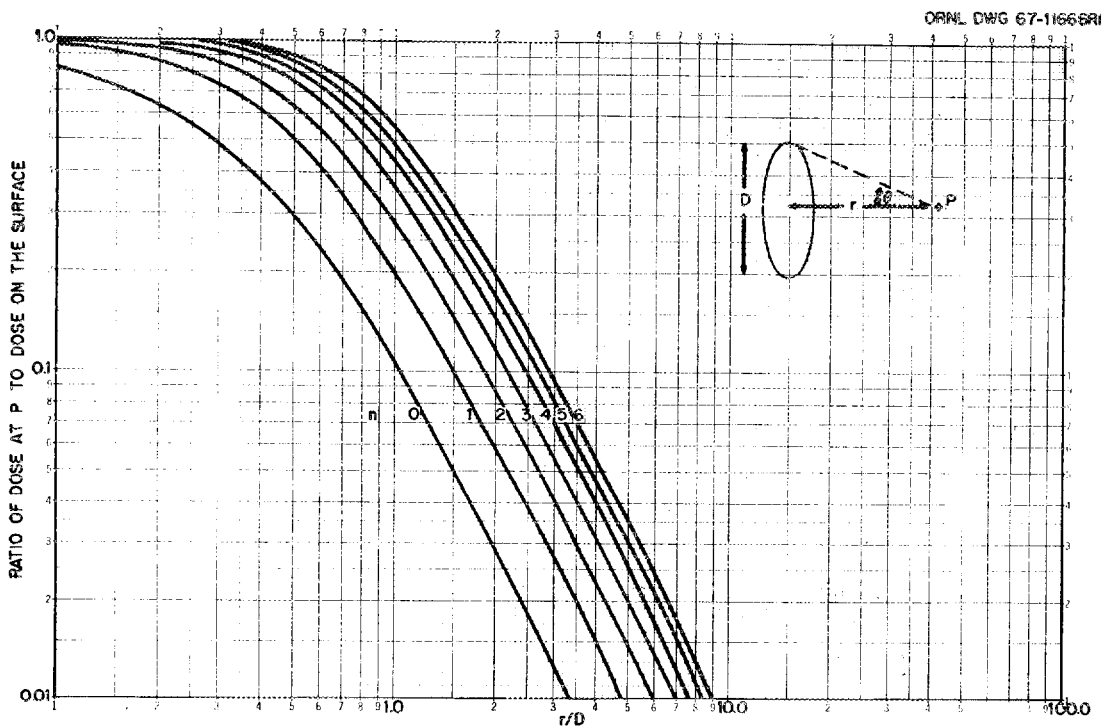


Fig. 7.9. Ratio of Dose at P to Dose on the Surface Based on Cosine¹ Flux Distribution on Surface.

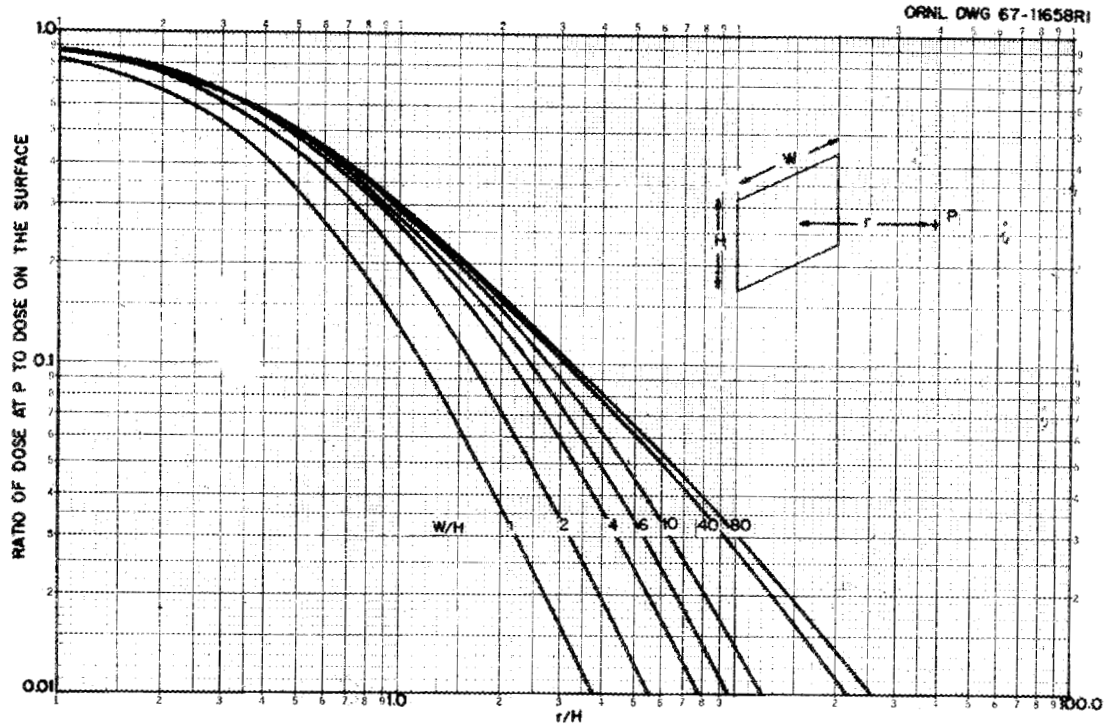


Fig. 7.10. Ratio of Dose at P to Dose on the Surface Based on Isotropic Flux Distribution on Surface.

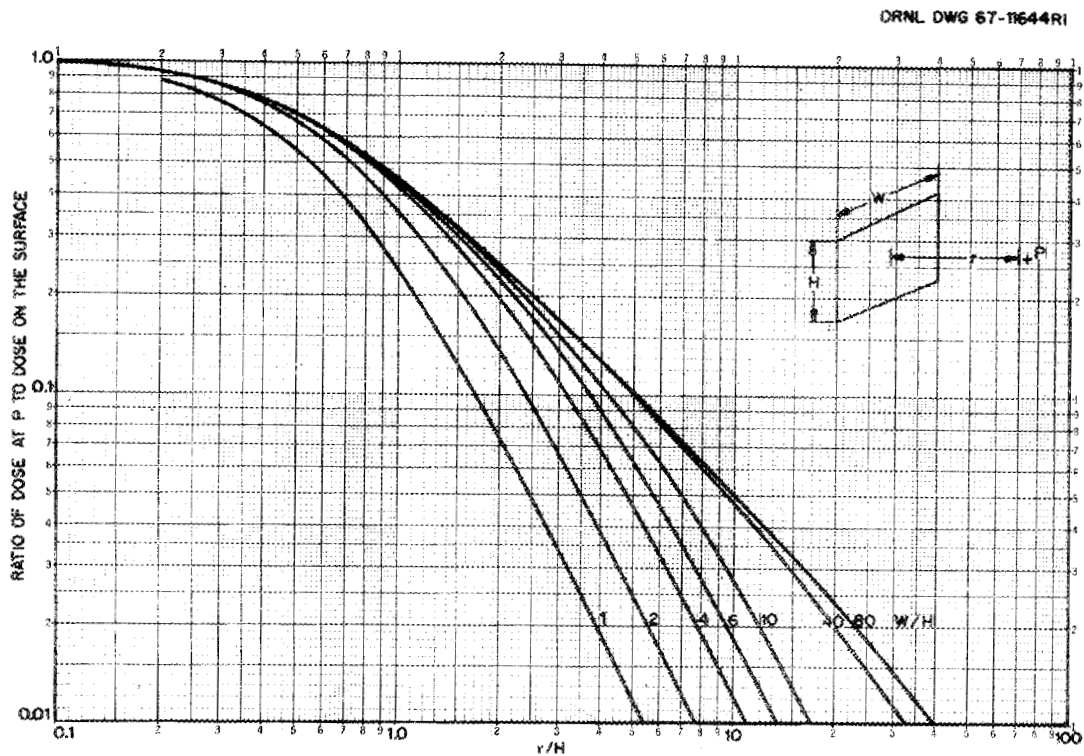


Fig. 7.11. Ratio of Dose at P to Dose on the Surface Based on Cosine¹ Flux Distribution on Surface.

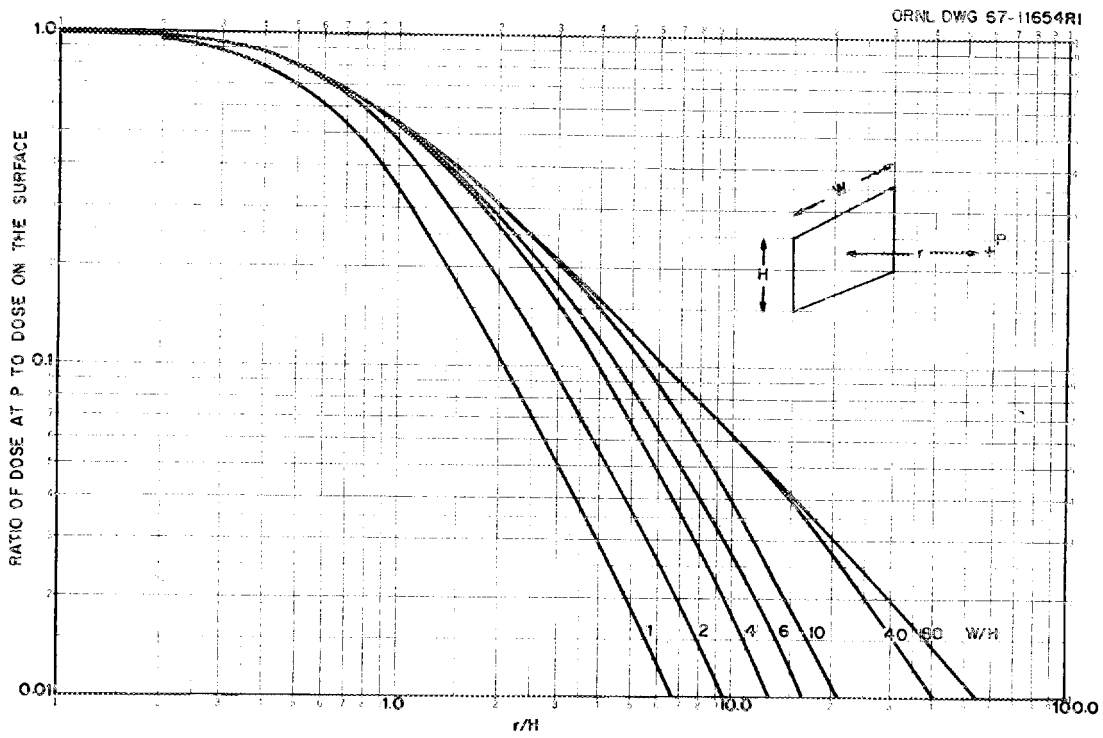


Fig. 7.12. Ratio of Dose at P to Dose on the Surface Based on Cosine² Flux Distribution on Surface.

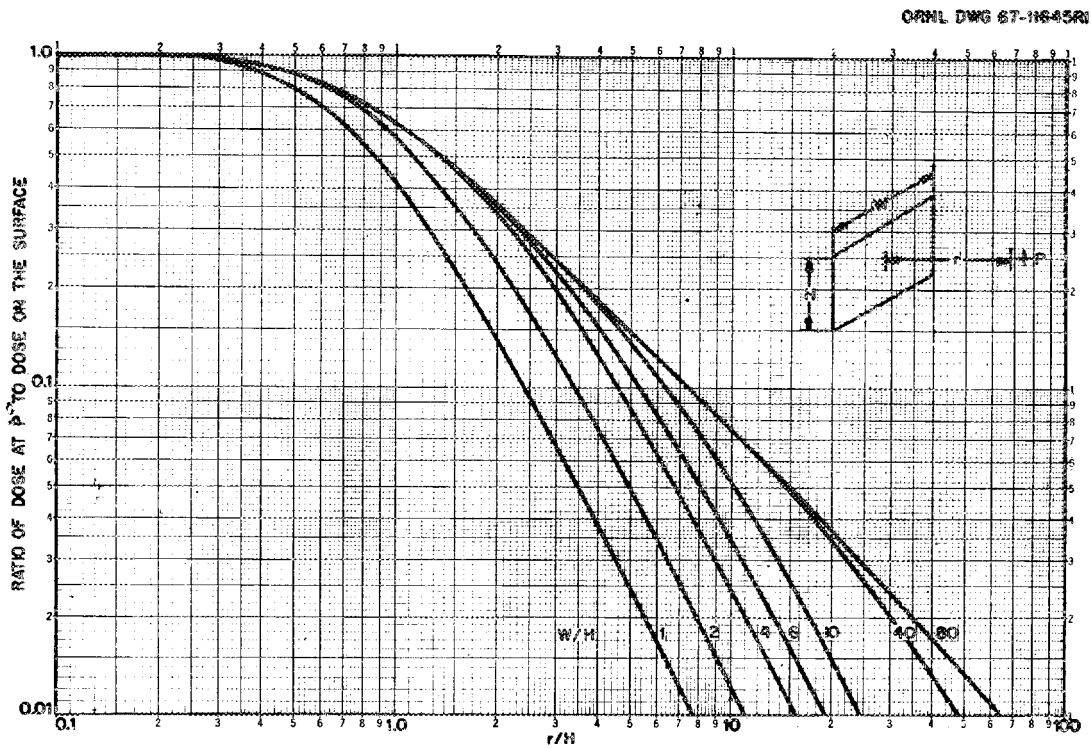


Fig. 7.13. Ratio of Dose at P to Dose on the Surface Based on Cosine³ Flux Distribution on Surface.

7.6 References

1. Code of Federal Regulations, Title 49, Part 173-178, Federal Register 33, No. 194, Part II (Oct. 4, 1968).
2. L. L. Zahn, et al., "Transportation of Radioactive Materials," Reactor Technology, Selected Reviews, 1965, TID-8541.
3. R. E. Malenfant, QAD; A Series of Point Kernel General Purpose Shielding Programs, LA-3573 (April 5, 1967).
4. J. W. Langhaar, E. I. DuPont, Wilmington, Delaware, personal communication.

INTERNAL DISTRIBUTION

- | | |
|--------------------------|---------------------------------|
| 1. T. A. Arehart | 38. R. J. Lauer |
| 2. E. E. Beauchamp | 39. A. J. Mallett, K-25 |
| 3. M. Bender | 40. J. L. Matherne |
| 4. C. E. Bettis | 41. J. R. McGuffey |
| 5. R. E. Blanco | 42. J. D. McLendon, Y-12 |
| 6. G. B. Brooks, K-25 | 43. H. A. Nelms |
| 7. R. E. Brooksbank | 44. C. E. Newlon, K-25 |
| 8. K. B. Brown | 45. J. P. Nichols |
| 9. F. R. Bruce | 46. A. M. Perry, Y-12 |
| 10. J. R. Buchanan | 47. J. E. Ratledge |
| 11. C. D. Cagle | 48. C. R. Riggs, Y-12 |
| 12. A. D. Callihan | 49. A. F. Rupp |
| 13. J. M. Case, Y-12 | 50. R. Salmon |
| 14. G. B. Child | 51. R. W. Schaich |
| 15. J. K. Cox, Y-12 | 52. R. D. Seagren |
| 16. E. C. Crume, Y-12 | 53. J. A. Setaro |
| 17. H. J. Culbert, K-25 | 54-73. L. B. Shappert |
| 18. F. L. Culler, Jr. | 74. M. R. Skidmore |
| 19. D. Dash, K-25 | 75. J. L. Smith, Y-12 |
| 20. R. L. Donahue | 76-80. W. C. Stoddart |
| 21. H. G. Duggan | 81. F. W. Stout, K-25 |
| 22. J. Dykstra, K-25 | 82. D. A. Sundberg |
| 23. J. H. Evans | 83. J. Thomas |
| 24. D. E. Ferguson | 84. G. M. Tolson, K-25 |
| 25. R. W. Forseman, Y-12 | 85. W. E. Unger |
| 26. W. R. Gall | 86. J. Wachter |
| 27. J. H. Gillette | 87. D. C. Watkin |
| 28. H. E. Goeller | 88. M. E. Whatley |
| 29. H. R. Gwinn | 89. R. G. Wymer |
| 30. K. W. Haff | 90. J. M. Young, K-25 |
| 31. G. W. Horde, Y-12 | 91-92. Central Research Library |
| 32. A. R. Irvine | 93. Document Reference Section |
| 33. W. M. Johnson | 94-95. Laboratory Records |
| 34. W. D. Jones | 96. Laboratory Records-RC |
| 35. O. A. Kelly | 97. ORNL Patent Office |
| 36. E. M. King | 98-112. DTIE |
| 37. B. B. Klima | |

EXTERNAL DISTRIBUTION

113. F. E. Adcock, The Dow Chemical Co., Rocky Flats Division,
P. O. Box 888, Golden, Colorado 80401
114. A. E. Aikens, Jr., Capintec, Inc., 527 Madison Avenue, Suite 920,
New York, N. Y. 10022
115. W. L. Albrecht, Tennessee Valley Authority, New Sprankle Building,
Knoxville, Tennessee 37902

116. A. P. Alton, Rolls-Royce & Associates, Ltd., P. O. Box 31, Derby, England
117. C. J. Anderson, Hittman Associates, 9190 Red Branch Road, Columbia, Maryland
118. R. Andree, USAEC, New York Operations Office, 376 Hudson Street, New York, N. Y. 10014
119. D. G. Andrews, University of Toronto, Toronto 5, Canada
120. A. Anselmo, Idaho Nuclear Corporation, P. O. Box 1845, Idaho Falls, Idaho 83401
121. S. Aoki, Tokyo Institute of Technology, Ookayama, Meguro-Kw, Tokyo, Japan
122. G. Ascione, Italian State Electricity Board, via G. G. Martini 3, Rome, Italy
123. A. Aupetit, Transnucleaire, S.A., 11/11 bis rue Christophe Colomb, 75 Paris 8^{eme}, France
124. H. Baatz, Transnuklear GmbH, 6 Frankfurt/Main, Zeil 79, Germany
125. G. E. Backman, Atlantic Richfield Hanford Co., Richland, Wash.
126. R. F. Barker, USAEC, Washington, D. C. 20545
127. R. J. Bass, E. I. duPont de Nemours & Co., Savannah River Plant, Aiken, South Carolina 29801
128. V. A. Beamish, Canadian General Electric Co., Ltd., 107 Park St. North, Peterborough, Ontario, Canada
129. D. Baderstadt, USAEC, Chicago Operations Office, 9800 South Cass Avenue, Argonne, Illinois 60439
130. C. K. Beck, USAEC, Washington, D. C. 20545
131. R. C. Becker, University of California, Lawrence Radiation Lab., P. O. Box 808, Livermore, California 94550
132. F. P. Beierle, Nuclear Engineering Company, Inc., P. O. Box 158, Sheffield, Illinois 61361
133. W. G. Belter, USAEC, Washington, D. C. 20545
134. H. Bernard, Commissariat A L'Energie Atomique, 29-33 Rue de la Federation, Paris XV^e, France
135. S. Bernstein, Union Carbide Corporation, P. O. Box 1410, Paducah, Kentucky 42001
136. S. N. Berry, Sam Edlow Associates, Suite 214, Port Columbus International Airport, Columbus, Ohio 43219
137. R. J. Berte, USAEC, Washington, D. C. 20545
138. R. W. Blackburn, Atomic Energy Control Board, P. O. Box 1046, Ottawa Ontario, Canada
139. P. S. Bland, Westinghouse Advanced Reactors Division, Westinghouse Corp., Pittsburgh, Pa.
140. M. G. Blechschmidt, P.T.B., Bundesallee 100, 33 Braunschweig, F.R. Germany
141. R. Blomquist, Aktiebolaget Atomenergi Studsvik, Fack, S-611 01, Nykoping 1, Sweden
142. D. E. Bloomfield, Battelle Northwest, P. O. Box 999, Richland, Washington 99352
143. P. Blum, Transnucleaire, S.A. Societe Lyonnaise de Plomberie Industrielle Lyons, France
144. P. A. Bohm, General Electric Co., P. O. Box 846, Pleasanton, California 94566
145. J. Bouillet, Commissariat A L'Energie Atomique 29-33 Rue de la Federation, Paris XV^e, France

146. T. B. Bowie, Combustion Engineering, Inc., P. O. Box 500, Windsor, Connecticut
147. G. Boyd, Tri-State Motor Transit Co., P. O. Box 113, Joplin, Mo. 64802
148. E. T. Borawski, Combustion Engineering, Inc., P. O. Box 500, Windsor, Connecticut
149. J. C. Bradburne, Jr., Lockheed Georgia Nuclear Laboratory, Dawsonville, Georgia
150. W. J. Bradley, U. S. Nuclear Division of I.C.N. Corporation, 801 North Lake Street, Burbank, California 91503
151. R. L. Bragg, Nuclear Materials & Equipment Corporation, Apollo, Pennsylvania 15613
152. W. A. Brobst, U. S. Dept. of Transportation, 6th and D Street S. W. Washington, D. C. 20590
153. J. M. Brooks, Ryan Industries, Inc., 4800 Allmond Avenue, Louisville, Kentucky 40214
154. C. L. Brown, Battelle Northwest, P. O. Box 999, Richland, Wash. 99352
155. J. F. Brown, National Lead Co., Foot of West Street, Wilmington, Delaware 19898
156. W. L. Bruckart, Precision Sheet Metal, Inc. 5235 W. 104th Street, Los Angeles, California 90054
157. C. W. Buckland, Los Alamos Scientific Laboratory, P. O. Box 1663, Los Alamos, New Mexico 87544
158. R. O. Budd, Battelle Northwest, P. O. Box 999, Richland, Wash. 99352
159. T. P. Bullock, Westinghouse - NFD, P. O. Box 355, Pittsburgh, Pa. 15230
160. J. P. Byrom, Idaho Nuclear Corporation, P. O. Box 1845, Idaho Falls, Idaho 83401
161. C. J. Campbell, 442 Eldert Lane, Brooklyn, N. Y. 11230
162. C. M. Campbell, USAEC, Nevada Operations Office, P. O. Box 14100, Las Vegas, Nevada 89114
163. R. E. Carlton, Department of the Navy, Naval Facilities Engineering Command, P. O. Box 610, Falls Church, Va. 22046
164. T. J. Castro, Schwarz BioResearch, Mountain View Avenue, Orangeburg, New York 10962
165. R. A. Chagnon, All American Engineering Company, P. O. Box 1247, Wilmington, Delaware 19899
166. G. R. Champion, Los Alamos Scientific Laboratory, P. O. Box 1663, Los Alamos, New Mexico 87544
167. G. A. Chandler, Australian Embassy, 1700 Massachusetts Avenue N. W., Washington, D. C. 20036
168. R. L. Chandler, USAEC, Savannah River Operations Office, P. O. Box A, Aiken, South Carolina 29801
169. F. D. Chin, Nuclear Energy Liability Insurance Association, 85 John Street, New York, N. Y. 10038
170. S. Chin, University of California, Lawrence Radiation Laboratory, P. O. Box 808, Livermore, California 94550
171. R. B. Chitwood, USAEC, Washington, D. C. 20545
172. R. L. Christenot, Reynolds Electric & Engineering Co., 2731 Stewart, Las Vegas, Nevada
173. J. J. Christie, Atomic Industrial Forum, Inc., 850 Third Avenue, New York, N. Y. 10022
174. B. C. Clark, American Nuclear Corporation, P. O. Box 426, Oak Ridge, Tennessee 37830

175. H. G. Clarke, Jr., The Franklin Institute, 20th and Parkway,
Philadelphia, Pennsylvania 19103
176. C. B. Clifford, Union Carbide Corporation, P. O. Box 1410, Paducah,
Kentucky 42001
177. D. C. Collins, USAEC, Savannah River Operations Office, P. O. Box A,
Aiken, South Carolina 29801
178. P. Colsmann, Brookhaven National Laboratory
179. J. E. Conway, Savannah River Plant, Aiken, South Carolina 29801
180. F. B. Conlon, National Center for Radiological Health, 12720 Twin-
brook Parkway, Rockville, Maryland 20852
181. I. L. T. Conn, Atomic Energy of Canada, Ltd., P. O. Box 93,
Ottawa, Ontario, Canada
182. J. W. Conway, Homalite - G. L. Industries, 11 Brookside Drive,
Wilmington, Delaware 19809
183. H. L. Cook, Jr., Ohmart Corporation, 4241 Allendorf Drive,
Cincinnati, Ohio 45209
184. J. N. Cook, USAEC, Albuquerque Operations Office, P. O. Box 5400,
Albuquerque, New Mexico 87115
185. W. J. Cooley, USAEC, San Francisco Operations Office, 2111 Bancroft
Way, Berkeley, California 94702
186. H. W. Crocker, USAEC, Washington, D. C. 20545
187. J. J. Cullen, National Lead Company, 1050 State Street, Perth Amboy,
New Jersey 08862
188. D. A. Currie, Canadian Nuclear Association, c/o Eldorado Nuclear
Ltd., Port Hope, Ontario, Canada
189. T. E. Dabrowski, Douglas United Nuclear, Inc. P. O. Box 490,
Richland, Washington 99352
190. C. R. Davis, Gulf General Atomic, Inc. T.O. 211, P. O. Box 608,
San Diego, California 92112
191. D. C. Davis, USAEC, Oak Ridge Operations Office, P. O. Box E, Oak
Ridge, Tennessee 37830
192. R. R. Dean, Edgewood Arsenal, Depot Operations Division, SMUEA-SSDO
Edgewood Arsenal, Maryland 21010
193. J. D. W. deLind van Wijngaarden, Atomic Energy of Canada, Ltd.,
P. O. Box 93, Ottawa, Ontario, Canada
194. A. W. DeMerschman, Battelle-Northwest, P. O. Box 99, Richland,
Washington 99352
195. J. A. Derry, USAEC, Washington, D. C. 20545
196. B. D. Devine, Argonne National Laboratory
197. B. Dewey, University of Tennessee, Knoxville, Tennessee 37916
198. J. S. Dewey, Kerr-McGee Corporation, Kerr-McGee Building, Oklahoma
City, Oklahoma 73102
199. F. E. Diebold, Sandia Corporation, P. O. Box 5800, Albuquerque,
New Mexico 87115
200. F. E. Dixon, United Kingdom Atomic Energy Authority, Bldg. 424,
Harwell, Didcot, Berkshire, England
201. A. O. Dodd, USAEC, Richland Operations Office, P. O. Box 550,
Richland, Washington 99352
202. T. L. Dunckel, USAEC, San Francisco Operations Office, 2111 Bancroft
Way, Berkeley, California 94704
203. F. A. Dugan, Brookhaven National Laboratory

204. D. L. Dunaway, National Lead Co. of Ohio, P. O. Box 39158
Cincinnati, Ohio 45239
205. K. A. Dunbar, USAEC, Chicago Operations Office, 9800 South Cass
Avenue, Argonne, Illinois 60439
206. C. H. Durham, USAEC, Oak Ridge Operations Office, P. O. Box E
Oak Ridge, Tennessee 37830
207. J. H. Edgerton, U. S. Army Transportation Engineering Agency,
Fort Eustis, Virginia 23604
208. D. A. Edling, Mound Laboratory, Monsanto Research Corporation,
Miamisburg, Ohio 45342
209. J. D. Edwards, Jr., U. S. Army Engineer Reactors Group, Fort
Belvoir, Virginia 22060
210. C. S. Ehrman, Allied Chemical Corporation, P. O. Box 70,
Morristown, New Jersey 07960
211. C. C. Eldridge, Bechtel Corporation, P. O. Box 3965, San
Francisco, California 94119
212. K. E. Elliott, USAEC, Oak Ridge Operations Office, P. O. Box E,
Oak Ridge, Tennessee 37830
213. T. R. Emswiler, Battelle Memorial Institute, 505 King Avenue,
Columbus, Ohio 43201
214. D. L. Erickson, Naval Nuclear Power Unit, Fort Belvoir, Va.
22060
215. B. Ernst, Nuclear Materials & Equipment Corp., Apollo, Pa.
216. B. F. Estes, USAEC, Albuquerque Operations Office, P. O.
Box 5400, Albuquerque, New Mexico 87115
217. S. W. Farkas, USAEC, Idaho Operations Office, P. O. Box 2108,
Idaho Falls, Idaho 83401
218. H. M. Faust, Battelle Memorial Institute, 505 King Avenue,
Columbus, Ohio 43201
219. A. Ferrelli, Comitato Nazionale Energia Nucleare, Via Belisario
15, Rome, Italy
220. J. T. Foley, Sandia Laboratories, P. O. Box 5800, Albuquerque,
New Mexico 87115
221. W. Foote, General Electric Co., Vallecitos Nuclear Center,
Pleasanton, California 94566
222. E. P. Forest, General Electric Co., P. O. Box 11508, St.
Petersburg, Florida 33733
223. R. F. Fraley, USAEC, Washington, D. C. 20545
224. E. J. Freeman, Allied Chemical Corporation, P. O. Box 430,
Metropolis, Illinois 62960
225. A. Frigo, Argonne National Laboratory
226. S. E. Frost, Eldorado Nuclear Ltd., Port Hope Ontario, Canada
227. P. H. Gantt, USAEC, Washington, D. C. 20545
- 228-237. W. P. Gammill, USAEC, Washington, D. C. 20545
238. J. M. Garner, Jr., Auburn University, Auburn, Ala. 36830
239. C. F. Garrison, HGS Technical Associates, Inc. P. O. Box 1156,
Johnson City, Tennessee 37601
240. L. D. Geiger, USAEC, Pittsburgh Naval Reactors Office,
P. O. Box 109, West Mifflin, Pa. 15122
241. T. C. George Bureau of Explosives, 63 Vesey Street, New York,
N. Y. 10007

242. J. E. Gillham, Pan American World Airways, Pan Am Building, New York, N. Y. 10017
243. W. L. Ginkel, USAEC, Idaho Operations Office, P. O. Box 2108, Idaho Falls, Idaho 83402
244. L. P. Gise, USAEC, Albuquerque Operations Office, P. O. Box 5400, Albuquerque, New Mexico 87115
245. J. C. Glynn, USAEC, Washington, D. C. 20545
246. J. C. Goodchild, Ellisco, Inc., 400 North American Street, Philadelphia, Pennsylvania
247. C. F. Goodner, USAEC, Richland Operations Office, P. O. Box 550, Richland, Washington 99352
248. T. W. Gore, Donald Douglas Laboratory, 2955 George Washington Way, Richland, Washington 99350
249. G. C. Gower, USAEC, Chicago Operations Office, 9800 South Cass Ave., Argonne, Illinois 60439
250. T. R. Grant, U. S. Coast Guard Headquarters (Sta. MHM-MEZ) Washington, D. C. 20591
251. K. W. Graybeal, American Nuclear Corporation, P. O. Box 426, Oak Ridge, Tennessee 37830
252. A. W. Grella, U. S. Dept. of Transportation, 6th and D Street, SW, Washington, D. C. 20590
253. R. P. Grill, University of California, Lawrence Radiation Lab., Berkeley, California 94720
254. D. L. Grover, Bettis Atomic Power Laboratory, P. O. Box 79, West Mifflin, Pennsylvania 15122
255. T. Gutman, Westinghouse Electric Corp., P. O. Box 217, Cheswick, Pennsylvania 15024
256. S. Hagsgard, Aktiebolaget Atomenergi, Studsvik, Fack, S-611 01 Nykoping, Sweden
257. J. J. Hairston, Neutron Products, Inc., P. O. Box 95, Dickerson, Maryland 20753
258. M. M. Ham, III, Lockheed-Georgia Company, Dawsonville, Ga. 30534
259. A. K. Hardin, Douglas United Nuclear, Inc., P. O. Box 490, Richland, Washington 99352
260. T. H. Hardin, USAEC, Oak Ridge Operations, P. O. Box E, Oak Ridge, Tennessee 37830
261. J. A. Harper, E. I. duPont deNemours & Co., Savannah River Plant, Aiken, South Carolina 29801
262. W. F. Harrington, Uniroyal, Inc., 312 N. Hill Street, Mishawaka, Indiana 46544
263. B. D. Harris, Nuclear Engineering Company, Inc., 855 N. Wilson Ave., Morehead, Kentucky 40351
264. J. T. Harris, USAEC, Chicago Operations Office, 9800 South Cass Ave., Argonne, Illinois 60439
265. J. H. Harrison, National Lead Company of Ohio, P. O. Box 39158, Cincinnati, Ohio 45239
266. A. F. Heitkamp, Monsanto Research Corporation, Mound Laboratory, Miamisburg, Ohio 45342
267. M. M. Hendrickson, Battelle Northwest, P. O. Box 999, Richland, Washington 99352
268. R. H. Hendron, Los Alamos Scientific Laboratory, P. O. Box 1663, Los Alamos, New Mexico 87544

269. M. R. Hersey, United Kingdom Atomic Energy Authority, Risley, Warrington, Lancashire, England
270. K. Heydorn, Danish Atomic Energy Commission, Riso DK 4000, Roskilde, Denmark
271. O. S. Hiestand, Jr., USAEC, Washington, D. C. 20545
272. J. R. Hill, USAEC, P. O. Box 392, West Valley, N. Y. 14171
273. R. N. Hill, Brookhaven National Laboratory
274. S. B. Hodge, Atomic Energy of Canada, Ltd., Chalk River, Ontario, Canada
275. G. D. Hoggatt, General Electric Co., 310 Deguigne Drive, Sunnyvale, California
276. J. J. Holloway, NUS Corporation, 1730 M Street N. W., Washington, D. C. 20036
277. A. W. Holmes, USAEC, Chicago Operations Office, 9800 South Cass Ave., Argonne, Illinois 60439
278. D. A. Hoover, Atlantic Richfield Hanford Co., Richland, Wash. 99352
279. D. R. Hopkins, Industrial Nucleonics Corporation, 650 Ackerman Rd., Columbus, Ohio 43202
280. L. H. Horn, Underwriters Laboratories, 207 E. Ohio Street, Chicago, Illinois 60611
281. W. R. Householder, HGS Technical Associates, Inc., P. O. Box 1156, Johnson City, Tennessee 37601
282. E. G. Howard, Association of American Railroads, Law Department, Transportation Building, Washington, D. C. 20006
283. R. A. Hunt, E. I. duPont, Savannah River Plant., Aiken, S. C. 29801
284. L. K. Hurst, Argonne National Laboratory
285. L. G. Hungerford, Nuclear Management, Inc., 2323 South Ninth St., Lafayette, Indiana 47905
286. J. F. Ingman, U. S. Army Nuclear Weapons Surety Group, Fort Belvoir, Virginia 22150
287. S. Ishii, Mitsubishi International Corp., 277 Park Avenue, New York, N. Y. 10017
288. C. E. Ishmael, USAEC, 9800 South Cass Avenue, Argonne, Ill. 60439
289. P. R. Janin, Transnuclear, Inc., 7 West 57th Street, New York, N. Y. 10019
290. T. M. Jelinek, USAEC, 21000 Brookpark Road, Cleveland, Ohio 44135
291. R. I. Jetter, Atomics International, P. O. Box 309, Canoga Park, California 91304
292. W. A. Johnson, USAEC, Oak Ridge Operations, P. O. Box E, Oak Ridge, Tennessee 37830
293. A. E. Jones, USAEC, Grand Junction Office, P. O. Box 2567, Grand Junction, Colorado 81501
294. J. W. Jones, Bettis Atomic Power Laboratory, P. O. Box 79, West Mifflin, Pa. 15122
295. O. H. Jones, The Babcock & Wilcox Co., P. O. Box 1260, Lynchburg, Virginia 24505
296. A. A. Jonke, Argonne National Laboratory
297. J. Kafkafi, The Embassy of Israel, 2916 Chesapeake St., Wash., D. C.
298. J. B. Kahle, Monsanto Research Corporation, Mound Laboratories, Miamisburg, Ohio 45342
299. D. W. Kamphaus, Navy Nuclear Power Unit, Fort Belvoir, Va. 22150

300. B. A. Karrasch, Babcock & Wilcox Co., P. O. Box 1260, Lynchburg, Virginia 24505
301. R. A. Kaye, USAEC, Washington, D. C. 20545
302. R. Kennedy, Engineering Research Laboratory, 1505 Richmond Road, Williamsburg, Virginia 23185
303. G. R. Kiel, Isochem, P. O. Box 250, Richland, Washington 99352
304. E. M. Kinderman, Stanford Research Institute, 333 Ravenswood Ave., Menlo Park, California 94025
305. R. G. Kitzer, Jr., Westinghouse Atomic Power Division, P. O. Box 355, Pittsburgh, Pennsylvania 15230
306. W. J. Klaassen, Parsons-Jurden Corporation, 26 Broadway, New York, N. Y. 10004
307. P. B. Klevin, USAEC, Brookhaven Operations Office, Upton, Long Island, New York 11973
308. W. H. Kline, Argonne National Laboratory
309. W. A. Kolb, P. T. B. Bundesallee 100, 33 Braunschweig, F. R. Germany
310. C. P. Koster, Union Carbide Corporation, Tuxedo, N. Y. 10987
311. S. S. Kowronek, United Nuclear Corporation, P. O. Box 1883, New Haven, Connecticut 06508
312. W. J. Kreeger, U. S. Army Engineer Reactors Group, Fort Belvoir, Virginia 22060
313. R. E. Kropp, United Nuclear Corporation, P. O. Box 1883, New Haven, Connecticut 06508
314. H. D. Kucherer, Westinghouse Electric Corporation, P. O. Box 355, Pittsburgh, Pennsylvania 15230
315. L. Kunsagi, Foster-Wheeler Corporation, Livingston, N. J. 07039
316. R. W. Kupp, S. M. Stoller Associates, 201 Park Avenue South, New York, N. Y. 10003
317. D. J. Kvam, Lawrence Radiation, P. O. Box 808, Livermore, California 94551
318. S. Ladich, Babcock & Wilcox Co. Barberton, Ohio 44203
319. T. LaGuardia, United Nuclear Corporation, Elmsford, N. Y. 10523
320. J. W. Langhaar, E. I. duPont de Nemours & Company, Wilmington, Delaware 19898
321. J. W. Lee, Tri-State Motor Transit Co., P. O. Box 9935, West Palm Beach, Florida 33404
322. J. A. Lenhard, USAEC, Oak Ridge Operations, P. O. Box E, Oak Ridge, Tennessee
323. L. Lewis, International Bridge Tunnel & Turnpike Association Port of New York Authority, 13th and Provost Street, Jersey City, New Jersey 07302
324. L. Lewis, Duke Power Company, P. O. Box 2178, Charlotte, N. C. 28201
325. J. A. Lieberman, USAEC, Washington, D. C. 20545
326. K. P. Lien, Norwegian Institute for Atomic Energy, P. O. Box 40, Kjeller, Norway
327. B. G. Lindberg, USAEC, Washington, D. C. 20545
328. J. B. Lingerfelt, USAEC, Oak Ridge Operations, P. O. Box E, Oak Ridge, Tennessee 37830
329. J. W. Loeding, Argonne National Laboratory
330. W. E. Lotz, USAEC, Richland Operations Office, P. O. Box 550, Richland, Washington 99352

331. C. W. Loveland, Union Carbide Corporation, P. O. Box 1410, Paducah, Kentucky 42001
332. H. L. Loy, General Electric Co., P. O. Box 254, 21518 First Street, San Jose, California 95100
333. C. D. Luke, USAEC, Washington, D. C. 20545
334. E. C. Lusk, Battelle Memorial Institute, 505 King Avenue, Columbus, Ohio 43201
335. R. J. Lusky, National Lead Company, 1130 Central Avenue, Albany, New York 12205
336. C. E. MacDonald, USAEC, Washington, D. C. 20545
337. R. S. MacKenzie, Jr., Commonwealth Edison Company, 72 West Adams Street, Chicago, Illinois 60690
338. H. J. McAlduff, USAEC, Oak Ridge Operations, P. O. Box E, Oak Ridge, Tennessee 37830
339. J. A. McBride, USAEC, Washington, D. C. 20545
340. L. D. McBride, General Electric Company, Vallecitos Nuclear Center, Pleasanton, California 94566
341. J. D. McCarthy, Dow Chemical Company, Rocky Flats Division, P. O. Box 888, Golden, Colorado 80401
342. J. J. McClister, Tennessee Valley Authority, Lupton Building, Chattanooga, Tennessee 37400
343. W. C. McCluggage, USAEC, Washington, D. C. 20545
344. J. D. McDaniels, Jr., Babcock & Wilcox Co., P. O. Box 1260, Lynchburg, Virginia 24505
345. F. L. McFarling, Sandia Corporation, P. O. Box 5800, Albuquerque, New Mexico 87115
346. S. McLain, Nuclear Management, Inc., 2323 South Ninth Street, LaFayette, Indiana 47905
347. J. R. McVey, Marsh & McLennan, 70 Pine Street, New York, N. Y. 10005
348. J. N. Maddox, USAEC, Washington, D. C. 20545
349. G. R. Maitland, Canadian Transport Commission, P. O. Box 283, Kanata, Ontario, Canada
350. R. F. Malecha, Argonne National Laboratory
351. H. A. Malson, Monsanto Research Corporation, 1515 Nicholas Road Station B, Box 8, Dayton, Ohio 45407
352. W. C. Manser, Jr., National Lead Company, Foot of West Street, Wilmington, Delaware 19898
353. A. R. Matheson, Gulf-General Atomic Corporation, P. O. Box 608, San Diego, California 92112
354. J. H. Mattare, Fire Fighters Local #36, 3001 Veasey Street NW, Washington, D. C.
355. R. A. Meldrum, Transportation Engineering, Department of the Army, Washington, D. C. 20310
356. G. Menichetti, Societa' Nazionale Transporti, Fratelli Direzione Generale, Milano Via Pontaccio 21, Italy
357. W. G. Meyer, Picker X-Ray Corporation, 595 Minor Road, Highland Heights, Ohio 44143
358. J. S. Milau, Brookhaven National Laboratory
359. G. J. Miller, Naval Nuclear Power Unit, Fort Belvoir, Va. 22060
360. R. H. Miller, USAEC, Oak Ridge Operations, P. O. Box E, Oak Ridge, Tennessee 37830

361. C. R. Moore, Nuclear Fuel Services, Inc., P. O. Box 124, West Valley, N. Y. 14171
362. R. A. Montgomery, Tennessee Valley Authority, New Sprinkle Building, Knoxville, Tennessee 37902
363. T. Moriya, Fire Research Institute of Japan, 700 Shinkawa, Mitake, Tokyo, Japan
364. W. G. Morrison, Idaho Nuclear Corporation, P. O. Box 1845, Idaho Falls, Idaho 83401
365. H. W. Morton, Nuclear Fuel Services, Inc., Irwin, Tenn. 37650
366. T. E. Morton, Nuclear Materials & Equipment Corporation, Apollo, Pennsylvania 15613
367. R. A. Moyer, E. I. DuPont, Savannah River Laboratory, Aiken, South Carolina 29801
368. W. L. Mullett, Southern Nuclear Engineering Inc., P. O. Box 10, Dunedin, Florida 33528
369. D. S. Myers, Lawrence Radiation Laboratory, P. O. Box 808, Livermore, California 94550
- 370-379. W. A. Nelson, USAEC, Washington, D. C. 20545
380. R. S. Nisson, Naval Facilities Engineering Command, P. O. Box 610, Falls Church, Va. 22046
381. S. W. Nitzman, Schenectady Naval Reactors Office, P. O. Box 1069, Schenectady, New York 12301
382. C. B. Noel, Mason & Hanger-Silas Mason Co., Inc., P. O. Box 261, Burlington, Iowa 52601
383. S. G. Nordlinger, USAEC, Washington, D. C. 20545
384. E. D. North, Nuclear Fuel Services, Inc., 906 Wheaton Plaza, Wheaton, Maryland 20902
385. H. E. Noyes, Los Alamos Scientific Laboratory, P. O. Box 1663, Los Alamos, New Mexico 87544
386. D. A. Nussbaumer, USAEC, Washington, D. C. 20545
387. J. W. O'Daniel, Babcock & Wilcox Company, P. O. Box 1260, Lynchburg, Va. 24505
388. C. E. Oddis, USAEC, Pittsburgh Naval Reactors Office, P. O. Box 109, West Mifflin, Pennsylvania 15122
389. R. J. O'Dea, Lawrence Radiation Laboratory, Berkeley, Cal. 94720
390. R. H. Odegaarden, USAEC, Washington, D. C. 20545
391. R. G. Olt, Monsanto Research Corporation, P. O. Box 8, Sta. B, Dayton, Ohio 45407
392. L. J. O'Neill, USAEC, Nevada Operations Office/NTSSO, P. O. Box 14100, Las Vegas, Nevada 89114
393. R. L. Pannemann, Minnesota Mining & Mfg. Co., St. Paul, Minn. 55119
394. D. E. Patterson, USAEC, Washington, D. C. 20545
395. S. G. Pearsall, Brookhaven National Laboratory
396. E. Pedersen, Nuclear Fuel Services, Irwin, Tennessee 37650
397. G. F. Penn, USAEC, Richland Operations Office, P. O. Box 550, Richland, Washington 99352
398. J. A. Penney, Brookhaven National Laboratory
399. J. R. Perrette, Transnuclear, Inc., 7 West 57th Street, New York, N. Y. 10019
400. G. Pesce, Comitato Nazionale Energia Nucleare, Viz Belisario 15, Rome, Italy

401. R. L. Peterson, American Insurance Association, 85 John Street, New York, N. Y. 10038
402. R. W. Peterson, National Lead Company, Foot of West Street, Wilmington, Delaware 19898
403. J. Pidkowicz, USAEC, Site Representative, 4500 Bldg., Oak Ridge Tennessee 37830
404. J. Pirro, Atcor Inc., 360 Bradhurst Avenue, Hawthorne, N. Y. 10532
405. W. L. Pie, Jr., E. I. duPont, Savannah River Plant, Aiken, S. C. 29801
406. W. A. Pryor, USAEC, Oak Ridge Operations, P. O. Box E, Oak Ridge, Tennessee 37830
407. S. L. Reese, Nuclear Safety Associates, Suite 200, 7735 Old Georgetown Road, Bethesda, Maryland 20014
408. H. B. Reid, Atomic Energy of Canada Limited, Chalk River, Ontario, Canada
409. J. E. Reeves, Nevada Operations Office, P. O. Box 14100, Las Vegas, Nevada 89114
410. T. Ricci, Atomics International, P. O. Box 309, Canoga Park, California 91304
411. N. J. Rigstad, Idaho Nuclear Corporation, P. O. Box 1845, Idaho Falls, Idaho 83401
412. M. Robatel, Robatel SLPI, 59 rue Baraban, 69-Lyon 3 eme, France
413. G. G. Rocco, New England Nuclear Corporation, 575 Albany Street, Boston, Massachusetts 02118
414. L. R. Rogers, USAEC, Washington, D. C. 20545
415. R. F. Rogers, E. I. duPont de Nemours & Company, Savannah River Plant, Aiken, South Carolina 29801
416. W. F. Romine, The Dow Chemical Company, P. O. Box 888, Golden, Colorado 80401
417. R. E. Rowley, Douglas United Nuclear, Inc., P. O. Box 490, Richland, Washington 99352
418. T. A. Russell, Atcor Inc., 360 Bradhurst Ave., Hawthorne, N. Y. 10038
419. E. O. Rutenkroger, Nuclear Fuel Services, Inc., P. O. Box 124, West Valley, N. Y. 14171
420. S. R. Sapirie, USAEC, Oak Ridge Operations, Post Office Box E Oak Ridge, Tennessee 37830
421. R. A. Scarano, Westinghouse Astronuclear Laboratory, P. O. Box 10864, Pittsburgh, Pennsylvania 15200
422. M. R. Schaeffer, Reactive Metals Inc., P. O. Box 579, Ashtabula, Ohio 44004
423. G. D. Schmidt, U. S. Public Health Service, National Center for Radiological Health, Rockville, Md. 20852
424. C. W. Schultz, Bureau of Explosives, 2 Pennsylvania Plaza, New York, N. Y. 10001
425. H. C. Schultze, South Carolina State Development Board, P. O. Box 927, Columbia, South Carolina 29202
426. A. Schwebel, National Bureau of Standards, Washington, D. C. 20234
427. R. G. Schwieger, Westinghouse Advanced Reactors Division, 800 Penn Center Boulevard, Pittsburgh, Pennsylvania 15235
428. B. Seid, Radiation Machinery Corporation, 1280 Rt. #46 Parsippany, New Jersey 07054

429. M. Selman, Nuclear Materials & Equipment Corporation, Apollo, Pennsylvania 15613
430. E. M. Shank, Eurochemic, Mol, Belgium
431. J. W. Shaver, North Carolina State Board of Health, P. O. Box 2091, Raleigh, North Carolina 27602
432. H. P. Shaw, Atlantic Richfield Hanford Company, P. O. Box 250, Richland, Washington 99352
433. W. Shaw, Canadian General Electric, Petersborough, Ontario, Canada
434. J. J. Shefcik, Gulf General Atomic Corporation, P. O. Box 608, San Diego, California 92112
435. L. R. Shobe, University of Tennessee, Knoxville, Tennessee 37916
436. F. J. Shon, USAEC, Washington, D. C. 20545
437. E. C. Shute, USAEC, San Francisco Operations Office, 2111 Bancroft Way, Berkeley, California 94702
- 438-447. J. A. Sisler, USAEC, Washington, D. C. 20545
448. W. L. Slagle, Phillips Petroleum Company, P. O. Box 2067, Idaho Falls, Idaho 83401
449. W. L. Smalley, USAEC, Oak Ridge Operations, P. O. Box E, Oak Ridge, Tennessee 37830
450. C. W. Smith, General Electric Company, 283 Brokaw Road, Santa Clara, California 95050
451. D. R. Smith, Los Alamos Scientific Laboratory, P. O. Box 1663, Los Alamos, New Mexico 87544
452. H. A. Smith, National Lead Company, Foot of West Street, Wilmington, Delaware 19898
453. V. A. Smith, Union Carbide Corporation, P. O. Box 1410, Paducah, Kentucky 42001
454. D. R. Snavely, U. S. Public Health Service, National Center for Rad. Health, Rockville, Maryland 20852
455. N. Srinivasan, Bhabha Research Centre, Fuel Reprocessing Division, Trombay, Bombay 74, India
456. N. Stetson, USAEC, Savannah River Operations Office, P. O. Box A, Aiken, South Carolina 29801
457. J. F. Stevens, USAEC, Dayton Area Office, P. O. Box 66, Miamisburg, Ohio 45342
458. J. J. Sullivan, O. G. Kelley Company, 98 Taylor Street, Boston, Massachusetts 02122
459. C. L. Sumrall, Gilbert Associates, Inc., 525 Lancaster Avenue, Redding, Pennsylvania 19603
460. A. Susanna, Comitato Nazionale Energia Nucleare, 15 Via Belisario, Rome, Italy
461. F. J. Sweeney, Associated Transport, Inc., 380 Madison Avenue, New York, N. Y. 10017
462. G. E. Swindell, International Atomic Energy Agency, 11 Kaerntnerring, A-1010 Vienna, Austria
463. D. R. Swindle, USAEC, Washington, D. C. 20545
464. W. R. Taylor, Atomic Energy of Canada Limited, Chalk River, Ontario, Canada
465. W. I. Thisell, E. I. duPont de Nemours & Co., Inc., Wilmington, Delaware 19898

466. R. H. Thompson, General Electric, Vallecitos Nuclear Center,
P. O. Box 846, Pleasanton, California 94566
467. R. J. Thompson, Stearns-Roger Corporation, P. O. Box 588,
Denver, Colorado 80217
468. D. A. Tobias, Idaho Nuclear Corporation, P. O. Box 1845,
Idaho Falls, Idaho 83401
469. S. A. Tompkins, Johns-Manville Corporation, 22 E. 40th Street
New York, N. Y. 10016
470. J. J. Toughey, REA Express, 219 E. 42nd Street, New York,
N. Y. 10017
471. C. L. Trenouth, Eldorado Nuclear Limited, Port Hope, Ontario,
Canada
472. E. L. Van Horn, USAEC, Brookhaven Operations Office, Upton,
N. Y. 11973
473. K. H. Veith, Bundesanstalt fur Materialprufung (BAM), Unter
den Eichen 87, Berlin, Dahlem, Germany
474. O. A. Vogtsberger, U. S. Army, Fort Belvoir, Virginia 22060
- 475-476. J. Votaw, National Lead of Ohio, M.P.O. Toledo, Ohio 43601
477. R. L. Vree, Argonne National Laboratory, 9700 S. Cass Avenue,
Argonne, Illinois 60439
478. W. F. Wackler, Dow Chemical Company, P. O. Box 888, Golden,
Colorado 80401
479. H. E. Walchli, Westinghouse Electric Corporation, P. O. Box
355, Pittsburgh, Pennsylvania 15230
480. R. B. Waite, Stearns-Roger Corporation, P. O. Box 5888,
Denver, Colorado 80217
481. R. T. Waite, American Insurance Association, 85 John Street,
New York, N. Y. 10038
482. J. E. S. Warden, Knolls Atomic Power Laboratory, P. O.
Box 1072, Schenectady, N. Y. 12301
483. M. J. Weiss, Duquesne Light Company, Shippingport Atomic Power
Station, Shippingport, Pennsylvania 15077
484. A. H. Wernecke, Goodyear Atomic Corporation, P. O. Box 628,
Piketon, Ohio 45661
485. P. H. Wigfull, Rolls-Royce & Associates Ltd., P. O. Box 31,
Derby, England
486. G. L. Wigle, Lawrence Radiation Laboratory, Berkeley,
California 94720
487. B. J. Wilson, General Electric Co., APED, P. O. Box 254
21518 First Street, San Jose, California 95100
488. D. G. Williams, USAEC, Richland Operations Office, P. O. Box
550, Richland, Washington 99352
489. C. A. Wilkins, E. I. duPont de Nemours & Company, Savannah
River Laboratory, Aiken, South Carolina 29801
490. D. H. Winkler, General Electric Company - N.S.P. P. O. Box 132,
Cincinnati, Ohio 45215
491. G. E. Wuller, Ker-McGee Corporation, Kerr-McGee Building,
Oklahoma City, Oklahoma 73102
492. B. J. Youngblood, USAEC, Washington, D. C. 20545
493. L. L. Zahn, Jr., Atlantic Richfield Hanford Co., P. O. Box 250,
Richland, Washington 99352

- 494. L. M. Zamory, Atcor, Inc., 360 Bradhurst Avenue, Hawthorne
N. Y. 10038
- 495. C. N. Zangar, Vitro/Hanford Engineering Services, P. O. Box
296, Richland, Washington 99352
- 496. M. R. Zigler, Goodyear Atomic Corporation, P. O. Box 628,
Piketon, Ohio 45661
- 497-514. Advisory Committee on Reactor Safeguards, R. F. Fraley,
Executive Secretary, USAEC, Washington, D. C. 20545
- 515. E. L. Daman, Foster Wheeler Corporation, 110 South Orange
Avenue, Livingston, New Jersey 07039
- 516. D. E. Haagensen, 4729 Newlons Drive West, Murrysville,
Pennsylvania 15668
- 517. F. R. Hubbard, Nuclear Technology Corporation, 116 Main St.,
White Plains, N. Y. 10601
- 518. Laboratory and University Division, OR.